TOWARDS THE TOTAL SYNTHESIS OF THE XIAMYCIN FAMILY OF INDOLOSESQUITERPENES: SYNTHESIS OF ORIDAMYCINS A AND B

A Dissertation

Presented to the Faculty of the Weill Cornell Graduate School

of Medical Sciences

in Partial Fulfillment of the Requirements for the Degree of

Doctor of Philosophy

by

Adam Howell Trotta

January 2018

TOWARDS THE TOTAL SYNTHESIS OF THE XIAMYCIN FAMILY OF INDOLOSESQUITERPENES: SYNTHESIS OF ORIDAMYCINS A AND B

Adam Howell Trotta

Cornell University 2018

The xiamycin family of indolosesquiterpenes comprises bioactive compounds isolated from several strains of *Streptomyces*. Several dimeric family members have shown strong activity against several strains of bacteria, including methicillin-resistant *Staphylococcus aureus* (MRSA) and vancomycin-resistant *Enterococcus* (VRE). These promising initial results, coupled with the limited production of these compounds from their natural sources, prompted the design of a unified synthetic strategy capable of producing several family members from a common synthetic intermediate.

Structurally, the xiamycin family members consist of a carbazole fused to a *trans*-decalin ring system. The difference between xiamycin A and oridamycin A is a single epimeric stereocenter at C16. It was envisioned that a key oxidative radical cyclization could produce both stereochemical patterns—with free-radical conditions generating the stereochemistry associated with oridamycin A, and chelated radical conditions producing the stereochemistry corresponding to xiamycin A.

The total synthesis of oridamycins A and B was completed, utilizing a free-radical cyclization that correctly set three contiguous stereocenters, including two quaternary carbons. The fused carbazole was produced using a 6π-electrocyclization/aromatization sequence. Finally, oridamycin B was accessed through a palladium-catalyzed, oxime-directed C-H oxidation.

BIOGRAPHICL SKETCH

Adam Howell Trotta was born in Lowell, Massachusetts in 1989, and spent his childhood in Andover, Massachusetts. In high school, Adam was primarily interested in biology, as it answered fundamental questions about life and nature. His first research experience was during the summer of 2007, when he was a research assistant in the laboratory of Prof. Ferdinando F. Bruno at UMass–Lowell. He conducted research in polymer chemistry, using enzymes to polymerize antioxidant polyphenols to augment their stability. During undergraduate studies at Tufts University, Adam became more interested in chemistry because it illuminated the underlying mechanisms of biology, and he switched his major from Biochemistry to Chemistry. While at Tufts, Adam conducted research under the supervision of Prof. Clay S. Bennett, working to streamline solid-phase oligosaccharide synthesis. Adam helped develop a methodology to directly transfer resin bound oligosaccharides to alcohol acceptors through activation of thioether linkers. He began his graduate career at Columbia University in the laboratory of Prof. Scott A. Snyder, where he worked on the synthesis of the coccinellid alkaloids using a family based strategy. Eight of the monomers and two of the dimers were completed using amine/enamine cascades. After Prof. Snyder's departure from Columbia, Adam transferred to the laboratory of Prof. Samuel J. Danishefsky at Memorial Sloan Kettering Cancer Center, where he has worked towards a unified synthetic strategy to access the xiamycin family of indolosesquiterpenes.

ACKNOWLEDGEMENTS

First and foremost, I would like to thank Prof. Samuel J. Danishefsky for accepting me into his laboratory and providing outstanding support throughout my doctoral studies. He has provided an excellent environment to conduct research, encouraging new ideas and exploration. He has also been extremely supportive in my efforts to publish, in my fellowship applications, and in my postdoctoral applications—I am certain that I owe a significant amount of my success in those endeavors to Prof. Danishefsky. I would also like to thank Sarah Danishefsky for her continued support during my doctoral studies.

Prof. Derek S. Tan has also been instrumental throughout my graduate school experience. Initially, he was instrumental in facilitating my transition from Columbia to the Tri-Institutional Training Program in Chemical Biology (TPCB). He made the entire process seamless, and I am grateful for that. As the chair of the program he has been spectacular. TPCB is an outstanding collaborative program that is only getting better. Derek makes sure that every aspect is meticulously designed and executed, and the quality of the training we receive reflects his hard work and dedication. He has also served as a second mentor to me after Prof. Danishefsky's retirement, supporting and encouraging my research endeavors and helping the remaining lab members manage resources and communicate with the administration. We would certainly be lost without you. Thank you.

I would also like to thank my committee members Prof. Minkui Luo and Prof. Anthony Sauve who have always provided excellent suggestions

and discussions. I appreciate your insightful comments and continued support throughout my graduate studies. I would also like to thank Prof. Howard Hang for serving as an additional committee member on short notice.

I would also like to thank several lab members. First, I would like to thank Dr. Adam Levinson, who has been my esteemed colleague throughout all of graduate school—Columbia included. Adam is an outstanding chemist, and has served as an incredible role model for me. He was always curious, trying new things, reading the current literature, drawing mechanisms, and making great chemistry puns about his dog Dooley. It's been extremely challenging and rewarding to try to live up to the lofty example he has set. Adam is now at Eli Lilly where I'm sure he'll rise through the ranks and do great things. I would also like to thank Dr. Gardner Creech, who was extremely helpful during my first year in the Danishefsky lab. Gardner was always willing to talk about anything, providing ample doses of insight, humor, and commentary. He is an intelligent, hard-working, practical, and thoughtful person, and I'm grateful that our paths crossed in the Danishefsky lab. I would also like to thank Prof. Andrew G. Roberts of the University of Utah. Andrew has always been there to talk about chemistry. He is remarkably patient, thoughtful, intelligent, and humorous, and his careful considerations and insightful comments have been influential during my graduate studies. He has a unique perspective, and I'm curious and excited to see what interesting chemistry comes out of his independent career. I owe him a tremendous debt of gratitude, he's been an excellent mentor and friend. I would also like to thank the current Danishefsky lab members: Dr. Abram Axelrod, Dr. Baptiste Aussedat, and Dr. Bill Walkowicz.

You are all awesome people, and I feel very fortunate to have shared the lab with you for all these years. I've learned a lot about chemistry and life from all of you, and I can't thank you enough for your support and comradery.

I would also like to thank one of my best friends, Maria Chiriac. I'm incredibly grateful for her support, wisdom, and guidance throughout my graduate studies. Maria is a great person and fantastic chemist, and our many conversations covered every topic imaginable. I always looked forward to delving head-first into complex topics with her. Merck is very lucky to have her! I would also like to thank my girlfriend, Michaelyn Lux. She has been the most supportive, understanding, rational, and consistent person throughout graduate school. I couldn't have done it without her. She is intelligent, fearless, compassionate, and wise, and we've had countless conversations that have significantly influenced my perspective on the world. I can't thank her enough for everything that she's done. She's also a brilliant chemist who has tremendous potential. I look forward to seeing what she decides to pursue—it will certainly be great! I'm extremely glad we met and I look forward to many more great experiences together.

I would also like to thank my family. My parents are my foundation. They are truly wonderful people and I owe the world to them. They are two of my most important role models, and they've shown me how to lead a balanced and fulfilling life full of love and laughter. Any success that I may have in life I owe to them. Finally, I would like to thank my sister Rachael. I can't believe how lucky I am to have such a fantastic sister. She's hilarious, brilliant, wise, and kind. I'm excited to finally live in the same city again next year!

TABLE OF CONTENTS

LIST OF FIGURES

Chapter 1

Chapter 2

Chapter 4

Appendix II

LIST OF SCHEMES

Chapter 1

Chapter 2

Chapter 3

Chapter 4

Chapter 5

LIST OF TABLES

Chapter 1

Chapter 2

Chapter 4

Appendix II

LIST OF ABBREVIATIONS

[H^-]	reductant
[O]	oxidant
7-ACA	7-aminocephalosporanic acid
Ac	acetyl
AcOH	acetic acid
AIBN	2,2'-azobisisobutyronitrile
approx.	approximately
Ar	aryl (substituted aryl ring)
BDSB	bromodiethylsulfonium bromopentachloroantimonate
Bn	benzyl
Boc	*tert*-butoxycarbonyl
bpy	2,2'-bipyridyl
Bz	benzoyl
cat.	catalyst
CE	Common Era
cod	1,5-cyclooctadiene
Cp	cyclopentadienyl
CXCR4	C-X-C chemokine receptor type 4
DABCO	1,4-diazabicyclo[2.2.2]octane
DBU	1,8-diazabicyclo[5.4.0]non-5-ene
decomp.	decomposition
dF-ppy	2-(2,4-difluorophenyl)pyridine
DMAP	*N*,*N*-4-dimethylaminopyridine
DME	1,2-dimethoxyethane
DMF	*N*,*N*-dimethylformamide
DMSO	dimethylsulfoxide
DNA	deoxyribonucleic acid
dr	diastereomeric ratio
dtbpy	4,4'-di-*tert*-butyl-2,2'-bipyridine
Enz	enzyme
equiv.	equivalents
ESI	electrospray ionization

Et	ethyl
EtOAc	ethyl acetate
EtOH	ethanol
FDA	Food and Drug Administration
FT/IR	Fourier-transform infrared spectroscopy
GlcNAc	N-acetylglucosamine
GPCR	G-protein coupled receptor
HCV	hepatitis C virus
hfacac	1,1,1,5,5,5-hexafluoroacetylacetone
HIV	human immunodeficiency virus
HMDS	1,1,1,3,3,3-hexamethyldisilazane
HMPA	hexamethylphosphoramide
HPLC	high-performance liquid chromatography
HRMS	high-resolution mass spectrometry
HSV	herpes simplex virus
HTS	high-throughput screening
Hz	Hertz
IC_{50}	half maximal inhibitory concentration
IMDA	intramolecular Diel–Alder cycloaddition
i-Pr	isopropyl
i-PrOH	isopropanol
LA	Lewis acid
LDA	lithium diisopropylamide
LED	light-emitting diode
L_n	*n* ligand(s), where *n* is an integer
M.S.	molecular sieves
Me	methyl
MIC	minimum inhibitory concentration
MOM	methoxymethyl
MRSA	methicillin-resistant *Staphylococcus aureus*
MS	mass spectrometry
Ms	mesyl (methanesulfonyl)
MsCl	methanesulfonyl chloride
MSKCC	Memorial Sloan Kettering Cancer Center

MurNAc	N-acetylmuramic acid
N/A	not available
NBS	N-bromosuccinimide
n-Bu	normal butyl (unbranched)
nd	not determined
NMR	nuclear magnetic resonance
Nu	nucleophile
Oxone	potassium peroxymonosulfate
PBP	penicillin-binding protein
PEDV	porcine epidemic diarrhea virus
Ph	phenyl
phen	1,10-phenanthroline
PhMe	toluene
pic	2-pyridinecarboxylate
PMDA	N,N,N',N",N"-pentamethyldiethylenetriamine
PP	pyrophosphate
ppy	2-phenylpyridinato-C^2,N
PTLC	preparatory thin-layer chromatography
p-TsCl	*para*-toluenesulfonyl chloride
pyr.	pyridine
R_f	retention factor
rxn.	reaction
SET	single-electron transfer
sm	starting material
TADA	transannular Diels–Alder cycloaddition
TBAI	tetra-*n*-butylammonium iodide
TBS	*tert*-butyldimethylsilyl
t-Bu	*tert*-butyl
t-BuOH	*tert*-butanol
TES	triethylsilyl
Tf	trifluoromethanesulfonyl
TFA	trifluoroacetic acid
TFE	2,2,2-trifluoroethanol
THF	tetrahydrofuran

TIPS	triisopropylsilyl
TLC	thin-layer chromatography
TMEDA	N,N,N',N'-tetramethylethylenediamine
TMS	trimethylsilyl
TMSE	2-(trimethylsilyl)ethyl
Ts	*para*-toluenesulfonyl
UPLC	ultra-performance liquid chromatography
UV	ultraviolet
VRE	vancomycin-resistant *Enterococcus*
xfer	transfer

Chapter 1. History and Development of Antibiotics

Preface

The purpose of this chapter is to outline the events that have informed the modern antibiotic drug discovery process, highlighting key insights gathered from decades of research. An important theme is that targeting bacteria is different than targeting mammalian cells, and effective practices for drug development in human disease may not be applicable to infectious diseases. Another important message is that simple structural modifications of drug molecules can have a profound impact on activity, highlighting the role of synthetic organic chemistry in the development of antibiotic medicines.

A. The Foundation of the Antibiotic Era

There is evidence that humans have been ingesting antibacterial compounds for thousands of years, but the modern conception of antibiotics has only arisen within the last century.[1] Tetracycline (**1**) has been found in skeletal remains dated between 350–550 CE, a discovery explicable only if these individuals had ingested tetracycline-containing materials (Figure 1.1.a).[2] There is speculation, however, that beer was the source, casting doubt onto whether the tetracycline was explicitly used to treat disease.[3] Further evidence of antibiotic use comes from red soils in Jordan, which have been traditionally used to treat skin infections. The antibacterial cyclic peptides actinomycin C2 (**2**) and C3 have since been extracted from strains of *Streptomyces* dwelling in these soils, implying that antibiotics were intentionally and effectively used in traditional medicines.[4]

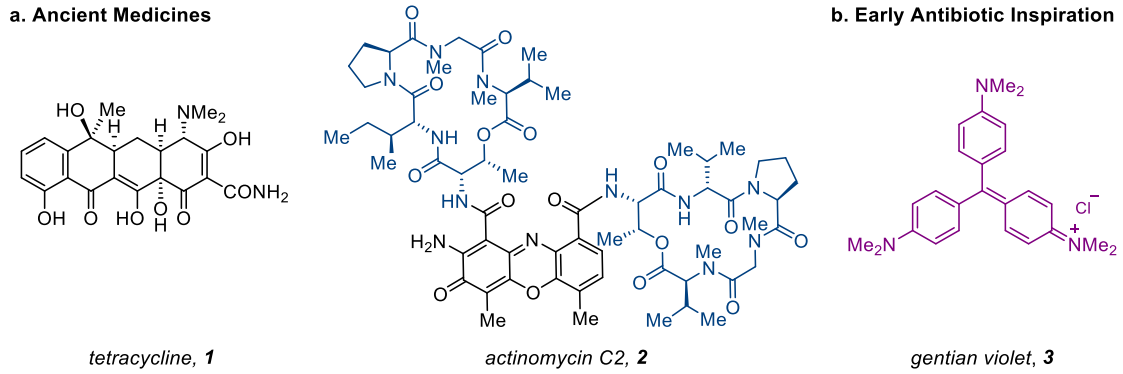

Figure 1.1.a Molecules implicated in ancient medicine: **1**, tetracycline has been found in ancient skeletons, possibly coming from ancient beer, and **2**, actinomycin C2 (peptide portions in blue) has been found in traditional medicines in Jordan. **b** Gentian violet (**3**) is the dye used for Gram staining, and inspired Paul Ehrlich to hypothesize the existence of chemoreceptors due to its selective action.

In spite of early efforts, treatments for systemic bacterial infections were lacking throughout human history. One of the most striking examples is the outbreak of the 'Black Death' between 1347 and 1351. The infection is caused by *Yersinia pestis*, a Gram-negative bacterium commonly found in ground rodents. The outbreak in the 14th century killed between 30-50% of the population of Europe in only five years—claiming the lives of over 30 million people.[5] In contrast, between 2010 and 2015 there were 3248 cases reported worldwide, 584 of which proved fatal—a dramatic difference of over two orders of magnitude between the 14th century and the present.[6] While sanitation has significantly contributed to the disappearance of the Black Death, the introduction of modern antibiotic treatments has also played a crucial role. Clearly, medicine has advanced significantly in the intervening centuries, having nearly eradicated a disease that once wreaked havoc on humanity.

The modern drug discovery process has been a key component in the battle against premature human mortality, with its origins in the late 19th

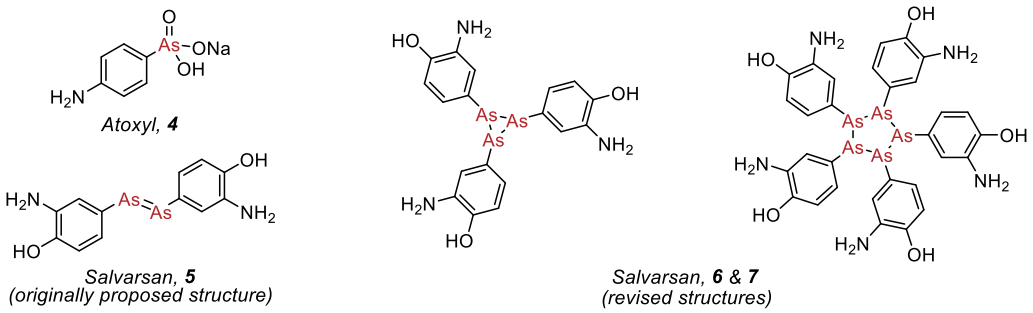

Figure 1.2 Atoxyl (**4**) was a highly toxic veterinary medicine that inspired the early syphilis medication Salvarsan. The originally proposed structure of Salvarsan is shown (**5**), and the 2005 revised structures are also depicted (**6** & **7**).

century. One of the early pioneers was Paul Ehrlich, a German physician and scientist. While Paul Ehrlich was a medical student in the early 1870s, he observed the selective affinity of dyes for biological tissue, leading him to postulate the existence of chemoreceptors on the cells that were selectively interacting with the dye molecules.[7] Several years later, in 1884, Hans Christian Gram discovered that certain bacteria could be selectively stained with a dye (gentian violet [**3**], Figure 1.1.b) in the presence of human cells and other types of organisms.[8] Using this observation, he invented a method to differentiate different types of bacteria, originating the terms Gram-positive and Gram-negative bacteria. Ehrlich's chemoreceptor concept coupled with Gram's dying method led Ehrlich to formulate the 'magic bullet' hypothesis, in which he argued that chemoreceptors on microorganisms, parasites, and cancer cells would be suitably differentiated from similar structures in host tissues to allow for the selective targeting of the infectious agent with a drug molecule. The first modern chemotherapeutic agent, Salvarsan (**5**/**6**/**7**, Figure 1.2), arose as a proof of this hypothesis.[1] In 1904, Paul Ehrlich began a systematic screening program to uncover an improved treatment for syphilis. He synthesized hundreds of

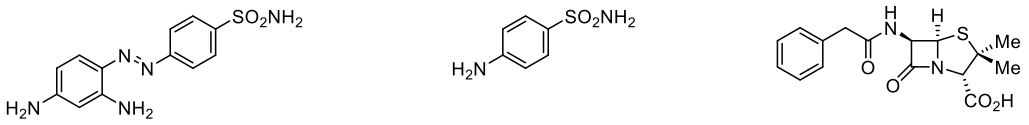

Prontosil, ***8*** *sulfanilamide,* ***9*** *penicillin,* ***10***

Figure 1.3 Early medicines: Prontosil (**8**) was the first sulfa drug, developed by screening azobenzene derived dyes. It was subsequently found that prontosil was a prodrug for sulfanilamide (**9**), the active species. Penicillin (**10**) was the first natural product derived antibiotic.

organoarsenic derivatives of the toxic drug Atoxyl (**4**), eventually discovering Salvarsan (**5**/**6**/**7**) in 1909[9]—replaced by the less toxic and more soluble Neosalvarsan in 1912.[10] Salvarsan and Neosalvarsan were highly successful, becoming the most frequently prescribed drugs until they were superseded by penicillin in the 1940s.[1] Surprisingly, the mechanism of action remains a mystery, and the controversy over its structure was only recently solved.[11] The discovery of Salvarsan gave rise to the modern era of medicinal chemistry. Ehrlich's 'magic bullet' concept has survived to this day, as most current drugs are effective because they selectively target a specific protein while leaving the rest of the proteome largely untouched. The modern drug discovery process is also structured in a manner similar to Ehrlich's discovery process in which a lead compound (Atoxyl) displaying desired activity is derivatized and systematically screened to produce a safer, more effective compound (Salvarsan/Neosalvarsan).

The systematic screening approach was subsequently applied at Bayer in their search for novel antibiotics. Inspired by the selectivity of dyes for specific cell types, they began screening azobenzene derivatives for activity against infectious agents.[12] This screening process eventually yielded Prontosil (**8**), the first of the synthetic sulfa drugs (Figure 1.3). Prontosil turned out to be a prodrug for sulfanilamide (**9**), which had

previously been described in the dye industry, and thus was not patentable.[1] Many companies began to mass produce sulfonamide derivatives, leading to the rapid development of a new class of antibiotics. In 1937, due to exuberance about the sulfa drugs and inconsistent quality control, over 100 people were poisoned from a poorly formulated drug known as Elixir Sulfanilamide.[13] This disaster prompted the passage of the 1938 Federal Food, Drug, and Cosmetic Act, which ultimately put the Food and Drug Administration (FDA) in charge of regulating drug safety in the United States.

The next advance in antibiotics stemmed from the serendipitous discovery of penicillin (**10**) by Alexander Fleming on September 3, 1928 (Figure 1.3).[1] Upon returning from vacation, Fleming noticed a mold colony contaminating one of his Petri dishes that had created a *Staphylococcus*-free zone forming a halo encircling the mold colony.[14] He subsequently developed conditions to produce the antibacterial substance, demonstrated its nontoxicity towards animals, and showed its selective action against various bacterial strains.[14] However, isolation of the pure compound eluded him, and he spent the next 12 years unsuccessfully attempting to convince chemists to resolve the problems with purification and stability.[1] Eventually, Florey and Chain disclosed a method for the purification of penicillin in 1940, leading to mass production and distribution in 1945.[15] While several analgesics and antimalarials had previously been isolated from plants—salicylic acid, morphine, quinine, etc[16]—penicillin was the first natural product developed as an antibacterial, and quickly became the most successful due to its potency and safety.[17] It

also become the first drug to be produced through fermentation on large scale, a practice that continues in modern medicine.

The early search for antibiotic compounds has had a profound impact on the modern drug discovery process. Ehrlich's 'magic bullet' hypothesis has survived to this day, and his strategy of systematic screening and derivatization is common practice in drug discovery campaigns. Another important finding from this era was the discovery that sulfanilamide inhibited carboanhydrase.[18] Derivatives of sulfanilamide were prepared with improved activity against carboanhydrase, leading to highly effective diuretics.[7] This work revealed that enzymes are excellent drug targets, further informing the drug discovery process, and strongly influencing future efforts.

B. Humans vs. Microorganisms

Following the introduction of penicillin in the 1940s, the pharmaceutical industry entered the 'golden age' of antibiotics, extending from the 1940s to the 1970s.[19] In these highly productive years, a number of novel antibiotics were introduced, improving efficacy and safety. Unfortunately, bacteria rapidly began to develop resistance to antibiotics, one after another, usually within a few years following widespread use. The continual battle between humans and bacteria, and the role that organic synthesis has played, is exemplified through two case studies: 1) the β-lactams, and 2) the tetracyclines. In both classes of compounds, bacteria have rapidly developed resistance, which has been countered by elucidation

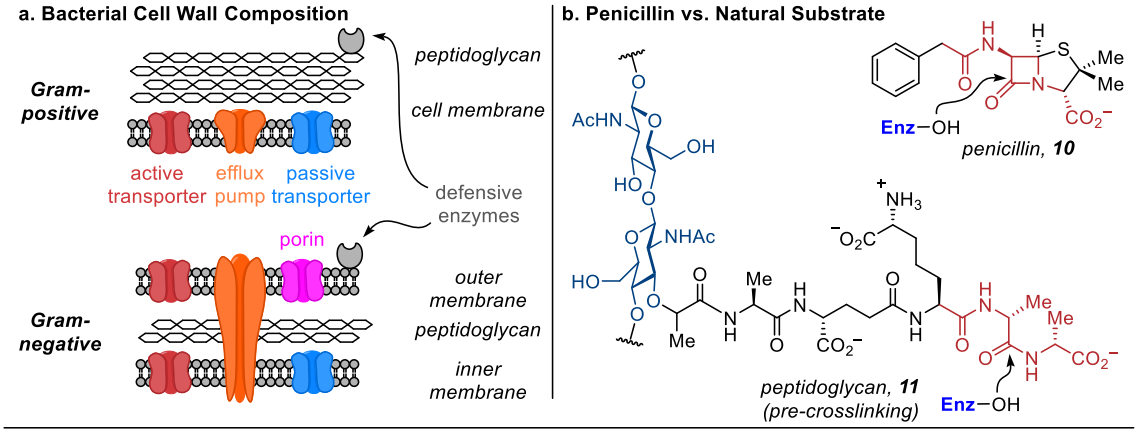

Figure 1.4.a The structural differences between the cell walls of Gram-positive and Gram-negative bacteria. **b** The structural similarities between the substrate (**11**) of the transpeptidase enzyme (Enz, also known as penicillin binding protein [PBP]) and the structure of penicillin (**10**).

of the resistance mechanism followed by structural modifications to the drug molecule.

To understand bacterial resistance, it is necessary to understand the targets of antibiotic compounds, as well as certain key elements of bacterial cell structure. As previously mentioned, there are two main classes of bacteria: 1) Gram-positive, those that can be stained with gentian violet dye, and 2) Gram-negative, those that cannot. Both types of bacteria employ protective outer coatings, differing in their composition and organization (Figure 1.4.a). Gram-positive bacteria utilize a cell wall composed of a thick layer of peptidoglycan, a cross-linked polymer consisting of two alternating monosaccharides (N-acetylglucosamine [GlcNAc] and N-acetylmuramic acid [MurNAc] with a β-1,4 glycosidic linkage) linked to a short polypeptide (4 or 5 amino acids).[20-21] In Gram-positive bacteria, the peptidoglycan layer protects a single cytoplasmic membrane, and interacts with gentian violet dye to produce a positive result in the Gram test.[22] In contrast,

Gram-negative bacteria have both inner and outer cytoplasmic membranes surrounding a thin layer of peptidoglycan and a periplasmic space. The outer cytoplasmic membrane of Gram-negative bacteria prevents gentian dye from interacting with the underlying peptidoglycan layer, producing a negative result in the Gram test. Both types of bacteria utilize active and passive methods (namely, porins) of transportation to migrate molecules across their membranes/walls, and both types of transportation are used during uptake of antibiotic drugs. In addition, both types of bacteria contain membrane-spanning efflux pumps that expunge toxins, defensive surface enzymes (including β-lactamases), and complex carbohydrate networks that create a protective capsule.[23] These numerous defense mechanisms pose a considerable challenge when designing antibacterial drugs, especially for Gram-negative bacteria, which contain an additional membrane relative to their Gram-positive relatives with nearly orthogonal permeability properties.[24]

One of the main targets of antibacterial compounds is the cell wall biosynthesis pathway. It was first proposed that penicillin was an inhibitor of bacterial cell wall biosynthesis in 1956, based on the observation that bacteria lost their cell wall upon treatment with penicillin.[25-26] Tipper and Strominger subsequently proposed that penicillin (**10**) inhibited a transpeptidase (also known as a penicillin-binding protein, or PBP) involved in the tail-to-tail crosslinking of peptidoglycan subunits by mimicking the acyl-D-Ala-D-Ala motif (**11**) found in the natural substrate (Figure 1.4.b).[27-29] Further experimentation suggested that the highly strained β-lactam ring was opened by the enzyme, forming an irreversible covalent linkage, and destroying the catalytic activity.

Microorganisms have been battling each other for millennia, and β-lactams, such as penicillin, have played an important role. Correspondingly, many bacteria developed resistance to β-lactams a billion years prior to their use by humans.[28] There are four main forms of resistance: 1) through the production of β-lactamase enzymes, proteins that are capable of hydrolyzing the β-lactam ring, rendering the compound inactive, 2) mutation of residues in the active site of the target transpeptidase to reduce the affinity of drug molecules (a notable example is PBP2a of methicillin resistant *Staphylococcus* spp.), 3) decreased expression of certain transport proteins, preventing entry of the antibiotic—especially prevalent among Gram-negative bacteria that are able to modulate the expression of passive porin proteins that span the outer membrane, and 4) efflux pumps, proteins that span the membrane(s) and eject undesired compounds from the interior of the cell.[30] In general, Gram-negative bacteria are more difficult targets due to decreased permeability, and generally higher expression of efflux pumps.[30]

To overcome the myriad resistance mechanisms, medicinal chemists have modified the structure of antibiotic compounds using the tools of organic synthesis. Many antibiotic scaffolds have undergone successive structural modifications to overcome resistance, but the cephalosporins have undergone one of the most striking transformations.[31] The precursor to many cephalosporin derivatives is 7-aminocephalosporanic acid (7-ACA, **13**), a semisynthetic compound derived from the natural product cephalosporin C (**12**, Scheme 1.1). Early experiments revealed that acidic hydrolysis of cephalosporin C could produce 7-ACA in low yield, but an improved procedure from chemists at Eli Lilly produced 7-ACA at a

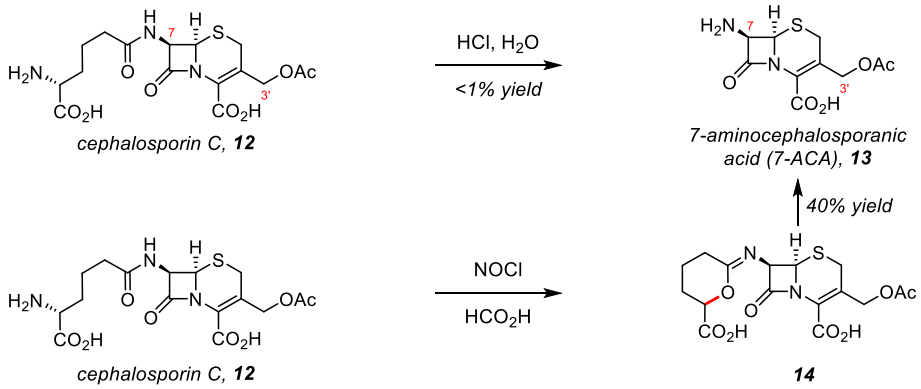

Scheme 1.1 Semisynthetic efforts towards 7-aminocephalosporanic acid (7-ACA, **13**), a common precursor to cephalosporin antibiotics.

commercial level.[31] The two readily modifiable sites on 7-ACA are the C7 amine and the C3' oxygen. Modification of these positions produced the first generation of cephalosporins, as exemplified by cephalothin (**15**, Figure 1.5).[32] The second generation of cephalosporins (**16**, for example) was engineered to have increased activity against Gram-negative bacteria due to increased cell penetration and reduced binding to β-lactamase enzymes.[33] The α-methoxyimino substituent in cefuroxime (**16**) was instrumental in sterically shielding the molecule from β-lactamases, highlighting the impact a simple chemical modification can have on activity.

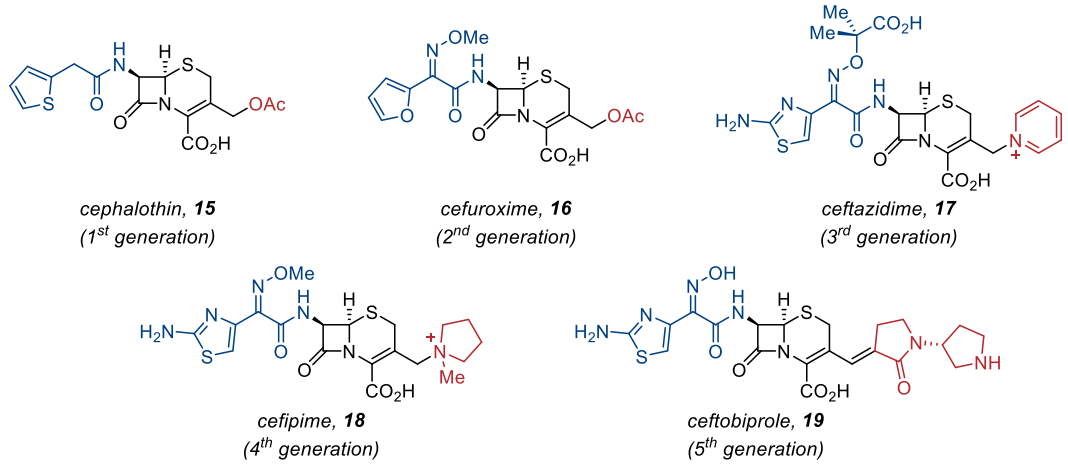

Figure 1.5 Five generations of cephalosporin antibiotics.

Further refinements produced third generation molecules (**17**), which contained an aminothioazole and several charged moieties, including a carboxylate on the oxime, as well as a pyridinium. The charged functionality allowed for enhanced penetration through porins, increasing activity against Gram-negative bacteria.[34] Unsurprisingly, resistance emerged to third generation cephalosporins, as well. Several β-lactamases arose that were able to break down these molecules, prompting the development of fourth generation molecules (**18**), further improving activity against both Gram-positive and Gram-negative bacterial strains.[35]

Structural modifications to the cephalosporins transformed an antibiotic active against Gram-positive bacteria into a broad-spectrum medicine. The inverse has also been achieved with the quinolone family of antibiotics. Early quinolones were active against Gram-negative bacteria, and were subsequently engineered to have activity against Gram-positive organisms, as well.[31] The successive chemical modification of the cephalosporins and the quinolones demonstrates that a lead compound active against only one type of bacteria may be engineered into a broad-spectrum agent, broadening the pool of potential lead compounds for the development of novel antibiotics.

The tetracyclines have undergone a similar evolution to produce antibiotics with increased activity and efficacy. One of the first modifications to the tetracyclines was the reductive removal of the C6 hydroxyl group of 6-demethyltetracycline (**20**) to produce sancycline (**21**), improving access to further derivatives by increasing acid and base tolerance (Scheme 1.2).[36-38] The increased stability enabled nitration of the D ring, leading to the synthesis of minocycline (**23**) after reduction and

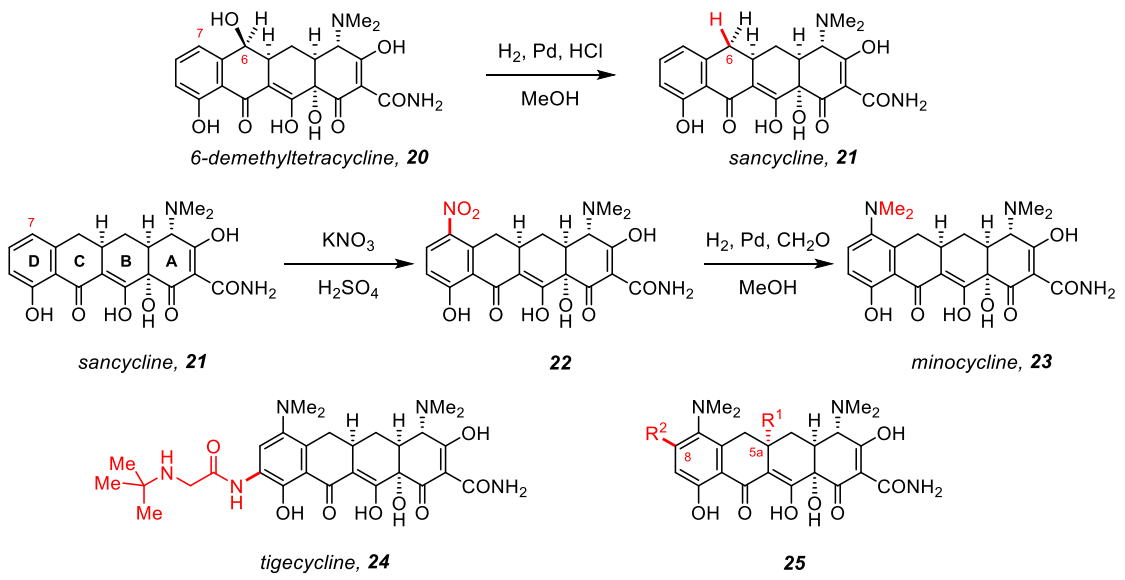

Scheme 1.2 Modifications to the tetracycline scaffold to produce compounds with increased activity.

methylation. Minocycline has a broader spectrum of activity than previous tetracyclines, including activity against resistant strains.[39-40] Further improvements were made in the late 1990s by Wyeth scientists attempting to overcome tetracycline resistance. Modification of minocycline at C9 produced tigecycline (**24**), which succeeded in improving activity toward tetracycline-resistant bacteria by increasing the strength of the binding interaction with its target (the small subunit of the bacterial ribosome),[41-43] and by decreasing binding to a common tetracycline efflux pump.[44] Simple structural modifications at C6, C7, and C9 have significantly altered the properties of the tetracyclines, providing safer and more effective drugs. Inspired by this, the Myers group set out to develop a scalable, diversifiable, fully synthetic route towards the tetracyclines, allowing them to modify the scaffold at previously inaccessible positions.[45-47] Their synthetic route has enabled the preparation of analogues with modifications at C5a[48] and C8,

among others (**25**). Additionally, an orally available tetracycline has been advanced to Phase III trials as a result of their endeavors.[49]

Synthetic organic chemistry has enabled the structural modification of a variety of antibiotics, improving their properties, and providing an indispensable tool in the fight against drug resistant bacteria. Simple structural modifications have enabled the creation of Gram-negative antibiotics from Gram-positive leads and vice versa. Modifications have enabled the creation of medicines that are active against strains of bacteria that have developed resistance to compounds of the same structural class—often due to modification of the binding interaction with the target protein or resistance-conferring protein(s) (β-lactamases or efflux pumps, for example). While semisynthetic preparations of antibiotics will continue to play an important role, total synthesis allows for the introduction of diverse, and otherwise inaccessible modifications to the scaffold, allowing scientists to probe chemical space more effectively. While it seems prudent to develop antibiotics with novel scaffolds and targets, total synthesis also enables the preparation of active compounds through structural modifications to known scaffolds, helping to stem the tide of infections arising from resistant bacterial strains.

C. Lead Discovery

There are two methods for the discovery of lead compounds, 1) phenotypic drug discovery, and 2) target-directed drug discovery. In phenotypic drug discovery, compounds are screened in live cell assays to elicit a specific phenotypic response (in the case of antibiotics, growth

inhibition or cell death) without regard for the mechanism of action. In target-directed drug discovery, leads are identified from *in vitro* assays that determine the activity of compounds against specific, isolated protein targets that have been implicated to be vital for the target organism to thrive.

Early efforts in antibiotic discovery relied on phenotypic drug discovery to discover leads for further optimization. The compounds used in phenotypic screening can be culled from diverse sources, as exemplified by early efforts in antibiotics research. As mentioned above, Salvarsan and the sulfa drugs were both discovered by screening synthetic dye derivatives, while the β-lactams and the tetracyclines are natural products isolated from microorganisms.

Nearly all current antibiotics are derived from natural products isolated between 1940 and 1960, largely discovered through phenotypic drug discovery by screening compounds derived from actinomycetes and fungi.[50-52] Several examples include the penicillins, cephalosporins, aminoglycosides, tetracyclines, erythromycin, and vancomycin.[52] More recently, antibiotic research has shifted from phenotypic drug discovery towards target-directed drug discovery. Part of the impetus for this shift was the observation that the major classes of antibiotics hit only four classical targets: 1) bacterial cell-wall biosynthesis, 2) DNA replication, 3) bacterial protein synthesis, and 4) folate coenzyme biosynthesis.[52] Novel targets were sought that would provide new tools in the fight against resistant bacteria. Another major factor in the shift towards target-directed drug discovery was the introduction of powerful genomics techniques beginning in 1995 with the determination of the complete genome sequence

of *Haemophilus influenza*.[53] This advance eventually provided the full genomes of hundreds of microbial species, allowing for the rapid identification of potential targets through genome mining.[54] Further optimism was derived from the possibility of identifying conserved targets that were present in numerous pathogens but absent in higher eukaryotes, ideally leading to the development of safe, broad-spectrum compounds. At the same time, the move towards target-directed drug discovery inspired a shift from screening natural products and towards synthetic molecules, as synthetic molecules are more amenable to high-throughput screening (HTS) techniques, allowing medicinal chemists to screen a large number of compounds in a shorter period of time.[52, 55] Furthermore, natural product screening became increasing inefficient because previously isolated compounds were continuously rediscovered.[56]

The modern antibiotic drug discovery efforts using target-directed methods and large libraries of synthetic molecules have largely failed. Published efforts from GlaxoSmithKline[57] and AstraZeneca[22] reveal the difficulties associated with target-directed drug discovery for antibiotics. These reports, along with several others, outline several possible reasons for failure. It is widely understood that a major problem is maintaining a high drug concentration within the target bacteria. Thus, even if compounds demonstrate sufficient biochemical activity, it does not translate to antimicrobial activity due to poor permeability through the cell wall/membrane and efflux.[55, 57] These problems are particularly challenging in Gram-negative bacteria, which contain multiple layers of defense. Another major difficulty lies in the composition of the libraries used in HTS efforts. These libraries are largely composed of molecules that obey

Lipinski's rule of five,[58] a set of guidelines developed for orally available drugs in areas other than infectious disease. In fact, it has been observed that known antibacterial compounds tend to disobey Lipinski's rules.[59] Furthermore, the majority of compounds in commercial libraries are aimed at interacting with G-protein coupled receptors (GPCRs), nuclear receptors, voltage-gated ion channels, and ligand-gated ion channels, with 50% of current drugs focused on these four classes.[60] In contrast, antibiotic targets for HTS campaigns have primarily been enzymes, which are not represented in the protein classes listed above.[19]

In summary, the golden age of antibacterial discovery utilized phenotypic drug discovery methods with natural products to generate an arsenal of life-saving molecules. Modern efforts have focused on target-directed drug discovery with synthetic molecules, and have encountered significant challenges that must be addressed given the increasing prevalence of bacterial resistance.

D. Outlook

The number of novel antibiotic scaffolds has dropped precipitously in recent decades—with every current antibiotic stemming from a scaffold discovered before 1984 (Table 1.1).[61] Given that resistance is certain to arise to all current antibiotics, and that resistance to one molecule within a class often leads to resistance of other molecules of the class, this lack of novel antibiotic scaffolds is concerning. Additionally, it is financially untenable for pharmaceutical companies to continue investing in antibiotic research. There are two main reasons for this: 1) treatment courses for antibiotics are short, only one or two weeks, and 2) deployment of novel antibiotics must

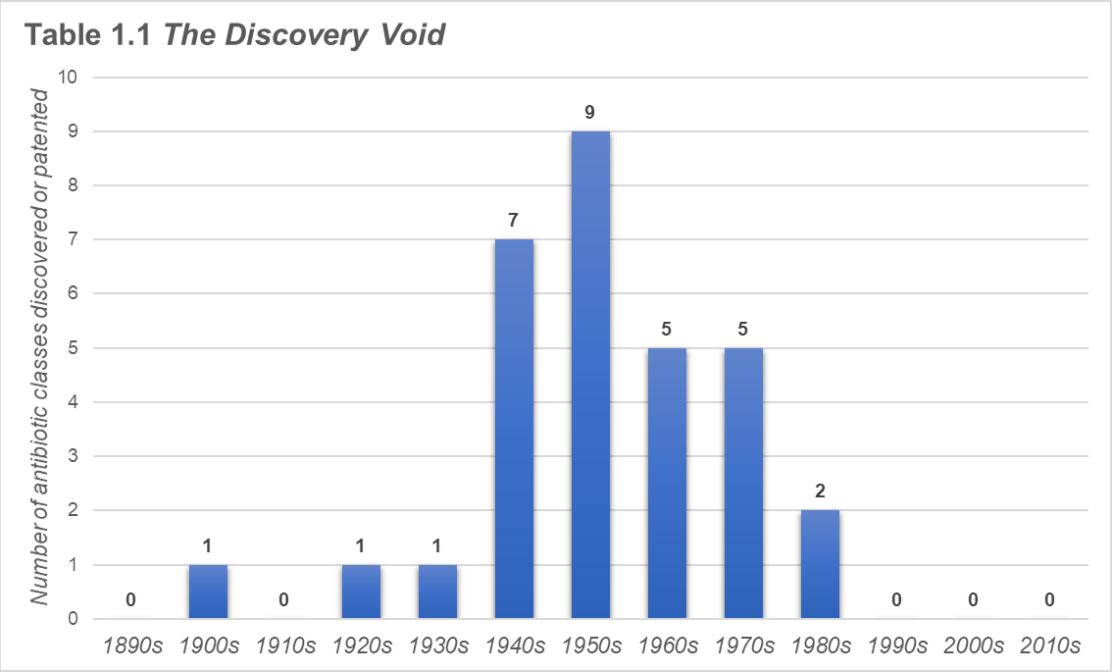

be restricted to slow the development of resistance, thereby maintaining a stable of effective antibiotics to treat life-threatening illnesses.[44] Furthermore, recent difficulties in the drug discovery process have further disincentivized antibiotic development, as it appears to be more difficult and expensive than previously imagined.[22, 57] Accordingly, there have been numerous funding proposals to overcome the challenges associated with antibiotic discovery, including increased government spending.[13, 62-63] Another discovery mechanism would be through academic labs, although this avenue would likely require longer development times.

Scientifically, there are several aspects of the antibiotic discovery process that could be improved. The composition of library compounds must be optimized for antibiotic discovery. As previously mentioned, current commercial libraries are composed of synthetic molecules designed for targets outside of infectious disease (such as GPCRs, etc). There is considerable agreement that screening libraries should be made

more ‘natural product-like’ by introducing more stereochemical features, reducing the number of aromatic rings, increasing molecular weight, and increasing polarity.[60, 64] In fact, it has been observed that 83% of the core ring scaffolds present in natural products are absent in current commercial libraries.[65] It has been proposed that because natural products are structurally akin to metabolites, they are more likely to be able to interact with transport systems, increasing the likelihood of successful drug delivery.[64-65]

Another proposal is to return to phenotypic screening methods, which are more likely to identify compounds that are capable of penetrating the cell wall/membrane than biochemical binding assays—it has been suggested that “it is easier to find the target of an antibacterial compound than it is to engineer permeability into an enzyme inhibitor”.[57] Even outside of antibiotic development there is discussion that HTS and target-directed drug discovery are detrimental to the productivity of the pharmaceutical industry.[66] Between 1999 and 2008 there were more target-directed drug discovery efforts than phenotypic drug discovery efforts, but phenotypic drug discovery accounted for 37% of first in class molecules, while target-directed accounted for 23%.[67] Another potential advantage of phenotypic drug discovery is that it facilitates the discovery of compounds that hit multiple targets because the discovery process does not select for binding to a single protein target. It has been proposed that the development of resistance may be delayed for molecules with multiple targets due to the increased requirements for resistance.[19, 55] Using the same logic, it has been proposed that a more thorough investigation of combination therapies is warranted.[55] The success of the combination

therapy Augmentin supports this hypothesis, pairing the β-lactam amoxicillin with a β-lactamase inhibitor clavulanate.

In conclusion, while there are many challenges associated with the modern antibiotic drug discovery process, there are also many possible solutions. Antibiotic resistance is well-documented, and many talented scientists are working hard to overcome the obstacles to antibiotic development.

E. Relevance to the Xiamycin & Oridamycin Family of Natural Products

The xiamycin and oridamycin family of natural products were extracted from several strains of bacteria and were discovered because of their activity in whole cell assays. In other words, they are natural products derived from a phenotypic drug discovery platform. They have novel molecular scaffolds and promising activity against several resistant strains of bacteria, including methicillin resistant *staphylococcus aureus* (MRSA) and vancomycin resistant *enterococcus* (VRE). Total synthesis of these antibacterial compounds could provide structural derivatives, allowing for the optimization of their physicochemical properties, and providing structurally modified compounds to combat resistance in the future. In light of this, a program aimed at the total synthesis of these families was undertaken.

REFERENCES

[1] Aminov, R. I., A brief history of the antibiotic era: lessons learned and challenges for the future. *Front. Microbiol.* **2010,** 1, 134.

[2] Nelson, M. L., Dinardo, A., Hochberg, J., & Armelagos, G. J., Brief communication: Mass spectroscopic characterization of tetracycline in the skeletal remains of an ancient population from Sudanese Nubia 350–550 CE. *Am. J. Phys. Anthropol.* **2010,** 143, 151–154.

[3] Armelagos, G., Take two beers and call me 1600 years. *Nat. Hist.* **2000,** 109, 50–54.

[4] Falkinham, J. O., Wall, T. E., Tanner, J. R., Tawaha, K., Alali, F. Q., Li, C., & Oberlies, N. H., Proliferation of antibiotic-producing bacteria and concomitant antibiotic production as the basis for the antibiotic activity of Jordan's red soils. *Appl. Environ. Microbiol.* **2009,** 75, 2735–2741.

[5] Bos, K. I., Schuenemann, V. J., Golding, G. B., Burbano, H. A., Waglechner, N., Coombes, B. K., McPhee, J. B., DeWitte, S. N., Meyer, M., Schmedes, S., Wood, J., Earn, D. J. D., Herring, D. A., Bauer, P., Poinar, H. N., & Krause, J., A draft genome of Yersinia pestis from victims of the Black Death. *Nature* **2011,** 478, 506–510.

[6] Lin, S., Yang, X., Jia, S., Weeks, A. M., Hornsby, M., Lee, P. S., Nichiporuk, R. V., Iavarone, A. T., Wells, J. A., Toste, F. D., & Chang, C. J., Redox-based reagents for chemoselective methionine bioconjugation. *Science* **2017,** 355, 597–602.

[7] Drews, J., Drug discovery: A historical perspective. *Science* **2000,** 287, 1960–1964.

[8] Wainwright, M., Dyes in the development of drugs and pharmaceuticals. *Dyes Pigments* **2008,** 76, 582–589.

[9] Ehrlich, P., & Hata, S., *Die experimentelle Chemotherapie der Spirillosen*. Springer Berlin Heidelberg: 1910.

[10] Strebhardt, K., & Ullrich, A., Paul Ehrlich's magic bullet concept: 100 years of progress. *Nat. Rev. Cancer* **2008,** 8, 473–480.

[11] Lloyd, N. C., Morgan, H. W., Nicholson, B. K., & Ronimus, R. S., The composition of Ehrlich's Salvarsan: Resolution of a century-old debate. *Angew. Chem. Int. Ed.* **2005,** 44, 941–944.

[12] Wainwright, M., & Kristiansen, J. E., On the 75th anniversary of Prontosil. *Dyes Pigments* **2011,** 88, 231–234.

[13] Kinch, M. S., Patridge, E., Plummer, M., & Hoyer, D., An analysis of FDA-approved drugs for infectious disease: Antibacterial agents. *Drug Discov. Today* **2014,** 19, 1283–1287.

[14] Bennett, J. W., & Chung, K. T., Alexander Fleming and the discovery of penicillin. *Adv. Appl. Microbiol.* **2001,** 49, 163–184.

[15] Chain, E., Florey, H. W., Gardner, A. D., Heatley, N. G., Jennings, M. A., Orr-Ewing, J., & Sanders, A. G., Penicillin as a chemotherapeutic agent. *Lancet* **1940,** 236, 226–228.

[16] Dias, D. A., Urban, S., & Roessner, U., A historical overview of natural products in drug discovery. *Metabolites* **2012,** 2, 303–336.

[17] Hewitt, W. L., Penicillin-historical impact on infection control. *Ann. N.Y. Acad. Sci.* **1967,** 145, 212–215.

[18] Schwartz , W. B., The effect of Sulfanilamide on salt and water excretion in congestive heart failure. *New Engl. J. Med.* **1949,** 240, 173–177.

[19] Silver, L. L., Challenges of antibacterial discovery. *Clin. Microbiol. Rev.* **2011,** 24, 71–109.

[20] Schleifer, K. H., & Kandler, O., Peptidoglycan types of bacterial cell walls and their taxonomic implications. *Bacteriol. Rev.* **1972,** 36, 407–477.

[21] Fisher, J. F., Meroueh, S. O., & Mobashery, S., Bacterial resistance to β -lactam antibiotics: Compelling opportunism, compelling opportunity. *Chem. Rev.* **2005,** 105, 395–424.

[22] Tommasi, R., Brown, D. G., Walkup, G. K., Manchester, J. I., & Miller, A. A., ESKAPEing the labyrinth of antibacterial discovery. *Nat. Rev. Drug Discov.* **2015,** 14, 529–542.

[23] Silhavy, T. J., Kahne, D., & Walker, S., The bacterial cell envelope. *Cold Spring Harb. Perspect. Biol.* **2010,** 2, a000414.

[24] Silver, L. L., A Gestalt approach to Gram-negative entry. *Bioorgan. Med. Chem.* **2016,** 24, 6379–6389.

[25] Lederberg, J., Bacterial protoplasts induced by penicillin. *P. Natl. Acad. Sci. U.S.A.* **1956,** 42, 574–577.

[26] Park, J. T., & Strominger, J. L., Mode of action of penicillin. *Science* **1957,** 125, 99–101.

[27] Tipper, D. J., & Strominger, J. L., Mechanism of action of penicillins: a proposal based on their structural similarity to acyl-D-alanyl-D-alanine. *P. Natl. Acad. Sci. U.S.A.* **1965,** 54, 1133–1141.

[28] Koch, A. L., Bacterial wall as target for attack past, present, and future research. *Clin. Microbiol. Rev.* **2003,** 16, 673–687.

[29] Waxman, D. J., Yocum, R. R., & Strominger, J. L., Penicillins and cephalosporins are active site-directed acylating agents: Evidence in support of the substrate analogue hypothesis. *Philos. T. R. Soc. B* **1980,** 289, 257–271.

[30] Drawz, S. M., & Bonomo, R. A., Three decades of β -lactamase inhibitors. *Clin. Microbiol. Rev.* **2010,** 23, 160-201.

[31] Wright, P. M., Seiple, I. B., & Myers, A. G., The evolving role of chemical synthesis in antibacterial drug discovery. *Angew. Chem. Int. Ed.* **2014,** 53, 8840–8869.

[32] Chauvette, R. R., Flynn, E. H., Jackson, B. G., Lavagnino, E. R., Morin, R. B., Mueller, R. A., Pioch, R. P., Roeske, R. W., Ryan, C. W., Spencer, J. L., & Van Heyningen, E., Chemistry of cephalosporin antibiotics. II. Preparation of a new class of antibiotics and the relation of structure to activity. *J. Am. Chem. Soc.* **1962,** 84, 3401–3402.

[33] O'Callaghan, C. H., Sykes, R., Griffiths, A., & Thornton, J., Cefuroxime, a new cephalosporin antibiotic: Activity in vitro. *Antimicrob. Agents Ch.* **1976,** 9, 511–519.

[34] O'callaghan, C., Acred, P., Harper, P., Ryan, D., Kirby, S., & Harding, S., GR 20263, A new broad-spectrum cephalosporin with anti-pseudomonal activity. *Antimicrob. Agents Ch.* **1980,** 17, 876–883.

[35] Garau, J., Wilson, W. W., Wood, M., & Carlet, J., Fourth-generation cephalosporins: A review of in vitro activity, pharmacokinetics, pharmacodynamics and clinical utility. *Clin. Microbiol. Infec.* **1997,** 3, s87–s101.

[36] Stephens, C. R., Murai, K., Rennhard, H. H., Conover, L. H., & Brunings, K. J., Hydrogenolysis studies in the tetracycline series—6-Deoxytetracyclines. *J. Am. Chem. Soc.* **1958,** *80*, 5324–5325.

[37] McCormick, J. R. D., Jensen, E. R., Miller, P. A., & Doerschuk, A. P., The 6-deoxytetracyclines. Further studies on the relationship between structure and antibacterial activity in the tetracycline series. *J. Am. Chem. Soc.* **1960,** *82*, 3381–3386.

[38] Stephens, C. R., Beereboom, J. J., Rennhard, H. H., Gordon, P. N., Murai, K., Blackwood, R. K., & von Wittenau, M. S., 6-Deoxytetracyclines. IV. Preparation, C-6 stereochemistry, and reactions. *J. Am. Chem. Soc.* **1963,** 85, 2643–2652.

[39] Martell, M. J., & Boothe, J. H., The 6-deoxytetracyclines. VII. Alkylated aminotetracyclines possessing unique antibacterial activity. *J. Med. Chem.* **1967,** 10, 44–46.

[40] Church, R. F. R., Schaub, R. E., & Weiss, M. J., Synthesis of 7-dimethylamino-6-demethyl-6-deoxytetracycline (minocycline) via 9-nitro-6-demethyl-6-deoxytetracycline. *J. Org. Chem.* **1971,** 36, 723–725.

[41] Sum, P. E., Lee, V. J., Testa, R. T., Hlavka, J. J., Ellestad, G. A., Bloom, J. D., Gluzman, Y., & Tally, F. P., Glycylcyclines. 1. A new generation of potent antibacterial agents through modification of 9-aminotetracyclines. *J. Med. Chem.* **1994,** 37, 184–188.

[42] Sum, P.-E., & Petersen, P., Synthesis and structure-activity relationship of novel glycylcycline derivatives leading to the discovery of GAR-936. *Bioorg. Med. Chem. Lett.* **1999,** 9, 1459–1462.

[43] Bergeron, J., Ammirati, M., Danley, D., James, L., Norcia, M., Retsema, J., Strick, C. A., Su, W.-G., Sutcliffe, J., & Wondrack, L., Glycylcyclines bind to the high-affinity tetracycline ribosomal binding site and evade Tet(M)-and Tet(O)-mediated ribosomal protection. *Antimicrob. Agents Ch.* **1996,** 40, 2226–2228.

[44] Fischbach, M. A., & Walsh, C. T., Antibiotics for emerging pathogens. *Science* **2009,** 325, 1089–1093.

[45] Charest, M. G., Lerner, C. D., Brubaker, J. D., Siegel, D. R., & Myers, A. G., A convergent enantioselective route to structurally diverse 6-deoxytetracycline antibiotics. *Science* **2005,** 308, 395–398.

[46] Kummer, D. A., Li, D., Dion, A., & Myers, A. G., A practical, convergent route to the key precursor to the tetracycline antibiotics. *Chem. Sci.* **2011,** 2, 1710–1718.

[47] Brubaker, J. D., & Myers, A. G., A practical, enantioselective synthetic route to a key precursor to the tetracycline antibiotics. *Org. Lett.* **2007,** 9, 3523–3525.

[48] Wright, P. M., & Myers, A. G., Methodological advances permit the stereocontrolled construction of diverse fully synthetic tetracyclines containing an all-carbon quaternary center at position C5a. *Tetrahedron* **2011,** 67, 9853–9869.

[49] Sun, C., Wang, Q., Brubaker, J. D., Wright, P. M., Lerner, C. D., Noson, K., Charest, M., Siegel, D. R., Wang, Y.-M., & Myers, A. G., A robust platform for the synthesis of new tetracycline antibiotics. *J. Am. Chem. Soc.* **2008,** 130, 17913–17927.

[50] Peláez, F., The historical delivery of antibiotics from microbial natural products—Can history repeat? *Biochem. Pharmacol.* **2006,** 71, 981-990.

[51] Lewis, K., Platforms for antibiotic discovery. *Nat. Rev. Drug Discov.* **2013,** 12, 371–387.

[52] Walsh, C., Where will new antibiotics come from? *Nat. Rev. Microbiol.* **2003,** 1, 65–70.

[53] Fleischmann, R. D., Adams, M. D., White, O., Clayton, R. A., Kirkness, E. F., Kerlavage, A. R., Bult, C. J., Tomb, J. F., Dougherty, B. A., Merrick, J. M., & et al., Whole-genome random sequencing and assembly of *Haemophilus influenzae* Rd. *Science* **1995,** 269, 496–512.

[54] McDevitt, D., & Rosenberg, M., Exploiting genomics to discover new antibiotics. *Trends Microbiol.* **2001,** 9, 611–617.

[55] Monaghan, R. L., & Barrett, J. F., Antibacterial drug discovery—Then, now and the genomics future. *Biochem. Pharmacol.* **2006,** *71*, 901–909.

[56] Baltz, R. H., Marcel Faber Roundtable: Is our antibiotic pipeline unproductive because of starvation, constipation or lack of inspiration? *J. Ind. Microbiol. Biot.* **2006,** 33, 507–513.

[57] Payne, D. J., Gwynn, M. N., Holmes, D. J., & Pompliano, D. L., Drugs for bad bugs: Confronting the challenges of antibacterial discovery. *Nat. Rev. Drug Discov.* **2007,** 6, 29–40.

[58] Lipinski, C. A., Drug-like properties and the causes of poor solubility and poor permeability. *J. Pharmacol. Tox. Met.* **2000,** 44, 235–249.

[59] O'Shea, R., & Moser, H. E., Physicochemical properties of antibacterial compounds: Implications for drug discovery. *J. Med. Chem.* **2008,** 51, 2871–2878.

[60] Bauer, R. A., Wurst, J. M., & Tan, D. S., Expanding the range of 'druggable' targets with natural product-based libraries: An academic perspective. *Curr. Opin. Chem. Biol.* **2010,** 14, 308–314.

[61] The PEW Charitable Trusts, *A scientific roadmap for antibiotic discovery*. http://www.pewtrusts.org/antibiotic-discovery, May 11 2016, (accessed May 16 2017).

[62] Cooper, M. A., & Shlaes, D., Fix the antibiotics pipeline. *Nature* **2011,** *472*, 32–32.

[63] Shore, C. K., & Coukell, A., Roadmap for antibiotic discovery. *Nat. Microbiol.* **2016,** 1, 16083.

[64] Harvey, A. L., Edrada-Ebel, R., & Quinn, R. J., The re-emergence of natural products for drug discovery in the genomics era. *Nat. Rev. Drug Discov.* **2015,** 14, 111–129.

[65] Hert, J., Irwin, J. J., Laggner, C., Keiser, M. J., & Shoichet, B. K., Quantifying biogenic bias in screening libraries. *Nat. Chem. Biol.* **2009,** 5, 479–483.

[66] Macarron, R., Banks, M. N., Bojanic, D., Burns, D. J., Cirovic, D. A., Garyantes, T., Green, D. V. S., Hertzberg, R. P., Janzen, W. P., Paslay, J. W., Schopfer, U., & Sittampalam, G. S., Impact of high-throughput

screening in biomedical research. *Nat. Rev. Drug Discov.* **2011,** *10*, 188–195.

[67] Lee, J. A., Uhlik, M. T., Moxham, C. M., Tomandl, D., & Sall, D. J., Modern phenotypic drug discovery is a viable, neoclassic pharma strategy. *J. Med. Chem.* **2012,** 55, 4527–4538.

Chapter 2. Introduction to the Xiamycin and Oridamycin Families of Indolosesquiterpenes

Preface

This chapter introduces the xiamycin and oridamycin families of indolosesquiterpenes, starting with their isolation and biosynthesis and moving through previous work on related natural product scaffolds and on the family, itself. Finally, a retrosynthesis is outlined that provides a strategy to access four monomeric family members.

A. Isolation & Biosynthesis

The first xiamycin family members to be isolated were oridamycin A (**26**) and oridamycin B (**27**) in 2010 (Figure 2.1).[1] These pentacyclic compounds were derived from a soil-dwelling actinomycete, *Streptomyces* sp. strain KS84. Interestingly, they were the first indolosesquiterpenes derived from prokaryotes, as all previous indolosesquiterpenes were isolated from plants or fungi. The oridamycins were discovered based on their activity against *Saprolegnia parasitica*, a common protozoan that infects freshwater fishes, particularly those contained in commercial aquacultures.

Several months later, xiamycin A (**28**) was isolated along with its methyl ester (**29**) from *Streptomyces* sp. GT20021503, an endophyte derived from the stem of a mangrove tree (*Bruguiera gymnorrhiza*).[2] The related family members xiamycin B (**32**), indosespene (**30**), and sespenine (**33**) were disclosed soon after, isolated from *Streptomyces* sp. HKI0595, an endophyte

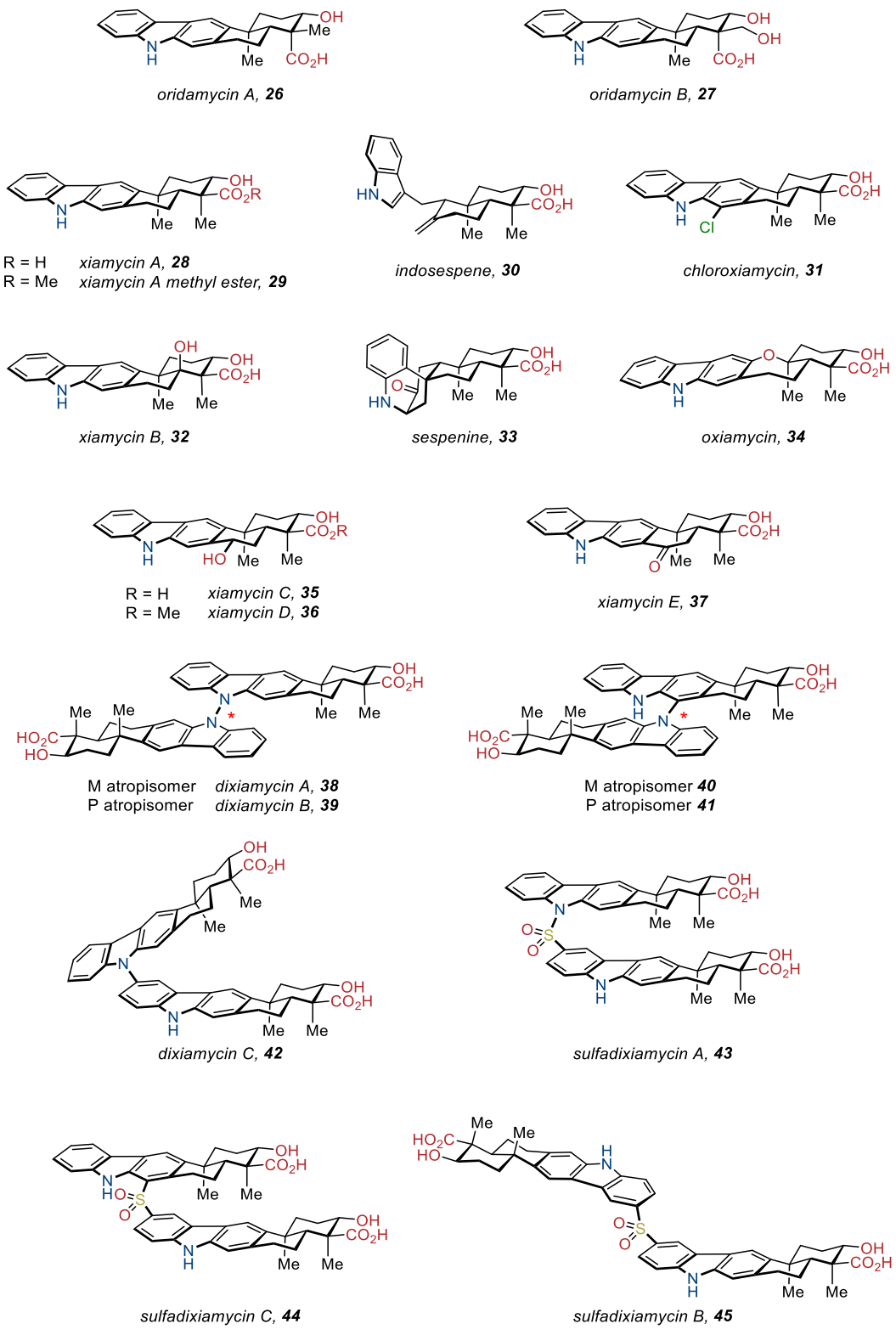

Figure 2.1 The xiamycin family of indolosesquiterpenes.

Table 2.1 Antibacterial activity of the xiamycin family.

Compound	*pseudomonas aeruginosa*	*staphylococcus aureus*	*bacillus subtilis*	*mycobacterium vaccae*	*escherichia coli*	*bacillus thuringiensis*	MRSA	VRE
xiamycin A (**28**)	Moderate	MIC: 50 μg/mL	Moderate	MIC: 50 μg/mL	MIC: 64 μg/mL	MIC: >128 μg/mL	Moderate	Moderate
indosespene (**30**)	None	Moderate	Moderate	Moderate	N/A	N/A	Moderate	Moderate
sespenine (**33**)	None	None	Moderate	Moderate	N/A	N/A	None	None
oxiamycin (**34**)	N/A	MIC: 128 μg/mL	MIC: >128 μg/mL	N/A	MIC: 64 μg/mL	MIC: >128 μg/mL	N/A	N/A
chloroxiamycin (**31**)	N/A	MIC: 64 μg/mL	MIC: >128 μg/mL	N/A	MIC: 64 μg/mL	MIC: 64 μg/mL	N/A	N/A
dixiamycin A (**38**)	N/A	MIC: 0.4 μg/mL	MIC: 12.5 μg/mL	MIC: 25 μg/mL	MIC: 8 μg/mL	MIC: 4 μg/mL	MIC: 0.2 μg/mL	MIC: 3.12 μg/mL
dixiamycin B (**39**)	N/A	MIC: 1.56 μg/mL	MIC: 3.12 μg/mL	MIC: 25 μg/mL	MIC: 8 μg/mL	MIC: 8 μg/mL	MIC: 3.12 μg/mL	MIC: 3.12 μg/mL
dixiamycin C (**42**)	N/A	MIC: 1.56 μg/mL	MIC: 3.12 μg/mL	MIC: 12.5 μg/mL	N/A	N/A	MIC: 1.56 μg/mL	MIC: 12.5 μg/mL
dixiamycin D' (**40**)	N/A	MIC: 25 μg/mL	MIC: 50 μg/mL	MIC: 25 μg/mL	N/A	N/A	MIC: 50 μg/mL	MIC: 50 μg/mL
dixiamycin E' (**41**)	N/A	MIC: 12.5 μg/mL	MIC: 25 μg/mL	MIC: 25 μg/mL	N/A	N/A	MIC: 25 μg/mL	MIC: 50 μg/mL
sulfadixiamycin A (**43**)	N/A	MIC: 3.12 μg/mL	MIC: 6.25 μg/mL	MIC: 25 μg/mL	N/A	N/A	MIC: 6.25 μg/mL	MIC: 50 μg/mL
sulfadixiamycin B (**45**)	N/A	MIC: 100 μg/mL	MIC: >100 μg/mL	MIC: 25 μg/mL	N/A	N/A	MIC: 100 μg/mL	MIC: >100 μg/mL

stemming from another mangrove tree (*Kandelia candel*).[3] During heterologous expression of the *xia* gene cluster in *Streptomyces albus*, the dimeric compounds dixiamycin A (**38**), dixiamycin B (**39**), **40** and **41** were discovered, further extending the family.[4] Another research team was able to isolate dixiamycin A (**38**) and dixiamycin B (**39**) from the marine-derived actinomycete SCSIO 02999, along with two new family members, oxiamycin (**34**) and chloroxiamycin (**31**).[5] Dixiamycin C (**42**) was soon discovered,[6] followed by three sulfone-bridged dimers, dixiamycins A-C (**43**-**45**)—also discovered through heterologous expression.[7] The final family members to be reported were xiamcycins C-E (**35**-**37**), which were isolated from a topsoil-dwelling acinomycetes, *Streptomyces* sp. HK18.[8]

The xiamycin family members have antibacterial and antiviral biological activity (Tables 2.1, 2.2, and 2.3). In general, the antibiotic activity is more consequential than the antiviral activity. Interestingly, these compounds show minimal cytotoxicity towards mammalian cells, implying that they are not DNA intercalators in eukaryotes, and revealing their potential as antibiotic lead compounds.[9] The monomers are generally less active than the dimers, and the sulfone linked dimers are less active than the N-N or C-N linked dimers. Interestingly, in both pairs of atropisomeric dimers, the *M* dimer (**38** and **40**) is slightly more active than the *P* dimer (**39** and **41**). The compounds also show activity against methicillin-resistant

Table 2.2 Biological activity of the oridamycins.

Compound	*saprolegnia parasitica* (protozoan)	*phoma* sp. CCF3818 (fungus)	*saccharomyces cerevisiae* (yeast)
oridamycin A (**26**)	MIC: 3.0 µg/mL	MIC: 242 µg/mL	MIC: >1000 µg/mL
oridamycin B (**27**)	MIC: >300 µg/mL	N/A	N/A

Table 2.3 Cytotoxic and antiviral activity of the xiamycin family.

Compound	*Cytotoxicity (human tumor)*	*Cytotoxicity (monkey)*	HIV-1	PEDV	HSV-1	HCV
xiamycin A (**28**)	IC_{50}: >30 μg/mL	IC_{50}: 138.12 μg/mL	Moderate (CXCR4)	IC_{50}: 20.14 μg/mL	Good	None
xiamycin A methyl ester (**29**)	IC_{50}: ~10 μg/mL	IC_{50}: 103.15 μg/mL	None	IC_{50}: 5.69 μg/mL	N/A	N/A
xiamycin C (**35**)	N/A	IC_{50}: 76.9 μg/mL	N/A	IC_{50}: 11.49 μg/mL	N/A	N/A
xiamycin D (**36**)	N/A	IC_{50}: 56.03 μg/mL	N/A	IC_{50}: 0.93 μg/mL	N/A	N/A
xiamycin E (**37**)	N/A	IC_{50}: 98.74 μg/mL	N/A	IC_{50}: 2.89 μg/mL	N/A	N/A
chloroxiamycin (**31**)	N/A	IC_{50}: 162.08 μg/mL	N/A	IC_{50}: 12.76 μg/mL	N/A	N/A
sespenine (**33**)	None	None	N/A	N/A	Moderate	None
indosespene (**30**)	None	None	N/A	N/A	Moderate	None
oridamycin A (**26**)	None	None	N/A	N/A	None	None
dixiamycin C (**42**)	None	None	N/A	N/A	Moderate	Moderate

Staphylococcus aureus (MRSA) and vancomycin-resistant *Enterococcus* (VRE), implying that they have a different mechanism of action than previous medicines, or that their novel scaffold avoids resistance mechanisms developed against previous classes of antibiotics.

The biosynthesis of these compounds has been independently studied by two groups, each of which has used different designations for the relevant enzymes and genes. The proteins will be labeled according to the designations put forth by the Zhang group[10-13], as opposed to those used by the Hertweck group.[3-4, 6-7] Using the non-mevalonate pathway, the xiamycin-producing bacteria generate farnesyl pyrophosphate (**46**), which is then coupled with indole to generate **47** (Scheme 2.1.a). A selective epoxidation ensues, catalyzed by the oxidoreductase *Xia*O, generating

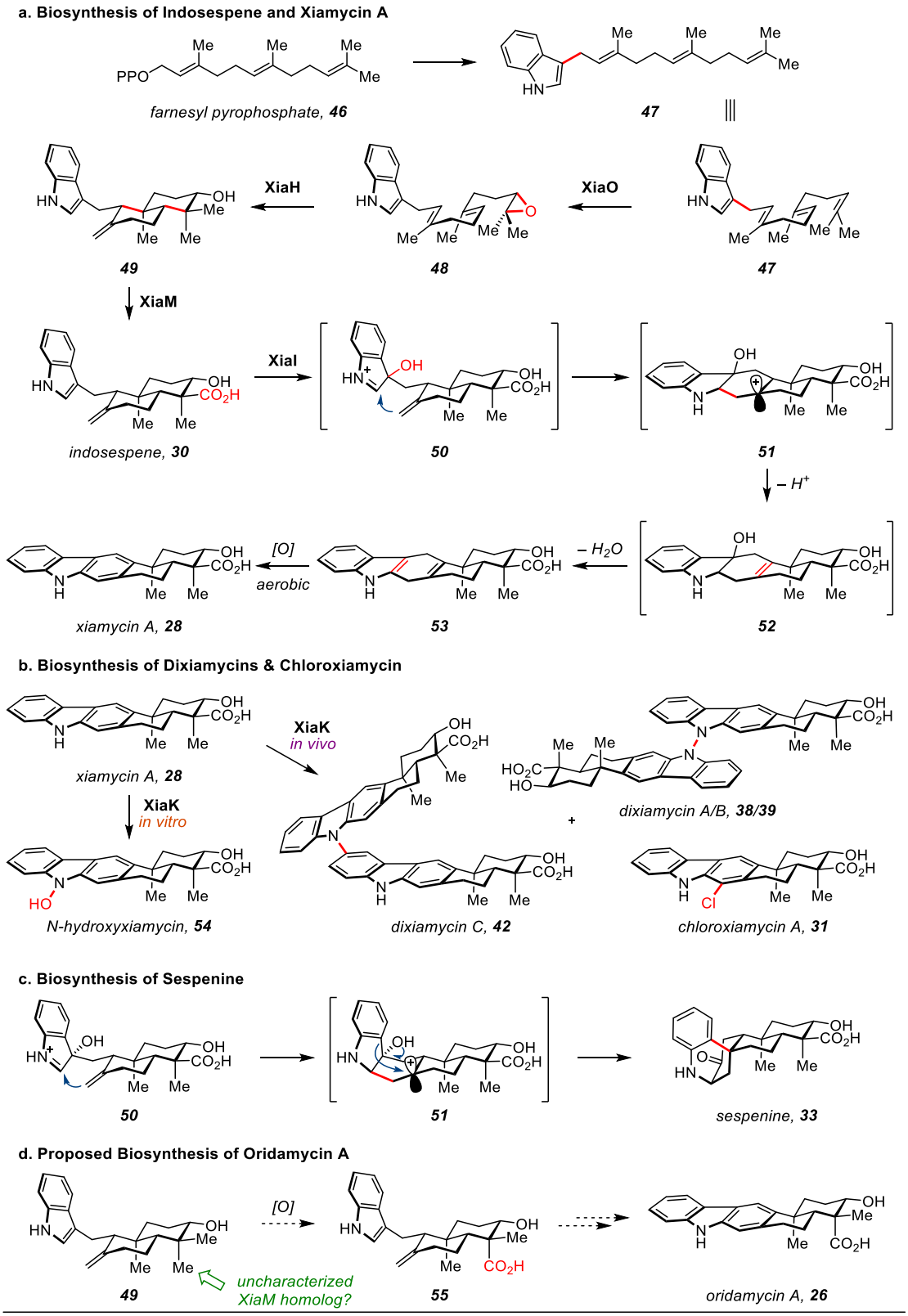

Scheme 2.1 Biosynthesis of the xiamycin family.

cyclization precursor **48**. The membrane protein *XiaH* catalyzes the terpene cyclization to form the *trans*-decalin ring system found in **49**. XiaM—a P450 enzyme—selectively oxidizes the equatorial methyl substituent to generate indosespene (**30**). Next, the indole oxygenase *XiaI* generates **50**, which undergoes cyclization, followed by elimination and dehydration to produce diene **53**. This compound spontaneously aromatizes to form xiamycin A (**28**).

The dixiamycins are generated from xiamycin A through an oxidation catalyzed by the flavoenzyme monooxygenase *XiaK* (Scheme 2.1.b).[13] Chloroxiamycin (**31**) is also generated, which is noteworthy given that no halogenase enzymes are encoded within the *Xia* gene cluster. When the reaction between *XiaK* and xiamycin A (**28**) is conducted *in vitro*, the dimers are not formed, but N-hydroxyxiamycin (**54**) can be isolated. It seems plausible that N-hydroxyxiamycin (**54**) is a precursor to the dimers, possibly through the intermediacy of a nitrogen-centered radical species (for further corroboration of this proposed intermediate see the Baran synthesis of dixiamycin B below[14]).

Sespenine (**33**) is formed in a similar manner to xiamycin A (Scheme 2.1.c). The same cationic intermediate **51** is formed, but instead of undergoing a base-promoted elimination to produce **52**, sespenine (**33**) is generated from an oxindole rearrangement. This pathway was hypothesized based on a related, unexpected rearrangement observed during the synthesis of hinckdentine A.[15] These observations led to a biosynthetic proposal for the formation of aspernomine from anominine, which was corroborated by quantum chemical calculations.[16] Further support for this rearrangement comes from the biomimetic synthesis of sespenine by the Li group, *vide infra* (Scheme 2.8.b).[17]

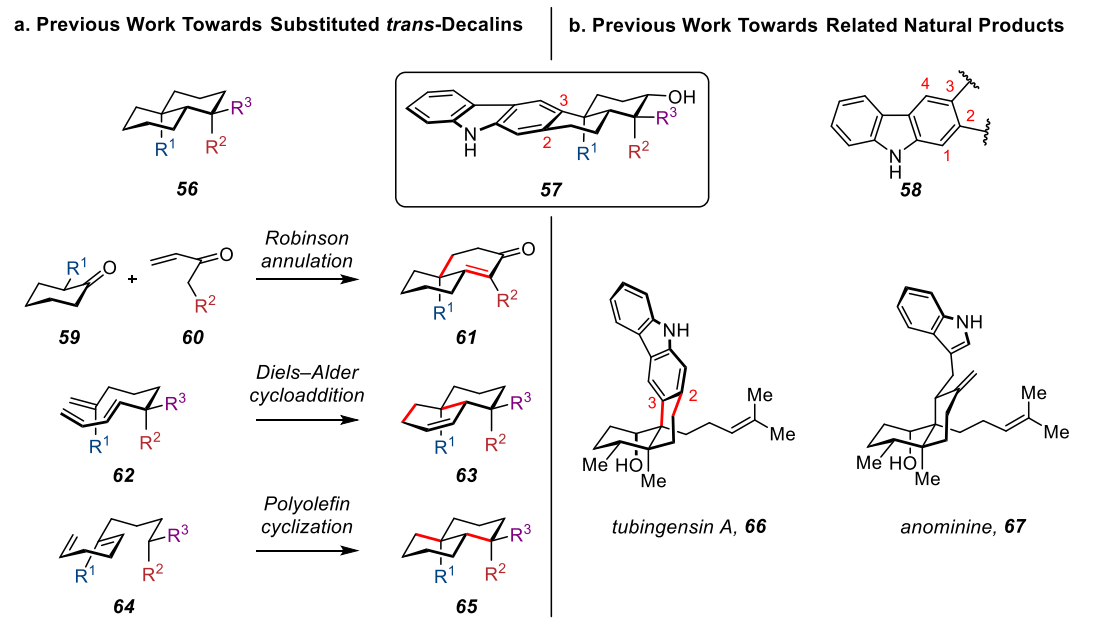

Scheme 2.2.a Synthetic approaches towards *trans*-decalin ring systems and **b** related natural products, one of which harbors a fused carbazole nucleus (tubingensin A, **66**).

While the biosynthetic pathway for xiamycin A (**28**) and related compounds has been thoroughly studied, no effort towards understanding the biogenesis of the oridamycins (**26** & **27**) has been undertaken. It seems possible that the oridamycins arise in an analogous manner to xiamycin A, except with a *XiaM* homolog that oxidizes the axial methyl instead of the equatorial methyl of intermediate **49** (Scheme 2.1.d).

B. Synthetic Challenges & Relevant Precedents

The major synthetic challenges of the xiamycin and oridamycin frameworks (**57**) can be split into two categories: 1) the substituted *trans*-decalin ring system (**56**, Scheme 2.2.a), and 2) the 2,3-fused carbazole (**58**, Scheme 2.2.b). The *trans*-decalin system is a common structural motif found in terpenoid natural products, resulting in the development of myriad

methods for its construction. The current discussion will be limited to the synthesis of substituted *trans*-decalins of type **56**, in which $R^1 \neq H$, $R^2 \neq H$, and $R^3 \neq H$. Examples of fused carbazoles are relatively sparse, and the present discussion will be focused on previous synthetic efforts towards tubingensin A (**66**), and the related family member anominine (**67**).

Three of the most common methods to synthesize the *trans*-decalin ring system are: 1) the Robinson annulation, requiring a subsequent enone reduction, 2) the Diels–Alder cycloaddition, either intramolecularly or through epimerization of a *cis*-decalin, and 3) polyolefin cyclizations, either cationic or radical (Scheme 2.2.a). [NOTE: *for the sake of clarity, all compounds are drawn in the same orientation with respect to the trans-decalin ring system, in certain instances the unnatural enantiomer is depicted.*]

Originally reported in 1935, the Robinson annulation was developed to construct the carbocyclic core of steroids.[18] Nucleophilic attack of the enolate derived from a cyclohexanone (**59**) onto an activated olefin (**60**) generates the first bond, and intramolecular aldol condensation and dehydration completes the annulation (Scheme 2.2.a). The resultant enone (**61**) must be stereoselectively reduced to yield the desired *trans*-decalin framework. The Wieland–Miescher ketone (**70**) is the product of a Robinson annulation between 2-methyl-1,3-cyclohexanedione (**68**) and methyl vinyl ketone (**69**) (Scheme 2.3.a), and it has found widespread use in the synthesis of dozens of natural products.[19] The proline-catalyzed asymmetric synthesis of the Wieland–Miescher ketone significantly improved access to useful chiral building blocks, and was one of the first examples of organocatalysis (Scheme 2.3.a).[20-21] In studies towards clerocidin (**73**), Markó

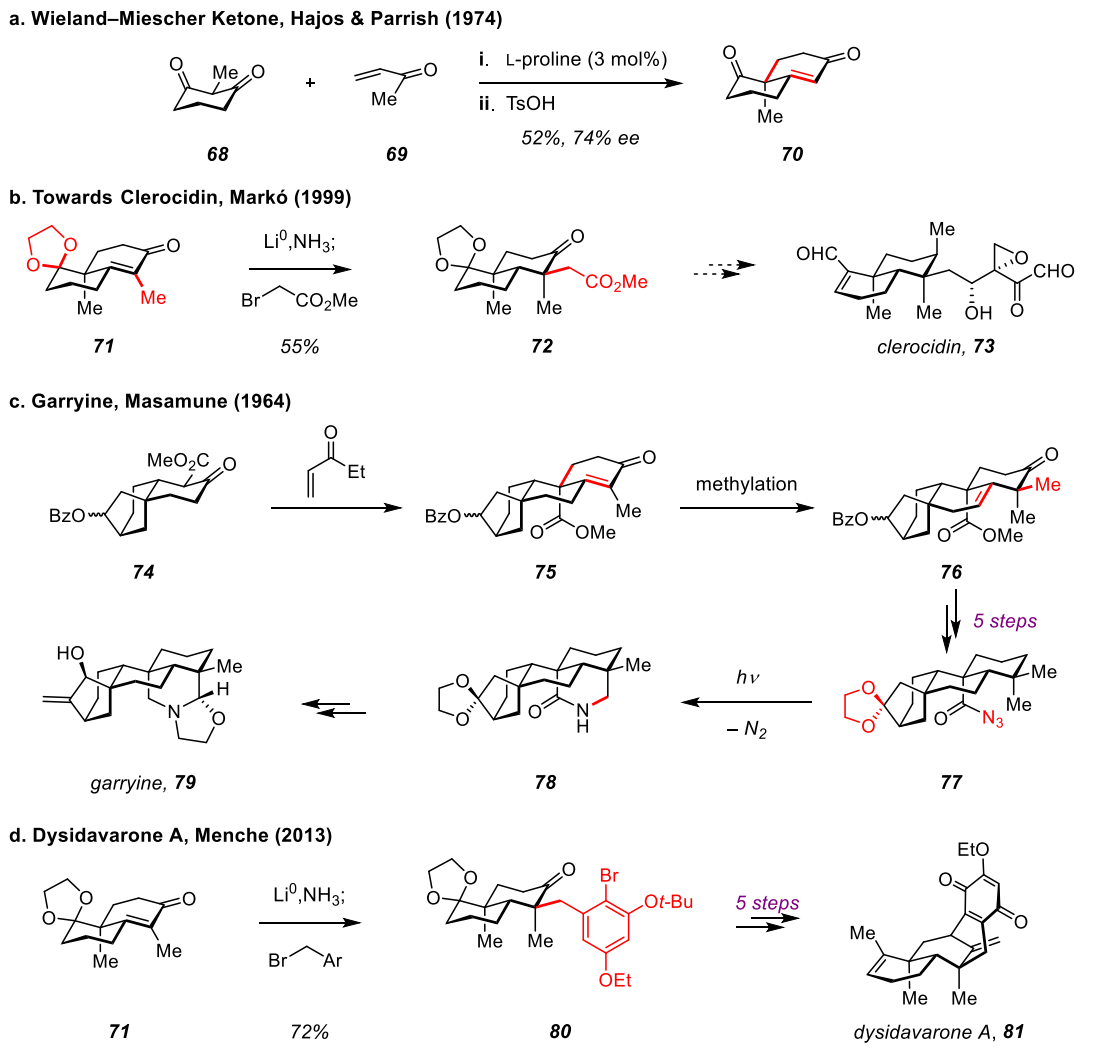

Scheme 2.3 Synthetic routes utilizing the Robinson annulation to construct *trans*-decalin ring systems.

and coworkers used the Wieland–Miescher ketone to access their key intermediate **71** (Scheme 2.3.b).[22] They generated the *trans*-decalin system through a dissolving-metal reduction of the enone, trapping the resultant enolate with methyl bromoacetate to form **72**. A single diastereomer was isolated, corresponding to an equatorial alkylation, producing a *syn*-pentane interaction between the two axial methyl substituents. The completion of clerocidin (**73**) using this strategy was never reported.

A Robinson annulation was also used in Masamune's route towards garryine (**79**) in 1964 (Scheme 2.3.c).[23-24] When tricycle **74** was condensed with ethyl vinyl ketone, key intermediate **75** was obtained. The *trans*-ring junction was established through a deconjugative alkylation producing **76**, with subsequent reduction occurring at the less hindered convex face to provide the desired stereochemistry. The requisite fused piperidine was forged when acyl azide **77** was irradiated with ultraviolet light, releasing N_2 and generating a nitrene intermediate, which inserted into the proximal methyl to generate **78**. Further elaboration ultimately produced garryine (**79**).

More recently, Menche *et al.* utilized a Wieland–Miescher-type ketone (**71**) in their synthesis of dysidavarone A (**81**, Scheme 2.3.d).[25] Using the same reduction/alkylation strategy as Markó, they were able to convert **71** to **80** through alkylation with a functionalized benzylic bromide. They observed the same stereoselectivity as Markó, generating the axial methyl through an equatorial alkylation. The bicyclic framework of the natural product was constructed through a Pd^{II}-catalyzed cross coupling between the aryl bromide and the ketone enolate, ultimately producing dysidavarone A (**81**).

The Diels–Alder cycloaddition has also found considerable use in the preparation of substituted *trans*-decalins.[26] The most direct method for obtaining *trans*-decalins using the Diels–Alder reaction is through an intramolecular Diels–Alder reaction (IMDA). One example comes from the synthesis of forskolin (**84**) by Ikegami and coworkers (Scheme 2.4.a).[27] Using catalytic thiophenol to equilibrate the diene, they were able to promote a thermal IMDA to generate **83** from **82**. The observed *exo* product is

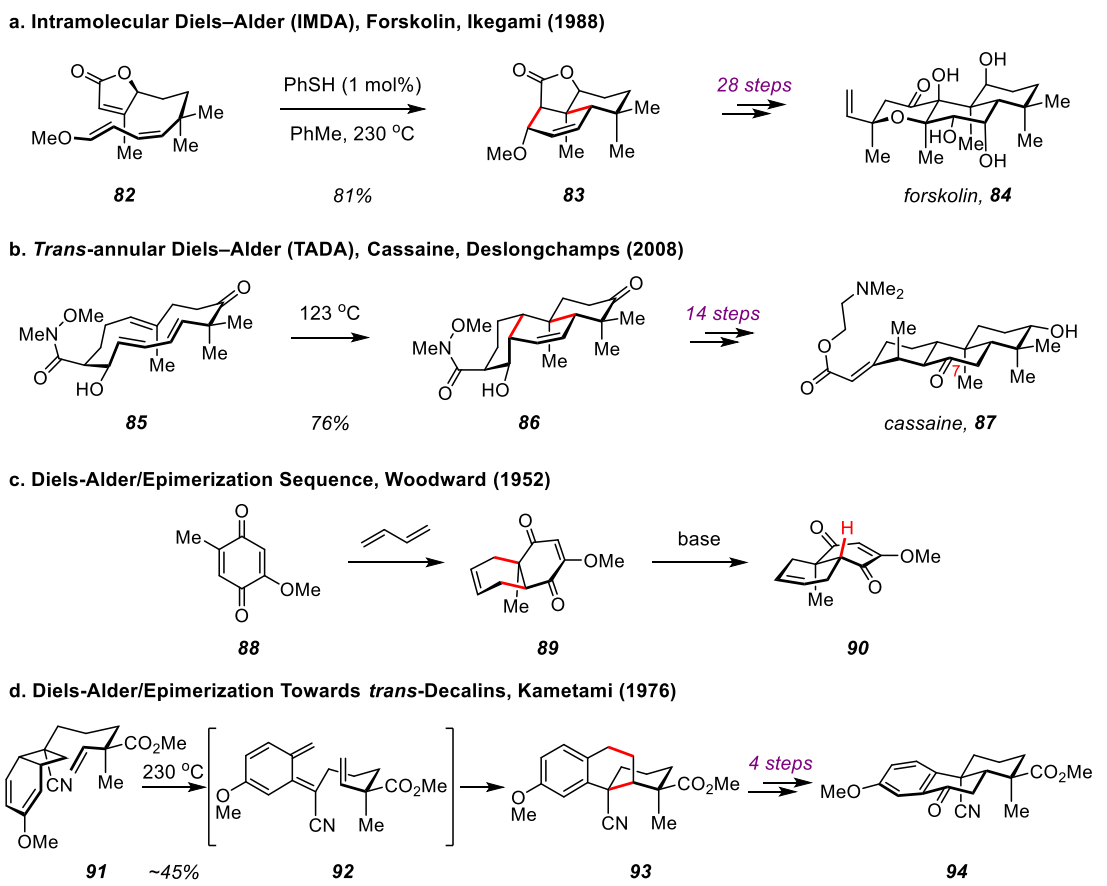

Scheme 2.4 Synthetic routes utilizing the Diels–Alder cycloaddition to construct *trans*-decalin ring systems.

hypothesized to arise because an asynchronous transition state is operant. The vinylogous enol ether adds to the electrophilic enoate first, so that steric interactions play a more important role than electronics. The resulting tricyclic product (**83**) was ultimately elaborated to the target natural product (**84**) in 28 steps.

Another version of the IMDA is the transannular Diels–Alder, a cycloaddition creating multiple smaller rings from a macrocyclic precursor. This strategy was used to generate a *trans*-decalin intermediate **86** en route to cassaine (**87**, Scheme 2.4.b).[28] In this case, the cycloaddition produced

both *cis*- and *trans*-fused ring junctions in product **86**. The *cis*-junction was epimerized after introduction of the C7 ketone to generate the requisite *trans*-junction found in cassaine. The Diels–Alder/epimerization strategy was first disclosed by Woodward during his studies on steroids in 1952 (Scheme 2.4.c).[29] He demonstrated that the bicyclic product (**89**) resulting from cycloaddition of butadiene and substituted quinone **88** could be equilibrated to the thermodynamically favored *trans*-isomer when treated with base. This strategy was subsequently used by Kametani to rapidly construct intermediate **94**, which could be elaborated to atisine, veatchine, garryine, and gibberellin A_{15} (Scheme 2.4.d).[30] The IMDA was initiated via thermolysis of the benzocyclobutane **91** to generate *ortho*-quinodimethane **92**, which produced the desired tricyclic compound **93**. Epimerization was realized through oxidation to the benzylic ketone, conversion to the α-bromoketone, dehydrobromination to form the enone, and catalytic hydrogenation.

The biomimetic strategy for the construction of *trans*-decalins is through a polyolefin cyclization. The two major mechanistic pathways for these types of cyclizations are cationic and radical. Early work by Johnson validated the Stork–Eschenmoser hypothesis, using acid to generate the symmetric bis-allylic cation from **95**, initiating the cascade to form tricyclic compound **96** (Scheme 2.5.a).[31] The subsequent addition of lithium aluminum hydride reduced the resulting trifluoroacetate esters to yield the desired alcohols. This strategy was employed by Corey in his synthesis of neotripterifordin (**99**, Scheme 2.5.b).[32] The cyclization was initiated through Lewis acid promoted epoxide-opening of linear compound **97**, generating tricycle **98** which was elaborated to the natural product.

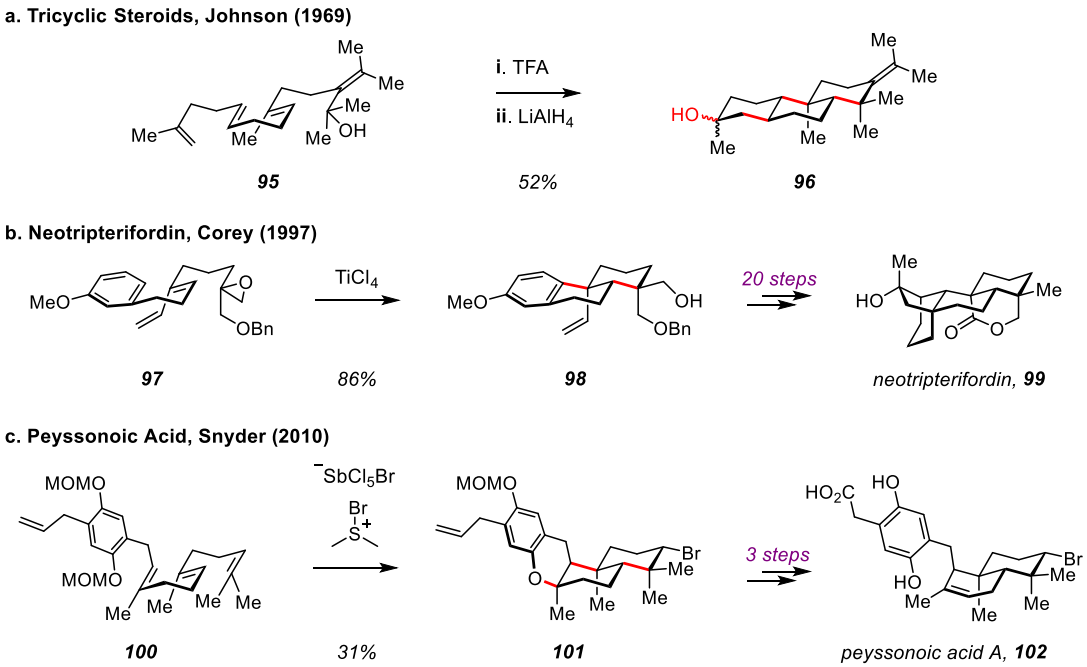

Scheme 2.5 Synthetic routes utilizing polyolefin cyclizations to construct *trans*-decalin ring systems.

Another method to initiate cationic polyolefin cyclizations involves the formation of a halonium cation. One example comes from Snyder and coworkers, who developed a method employing bromodiethylsulfonium bromopentachloroantimonate (BDSB), an electrophilic bromine source that reacts preferentially with olefins (Scheme 2.5.c).[33] They were able to construct a variety of natural products using this methodology, including peyssonoic acid A (**102**). Interestingly, they were able to construct both *cis*- and *trans*-decalins depending on the olefin geometry of the starting polyolefin. Furthermore, they successfully extended this technology to iodonium and chloronium analogues.

Radical-based methods for polyolefin cyclizations have also been employed, with one of the earliest examples coming from Breslow in 1968.[34] *Trans*,*trans*-farnesyl acetate (**103**) was cyclized to produce substituted

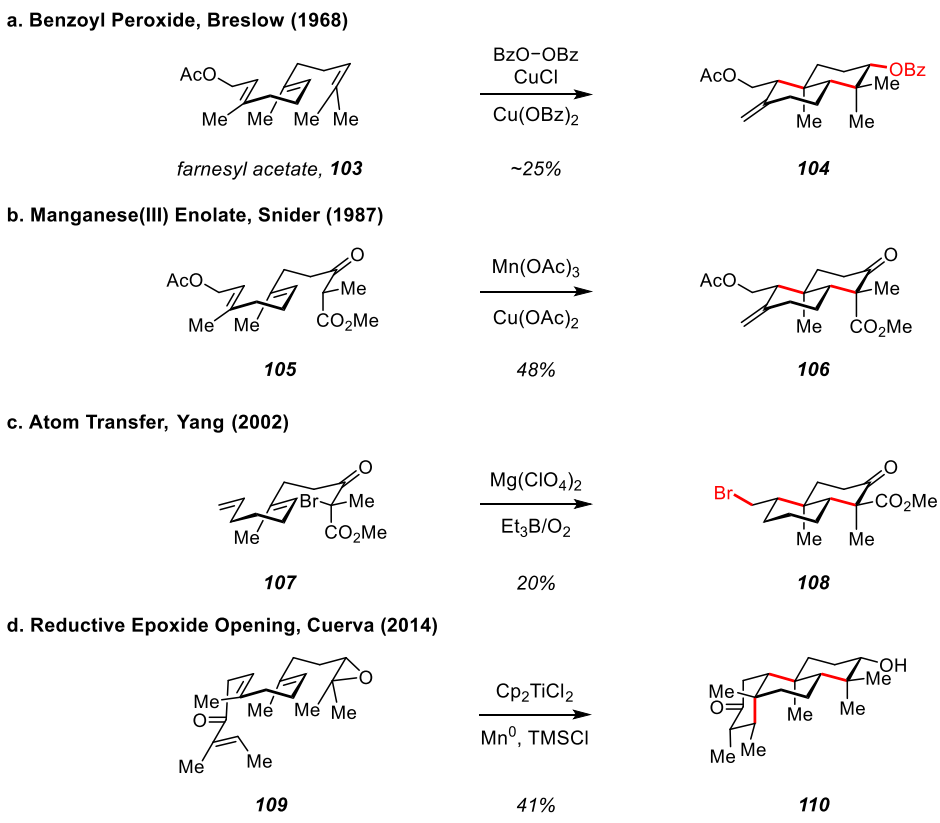

Scheme 2.6 Synthetic routes utilizing radical cyclizations to construct *trans*-decalin ring systems.

trans-decalin **104** (Scheme 2.6.a). CuCl aided in the thermal decomposition of benzoyl peroxide to form the desired benzoyl radical, and $Cu(OBz)_2$ served to terminate the cyclization through oxidation of the resultant radical. The cyclization could also be initiated through photosensitization of fluorescein to generate the desired benzoyl radical.

Radical cyclizations can also be initiated using Mn^{III} salts with enolizable carbonyl compounds, especially 1,3-dicarbonyls (Scheme 2.6.b).[35-36] The carbonyl compound exists in an equilibrium between the neutral carbonyl and the Mn^{III} enolate. Upon formation of the enolate, the oxygen-Mn^{III} bond homolytically cleaves to generate the desired α-carbonyl radical and a Mn^{II} species. Snider and coworkers demonstrated the utility of

this technology by synthesizing *trans*-decalin **106** from *β*-keto ester **105**. The axial ester stereochemistry is hypothesized to arise in order to minimize steric interactions between the axial substituents in the transition state, as methyl esters have smaller A-values (~1.25) than methyl substituents (1.74).

Atom-transfer cyclizations have also been used to construct substituted *trans*-decalins (Scheme 2.6.c). One relevant example comes from Yang and coworkers, who were able to generate bicycle **108** using Et_3B/O_2 as the radical initiator.[37] The Lewis acid chelated the carbonyl substituents to form the *trans*-decalin containing two axially disposed methyl substituents. The yield is low due to the formation of monocyclic products arising from premature termination of the cyclization. Presumably, the second cyclization is slow due to the congested transition state arising from the *syn*-pentane interaction of the two axial methyl substituents.

Epoxides can also serve as starting materials for radical cyclizations. *In situ* generated Ti^{III} salts can reductively homolyze epoxides to form the Ti^{IV} alkoxide and an alkyl radical. Cuerva and coworkers used this method to construct complex polycycles, avoiding premature termination through the strategic introduction of carbonyls along the linear precursors. One example is depicted in Scheme 2.6.d, in which a *cis*-decalin fused to the expected *trans*-decalin is formed (**110**) due to the modified conformational restraints stemming from the unsaturation introduced by the carbonyl substituent.

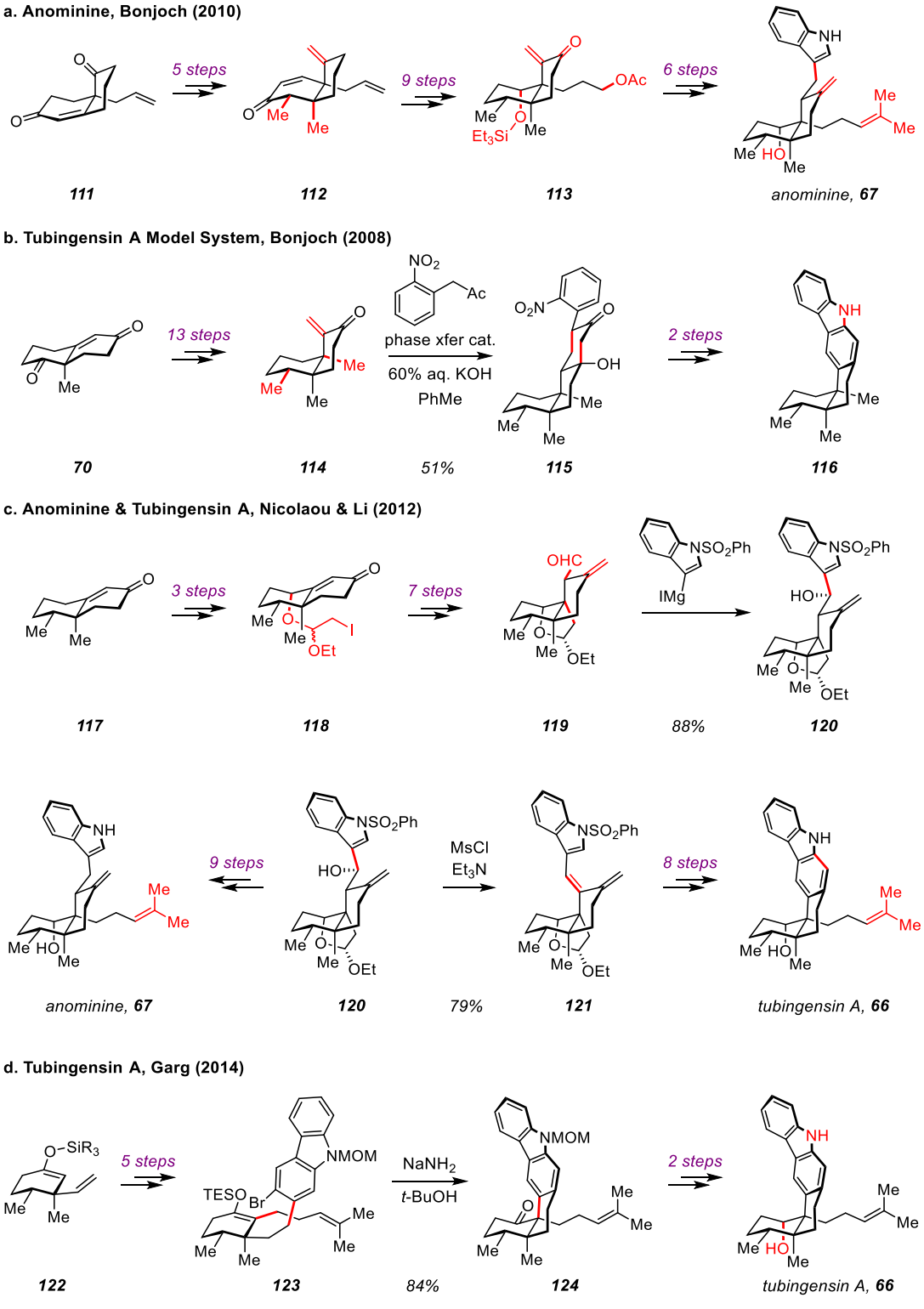

Scheme 2.7 Approaches towards related family members.

The second challenge in the xiamycin and oridamycin molecules is the fused carbazole (Scheme 2.2.b). Relevant precedent for the synthesis of this motif comes from tubingensin A (**66**), which contains a carbazole fused to a decalin ring system with the same regiochemistry as the xiamycin/oridamycin molecules. The related family member anominine (**67**) bears resemblance to indosespene (**30**), the biosynthetic precursor of xiamycin A, and will also be included in the present discussion.

Bonjoch reported the first synthesis of these natural products, reporting a successful route to anominine in 2010 (Scheme 2.7.a).[38] The synthesis begins with an organocatalyzed, asymmetric Robinson annulation to form Wieland–Miescher-type ketone **111.** This substrate was elaborated to *cis*-decalin **112** in five steps, which was converted to exocyclic enone **113** in nine steps, including a key selenium-oxide mediated allylic oxidation. The indole was installed through a Michael addition onto the exocyclic enone, and a cross metathesis forged the prenyl olefin. Bonjoch also reported progress towards tubingensin A (**66**), completing a synthesis of the core scaffold (Scheme 2.7.b).[39] This synthesis began with the Wieland Miescher ketone (**70**), which was elaborated into Michael acceptor **114**. To generate the fused carbazole, a Michael addition/aldol condensation cascade was executed using phase transfer catalysis. The aryl nitro group was reduced, and the resulting aniline condensed onto the proximal ketone to produce the indole. The carbazole was generated through dehydration followed by spontaneous aerobic oxidation.

Nicolaou and Li reported the synthesis of both anominine and tubingensin A from a common synthetic intermediate (**120**) in 2012 (Scheme 2.7.c).[40] Compound **117** was derived from a Robinson annulation, and was

converted to the Stork–Ueno cyclization precursor **118** in three steps.[41-42] After cyclization and functional group manipulation, Grignard addition into aldehyde **119** produced common synthetic intermediate **120.** To access anominine, **120** was deoxygenated via the xanthate, eventually yielding the natural product after introduction of the prenyl side chain. To synthesize tubingensin A, alcohol **120** was converted to the mesylate and eliminated to form triene **121**. A 6π-electrocyclization/aromatization sequence furnished the desired fused carbazole, ultimately leading to a successful synthesis of the natural product.

The most recent synthesis of tubingensin A comes from the Garg lab in 2014 (Scheme 2.7.d).[43] Starting from dihydrocarvone they were able to produce **122**, which was hydroborated and cross coupled with a protected carbazole triflate to connect the heterocycle with the aliphatic framework. The fused carbazole was generated from a benzyne intermediate, formed through elimination of aryl bromide **123** using $NaNH_2$. The benzyne was intercepted by the enolate derived from the silyl enol ether to produce the fused *cis*-decalin. Tubingensin A was synthesized after deprotection and reduction.

Three strategies emerge for the construction of fused carbazoles based on previous work. Bonjoch used a Michael addition, aldol condensation, nitro reduction, amine condensation, aromatization sequence on a model system, though this strategy was never successfully applied to tubingensin A (Scheme 2.7.b). Nicolaou and Li used a Grignard addition, alcohol elimination, 6π-electrocyclization, aromatization strategy (Scheme 2.7.c), and Garg used a benzyne annulation (Scheme 2.7.d).

C. Previous Syntheses of the Xiamycin and Oridamycin Family Members

Due to their interesting molecular architecture and promising biological activity, the xiamycin family of indolosesquiterpenes has piqued the interest of the synthetic community. The first synthetic effort towards any of the family members was reported by the Baran lab, disclosing the completion of xiamycin A and dixiamycin B (Scheme 2.8.a).[14] They accessed linear intermediate **125** in eight steps from geraniol, using a Suzuki coupling to link the carbazole to the terpenoid portion. Their key step involved formation of the *trans*-decalin ring system **126** through a cationic, epoxide-opening cyclization of substrate **125** as promoted by BF_3•OEt_2. After functional group tailoring they were able to produce xiamycin A (**28**) on gram scale. Initial attempts to chemically dimerize xiamycin A to dixiamycin A or B (**38** or **39**) using a variety of oxidants failed. Ultimately, it was discovered that dixiamycin B (**39**) could be generated from an electrochemical oxidation, along with bromodixiamycin, which is related to the natural product chloroxiamycin (**31**). The electrochemical dimerization likely proceeds through a nitrogen-centered radical, providing support for the biosynthetic hypothesis for dixiamycin A and dixiamycin B (Scheme 2.1.b). Currently, it is unclear why only one atropdiastereomer arises from the electrochemical dimerization.

Sespenine was the next family member to be synthesized (Scheme 2.8.b).[17] Li and coworkers accessed cyclization precursor **128** from geraniol (**127**) in 12 steps, forming desired bicycle **129** through a reductive epoxide-opening radical cyclization initiated by *in situ* generated Ti^{III}.

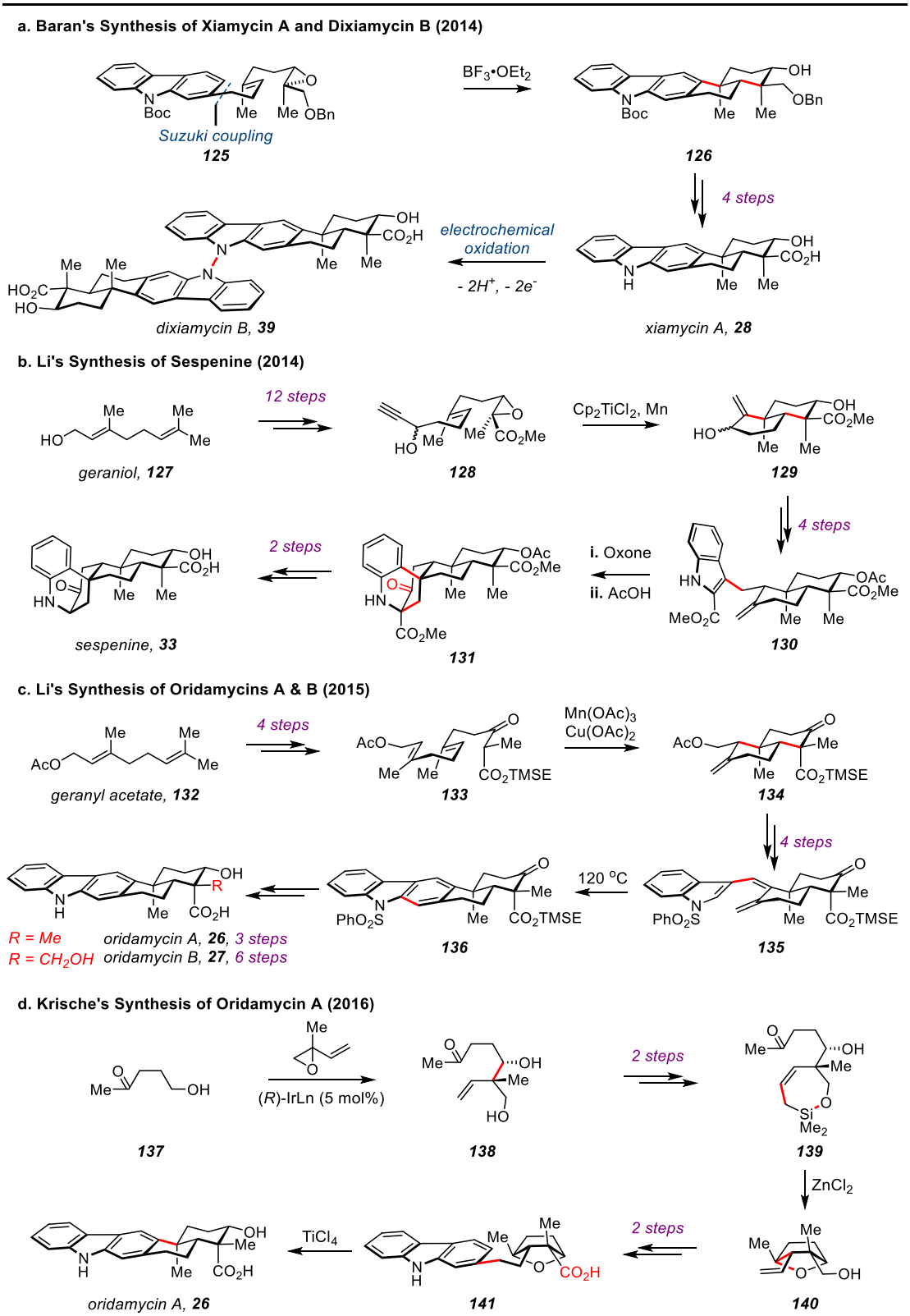

Scheme 2.8 Prior approaches towards xiamycin family members.

Oxidation of the resultant secondary alcohol produced an enone, which allowed for attachment of C2-methoxycarbonyl indole through a Michael addition, eventually producing rearrangement precursor **130**. The C2 ester substituent was required for the biomimetic rearrangement, as the unsubstituted derivative produced only complex mixtures. The indole was subsequently oxidized at C3 with Oxone, and the rearrangement was promoted with acetic acid at room temperature to produce compound **131**. Sespenine (**33**) was constructed after decarboxylation and deprotection. Interestingly, only one of the two C3 alcohol epimers underwent the desired skeletal rearrangement (see **51**, Scheme 2.1.c)—the other epimer primarily underwent an aza-Prins cyclization (see **50** to **28**, Scheme 2.1.a).

While the research described in this thesis was underway, Li and coworkers published the synthesis of oridamycin A (**26**), oridamycin B (**27**), xiamycin A (**28**), indosespene (**30**), and dixiamycin C (**42**).[44] They disclosed two routes to access xiamycin A, both of which used a reductive, epoxide-opening radical cyclization analogous to that used for the synthesis of sespenine (**33**). Dixiamycin C (**42**) was accessed through a Buchwald–Hartwig cross coupling between xiamycin A and a brominated derivative of xiamycin A. Li and coworkers also disclosed two routes to oridamycins A and B. The first route elaborated geranyl acetate (**132**) to the cyclization precursor **133** through a dianion alkylation (Scheme 2.8.c). Oxidative radical cyclization produced the desired *trans*-decalin **134** with the axially disposed ester substituent and equatorial methyl. Phenyl sulfone protected indole was attached through a Grignard addition, and the resulting secondary alcohol was eliminated to form triene **135**. The carbazole was forged using a 6π-electrocyclization/aromatization

sequence to yield **136**, which was converted to oridamycin A (**26**) upon reduction and deprotection. Oridamycin B (**27**) was synthesized using an oxime-directed, Pd^{II}-catalyzed, C-H oxidation to install the equatorial hydroxymethyl. The second route used the same key steps, but the indole was appended prior to cyclization, and the carbazole was forged through an oxidative Heck cyclization.[45]

The Li group's first route towards the oridamycins is strikingly similar to the route outlined in this document, *vide infra* Chapter 3. All of the key steps are the same, including oxidative radical cyclization, Grignard addition, 6π-electrocyclization, and oxime-directed C-H oxidation. The only significant difference between the strategies is the choice of protecting groups.[46]

More recently, the Krische group published a synthesis of oridamycin A using their direct alcohol C-H functionalization via C-C bond-forming transfer hydrogenation methodology (Scheme 2.8.d).[47] The first step in their synthesis joined **137** with isoprene oxide to form **138** asymmetrically. Treatment of silacycle **139** with $ZnCl_2$ generated a cyclic oxocarbenium intermediate, which was trapped by an intramolecular Sakurai allylation to produce bicycle **140**. This fragment was joined to carbazole, and an intramolecular Friedel–Crafts cyclization of **141** furnished oridamycin A (**26**).

All of the syntheses of the xiamycin family, with the exception of the Krische route, utilize a biomimetic cyclization strategy, forming two bonds, multiple stereocenters, and the desired *trans*-decalin ring system in a single step. This strategy selection is unsurprising, as there is considerable precedent for successful polyolefin cyclization cascades in natural product

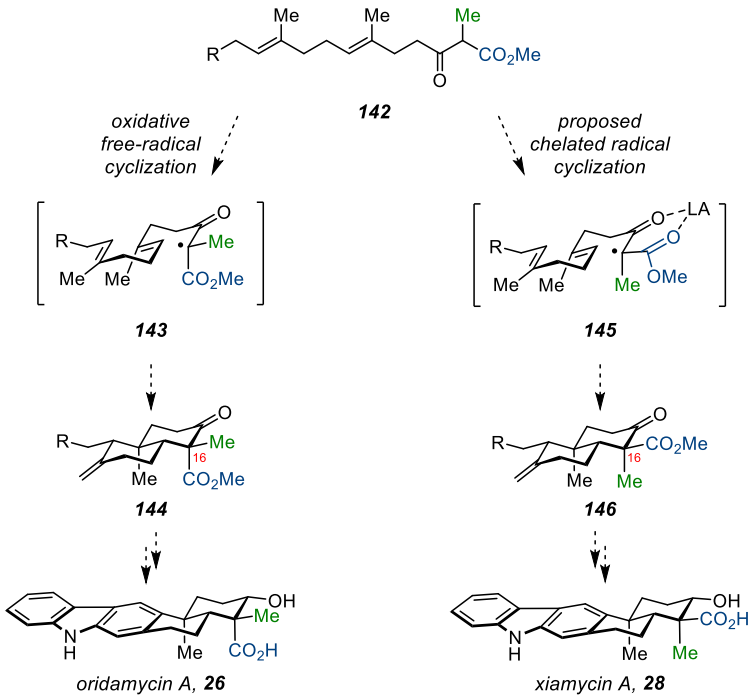

Scheme 2.9 A unified synthetic approach towards oridamycin A (**26**) and xiamycin A (**28**) from common synthetic starting material **142**.

total synthesis[48], with origins in the Stork–Eschenmoser hypothesis put forth in 1955.[49-50]

D. Retrosynthesis

The goal of this project is to find a solution to both the xiamycin and oridamycin scaffolds from a common synthetic intermediate (Scheme 2.9). With regards to efficiency, a biomimetic strategy would yield optimal results, as it could construct multiple bonds and stereocenters in a single operation. With these considerations in mind, a retrosynthesis is presented that accesses oridamycin A (**26**), oridamycin B (**27**), xiamycin A (**28**), and

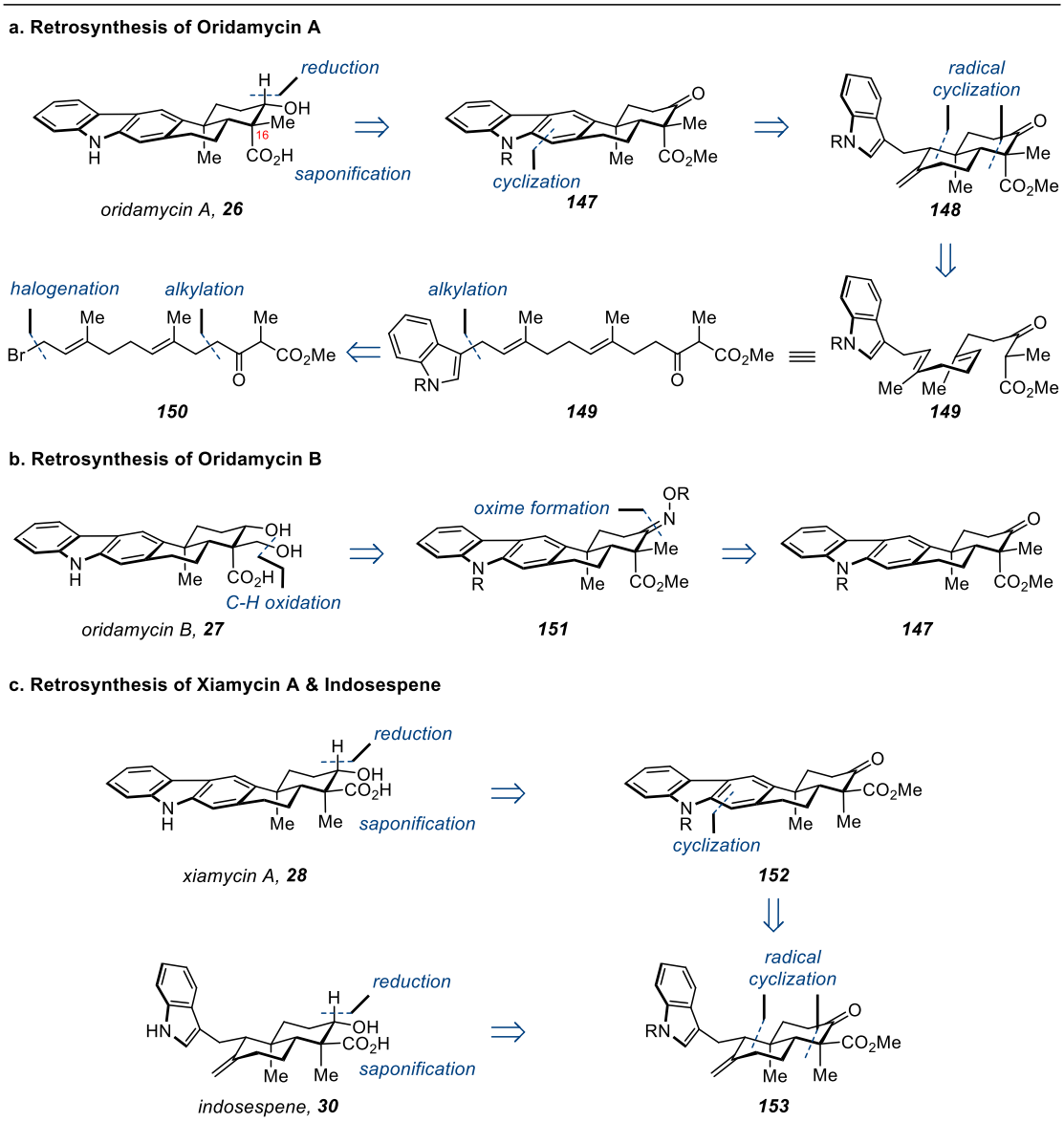

Scheme 2.10 Retrosynthetic analysis for several members of the xiamycin family.

indosespene (**30**), (Scheme 2.10). The dimeric compounds could be addressed upon completion of xiamycin A.

The key step for all monomers is the oxidative radical cyclization of linear *β*-keto ester **142**, forming three consecutive stereocenters, and producing the requisite *trans*-decalin system (Scheme 2.9). The radical

cyclization of a *β*-keto ester was selected for the key step because it produces a *trans*-decalin with an oxidation state similar to that of the natural products. Specifically, the C16 substituents will arrive in the correct oxidation state, containing an ester and a methyl substituent. Other methods provide the C16 *gem*-dimethyl (see Schemes 2.5.a, 2.5.c, 2.6.a, and 2.6.d), or other oxidation patterns that would require further manipulation (see Scheme 2.5.b). Atom-transfer cyclization was avoided because of the extra steps required for the synthesis of the starting α-bromo compounds, and for the conversion of the resultant bromide to the desired olefin. The Mn^{III}-mediated free radical cyclization, as reported by Snider and coworkers, is known to produce a *trans*-decalin corresponding to the oridamycins, in which the methyl group is equatorial and the ester is axial (Scheme 2.9, left side).[35-36] In order to access the C16 epimeric *trans*-decalin corresponding to indosespene (**30**), xiamycin A (**28**), and the dimers, a chelated radical cyclization is proposed (Scheme 2.9, right side). Chelated radical intermediates stemming from *β*-keto ester precursors have been reported for Mn^{III}-mediated cylclizations[51-53], as well as for atom-transfer cyclizations, providing promising precedent.[37, 54]

Based on previous reports, it seemed likely that the free radical cyclization towards the oridamycins (**26** & **27**) would be more straightforward than the chelated radical cyclization towards xiamycin A (**28**) and indosespene (**30**). Accordingly, the initial focus was on the synthesis of oridamycin A and oridamycin B in order to validate the late stage transformations before attempting to develop a novel radical cyclization methodology. The C16 carboxylic acid of oridamycin A (**26**) would stem from saponification of an appropriate ester precursor, while the secondary

alcohol would arise from the ketone of precursor **147** (Scheme 2.10.a). Axial hydride delivery is expected, as it would have a lower steric penalty than equatorial delivery due to the axial methyl and carboxy substituents. The carbazole could arise from a biomimetic cyclization of tetracycle **148** (see Scheme 2.1.a), entailing oxidation at the indole C3, aza-Prins cyclization, dehydration, and aromatization. Alternatively, a Pd^{II}-catalyzed oxidative cyclization could be explored[45] (after the development of this retrosynthesis, Li and coworkers reported the realization of this cyclization strategy[44]). Tetracycle **148** would arise from the key radical cyclization of common precursor **149**, producing two rings and three consecutive stereocenters in a single operation. Based on previous work, it seemed probable that the desired *trans*-decalin would be generated (for further discussion, see Chapter 3).[35-36, 55-57] A potential difficulty with this retrosynthesis is the possibility that the tertiary radical produced after the second cyclization could cyclize onto the indole, as these types of radicals have been shown to interact with aromatic systems.[55, 58] Alternatively, the cation that would result from oxidation of this radical could cyclize in a Friedel–Crafts fashion. The linear cyclization precursor **149** would be derived from indole and allylic bromide **150**.[59] The allylic bromide **150** would be synthesized from the corresponding allylic alcohol, which would be derived from oxidized geranyl acetate and the dianion of methyl 2-methyl-3-oxobutanoate.[58, 60-61] To produce the hydroxymethyl substituent of oridamycin B (**27**), a late stage, oxime-directed, Pd^{II}-catalyzed C-H oxidation was envisioned (Scheme 2.10.b). It was anticipated that coordination to the Lewis basic oxime (**151**) would allow for selective insertion into the equatorial methyl via a five-membered palladacycle, with subsequent

reductive elimination forming the desired C-O bond and regenerating the Pd^{II} catalyst.[62-63] The requisite oxime **151** could be readily synthesized from compound **147**, a proposed intermediate in the synthesis of oridamycin A (**26**).

Xiamycin A (**28**) was envisioned to arise from pentacyclic ketone **152** using the same disconnections as the oridamycins (Scheme 2.10.c). Pentacyclic ketone **152** would arise from tetracycle **153** using the same biomimetic cyclization strategy proposed for the oridamycins (Scheme 2.10.a). The key step in the synthesis would be the radical cyclization, forming the *trans*-decalin framework in a single step from common linear precursor **149**. As previously mentioned, the oxidative radical cyclization for xiamycin A requires chelation of the two carbonyls during cyclization to enforce formation of the *trans*-decalin bearing an axial methyl substituent and equatorial ester (see Scheme 2.9). The product of the desired radical cyclization would be readily converted into indosespene (**30**) through reduction and saponification.

In summary, a retrosynthesis is described that would provide access to oridamycin A (**26**), oridamycin B (**27**), xiamycin A (**28**), and indosespene (**30**) from a common synthetic precursor **149**. The key step in the retrosynthesis involves an oxidative radical cyclization to form the desired *trans*-decalin ring system in a biomimetic polyolefin cyclization. The framework associated with the oridamycins would arise from a free radical cyclization, while the framework associated with xiamycin A would arise from a chelated radical cyclization.

REFERENCES

[1] Takada, K., Kajiwara, H., & Imamura, N., Oridamycins A and B, anti-*Saprolegnia parasitica* indolosesquiterpenes isolated from *Streptomyces* sp. KS84. *J. Nat. Prod.* **2010,** 73, 698–701.

[2] Ding, L., Munch, J., Goerls, H., Maier, A., Fiebig, H. H., Lin, W. H., & Hertweck, C., Xiamycin, a pentacyclic indolosesquiterpene with selective anti-HIV activity from a bacterial mangrove endophyte. *Bioorg. Med. Chem. Lett.* **2010,** *20*, 6685–6687.

[3] Ding, L., Maier, A., Fiebig, H. H., Lin, W. H., & Hertweck, C., A family of multicyclic indolosesquiterpenes from a bacterial endophyte. *Org. Biomol. Chem.* **2011,** 9, 4029–4031.

[4] Xu, Z., Baunach, M., Ding, L., & Hertweck, C., Bacterial synthesis of diverse indole terpene alkaloids by an unparalleled cyclization sequence. *Angew. Chem. Int. Ed.* **2012,** 51, 10293–10297.

[5] Zhang, Q. B., Mandi, A., Li, S. M., Chen, Y. C., Zhang, W. J., Tian, X. P., Zhang, H. B., Li, H. X., Zhang, W. M., Zhang, S., Ju, J. H., Kurtan, T., & Zhang, C. S., N-N-Coupled indolo-sesquiterpene atropo-diastereomers from a marine-derived actinomycete. *Eur. J. Org. Chem.* **2012,** 5256–5262.

[6] Baunach, M., Ding, L., Bruhn, T., Bringmann, G., & Hertweck, C., Regiodivergent N-C and N-N aryl coupling reactions of indoloterpenes and cycloether formation mediated by a single bacterial flavoenzyme. *Angew. Chem. Int. Ed.* **2013,** 52, 9040–9043.

[7] Baunach, M., Ding, L., Willing, K., & Hertweck, C., Bacterial synthesis of unusual sulfonamide and sulfone antibiotics by flavoenzyme-mediated sulfur dioxide capture. *Angew. Chem. Int. Ed.* **2015,** 54, 13279–13283.

[8] Kim, S. H., Ha, T. K., Oh, W. K., Shin, J., & Oh, D. C., Antiviral indolosesquiterpenoid xiamycins C-E from a halophilic actinomycete. *J. Nat. Prod.* **2016,** 79, 51–58.

[9] Hurley, L. H., DNA and its associated processes as targets for cancer therapy. *Nat. Rev. Cancer* **2002,** 2, 188–200.

[10] Li, H., Zhang, Q., Li, S., Zhu, Y., Zhang, G., Zhang, H., Tian, X., Zhang, S., Ju, J., & Zhang, C., Identification and characterization of xiamycin

A and oxiamycin gene cluster reveals an oxidative cyclization strategy tailoring indolosesquiterpene biosynthesis. *J. Am. Chem. Soc.* **2012,** *134*, 8996–9005.

[11] Zhang, Q., Li, H., Li, S., Zhu, Y., Zhang, G., Zhang, H., Zhang, W., Shi, R., & Zhang, C., Carboxyl formation from methyl via triple hydroxylations by *XiaM* in xiamycin A biosynthesis. *Org. Lett.* **2012,** *14*, 6142–6145.

[12] Li, H., Sun, Y., Zhang, Q., Zhu, Y., Li, S. M., Li, A., & Zhang, C., Elucidating the cyclization cascades in xiamycin biosynthesis by substrate synthesis and enzyme characterizations. *Org. Lett.* **2015,** *17*, 306–309.

[13] Zhang, Q. B., Li, H. X., Yu, L., Sun, Y., Zhu, Y. G., Zhu, H. N., Zhang, L. P., Li, S. M., Shen, Y. M., Tian, C. L., Li, A., Liu, H. W., & Zhang, C. S., Characterization of the flavoenzyme *XiaK* as an N-hydroxylase and implications in indolosesquiterpene diversification. *Chem. Sci.* **2017,** *8*, 5067–5077.

[14] Rosen, B. R., Werner, E. W., O'Brien, A. G., & Baran, P. S., Total synthesis of dixiamycin B by electrochemical oxidation. *J. Am. Chem. Soc.* **2014,** *136*, 5571–5574.

[15] Liu, Y., McWhorter, W. W., Jr., & Hadden, C. E., Novel rearrangement of a 2-aryl-3-alkyl-3H-indol-3-ol to a 1,4,5,6-tetrahydro-2,6-methano-1-benzazocin-3(2H)-one with implications for the biosynthesis of aspernomine. *Org. Lett.* **2003,** *5*, 333–335.

[16] Ho, G. A., Nouri, D. H., & Tantillo, D. J., Carbocation rearrangements in aspernomine biosynthesis. *Tetrahedron Lett.* **2009,** *50*, 1578–1581.

[17] Sun, Y., Chen, P., Zhang, D., Baunach, M., Hertweck, C., & Li, A., Bioinspired total synthesis of sespenine. *Angew. Chem. Int. Ed.* **2014,** *53*, 9012–9016.

[18] Rapson, W. S., & Robinson, R., 307. Experiments on the synthesis of substances related to the sterols. Part II. A new general method for the synthesis of substituted cyclohexenones. *J. Chem. Soc.* **1935,** 1285–1288.

[19] Wieland, P., & Miescher, K., Über die herstellung mehrkerniger ketone. *Helv. Chim. Acta* **1950,** *33*, 2215–2228.

[20] Eder, U., Sauer, G., & Weichert, R., New type of asymmetric cyclization to optically active steroid CD partial structures. *Angew. Chem. Int. Ed.* **1971,** 10, 496–497.

[21] Hajos, Z. G., & Parrish, D. R., Asymmetric synthesis of bicyclic intermediates of natural product chemistry. *J. Org. Chem.* **1974,** 39, 1615–1621.

[22] Marko, I. E., Wiaux, M., Warriner, S. M., Giles, P. R., Eustace, P., Dean, D., & Bailey, M., Towards the total synthesis of clerocidin. Efficient assembly of the decalin subunit. *Tetrahedron Lett.* **1999,** 40, 5629–5632.

[23] Masamune, S., Total syntheses of diterpenes and diterpene alkaloids. III. Kaurene. *J. Am. Chem. Soc.* **1964,** 86, 289–290.

[24] Masamune, S., Total syntheses of diterpenes and diterpene alkaloids. IV. Garryine. *J. Am. Chem. Soc.* **1964,** 86, 290–291.

[25] Schmalzbauer, B., Herrmann, J., Muller, R., & Menche, D., Total synthesis and antibacterial activity of dysidavarone A. *Org. Lett.* **2013,** 15, 964–967.

[26] Diels, O., & Alder, K., Synthesen in der hydroaromatischen reihe. *Liebigs Ann. Chem.* **1928,** 460, 98–122.

[27] Hashimoto, S., Sakata, S., Sonegawa, M., & Ikegami, S., A total synthesis of (±)-forskolin. *J. Am. Chem. Soc.* **1988,** 110, 3670–3672.

[28] Phoenix, S., Reddy, M. S., & Deslongchamps, P., Total synthesis of (+)-cassaine via transannular Diels–Alder reaction. *J. Am. Chem. Soc.* **2008,** 130, 13989–13995.

[29] Woodward, R. B., Sondheimer, F., Taub, D., Heusler, K., & McLamore, W. M., The total synthesis of steroids. *J. Am. Chem. Soc.* **1952,** 74, 4223–4251.

[30] Kametani, T., Kato, Y., Honda, T., & Fukumoto, K., Studies on the syntheses of heterocyclic compounds. 675. A facile regiospecific and stereocontrolled synthesis of a diterpene alkaloid intermediate from benzocyclobutenes. *J. Am. Chem. Soc.* **1976,** 98, 8185–8190.

[31] Johnson, W. S., & Schaaf, T. K., Entry into the podocarpane series through a biogenetic-like stereoselective olefin cyclization. *J. Chem. Soc. Chem. Comm.* **1969,** 611–612.

[32] Corey, E. J., & Liu, K., Enantioselective total synthesis of the potent anti-HIV agent neotripterifordin. Reassignment of stereochemistry at C(16). *J. Am. Chem. Soc.* **1997,** *119*, 9929–9930.

[33] Snyder, S. A., Treitler, D. S., & Brucks, A. P., Simple reagents for direct halonium-induced polyene cyclizations. *J. Am. Chem. Soc.* **2010,** *132*, 14303–14314.

[34] Breslow, R., Olin, S. S., & Groves, J. T., Oxidative cyclization of farnesyl acetate by a free-radical path. *Tetrahedron Lett.* **1968,** 1837–1840.

[35] Snider, B. B., Manganese(III)-based oxidative free-radical cyclizations. *Chem. Rev.* **1996,** *96*, 339–364.

[36] Snider, B. B., Mohan, R., & Kates, S. A., Manganese(III)-based oxidative free-radical cyclizations 2. Polycyclization reactions proceeding through tertiary cations. *Tetrahedron Lett.* **1987,** *28*, 841–844.

[37] Yang, D., Gu, S., Yan, Y. L., Zhao, H. W., & Zhu, N. Y., Atom-transfer tandem radical cyclization reactions promoted by Lewis acids. *Angew. Chem. Int. Ed.* **2002,** *41*, 3014–3017.

[38] Bradshaw, B., Etxebarria-Jardi, G., & Bonjoch, J., Total synthesis of (-)-anominine. *J. Am. Chem. Soc.* **2010,** *132*, 5966–5967.

[39] Bradshaw, B., Etxebarria-Jardi, G., & Bonjoch, J., Polycyclic framework synthesis of anominine and tubingensin A indole diterpenoids. *Org. Biomol. Chem.* **2008,** *6*, 772–778.

[40] Bian, M., Wang, Z., Xiong, X., Sun, Y., Matera, C., Nicolaou, K. C., & Li, A., Total syntheses of anominine and tubingensin A. *J. Am. Chem. Soc.* **2012,** *134*, 8078–8081.

[41] Stork, G., Mook, R., Biller, S. A., & Rychnovsky, S. D., Free-radical cyclization of bromo acetals. Use in the construction of bicyclic acetals and lactones. *J. Am. Chem. Soc.* **1983,** *105*, 3741–3742.

[42] Ueno, Y., Chino, K., Watanabe, M., Moriya, O., & Okawara, M., Homolytic carbocyclization by use of heterogeneous supported organotin catalyst - A new synthetic route to 2-

alkoxytetrahydrofurans and γ -butyrolactones. *J. Am. Chem. Soc.* **1982,** *104*, 5564-5566.

[43] Goetz, A. E., Silberstein, A. L., Corsello, M. A., & Garg, N. K., Concise enantiospecific total synthesis of tubingensin A. *J. Am. Chem. Soc.* **2014,** *136*, 3036–3039.

[44] Meng, Z., Yu, H., Li, L., Tao, W., Chen, H., Wan, M., Yang, P., Edmonds, D. J., Zhong, J., & Li, A., Total synthesis and antiviral activity of indolosesquiterpenoids from the xiamycin and oridamycin families. *Nat. Commun.* **2015,** *6*, 6096.

[45] Kong, A., Han, X., & Lu, X., Highly efficient construction of benzene ring in carbazoles by palladium-catalyzed endo-mode oxidative cyclization of 3-(3'-alkenyl)indoles. *Org. Lett.* **2006,** *8*, 1339–1342.

[46] Trotta, A. H., Total synthesis of oridamycins A and B. *Org. Lett.* **2015,** *17*, 3358–3361.

[47] Feng, J., Noack, F., & Krische, M. J., Modular terpenoid construction via catalytic enantioselective formation of all-carbon quaternary centers: Total synthesis of oridamycin A, triptoquinones B and C, and isoiresin. *J. Am. Chem. Soc.* **2016,** *138*, 12364–12367.

[48] Yoder, R. A., & Johnston, J. N., A case study in biomimetic total synthesis: Polyolefin carbocyclizations to terpenes and steroids. *Chem. Rev.* **2005,** *105*, 4730–4756.

[49] Eschenmoser, A., Ruzicka, L., Jeger, O., & Arigoni, D., Zur kenntnis der triterpene. 190. Mitteilung. Eine stereochemische interpretation der biogenetischen isoprenregel bei den triterpenen. *Helv. Chim. Acta* **1955,** *38*, 1890–1904.

[50] Stork, G., & Burgstahler, A. W., The stereochemistry of polyene cyclization. *J. Am. Chem. Soc.* **1955,** *77*, 5068–5077.

[51] Yang, D., Ye, X. Y., Gu, S., & Xu, M., Lanthanide triflates catalyze Mn(III)-based oxidative radical cyclization reactions. Enantioselective synthesis of (-)-triptolide, (-)-triptonide, and (+)-triptophenolide. *J. Am. Chem. Soc.* **1999,** *121*, 5579–5580.

[52] Yang, D., Ye, X. Y., Xu, M., Pang, K. W., & Cheung, K. K., Investigation of Mn(III)-based oxidative free-radical cyclization reactions toward the synthesis of Triptolide: The effects of lanthanide triflates and

substituents on stereoselectivity. *J. Am. Chem. Soc.* **2000,** *122*, 1658–1663.

[53] Yang, D., Ye, X. Y., & Xu, M., Enantioselective total synthesis of (-)-triptolide, (-)-triptonide, (+)-triptophenolide, and (+)-triptoquinonide. *J. Org. Chem.* **2000,** 65, 2208–2217.

[54] Yang, D., Zheng, B. F., Gao, Q., Gu, S., & Zhu, N. Y., Enantioselective PhSe-group-transfer tandem radical cyclization reactions catalyzed by a chiral Lewis acid. *Angew. Chem. Int. Ed.* **2005,** 45, 255–258.

[55] Snider, B. B., Mohan, R., & Kates, S. A., Manganese(III)-based oxidative free-radical cyclization. Synthesis of (±)-podocarpic acid. *J. Org. Chem.* **1985,** 50, 3659–3661.

[56] Zoretic, P. A., Fang, H. Q., & Ribeiro, A. A., Synthesis of *d*,*l*-norlabdane oxide and related odorants: An intramolecular radical approach. *J. Org. Chem.* **1998,** 63, 4779–4785.

[57] Dombroski, M. A., Kates, S. A., & Snider, B. B., Manganese(III)-based oxidative free-radical tandem and triple cyclizations. *J. Am. Chem. Soc.* **1990,** *112*, 2759–2767.

[58] Gonzalez, M. A., & Molina-Navarro, S., Attempted synthesis of spongidines by a radical cascade terminating onto a pyridine ring. *J. Org. Chem.* **2007,** 72, 7462–7465.

[59] Zhu, X., & Ganesan, A., Regioselective synthesis of 3-alkylindoles mediated by zinc triflate. *J. Org. Chem.* **2002,** 67, 2705–2708.

[60] Kitagawa, Y., Itoh, A., Hashimoto, S., Yamamoto, H., & Nozaki, H., Total synthesis of humulene - Stereoselective approach. *J. Am. Chem. Soc.* **1977,** 99, 3864–3867.

[61] Jenny, L., & Borschberg, H. J., Synthesis of the dolabellane diterpene hydrocarbon (±)- δ -araneosene. *Helv. Chim. Acta* **1995,** 78, 715-731.

[62] Neufeldt, S. R., & Sanford, M. S., O-Acetyl oximes as transformable directing groups for Pd-catalyzed C-H bond functionalization. *Org. Lett.* **2010,** *12*, 532–535.

[63] Desai, L. V., Hull, K. L., & Sanford, M. S., Palladium-catalyzed oxygenation of unactivated sp3 C-H bonds. *J. Am. Chem. Soc.* **2004,** *126*, 9542–9543.

Chapter 3. Synthesis of Oridamycin A & Oridamycin B

Preface

This chapter outlines the evolution of the synthetic strategy used to synthesize both oridamycin A *and oridamycin* B*. The initial retrosynthesis was modified multiple times as a result of unexpected results during studies towards both natural products. The final sequence utilizes a free-radical cyclization to form the* trans*-decalin ring system, setting three contiguous stereocenters in a single operation. The carbazole is constructed using a 6π-electrocyclization to fuse the* trans*-decalin to the aromatic system.*

A. Initial Efforts

The first goal was to synthesize a suitable cyclization precursor to validate the hypothesis that a *trans*-decalin harboring the stereochemistry associated with the oridamycins could be accessed from a Mn^{III}-mediated free-radical cyclization. As previously outlined in Chapter 2, cyclization precursor **149** was the initial target for testing this premise. This compound was envisioned to arise from indole alkylation of allylic bromide **150**, which could be accessed from known linear alcohol **154** (Scheme 3.1.a).[1-3] This compound (**154**) could be derived from allylic oxidation of geranyl acetate, conversion of the resultant allylic alcohol **156** to an allylic bromide, and alkylation with the dianion of methyl 2-methyl-3-oxobutanoate (**155**).

Implementation of this retrosynthetic analysis began with SeO_2-mediated allylic oxidation of geranyl acetate (Scheme 3.1.b, **157**). Mechanistically, the oxidation begins with an ene reaction, in which the

a. Retrosynthetic Analysis of Cyclization Precursor

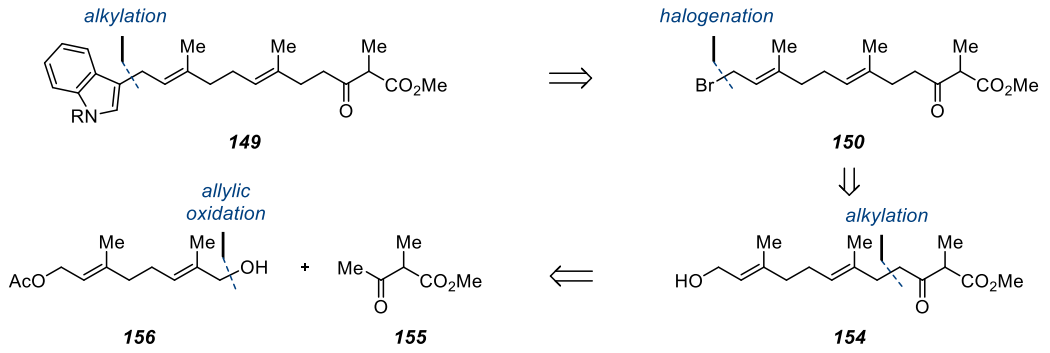

b. Synthesis of Cyclization Precursor(s) from Geranyl Acetate

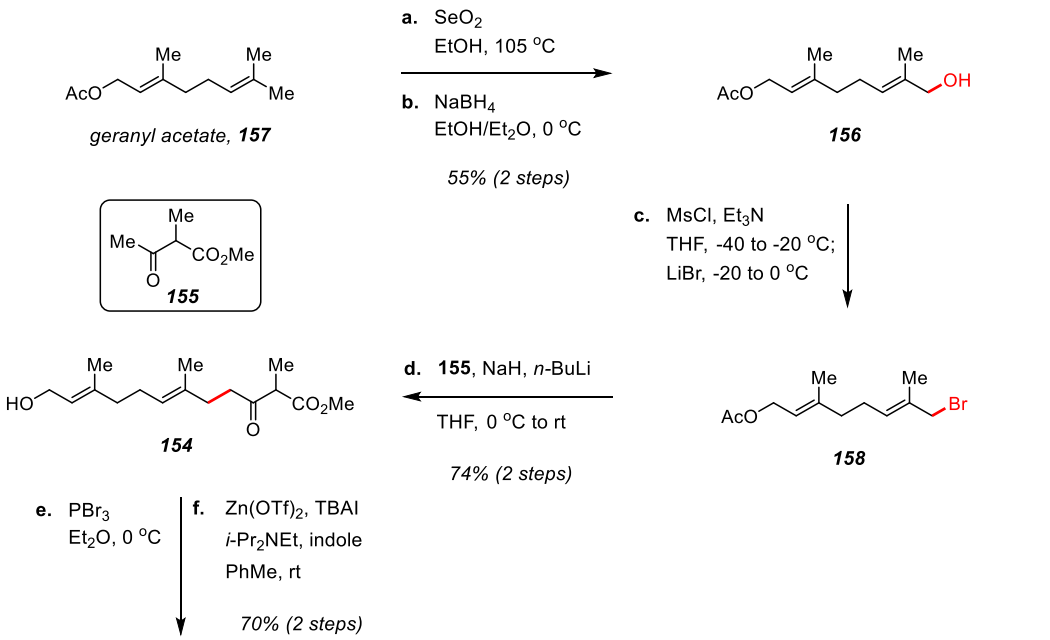

c. Attempted Cyclizations

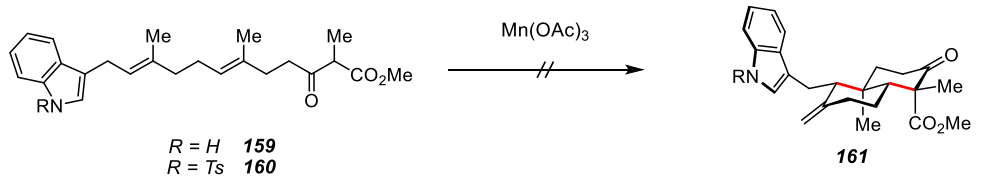

Scheme 3.1 Initial studies towards oridamycin A.

olefin engages the electrophilic selenium species. This is followed by a [2,3]-sigmatropic rearrangement to form the desired oxidized product **156**.[4-6] The ene reaction determines the regioselectivity, with the electrophilic SeO_2 preferentially engaging the more electron rich olefin. Oxidized product **156** is selectively produced from geranyl acetate due to the deactivation of the other olefin by the allylic acetate. Next, the allylic alcohol **156** was converted to allylic bromide **158**. Initial attempts using Appel conditions (CBr_4 and PPh_3) were complicated by large amounts of $P(O)Ph_3$ byproduct, leading to difficult purifications and loss of product. It was found that a one-pot, two-step procedure involving mesylate formation followed by Finkelstein reaction provided the desired material in significantly higher yield without requiring chromatographic purification (Scheme 3.1.b). The necessary acetoacetate derivative was produced through alkylation of methyl acetoacetate with methyl iodide to generate methyl 2-methyl-3-oxobutanoate (**155**).[7] The dianion of **155** was generated using sequential addition of NaH and *n*-BuLi and was alkylated with allylic bromide **158** to produce linear alcohol **154**. Presumably, excess dianion (5 equivalents were used) cleaved the allylic acetate *in situ* to directly afford the linear alcohol **154**. A similar process was employed to link indole to the linear β-keto ester. Allylic alcohol **154** was converted to the bromide through the action of PBr_3, and the resultant crude bromide was condensed with indole using $Zn(OTf)_2$ to yield the desired cyclization substrate **159**.[8]

With the desired cyclization precursor **159** in hand, several attempts were made to generate the desired *trans*-decalin **161** using Mn^{III}-mediated free-radical conditions (Scheme 3.1.c). Unfortunately, the desired *trans*-decalin **161** was not isolated from these reactions. It was hypothesized

that protection of the indole might be beneficial, and a tosyl-protected cyclization precursor **160** was prepared through the dianion of linear indole **159** (Scheme 3.1.b). The *trans*-decalin **161** remained elusive when tosyl-protected cyclization precursor **160** was used, prompting reconsideration of the strategy. It seemed plausible that the transient radical and/or cationic intermediates were unproductively interacting with the aromatic system, complicating the reaction and producing a mixture of unwanted side products. Indeed, previous studies have leveraged the ability of intermediate radicals/cations in free-radical cyclizations to engage aromatic systems, generating additional rings in cascade reactions.[9-10] These studies further support the hypothesis that the indole may be problematic for the free-radical cyclization.

B. Redesign & Completion of Oridamycin A

To overcome the difficulties encountered when attempting to cyclize indole derivatives **159** and **160**, it was hypothesized that cyclization prior to indole attachment would prove beneficial, eliminating the possibility of undesired interactions with the indole. Examination of the literature regarding Mn^{III}-mediated free-radical cyclizations revealed that molecules related to linear alcohol **154** have been successfully cyclized to produce the desired type of *trans*-decalin ring system.[11-12] Gratifyingly, treatment of linear alcohol **154** with $Mn(OAc)_3$ and $Cu(OAc)_2$ in AcOH afforded the desired *trans*-decalin **162** in 50% yield as a single diastereomer and as a single olefin isomer (Scheme 3.2.a). This cyclization correctly sets three contiguous stereocenters present in the target molecule, including two quaternary

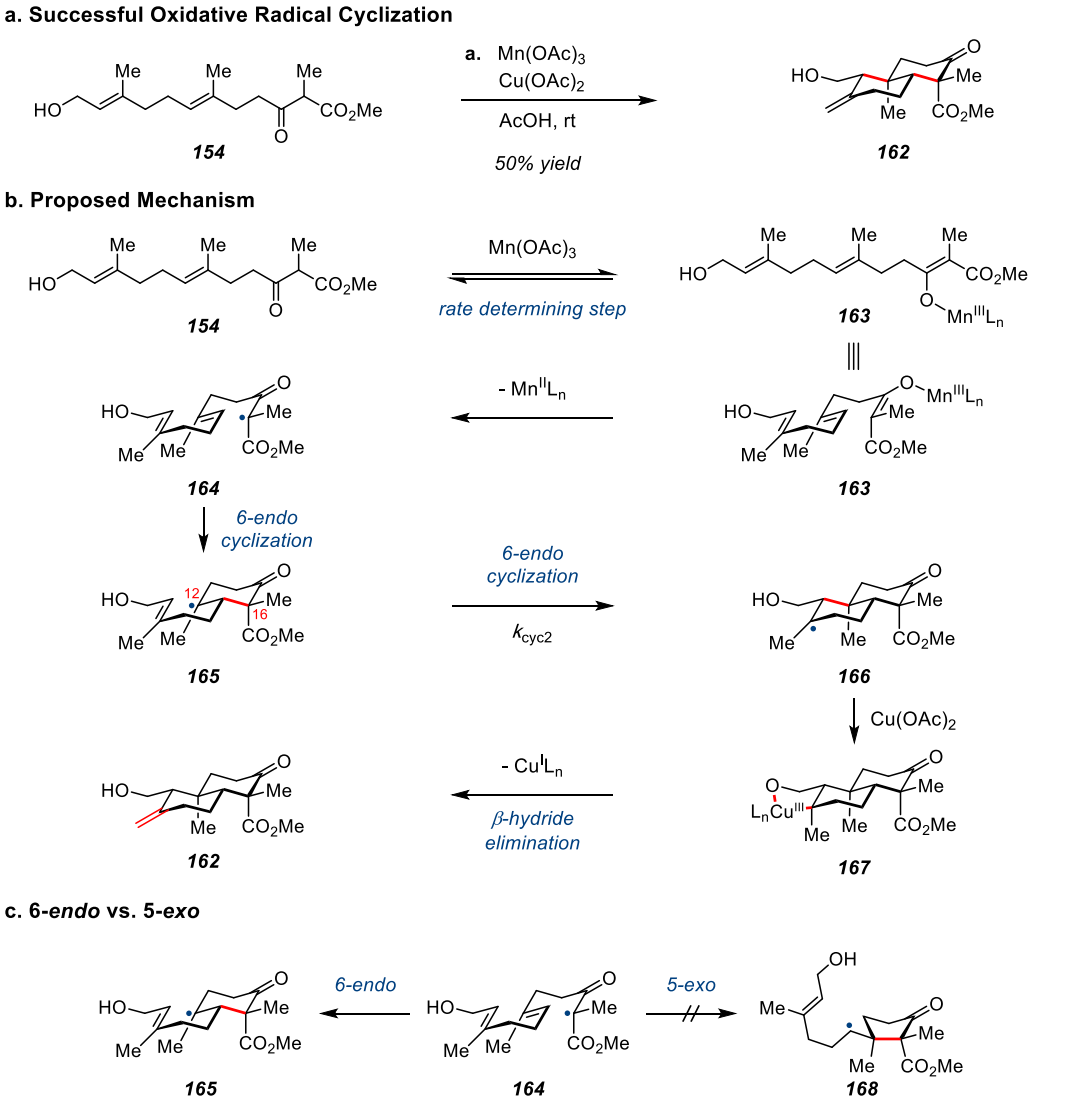

Scheme 3.2 Successful oxidative radical cyclization and mechanistic rationale.

centers. The remarkable selectivity of this transformation deserves further discussion.

The mechanism of the Mn^{III}-mediated oxidative radical cyclization has been studied, and the first step is formation of the Mn^{III}-enolate (Scheme 3.2.b).[13-14] When the substrate is an α-substituted β-keto ester (such

as **154**), the formation of the Mn^{III} enolate **163** is the rate-determining step, as the enolate rapidly undergoes electron transfer to form a Mn^{II} species and the free radical **164**. Interestingly, when the substrate is an α-unsubstituted β-keto ester, formation of the Mn^{III}-enolate is not the rate-determining step. In fact, an entirely different mechanism is operant with these substrates, in which the alkene acts as a nucleophile to directly engage the Mn^{III}-enolate. This hypothesis is based on the observation that alkene concentration changes the reaction rate for intermolecular additions, and that tether length effects the reaction rate in intramolecular cyclizations.[13, 15]

Oxidative radical cyclizations mediated by $Mn(OAc)_3$ are thought to proceed through free-radical intermediates, as opposed to Mn-complexed radicals. Comparisons between atom-transfer cyclizations and oxidative radical cyclizations have confirmed that both methods produce the same stereochemistry on equivalent substrates.[16] Since it is well known that atom-transfer radical cyclizations proceed through free-radical intermediates,[17] it can be postulated that Mn^{III}-mediated oxidative radical cyclizations also proceed through free-radical intermediates. Apparently, the Mn^{II} salt formed after electron transfer does not maintain an interaction with the substrate, instead free-radical intermediate **164** undergoes a 6-*endo* cyclization onto the proximal olefin to form tertiary radical **165** (Scheme 3.2.b & 3.2.c). The selectivity of the 6-*endo* cyclization is predicated on the presence of the vinyl methyl substituent on the nucleophilic olefin, as 1,2-disubstited olefins form products arising from 5-*exo* cyclization over those arising from 6-*endo* cyclization.[18] One explanation for the observed regioselectivity is that the first cyclization is reversible, allowing for the

formation of the thermodynamic 6-*endo* product, which is favored due to the increased stability of the resultant tertiary radical **165** and the formation of the thermodynamically favored six-membered ring. This hypothesis has been put forth to explain observed regioselectivities of other radical cyclizations,[19] but it seems unlikely in this case. For the first cyclization to be reversible the rate of ring-opening (**165** to **164**, k_{open}) would have to be faster than the second cyclization (**165** to **166**, k_{cyc2}). The second cyclization is faster than oxidation of **165** with $Cu(OAc)_2$ (k_{ox}) since no monocyclic products are observed ($k_{cyc2} > k_{ox}$). It has previously been shown that oxidation of alkyl radicals with $Cu(OAc)_2$ is faster than six-membered ring-opening reactions of related β-keto ester substrates ($k_{ox} > k_{open}$),[16] meaning that the second cyclization is faster than the ring-opening reaction (by the transitive relation, if $k_{cyc2} > k_{ox}$ and $k_{ox} > k_{open}$, then $k_{cyc2} > k_{open}$). This means that the first cyclization is under kinetic control rather than thermodynamic control in this system, ruling out the thermodynamic explanation predicated on the reversibility of the cyclization. Part of the argument is still applicable, however. The relative stability of the resultant radicals may have a role in the transition state. Since the secondary radical from a 5-*exo* cyclization is significantly less stable than the tertiary radical formed from 6-*endo* cyclization, the 6-*endo* transition state may have a lower energy barrier than the 5-*exo* transition state (Scheme 3.2.c). To argue that the stability of the product has an impact on a kinetically controlled reaction, a late transition state must be operant. In this case, a late transition state seems plausible since the initial radical is more stabilized than the resultant radical, implying that the process may be endothermic, or, at least, not highly exothermic. Another possible explanation for the

preference for 6-*endo* vs. 5-*exo* is that formation of two *vicinal* quaternary centers is sterically disfavored, bringing several substituents in close proximity in the transition state.

The stereochemistry arising from the first cyclization places the ester substituent in the axial position and the methyl substituent in the equatorial position (**165**). There are two explanations for this empirical result: 1) the transition state leading to the observed stereochemistry minimizes unfavorable dipole interactions,[16] and 2) the relative size of the methyl group is larger than the methyl ester. To minimize the overall dipole of the molecule, the two carbonyl substituents would have to point away from each other. In order to do this efficiently, the ester would need to occupy an axial position, as observed in *trans*-decalin **162**. Furthermore, the methyl ester is less sterically demanding than the methyl group (A-values: Me = 1.74 & CO_2Me = 1.2-1.3). As the six-membered ring **165** forms, the axial C16 substituent and the C12 methyl begin to engage in a *syn*-pentane interaction. Placing the smaller substituent in the axial position at C16 would incur less of a steric penalty, lowering the energy of the transition state. It is certainly possible that both dipole minimization and steric interactions play a role in determining the diastereoselectivity of the reaction.

The regioselectivity of the second cyclization (**165** to **166**) can be explained using the same principles outlined for the first 6-*endo* cyclization. In this case, the relative stability of the initial and terminal radicals is almost identical, since they are both tertiary alkyl radicals. This makes it more difficult to assert that the transition state is late rather than early. Since they are of similar energy, it can be posited that the reaction is not highly

exothermic, meaning that the stability of the resultant radical will influence the product ratio.

To aid in the oxidative termination of the resultant radical **166**, a Cu^{II}-carboxylate salt is added to the reaction—$Cu(OAc)_2$ reacts 350 times faster with secondary radicals than $Mn(OAc)_3$.[20-21] The Cu^{II} salt interacts with the alkyl radical to form a Cu^{III} intermediate **167** that can either form an olefin through β-hydride elimination, transfer a ligand through reductive elimination, or form a carbocation.[22] Interestingly, only one of three possible olefin isomers is formed in the cyclization of linear alcohol **154** to bicycle **162**. Similar observations have been made on related systems.[12] It seems likely that intramolecular complexation of the alcohol with the Cu^{III} species occurs, producing an intermediate that undergoes β-hydride elimination from the methyl group to selectively produce the exocyclic methylene **162**. In this instance, there are six proximal hydrogen atoms that are candidates for β-H elimination. The methyl group is statistically favored since there are three equivalent protons fit for elimination. Furthermore, for the methine or methylene protons to correctly align in a *syn* orientation with the C–Cu bond, the entire tricyclic ring system would have to twist slightly, increasing the strain energy relative to the chair–chair system **167**. The methyl protons are free to rotate without incurring a twist motion, implying that there is less of an energy barrier for β-H elimination from the methyl group, explaining the observed selectivity for the exocyclic olefin. Furthermore, it is possible that several olefins are produced in the reaction, but are equilibrated by the solvent, AcOH, to the exocyclic olefin.

After successful oxidative radical cyclization, the next challenge was to append indole onto bicyclic alcohol **162**. Initial experiments were aimed

at converting the alcohol into a leaving group, allowing for an alkylation using the nucleophilic C3 of indole. Conversion to the bromide was unsuccessful using PBr_3 and CBr_4/PPh_3. Mesylate formation followed by Finkelstein reaction was also unable to produce the desired bromide, though the mesylate was successfully generated. Several attempts using the mesylate as the electrophile were also futile.

An alternative strategy for indole attachment would be a Grignard addition into bicyclic aldehyde **169**, readily derived from bicyclic alcohol **162** through oxidation with the Dess–Martin periodinane (Scheme 3.3.a).[23-24] The product from this reaction would be a secondary alcohol, which would require deoxygenation prior to the proposed biomimetic carbazole formation *en route* to oridamycin A/B (see Scheme 2.1.a). Furthermore, the deoxygenated product was targeted because the C16 epimeric compound, which would be generated from a chelated radical cyclization, would readily lead to the natural product indosespene (**30**) upon deoxygenation. The Grignard precursor was prepared in two steps from indole,[25] and subsequent metal–halogen exchange using EtMgBr generated the desired Grignard reagent **170**.[26] Addition into bicyclic aldehyde **169** proceeded smoothly to yield secondary alcohol **171** as a mixture of diastereomers (Scheme 3.3.a). The Barton–McCombie deoxygenation method was considered, as there was literature precedent for success in related natural products,[26] but it seemed more expeditious to attempt the reduction of an extended iminium species instead (Scheme 3.3.b).[27-28] It was anticipated that addition of TFA would remove the *tert*-butyl carbamate protecting group of **171**, increasing the electron density of the indole nitrogen and facilitating dehydration to form the extended iminium species **173**, which could then be

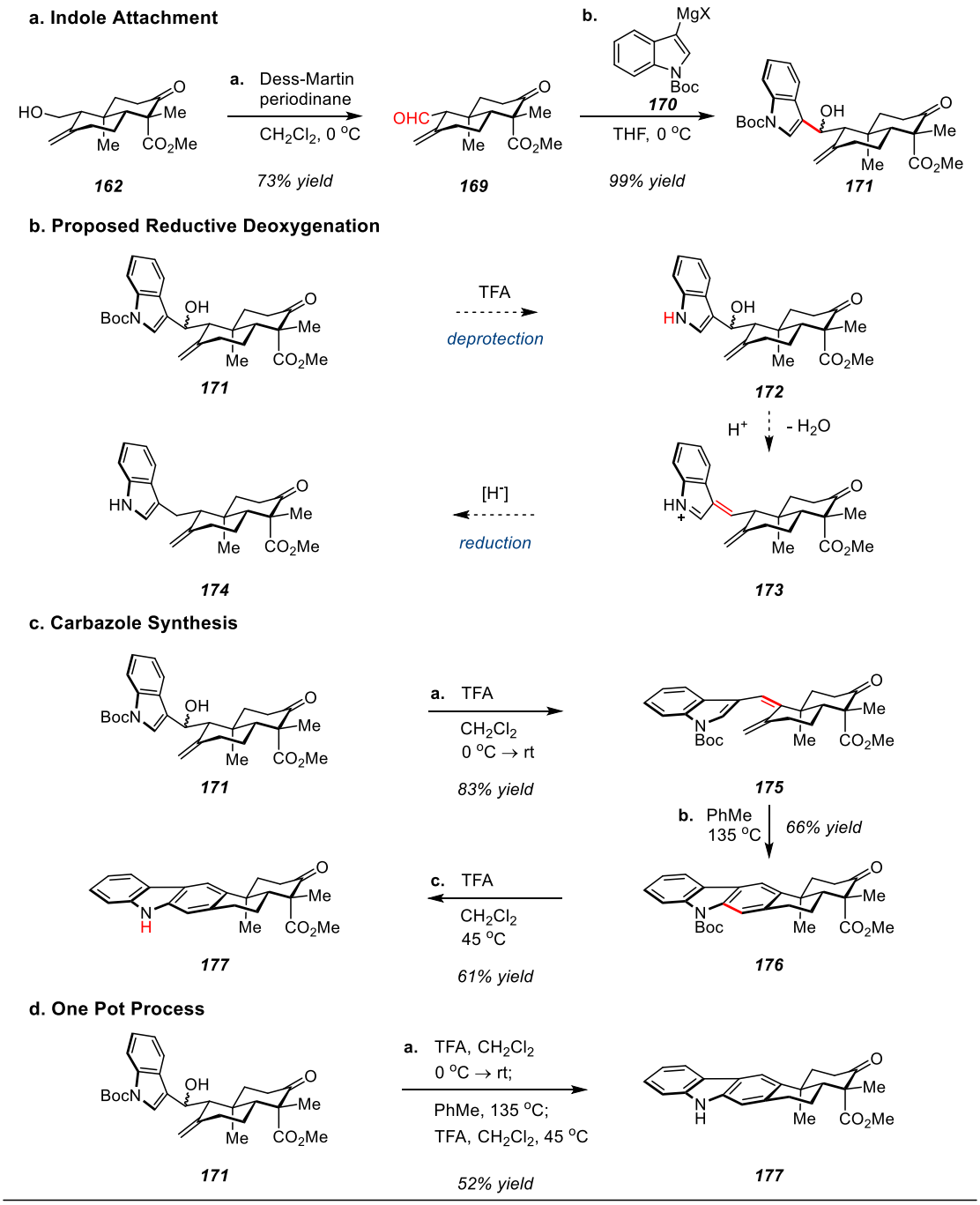

Scheme 3.3 Successful synthesis of the pentacyclic scaffold.

trapped with a silane reductant to form **174**. Surprisingly, the addition of TFA cleanly afforded the triene product **175**, arising from dehydration of the

secondary alcohol (Scheme 3.3.c). None of the deprotected material **172** was detected.

In light of the unexpected dehydration, a new strategy was adopted for the synthesis of oridamycin A. It was envisioned that the triene **175** could be induced to undergo a 6π-electrocyclization/aromatization sequence to generate the desired carbazole. Previous work on anominine further supported this strategy.[26] Heating triene **175** in PhMe at 100 °C failed to induce electrocyclization, but increasing the temperature to 135 °C successfully provided the desired protected carbazole **176** (Scheme 3.3.c). The carbamate protecting group was successfully removed using TFA at 45 °C to produce carbazole **177**. At this stage, a one-pot procedure was considered to increase the efficiency of the synthesis. The three preceding operations seemed primed for adaptation to a telescoped protocol. To start the one-pot process, TFA was added to dehydrate secondary alcohol **171**, forming triene **175** (Scheme 3.3.d). The resultant solution was condensed via rotary evaporation, removing both solvent and acid (TFA b.p. = 72.4 °C). After condensation, the crude material was dissolved in PhMe, transferred to a pressure tube, and heated to 135 °C to affect the desired 6π-electrocyclization/aromatization. After completion, the solution was cooled to 45 °C and TFA was added to remove the *tert*-butyl carbamate protecting group, yielding carbazole **177**. This three-step, one-pot procedure proved efficient, generating carbazole **177** in 52% yield from secondary alcohol **171**.

Only two operations separated carbazole **177** from oridamycin A: reduction of the ketone to the secondary alcohol, and saponification of the methyl ester to the free acid. Reduction with $NaBH_4$ proceeded

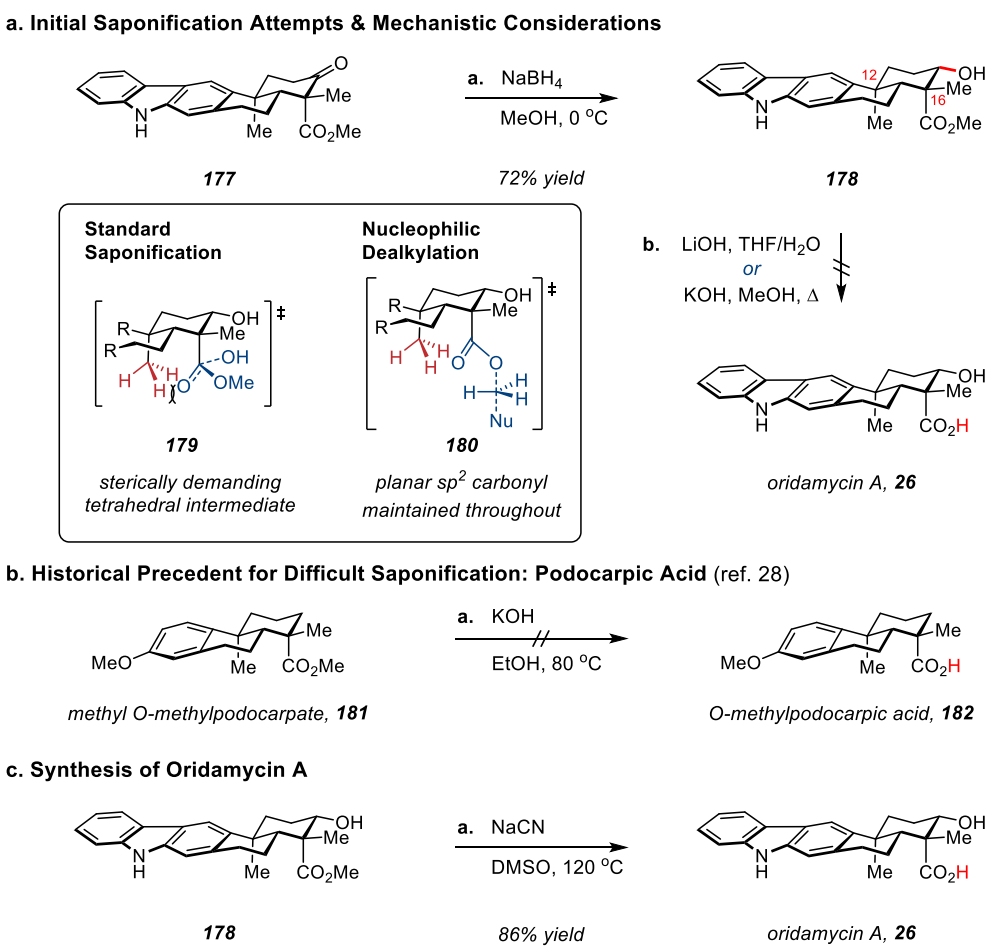

Scheme 3.4 Successful synthesis of oridamycin A using a nucleophilic ester dealkylation.

uneventfully, successfully delivering hydride from the less hindered face to selectively produce desired secondary alcohol **178** (Scheme 3.4.a). All that remained was saponification of the methyl ester. Initial attempts using standard saponification conditions (LiOH in THF/H_2O, KOH in MeOH) either returned starting material at low temperature, or decomposed starting material at elevated temperature (>100 °C). It seemed likely that formation of the requisite tetrahedral intermediate **179** *en route* to the desired acid was disfavored due to the sterically demanding 1,3-diaxial

relationship between the C16 ester–hydroxide adduct **179** and the C12 methyl group. Similar observations have been made on the structurally related derivatives of podocarpic acid **181**, dating back to structural determination studies conducted in the 1930s (Scheme 3.4.b).[29-31] In fact, it was reported that the ester was "unaffected by boiling 0.5N-alcoholic potassium hydroxide; hydrolysis of methyl O-methylpodocarpate with excess of concentrated alcoholic potash at 150°, however, afforded O-methylpodocarpic acid."[29] Since potash was unavailable, an alternate strategy was considered. If the ester could remain planar throughout the saponification process, then the steric requirement of the tetrahedral intermediate could be eliminated. It was hypothesized that a nucleophilic cleavage protocol would be possible, in which a nucleophile would engage the alkyl group on the ester in an S_N2 fashion to generate the free acid (Scheme 3.4.a, **180**). Krapcho decarboxylation conditions were employed for this transformation, as the Krapcho decarboxylation is thought to proceed through a similar mechanism, except the traditional Krapcho includes an anion stabilizing group such that the resultant free acid is lost as CO_2. Pleasingly, treatment of ester **178** with LiCl in DMF at 160 °C provided detectable quantities of oridamycin A. It was then found that NaCN in DMSO at 120 °C was a more effective combination, directly providing pure oridamycin A in 86% yield (Scheme 3.4.c).

In conclusion, oridamycin A was accessed in 9 steps from geranyl acetate in 4.7% overall yield. The sequence employs a key free-radical cyclization of a linear precursor to generate the *trans*-decalin ring system, correctly producing three contiguous stereocenters in a single operation. The carbazole was forged through a 6π-electrocyclization/aromatization

sequence, fusing the *trans*-decalin to the aromatic system. Finally, a difficult saponification was overcome through nucleophilic dealkylation, allowing the carbonyl to remain planar throughout the process. The next challenge was to install the hydroxymethyl substituent present in oridamycin B.

C. Synthesis of Oridamycin B

The difference between oridamycin A and oridamycin B is a single hydroxyl group. Oridamycin B harbors a hydroxymethyl substituent at C16, while oridamycin A contains a methyl at that position. Late-stage conversion of oridamycin A to oridamycin B would require a C-H oxidation, converting an inert C-H bond into a C-O bond. Thankfully, there is proximal functionality available in oridamycin A that could serve to direct a transition-metal mediated C-H oxidation. Specifically, it was envisioned that the secondary alcohol of **178/183** could serve as a directing group for an Ir-catalyzed C-H silylation, producing a silacycle (**184/185**) that could be oxidized using the Tamao method to produce the desired C-O bond (Scheme 3.5.a).[32] When these conditions were employed on ester **178** or **183**, the desired silacycles **184/185** were detected by UPLC-MS, but the reaction mixture was complicated by side products, and the desired product could not be purified and isolated. The protocol for the Ir-catalyzed C-H silylation involves the use of a glove box to exclude H_2O and O_2. Unfortunately, no glove box was readily available, so this strategy was abandoned.

As an alternative, a Pd^{II}-catalyzed C-H oxidation was explored. This method requires the installation of a strongly Lewis basic oxime to act as a

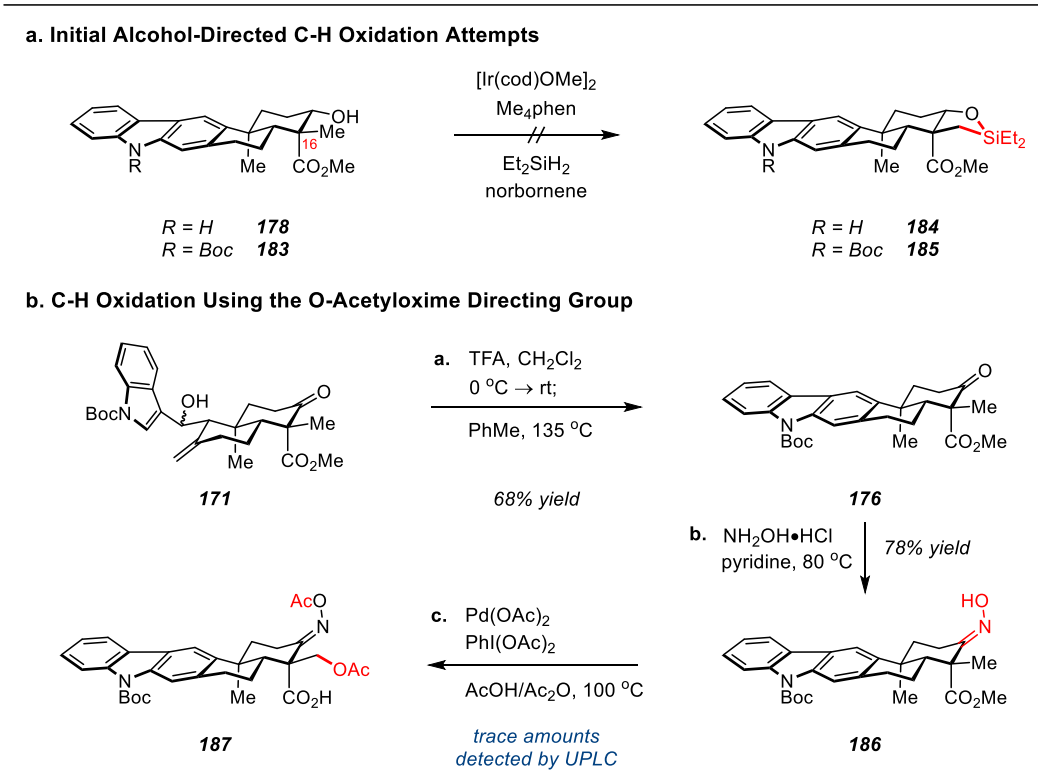

Scheme 3.5 Initial attempts to install the hydroxymethyl substituent through a directed C-H oxidation.

directing group.[33-34] O-Methyloximes are often used as directing groups for these transformations, but they are difficult to remove, requiring strong acidic conditions. With the hope of avoiding these harsh conditions, a method reported by Sanford was explored in which an oxime is installed and is converted to an O-acetyloxime *in situ* (Ac_2O/AcOH as solvent).[35] The O-acetyloxime serves as the directing group, and is significantly easier to remove than an O-methyloxime.

Anticipating difficulties conducting the C-H oxidation in the presence of the Lewis basic carbazole nitrogen, the *tert*-butyl carbamate protected carbazole **176** was prepared. The three-step, one-pot protocol for carbazole formation was modified to a two-step, one-pot protocol by

withholding TFA addition at the end of the sequence, directly yielding *tert*-butyl carbamate carbazole **176** from secondary alcohol **171** in 68% yield (Scheme 3.5.b). The oxime was installed without difficulty, and the resulting oxime **186** was treated with $Pd(OAc)_2$ and $PhI(OAc)_2$ in 1/1 $AcOH/Ac_2O$ at 100 °C. The resultant material was a complex mixture of compounds, but the desired compound **187** could be detected by mass via UPLC. The mass analysis also revealed that a significant amount of deprotected carbazole was present, indicating that AcOH at elevated temperature was sufficient to cleave the *tert*-butyl carbamate. Furthermore, approximately equal amounts of oxime and O-acetyloxime were present, indicating that the formation of the O-acetyloxime directing group was inefficient under the conditions. The resulting complex mixture resisted purification, and the desired compound could not be isolated. To avoid complications with the protecting group, the C-H oxidation was attempted on the unprotected carbazole, but that strategy proved untenable, generating a complex mixture.

To further minimize the number of possible side products, a more robust protecting group and a more predictable oxime were used. Specifically, the tosyl-protected carbazole harboring an O-methyloxime was synthesized (Scheme 3.6.a). Successful installation of the tosyl group required deprotonation with NaH and treatment with *p*-TsCl at 50 °C. Introduction of the oxime was straightforward, and the resulting O-methyloxime **187** was subjected to the reported C-H oxidation conditions.[33] Pleasingly, the desired acetoxymethyl **189** was formed, presumably via the five-membered palladacycle **188**.

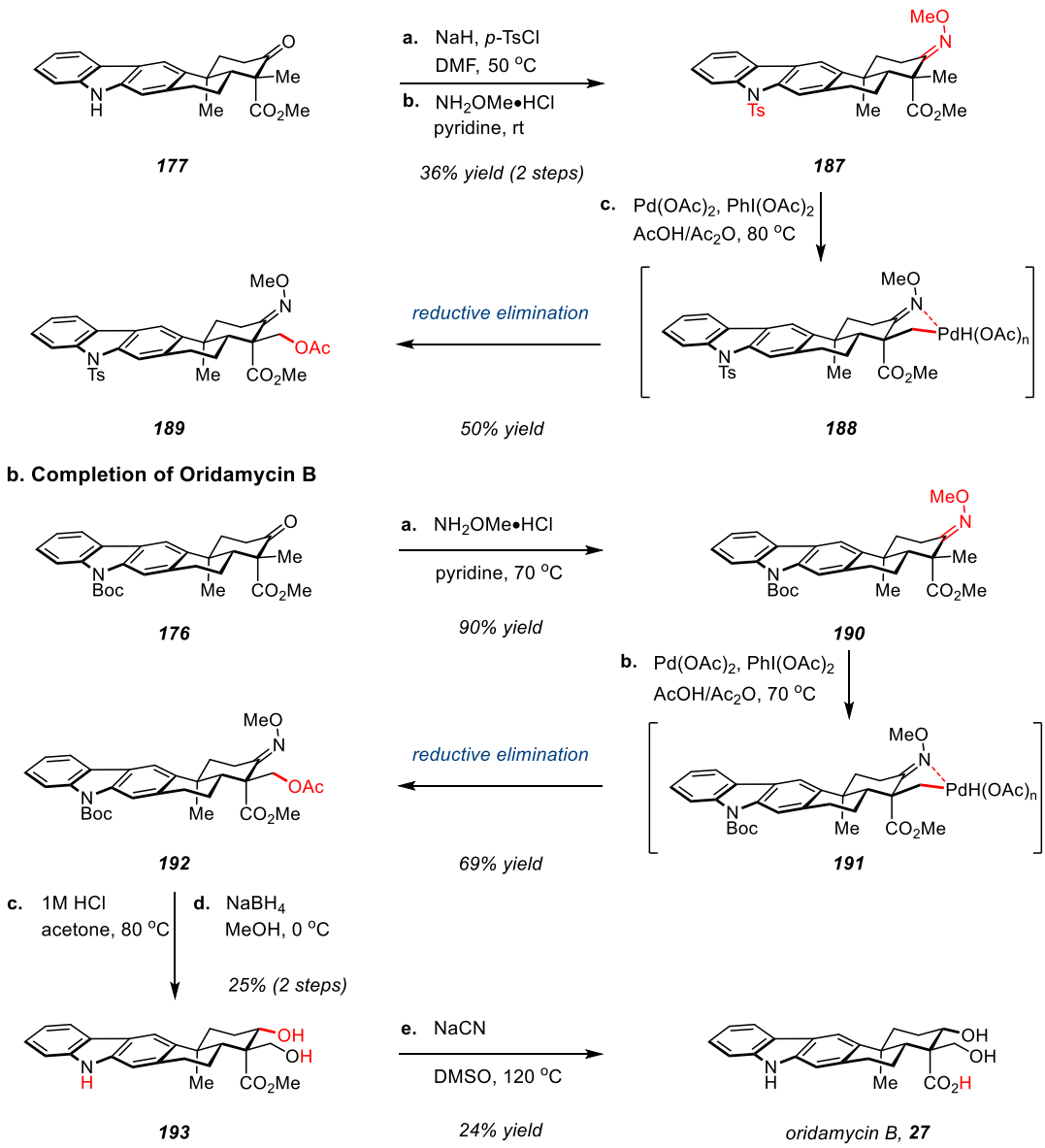

Scheme 3.6.a Successful C-H oxidation on tosyl-protected model compound **187**, **b** completion of oridamycin B (**27**).

The promising result on tosyl protected O-methyloxime **187** prompted reexamination of the *tert*-butyl carbamate protected compound **176**. The *tert*-butyl carbamate protecting group is already present earlier in the synthesis, eliminating the unnecessary deprotection, re-protection, and

deprotection sequence required for the tosyl protected series. Furthermore, the deprotection of the *tert*-butyl carbamate could be conducted at the same time as removal of the oxime and acetate protecting groups, allowing for a global deprotection protocol using aqueous acid. Initial C-H oxidation experiments yielded the desired product **192**, but in relatively low yield. Lowering the temperature and increasing the reaction time increased the yield, presumably by decreasing the formation of deprotected carbazole, which likely interferes with the palladium catalyst. Ultimately, optimal conditions were found that yield oxidized product **192** in 69% yield. The final remaining steps to complete oridamycin B include global deprotection, reduction of the ketone, and saponification of the ester.

Global deprotection of O-methyloxime **192** was problematic. More specifically, removal of the O-methyloxime was difficult—cleavage of the carbamate and acetyl groups proceeded under relatively mild conditions. As predicted, the harsh conditions required to remove the O-methyloxime caused significant loss of material. After extensive experimentation, it was found that the desired diol **193** could be obtained through treatment of protected O-methyloxime **192** with a mixture of aqueous 1M HCl and acetone at 80 °C, which was immediately followed by treatment of the crude material with $NaBH_4$ to reduce the ketone. Conversion of diol **193** into oridamycin B (**27**) ensued using the conditions optimized for oridamycin A, albeit in lower yield.

In conclusion, oridamycin B was accessed in 12 steps from geranyl acetate in 0.37% overall yield. The yield is lower for oridamycin B relative to oridamycin A because of difficulties with the last steps, including oxime

removal. Ultimately, however, this strategy still represents an efficient protocol for producing this pentacyclic natural product, accessing oridamycin B from common synthetic intermediate **171** in just 6 steps.

REFERENCES

[1] Gonzalez, M. A., & Molina-Navarro, S., Attempted synthesis of spongidines by a radical cascade terminating onto a pyridine ring. *J. Org. Chem.* **2007,** 72, 7462–7465.

[2] Jenny, L., & Borschberg, H. J., Synthesis of the dolabellane diterpene hydrocarbon (±)- δ -araneosene. *Helv. Chim. Acta* **1995,** 78, 715-731.

[3] Kitagawa, Y., Itoh, A., Hashimoto, S., Yamamoto, H., & Nozaki, H., Total synthesis of humulene - Stereoselective approach. *J. Am. Chem. Soc.* **1977,** 99, 3864–3867.

[4] Arigoni, D., Vasella, A., Sharpless, K. B., & Jensen, H. P., Selenium dioxide oxidations of olefins. Trapping of the allylic seleninic acid intermediate as a seleninolactone. *J. Am. Chem. Soc.* **1973,** 95, 7917–7919.

[5] Sharpless, K. B., & Lauer, R. F., Selenium dioxide oxidation of olefins. Evidence for the intermediacy of allylseleninic acids. *J. Am. Chem. Soc.* **1972,** 94, 7154–7155.

[6] Warpehoski, M. A., Chabaud, B., & Sharpless, K. B., Selenium dioxide oxidation of endocyclic olefins. Evidence for a dissociation-recombination pathway. *J. Org. Chem.* **1982,** 47, 2897–2900.

[7] Nawrat, C. C., Lewis, W., & Moody, C. J., Synthesis of amino-1,4-benzoquinones and their use in Diels–Alder approaches to the aminonaphthoquinone antibiotics. *J. Org. Chem.* **2011,** 76, 7872–7881.

[8] Zhu, X., & Ganesan, A., Regioselective synthesis of 3-alkylindoles mediated by zinc triflate. *J. Org. Chem.* **2002,** 67, 2705–2708.

[9] Yang, D., Xu, M., & Bian, M.-Y., Chiral auxiliaries for asymmetric radical cyclization reactions: Application to the enantioselective synthesis of (+)-triptocallol. *Org. Lett.* **2000,** 3, 111–114.

[10] Snider, B. B., Mohan, R., & Kates, S. A., Manganese(III)-based oxidative free-radical cyclization. Synthesis of (±)-podocarpic acid. *J. Org. Chem.* **1985,** 50, 3659–3661.

[11] Snider, B. B., Mohan, R., & Kates, S. A., Manganese(III)-based oxidative free-radical cyclizations 2. Polycyclization reactions proceeding through tertiary cations. *Tetrahedron Lett.* **1987,** 28, 841–844.

[12] Zoretic, P. A., Fang, H. Q., & Ribeiro, A. A., Synthesis of *d*,*l*-norlabdane oxide and related odorants: An intramolecular radical approach. *J. Org. Chem.* **1998,** 63, 4779–4785.

[13] Snider, B. B., Patricia, J. J., & Kates, S. A., Mechanism of manganese(III)-based oxidation of β -keto-esters. *J. Org. Chem.* **1988,** 53, 2137-2143.

[14] Snider, B. B., Manganese(III)-based oxidative free-radical cyclizations. *Chem. Rev.* **1996,** 96, 339–364.

[15] Corey, E. J., & Kang, M. C., A new and general synthesis of polycyclic γ -lactones by double annulation. *J. Am. Chem. Soc.* **1984,** 106, 5384-5385.

[16] Curran, D. P., Morgan, T. M., Schwartz, C. E., Snider, B. B., & Dombroski, M. A., Cyclizations of unsaturated •$CR(COX)_2$ radicals. Manganese(III) acetate oxidative cyclizations of unsaturated acetoacetates and atom-transfer cyclizations of unsaturated haloacetoacetates give the same radicals. *J. Am. Chem. Soc.* **1991,** 113, 6607–6617.

[17] Curran, D. P., Chen, M. H., & Kim, D., Atom transfer cyclization reactions of hex-5-ynyl iodides: Synthetic and mechanistic studies. *J. Am. Chem. Soc.* **1989,** 111, 6265–6276.

[18] Kates, S. A., Dombroski, M. A., & Snider, B. B., Manganese(III)-based oxidative free-radical cyclization of unsaturated β -keto esters, 1,3-diketones, and malonate diesters. *J. Org. Chem.* **1990,** 55, 2427-2436.

[19] Julia, M., Free-radical cyclizations. *Acc. Chem. Res.* **1971,** 4, 386–392.

[20] Heiba, E. I., & Dessau, R. M., Oxidation by metal salts. IX. Formation of cyclic ketones. *J. Am. Chem. Soc.* **1972,** 94, 2888–2889.

[21] Heiba, E.-A. I., & Dessau, R. M., Oxidation by metal salts. VII. Syntheses based on the selective oxidation of organic free radicals. *J. Am. Chem. Soc.* **1971,** 93, 524–527.

[22] Kochi, J. K., Electron-transfer mechanisms for organometallic intermediates in catalytic reactions. *Acc. Chem. Res.* **1974,** 7, 351–360.

[23] Dess, D. B., & Martin, J. C., A useful 12-I-5 triacetoxyperiodinane (the Dess–Martin periodinane) for the selective oxidation of primary or

secondary alcohols and a variety of related 12-I-5 species. *J. Am. Chem. Soc.* **1991,** *113*, 7277–7287.

[24] Dess, D. B., & Martin, J. C., Readily accessible 12-I-5 oxidant for the conversion of primary and secondary alcohols to aldehydes and ketones. *J. Org. Chem.* **1983,** *48*, 4155–4156.

[25] Watson, C. G., & Aggarwal, V. K., Asymmetric synthesis of 1-heteroaryl-1-arylalkyl tertiary alcohols and 1-pyridyl-1-arylethanes by lithiation–borylation Methodology. *Org. Lett.* **2013,** *15*, 1346–1349.

[26] Bian, M., Wang, Z., Xiong, X., Sun, Y., Matera, C., Nicolaou, K. C., & Li, A., Total syntheses of anominine and tubingensin A. *J. Am. Chem. Soc.* **2012,** *134*, 8078–8081.

[27] Bennasar, M. L., Zulaica, E., Jimenez, J. M., & Bosch, J., Studies on the synthesis of mavacurine-type indole alkaloids. First total synthesis of (±)-2,7-dihydropleiocarpamine. *J. Org. Chem.* **1993,** *58*, 7756–7767.

[28] Mewshaw, R. E., Meagher, K. L., Zhou, P., Zhou, D., Shi, X., Scerni, R., Smith, D., Schechter, L. E., & Andree, T. H., Studies toward the discovery of the next generation of antidepressants. Part 2: Incorporating a 5-HT1A antagonist component into a class of serotonin reuptake inhibitors. *Bioorg. Med. Chem. Lett.* **2002,** *12*, 307–310.

[29] Sherwood, I. R., & Short, W. F., 192. Podocarpic acid. Part I. *J. Chem. Soc.* **1938,** 1006–1013.

[30] Wenkert, E., Afonso, A., Bredenberg, J. B. s., Kaneko, C., & Tahara, A., Synthesis of some resin acids. *J. Am. Chem. Soc.* **1964,** *86*, 2038–2043.

[31] Wenkert, E., & Jackson, B. G., Partial degradation and reconstitution of podocarpic acid. A novel method of hydrolysis of highly sterically hindered esters. *J. Am. Chem. Soc.* **1958,** *80*, 217–219.

[32] Simmons, E. M., & Hartwig, J. F., Catalytic functionalization of unactivated primary C-H bonds directed by an alcohol. *Nature* **2012,** *483*, 70–73.

[33] Desai, L. V., Hull, K. L., & Sanford, M. S., Palladium-catalyzed oxygenation of unactivated sp3 C-H bonds. *J. Am. Chem. Soc.* **2004,** *126*, 9542–9543.

[34] Baldwin, J. E., Jones, R. H., Najera, C., & Yus, M., Functionalisation of unactivated methyl groups through cyclopalladation reactions. *Tetrahedron* **1985,** *41*, 699–711.

[35] Neufeldt, S. R., & Sanford, M. S., O-Acetyl oximes as transformable directing groups for Pd-catalyzed C-H bond functionalization. *Org. Lett.* **2010,** *12*, 532–535.

Chapter 4. Progress Towards Xiamycin A

Preface

This chapter outlines strategies used towards the trans*-decalin associated with xiamycin A and the dimeric natural products. The approaches were developed through mechanistic considerations and relevant literature precedent, with photoredox catalysis proving to be the most promising avenue to date.*

A. Initial Efforts

As previously outlined, xiamycin A (**28**) was envisioned to arise from the same linear precursor used to access the oridamycins. Introduction of a Lewis acid would produce chelated radical intermediate **194**, leading to the formation of the C16 epimeric *trans*-decalin (Scheme 4.1.a, **195**). The simplest strategy to access the desired intermediate **194** involves addition of a Lewis acid to the Mn^{III}-mediated oxidative radical cyclization. There is literature precedent that this is a viable option. Yang and coworkers

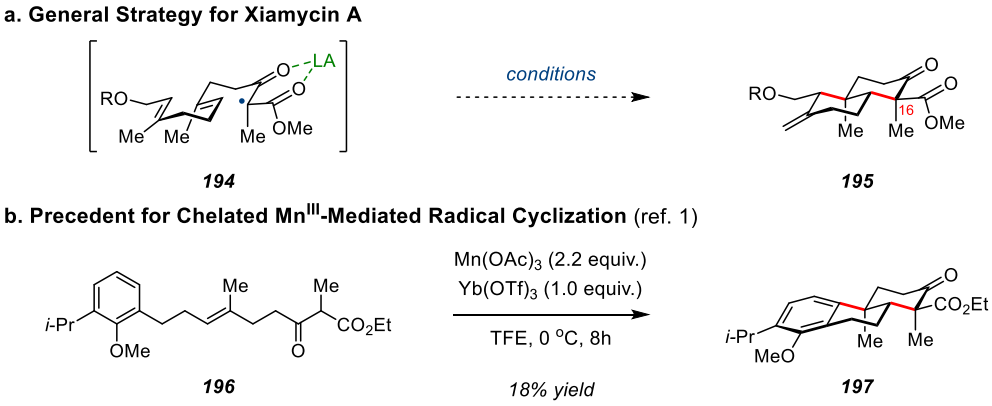

Scheme 4.1.a General strategy for chelated cyclization, and **b** precedent.

Table 4.1 Attempts at a chelated Mn^{III}-mediated oxidative radical cyclization.

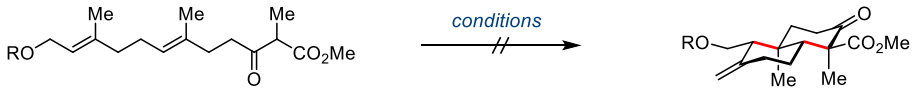

198 *195*

Entry	*Substrate (R)*	*Solvent*	*Oxidant (equiv.)*	*Co-oxidant (equiv.)*	*Lewis acid (equiv.)*	*Temp (°C)*	*Time*	*Result*
1	H	TFE	$Mn(OAc)_3$ (2.1)	–	$Yb(OTf)_3$ (1.0)	0	3h	decomp.
2	H	TFE	$Mn(OAc)_3$ (2.1)	–	$Yb(OTf)_3$ (1.0)	-20	36h	decomp.
3	Ac	TFE	$Mn(OAc)_3$ (2.1)	–	$Yb(OTf)_3$ (1.0)	0	7h	complex mixture
4	H	TFE	$Mn(OAc)_3$ (2.1)	$Cu(OAc)_2$ (1.0)	$Yb(OTf)_3$ (1.0)	-20	36h	complex mixture
5	H	TFE	$Mn(OAc)_3$ (2.2)	$Cu(OAc)_2$ (1.0)	$Yb(OTf)_3$ (1.0)	0	0.3h	decomp.
6	H	TFE	$Mn(OAc)_3$ (2.0)	$Cu(OAc)_2$ (1.0)	–	0	12h	decomp.
7	H	CH_2Cl_2	$Mn(OAc)_3$ (2.1)	$Cu(OAc)_2$ (1.0)	$Yb(OTf)_3$ (1.0)	-78 to 40	48h	complex mixture
8	H	THF	$Mn(OAc)_3$ (2.2)	$Cu(OAc)_2$ (1.0)	$MgCl_2$ (5.0)	rt	4h	decomp.
9	H	CH_2Cl_2	$Mn(OAc)_3$ (2.1)	$Cu(OAc)_2$ (1.0)	$Mg(ClO_4)_2$ (1.0)	-78 to 40	48h	decomp.

reported that addition of $Yb(OTf)_3$ to a $Mn(OAc)_3$-mediated cyclization of **196** yielded the tricyclic compound **197** containing the desired stereochemistry (Scheme 4.1.b).[1] The yield was low (18%), but these results appeared to be a promising lead for further optimization. Unfortunately, employing the conditions described by Yang *et al.* did not provide the desired *trans*-decalin **195** (Table 4.1, Entry 1). Lower temperature and longer reaction time failed to improve the results (Entry 2). The allylic alcohol was protected as the acetate to minimize potential disruptive interactions with the Lewis acid, but this also failed to improve the reaction (Entry 3). The co-oxidant $Cu(OAc)_2$ was introduced to assist with termination of the final alkyl radical species, but this strategy was unsuccessful (Entries 4-9). Interestingly, the cyclization failed without Lewis acid if TFE was used as the solvent, even when all other variables were identical to the conditions successfully employed for the synthesis of the oridamycins (Entry 6). Using

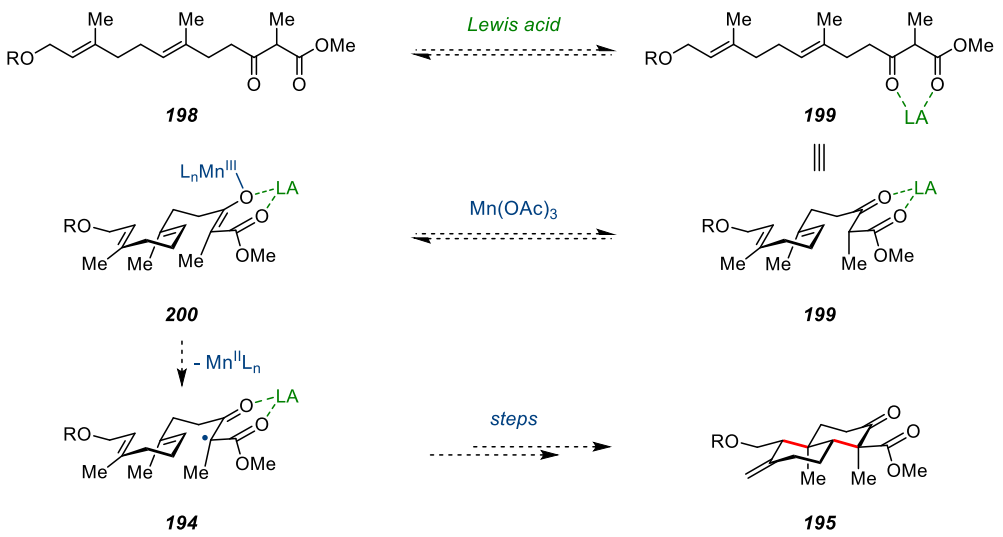

Scheme 4.2 Mechanistic considerations for the chelated Mn^{III}-mediated oxidative radical cyclization.

other solvents (THF, CH_2Cl_2) and other Lewis acids ($MgCl_2$, $Mg(ClO_4)_2$) also failed to provide the desired material (Entries 7-9). Ultimately, this avenue was abandoned.

B. Mechanistic Considerations & Alternate Strategies

Before considering alternate strategies for chelated radical cyclizations, the mechanism of the chelated Mn^{III}-mediated oxidative radical cyclization was examined. For a successful chelated cyclization, the first step would involve engagement of the Lewis acid with the β-keto ester to form intermediate **199** (Scheme 4.2). Next, the Mn^{III} enolate **200** would arise in a process analogous to the unchelated cyclization (see Scheme 3.2.b). The resultant enolate **200** would undergo electron transfer to generate the chelated radical **194** and a Mn^{II} species. As previously mentioned, the resultant Mn^{II} salt does not maintain an interaction with the

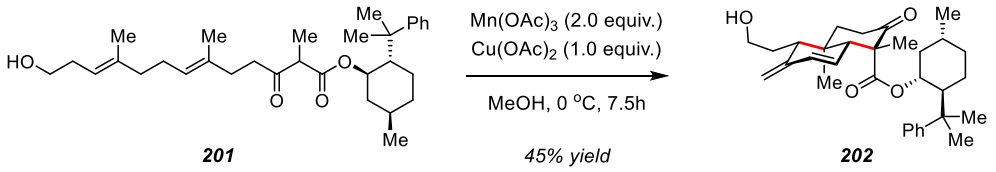

Scheme 4.3 Precedent indicating that increasing the steric bulk of the ester will not change the diastereoselectivity.

substrate after electron transfer.[2] To produce chelated radical intermediate **194**, the Lewis acid would need to maintain coordination to the substrate throughout this process (**199** to **194**). It seems unlikely that a free radical intermediate would exist long enough to allow for the Lewis acid to intercept it prior to cyclization, requiring an intermolecular interaction to outcompete the intramolecular cyclization of a highly reactive intermediate. Generating a substrate bound to two different transition metal complexes while generating a highly reactive radical intermediate seemed like a difficult construct to engineer (Scheme 4.2, **200**). A simpler solution was sought.

Since the transition state with an equatorial ester and an axial methyl group was sought, it seemed possible that increasing the steric bulk of the ester substituent so that it became larger than the methyl group could provide the desired stereochemical arrangement. Unfortunately, even isopropyl esters (~1.2) have a smaller A-value than methyl groups (~1.7), presumably because the ester can orient the bulky alkyl substituent away from the ring to minimize steric interactions. Furthermore, large chiral auxiliaries have been used in Mn^{III}-mediated cyclizations that produce the stereochemistry associated with the oridamycins (Scheme 4.3).[3] These

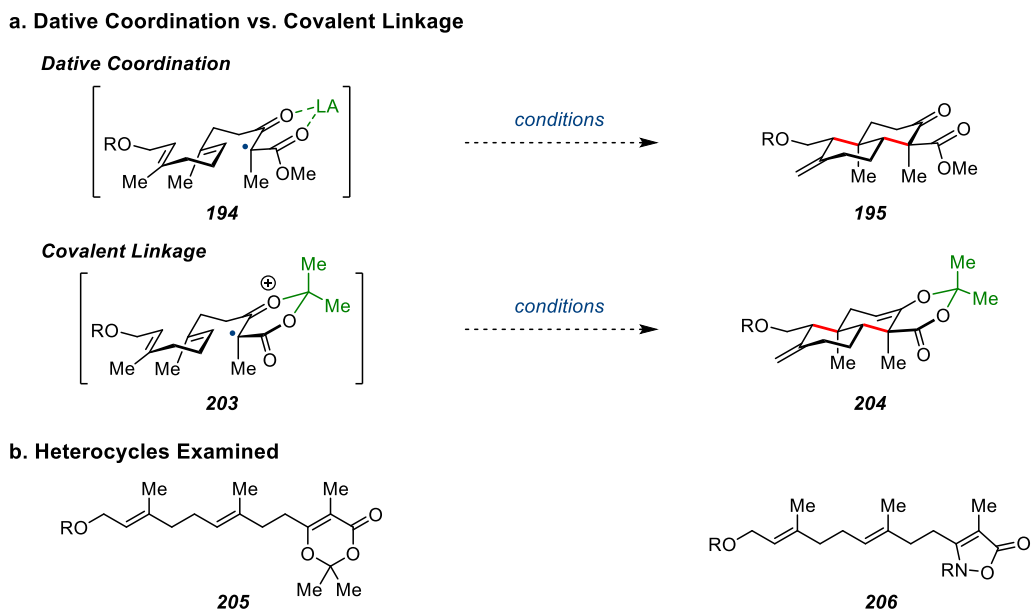

Scheme 4.4 Attempts at using heterocycles to obtain the desired stereochemistry.

results suggest that ester modification would be a fruitless endeavor towards xiamycin A.

Another strategy would be to use a covalent linkage instead of a dative coordination to hold the two functional groups in the correct orientation. The most straightforward example would be acetonide **203** (Scheme 4.4.a). In fact, this avenue was briefly explored on acetonide **205** and 5-isoxozolone **206** (Scheme 4.4.b). Several experiments using Mn^{III}-based and Ce^{IV}-based oxidants failed to produce the desired compound. Furthermore, this strategy required *de novo* synthesis of heterocyclic cyclization precursors, a process that abandons the original strategy of producing the xiamycin and oridamycin families from a common synthetic precursor.

C. Single-Electron Oxidation of Chelated Enolates

Another strategy would be to introduce the Lewis acid as the counterion for enolate **207** and then perform a single-electron transfer (SET) oxidation to generate the chelated radical cation **208** (Scheme 4.5.a). For the integrity of the counterion-substrate interaction to be maintained throughout the process, the SET oxidant must act through an outer sphere process, rather than an inner sphere process. An inner sphere process occurs when the substrate becomes a ligand for the oxidant, as exemplified by the Mn^{III}-mediated oxidation of β-keto esters (**199** to **194**). An outer sphere oxidation occurs without this requirement—the electron can move through space between the oxidant and the substrate.[4] The outer sphere oxidant would not disrupt the interaction between the enolate counterion

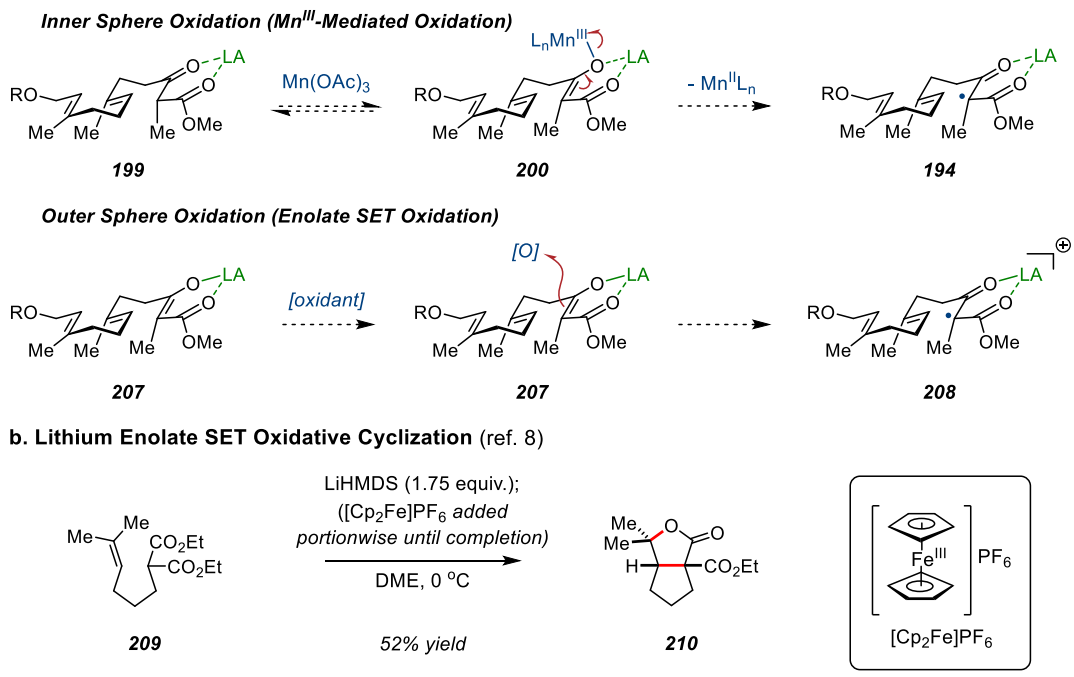

Scheme 4.5 Enolate SET strategy to access chelated radical cations.

and the substrate during oxidation, while an inner sphere oxidant would likely replace the counterion.

Relevant precedent includes oxidative radical cyclizations of enolates using ferrocenium-based oxidants such as $[Cp_2Fe]PF_6$ (Scheme 4.5.b).[5–18] Importantly, cyclizations of β-dicarbonyl compounds such as **209** have been demonstrated. Importantly, there is evidence that ferrocenium salts are outer sphere oxidants, minimizing disruption of the enolate–counterion interaction.[19] The majority of these cyclizations employ lithium enolates, but sodium, potassium, magnesium, zinc, silicon, and titanium enolates/enol ethers have also been cyclized with varying degrees of success.[10] Lithium enolates were chosen for pilot studies, since they have been reported to be the most consistent and straightforward for a wide variety of enolate oxidations.[20] At the outset, it was unclear if the lithium counterion would maintain a chelation interaction with both carbonyl substituents after SET oxidation. Optimism was derived from the Masamune–Roush modification of the Horner–Wadsworth–Emmons reaction, which employs LiCl to chelate β-phosphonate esters, lowering their pK_a values to so that they can be deprotonated with an amine base.[21]

Several substrates were prepared through protection of the allylic alcohol to prevent unwanted interactions between the allylic alcohol and the chelating counterions (Table 4.2). Lithium enolates were prepared using several different bases (LDA, *n*-BuLi, and LiHMDS) and in several solvents (THF, DME, and PhMe). In all cases, the desired *trans*-decalin **195** failed to form upon treatment with $[Cp_2Fe]PF_6$. Several reactions produced promising crude mixtures, but characterization of the resultant material was foiled because the products had the same R_f (these experiments are

Table 4.2 Enolate SET experiments with lithium enolates.

198 *195* *211*

Entry	*Substrate (R)*	*Solvent*	*Oxidant (equiv.)*	*Co-oxidant (equiv.)*	*Base (equiv.)*	*Temp (°C)*	*Time*	*Result*
1	TBS	THF	$[Cp_2Fe]PF_6$ (2.5)	—	nBuLi (1.3)/ i-Pr_2NH (1.2)	-78 to 0	1h	complex mixture
2	TBS	THF	$[Cp_2Fe]PF_6$ (2.5)	—	nBuLi (2.1)/ i-Pr_2NH (2.2)	-78 to 0	1h	complex mixture
3	TIPS	DME	$[Cp_2Fe]PF_6$ (2.5)	—	nBuLi (1.3)/ i-Pr_2NH (1.2)	-60 to 0	25h	inseparable mixture
4	TIPS	DME	$[Cp_2Fe]PF_6$ (2.5)	—	nBuLi (1.1)	-65 to -40	32h	inseparable mixture
5	TBS	DME	$[Cp_2Fe]PF_6$ (3.5)	—	LiHMDS (1.5)	-65 to -10	27h	inseparable mixture
6	TBS	DME	$[Cp_2Fe]PF_6$ (3.0)	—	LiHMDS (1.5)	0 to rt	6h	inseparable mixture
7	TBS	THF	$[Cp_2Fe]PF_6$ (2.5)	—	LiHMDS (1.2)	0	2h	inseparable mixture
8	TBS	PhMe	$[Cp_2Fe]PF_6$ (2.5)	—	LiHMDS (1.3)	-78 to rt	20h	inseparable mixture (contains **211**)
9	H	THF	$[Cp_2Fe]PF_6$ (2.5)	—	LiHMDS (1.1)	-78 to 0	2h	complex mixture
10	TBS	THF	$[Cp_2Fe]PF_6$ (2.5)	$Cu(OAc)_2$ (1.0)	LiHMDS (1.2)	0	2.5h	complex mixture
11	TBS	DME	$[Cp_2Fe]PF_6$ (3.5)	$Cu(OTf)_2$ (1.0)	LiHMDS (1.5)	-70 to 0	29h	decomp.
12	TBS	THF	$Cu(OTf)_2$ (2.5)	—	LiHMDS (1.5)	-78 to rt	24h	no rxn.
13	TBS	THF	$Cu(OTf)_2$ (3.5)	—	LiHMDS (1.5)	-78 to rt	48h	no rxn.
14	TBS	THF	$Fe(phen)_3(PF_6)_3$ (2.5)	—	LiHMDS (1.5)	-78 to 0	3h	decomp.

denoted by 'inseparable mixture,' Entries 3-8). Other outer sphere oxidants were examined, including $Cu(OTf)_2$ and $Fe(phen)_3(PF_6)_3$, but these also failed to produce the desired bicycle **195**. In one instance, trace bicycle **211** was detected in the crude NMR (Entry 8, yield not determined).

Table 4.3 Enolate SET experiments with zinc enolates. [A] Syringe pump.

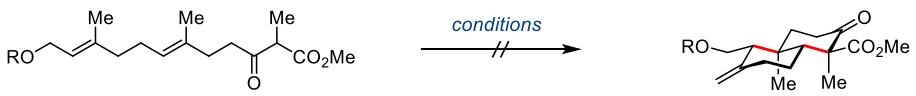

198 *195*

Entry	Substrate (R)	Solvent	Lewis acid / counterion (equiv.)	Oxidant (equiv.)	Co-oxidant (equiv.)	Base (equiv.)	Temp (°C)	Time	Result
1	H	THF	$Zn(OTf)_2$ (2.0)	$[Cp_2Fe]PF_6$ (2.5)	—	LiHMDS (1.1)	-78 to rt	1h	no rxn.
2	H	THF	$Zn(OTf)_2$ (2.0)	$[Cp_2Fe]PF_6$ (2.5)	$Cu(OAc)_2$ (1.0)	LiHMDS (1.1)	-78 to rt	1h	no rxn.
3	H	THF	$Zn(OTf)_2$ (1.5)	$Fe(phen)_3(PF_6)_3$ (2.5)	—	LiHMDS (1.1)	-78 to 0	0.5h	no rxn.
4	TBS	THF	$Zn(OTf)_2$ (1.5)	$Fe(phen)_3(PF_6)_3$ (2.5)	—	LiHMDS (1.3)	-80 to -20	19h	decomp.
5	TBS	THF	$Zn(OTf)_2$ (1.5)	$Fe(phen)_3(PF_6)_3$ (2.5)	—	LiHMDS (1.3)	-78 to rt	21h	complex mixture
6	TBS	THF	$Zn(OTf)_2$ (1.5)	$Fe(phen)_3(PF_6)_3$ (2.5)[A]	—	LiHMDS (1.3)	-78 to rt	16h	decomp.
7	TBS	THF	$Zn(OTf)_2$ (1.4)	$Fe(phen)_3(PF_6)_3$ (2.5)[A]	—	NaH (1.2)	rt	4h	decomp.
8	TBS	DME	$Zn(OTf)_2$ (1.5)	$Fe(phen)_3(PF_6)_3$ (2.5)	—	LiHMDS (1.3)	-78 to 0	7.5h	decomp.
9	TBS	MeCN	$Zn(OTf)_2$ (1.5)	$Fe(phen)_3(PF_6)_3$ (2.5)	—	LiHMDS (1.3)	-45 to -15	2.5h	no rxn.
10	TBS	DME	$Zn(OTf)_2$ (1.5)	$Fe(phen)_3(PF_6)_3$ (2.5)	$Cu(OAc)_2$ (1.0)	LiHMDS (1.3)	-78 to 0	7.5h	decomp.
11	TBS	THF	$Zn(OTf)_2$ (1.5)	$Ce(NH_4)_2(NO_3)_6$ (2.5)	—	LiHMDS (1.3)	-78	3h	no rxn.

Oxidations of zinc enolates were also conducted (Table 4.3). The enolates were formed through initial deprotonation with LiHMDS or NaH, followed by incubation of the resultant enolate with $Zn(OTf)_2$ at room temperature. The oxidation potential of $[Cp_2Fe]PF_6$ was too low to initiate radical cyclization, so the stronger oxidant $Fe(phen)_3(PF_6)_3$ was used (Entries 3-10). Unfortunately, none of the desired *trans*-decalin **195** was formed.

Promising precedent exists for the SET oxidation of titanium enolates (Scheme 4.6.a).[22-24] Specifically, it is known that the radical cation formed from titanium enolates derived from Cp_2TiCl_2 dissociates relatively slowly

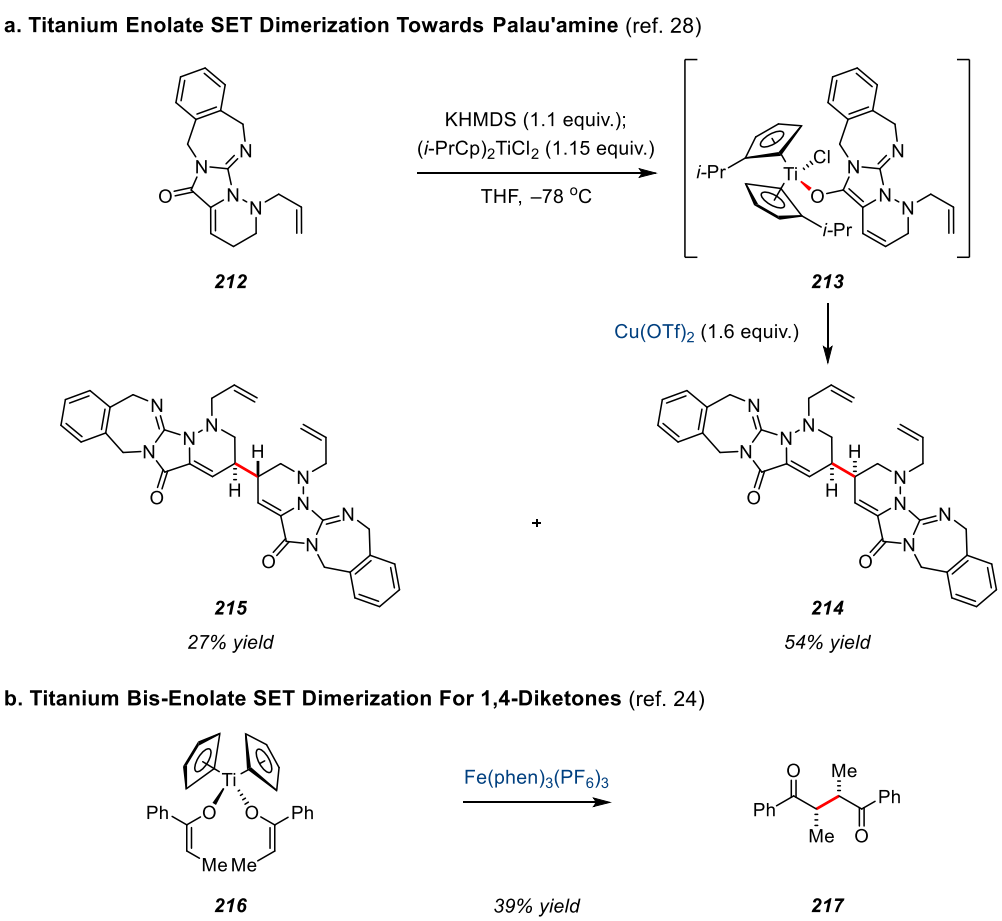

Scheme 4.6 Precedent for titanium enolate SET to generate electrophilic radical cations.

($k_{Ti\text{-}O}$ = ~3 x 10^{-2} s^{-1} in CH_2Cl_2), allowing for a chelated cyclization to occur before radical cation decomposition.[25-27] Harran and coworkers demonstrated the utility of titanium enolate oxidations in their work towards palau'amine, generating dimeric compounds **214** and **215** in good yield from titanium enolate **213** (Scheme 4.6.a).[28] While Harran et. al. used (*i*-PrCp)$_2$TiCl$_2$ as the counterion and Cu(OTf)$_2$ as the oxidant, the majority of studies use Cp$_2$TiCl$_2$ as the counterion and Fe(phen)$_3$(PF$_6$)$_3$ as the oxidant (Scheme 4.6.b).[22-27] Unfortunately, none of the conditions employed yielded the desired *trans*-decalin **195** (Table 4.4). At low temperature, starting

Table 4.4 Enolate SET experiments with titanium enolates. [A] Added with syringe pump.

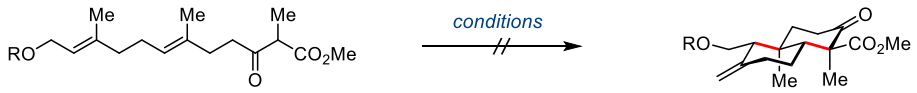

198 *195*

Entry	Substrate (R)	Solvent	Lewis acid / counterion (equiv.)	Oxidant (equiv.)	Base (equiv.)	Temp (°C)	Time	Result
1	TBS	THF	Cp_2TiCl_2 (1.1)	$Fe(phen)_3(PF_6)_3$ (2.5)	NaH (1.1)	-50	5h	no rxn.
2	TBS	THF	Cp_2TiCl_2 (1.1)	$Fe(phen)_3(PF_6)_3$ (2.5)	NaH (1.2)	-20	12h	mostly sm
3	TBS	THF	Cp_2TiCl_2 (1.5)	$Fe(phen)_3(PF_6)_3$ (2.5)[A]	LiHMDS (1.3)	-78 to rt	4h	no rxn.
4	TBS	PhMe	Cp_2TiCl_2 (1.3)	$Fe(phen)_3(PF_6)_3$ (2.5)	NaH (1.1) / K_2CO_3 (2.5)	0 to 85	24h	complex mixture
5	TBS	THF	Cp_2TiCl_2 (1.5)	$Ce(NH_4)_2(NO_3)_6$ (2.5)	LiHMDS (1.3)	-78 to rt	14h	complex mixture
6	Ac	MeCN	Cp_2TiCl_2 (1.2)	$Ce(NH_4)_2(NO_3)_6$ (2.5)	LiHMDS (1.1)	0	12h	decomp. (mostly sm)
7	TBS	THF	$Ti(Oi\text{-}Pr)_4$ (1.15)	$Fe(phen)_3(PF_6)_3$ (2.5)	NaH (1.1)	-50 to -10	23h	decomp.
8	TBS	THF	$Ti(Oi\text{-}Pr)_4$ (1.4)	$[Cp_2Fe]PF_6$ (2.5)	NaH (1.4)	-5	4h	inseparable mixture

material was returned (Entries 1-3), and at higher temperatures a complex mixture of compounds was obtained (Entry 4). Further efforts using $Ce(NH_4)_2(NO_3)_6$ and $[Cp_2Fe]PF_6$ as oxidants, and $Ti(Oi\text{-}Pr)_4$ as the counterion were also unsuccessful (Entries 5-8).

Several other attempts were made to oxidize various metal enolates to promote a chelated radical cyclization (Table 4.5). Entry 1 was inspired by a recent publication detailing the diradical character of enolates derived from $TiCl_4$ (Scheme 4.7).[29] Zakarian and coworkers have leveraged this property to trap *in situ* generated $\bullet CCl_3$ to diastereoselctively produce **221** from oxazolidinone **218**. In the present case, it was hypothesized that a diradical intermediate could be intramolecularly intercepted by the internal

Table 4.5 Other enolate SET experiments.

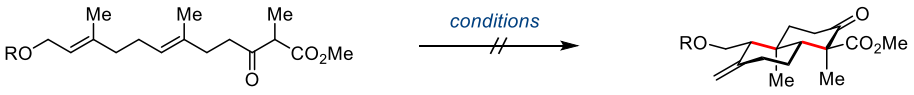

198 *195*

Entry	*Substrate (R)*	*Solvent*	*Lewis acid / counterion (equiv.)*	*Oxidant (equiv.)*	*Base (equiv.)*	*Temp (°C)*	*Time*	*Result*
1	H	CH_2Cl_2	—	$TiCl_4$ (1.1)	*i*-Pr_2NEt (1.1)	0	10 min	decomp.
2	H	AcOH	—	$Ce(NH_4)_2(NO_3)_6$ (2.5)	—	rt	23h	decomp.
3	TBS	THF	—	$[Cp_2Fe]PF_6$ (2.5)	EtMgBr (1.2)/ *i*-Pr_2NH (1.3)	-30 to 0	6h	no rxn.
4	TBS	THF/HMPA	—	$[Cp_2Fe]PF_6$ (2.5)	EtMgBr (1.2)/ *i*-Pr_2NH (1.3)	-78 to 0	5.5h	mostly sm
5	Ac	THF	$EtAlCl_2$ (1.1)	$Ce(NH_4)_2(NO_3)_6$ (2.5)	LiHMDS (1.1)	-78 to rt	17.5h	no rxn.
6	Ac	PhMe	$Yb(OTf)_3$ (1.3)	$Fe(phen)_3(PF_6)_3$ (2.5)	LiHMDS (1.2)	0 to 50	25h	decomp.

olefin to produce the desired bicycle **195**, using Ti^{IV} as both the oxidant and the Lewis acid. The reaction was unsuccessful, but the concept would become important in future studies.

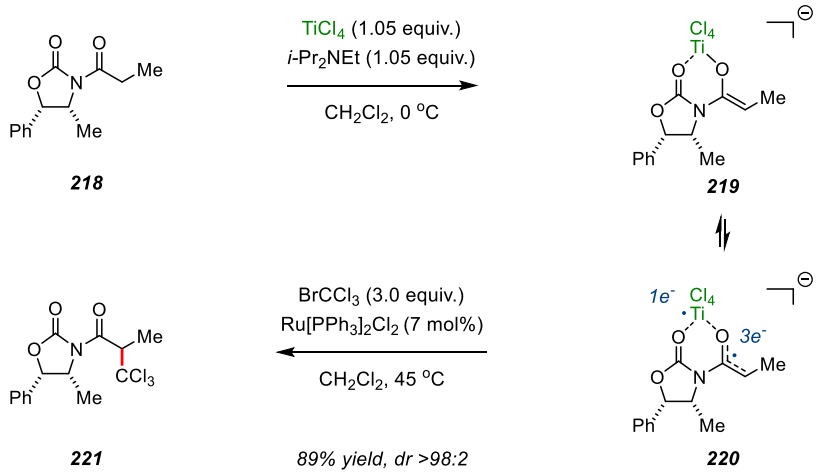

218 *219*

221 *89% yield, dr >98:2* *220*

Scheme 4.7 Precedent for using titanium enolates as both Lewis acids and oxidants to generate chelated radical cations.

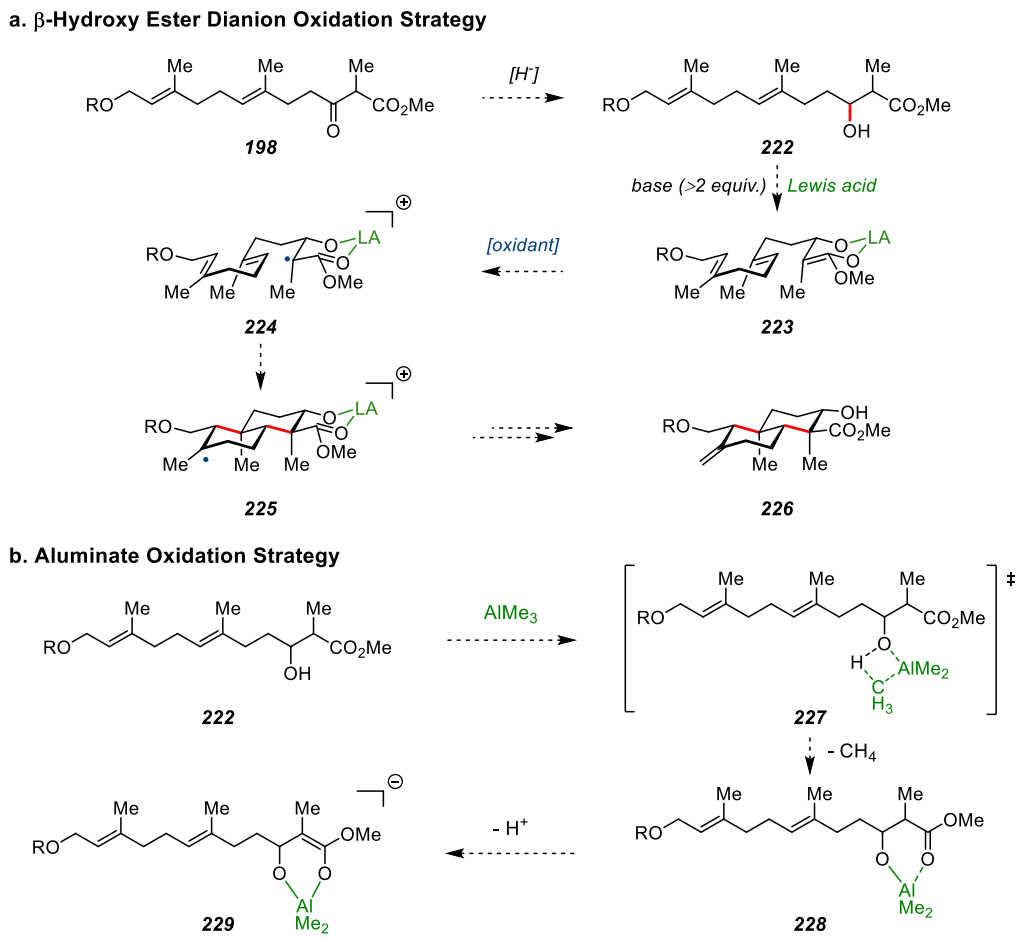

Scheme 4.8 Enolate SET oxidations with β-hydroxy ester substrates.

Another avenue that was explored was oxidation of the β-hydroxy ester dianion **223** (Scheme 4.8.a). Adding two equivalents of base to the substrate could generate the dianion, and subsequent addition of a Lewis acid capable of chelating both functional groups would produce cyclic enolate intermediate **223**. Oxidation could lead to radical cation **224** that would maintain a strong metal–substrate coordination through the alkoxy–metal interaction, potentially leading to a chelated intermediate with a longer half-life. Unfortunately, experiments employing Cp_2TiCl_2 as the counterion were unsuccessful (Table 4.6, Entries 1-6). A variation of this

Table 4.6 Enolate SET oxidations with β-hydroxy ester substrates.

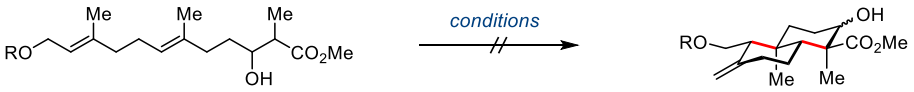

222 **226**

Entry	Substrate (R)	Solvent	Lewis acid / counterion (equiv.)	Oxidant (equiv.)	Base (equiv.)	Temp (°C)	Time	Result
1	TBS	THF	Cp_2TiCl_2 (1.2)	$Fe(phen)_3(PF_6)_3$ (2.5)	LiHMDS (2.1) / Na_3PO_4 (2.5)	-78 to rt	22.5h	no rxn.
2	Ac	THF	Cp_2TiCl_2 (2.2)	$Ce(NH_4)_2(NO_3)_6$ (2.5)	KHMDS (2.1) / K_2CO_3 (3.0)	-78 to rt	18h	inseparable mix. (mostly sm)
3	Ac	THF	Cp_2TiCl_2 (1.1)	$Ce(NH_4)_2(NO_3)_6$ (2.5)	KHMDS (2.1) / K_2CO_3 (3.0)	-78 to -25	4.5h	no rxn.
4	Ac	THF	Cp_2TiCl_2 (1.1)	$Cu(OTf)_2$ (2.5)	LiHMDS (2.1)	-78 to rt	20.5h	inseparable mix. (mostly sm)
5	TBS	PhMe	Cp_2TiCl_2 (1.2)	$Cu(OTf)_2$ (2.5)	LiHMDS (2.1) / K_2CO_3 (2.5)	-78 to rt	20h	no rxn.
6	TBS	THF	Cp_2TiCl_2 (1.2)	$Cu(OTf)_2$ (2.5)	LiHMDS (2.1) / Na_2HPO_4 (2.5)	-78 to rt	15h	no rxn.
7	Ac	THF	$ClTi(Oi\text{-}Pr)_3$ (1.1)	$Ce(NH_4)_2(NO_3)_6$ (2.5)	LiHMDS (2.1)	-78 to rt	17.5h	complex mixture
8	Ac	THF	$AlMe_3$ (1.1)	$Ce(NH_4)_2(NO_3)_6$ (2.5)	LiHMDS (1.1)	-78 to rt	14h	no rxn.
9	Ac	PhMe	$AlMe_3$ (1.1)	$V(O)Cl_3$ (2.5)	LiHMDS (1.1)	-78 to rt	17h	decomp.
10	Ac	PhMe	$AlMe_3$ (1.1)	$V(O)Cl_2$(OTFE) (2.5)	LiHMDS (1.1)	-78 to 5	16h	no rxn.
11	Ac	THF	$AlMe_3$ (1.1)	$Ag(pic)_2$ (2.5)	LiHMDS (1.1)	-78 to rt	16.5h	no rxn.

strategy entails generation of an aluminum chelated radical using $AlMe_3$, in which a bond metathesis occurs, releasing methane and generating the aluminum alkoxide **228** (Scheme 4.8.b). Subsequent addition of base could generate the cyclic aluminate complex **229**. Several oxidants were added to the presumed aluminate, and none of these experiments produced the desired *trans*-decalin **226** (Entries 8-11).

D. Dual-Function Vanadium Reagents: Both a Lewis Acid and an Oxidant

Another strategy for producing the desired chelated radical was to use the enolate counterion as both the oxidant and the chelating metal (see Table 4.5, Entry 1 for first example). It seemed strange that the Mn^{II} species formed after electron transfer did not maintain an interaction with the substrate in the Mn^{III}-mediated radical cyclization (Scheme 4.9.a, **200** to

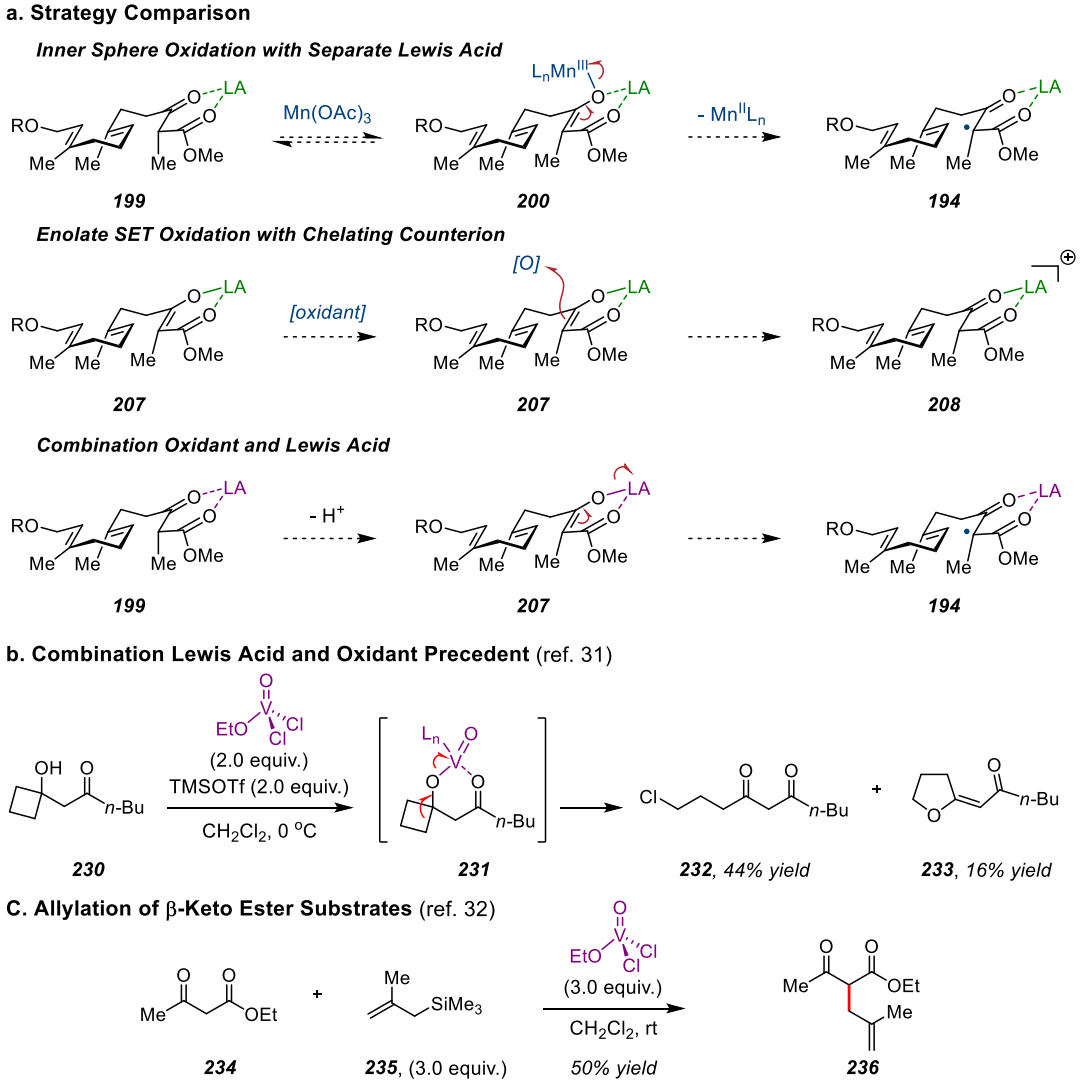

Scheme 4.9 Using vanadium(V) reagents as both oxidants and Lewis acids to generate chelated radicals.

194). It was hoped that a more Lewis acidic species could be found that would maintain a chelating interaction with the substrate after electron transfer. This would require an inner sphere oxidant that would form the enolate intermediate **199**, then undergo electron transfer to form the desired chelated radical intermediate **207** (Scheme 4.9.a). The high energy radical cation intermediate **208** implicated in the enolate SET oxidation strategy could be avoided, and there would be fewer reagents required, minimizing the number of possible interacting entities. Literature precedent for this type of reactivity was sparse, but there are reports of oxo-vanadium complexes that can act as both Lewis acids and oxidants, undergoing electron transfer while interacting with the substrate through bidentate chelation (Scheme 4.9.b, **231**).[30-31] Furthermore, oxo-vanadium oxidants have been shown to generate electrophilic radicals from β-keto esters (**234**), which can be trapped with nucleophilic olefins, a process analogous to the desired cyclization (Scheme 4.9.c).[32-33] The oxo-vanadium compound developed by Livinghouse was employed, which has been shown to be more reactive and selective than the standard alkoxy variants.[34] The first experiment rapidly decomposed the substrate (Table 4.7, Entry 1). Upon consideration of the mechanism, it was clear that HCl was generated upon formation of the initial radical, which could promote decomposition. To buffer the solution, 2,6-lutidine was added, but the reaction stalled at low temperature, and produced a complex mixture of products at higher temperature (Entries 3-4). It has previously been observed that addition of TMSOTf or AgOTf to oxo-vanadium oxidations increases reactivity.[35] There is no mechanistic rationale, but this observation coupled with the observation that base reduces reactivity has led to a mechanistic

Table 4.7 Attempts at using vanadium(V) reagents as both oxidants and Lewis acids to generate chelated radicals. [A] Added with syringe pump.

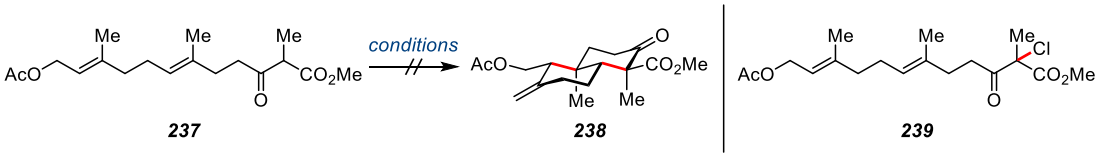

237 ***238*** ***239***

Entry	*Solvent*	*Oxidant (equiv.)*	*Additive (equiv.)*	*Base (equiv.)*	*Temp (°C)*	*Time*	*Result*
1	CH_2Cl_2	$V(O)Cl_2$(OTFE) (3.0)	—	—	0	2h	decomp.
2	CH_2Cl_2	$V(O)Cl_2$(OTFE) (3.0)	—	2,6-lutidine (4.0)	-78	10h	complex mixture (mostly sm)
3	CH_2Cl_2	$V(O)Cl_2$(OTFE) (3.0)	—	2,6-lutidine (4.0)	-40	4h	complex mixture
4	CH_2Cl_2	$V(O)Cl_2$(OTFE) (2.5)[A]	—	2,6-lutidine (4.0)	-70 to -40	23h	inseparable mixture (mostly sm)
5	CH_2Cl_2	$V(O)Cl_2$(OTFE) (3.0)[A]	$CuCl_2$ (1.2)	2,6-lutidine (4.0)	-40	22h	α-chloro **239** (yield nd), and sm
6	CH_2Cl_2	$V(O)Cl_2$(OTFE) (3.0)[A]	—	2,4,6-tri-*t* Bupyr. (4.0)	-40 to rt	18h	inseparable mixture (mostly sm)
7	PhMe	$V(O)Cl_2$(OTFE) (3.0)[A]	—	2,4,6-tri-*t* Bupyr. (4.0)	-40 to rt	18h	no rxn.
8	CH_2Cl_2	$V(O)Cl_2$(OTFE) (3.0)[A]	TMSCl (1.0)	2,4,6-tri-*t* Bupyr. (4.0)	rt	15h	inseparable mixture
9	CH_2Cl_2	$V(O)Cl_2$(OTFE) (3.0)	AgOTf (3.0)	2,4,6-tri-*t* Bupyr. (4.0)	-78 to -20	5.5h	no rxn.
10	CH_2Cl_2	$V(O)Cl_2$(OTFE) (3.0)	TMSOTf (3.0)	2,4,6-tri-*t* Bupyr. (4.0)	-40 to -20	13h	inseparable mixture
11	PhMe	$V(O)Cl_2$(OTFE) (3.0)	TMSOTf (3.0)	2,4,6-tri-*t* Bupyr. (4.0)	-78 to rt	22h	inseparable mixture
12	PhMe	$V(O)Cl_2$(OTFE) (3.0)	$Cu(OTf)_2$ (3.0)	2,4,6-tri-*t* Bupyr. (4.0)	-55 to -25	2.5h	α-chloro **239** (56%)
13	PhMe	$V(O)Cl_2$(OTFE) (2.0)	$Cu(OTf)_2$ (1.0)	2,4,6-tri-*t* Bupyr. (4.0)	-55 to -35	4.5h	α-chloro **239** (yield nd), and sm
14	PhMe	$V(O)Cl_2$(OTFE) (2.0)	$Cu(OTf)_2$ (1.0)/ $Zn(OTf)_2$ (1.0)	2,4,6-tri-*t* Bupyr. (4.0)	-65 to -25	6.5h	α-chloro **239** (yield nd), and sm
15	PhMe	$V(O)Cl_2$(OTFE) (2.0)	AgOTf (4.0)/ $Cu(OTf)_2$ (1.0)	2,4,6-tri-*t* Bupyr. (4.0)	-60 to 50	20.5h	inseparable mixture
16	PhMe	$V(O)Cl_2$(OTFE) (2.0)	$Cu(OAc)_2$ (1.0)	2,4,6-tri-*t* Bupyr. (4.0)	-60 to -15	23h	α-chloro **239**, and sm

hypothesis; perhaps the Brønsted or Lewis acid interacts with the oxo-vanadium compound at the oxygen atom, decreasing the electron

density at vanadium and increasing reactivity in a manner analogous to carbonyl activation. An initial foray using TMSCl seemed to improve the reaction, yielding a less complex mixture of products. Unfortunately, the mixture still resisted purification and characterization (Entry 8). Further experiments with TMSOTf yielded similar results (Entries 10-11). Addition of AgOTf precipitated a sticky black solid and returned starting material (Entry 9). Based on the hypothesis that protic or Lewis acids activate the oxo-vanadium species, several other Lewis acids were explored (Entries 12-16). Interestingly, addition of $Cu(OTf)_2$ yielded α-chlorinated product **239** in 56% yield. Characterization of this material led to its retroactive identification in previous crude reaction mixtures (most notably in Entry 5). Further experiments failed to yield any of the desired *trans*-decalin **238**.

E. Atom-Transfer Cyclizations

Difficulties encountered with the enolate SET oxidation strategy prompted the exploration of atom transfer cyclizations. Conceptually, generation of the desired chelated radical would be similar to the enolate SET oxidation (Scheme 4.10.a). First, the Lewis acid would engage the substrate to form chelated intermediate **240**. Next, the initiator would reduce the C-Br bond to form the desired chelated radical **194**. Similar to the enolate SET oxidation, the electron transfer would not interrupt the Lewis acid-substrate interaction. Promising literature precedent exists for chelated atom-transfer cyclizations of α-seleno β-keto esters (**241**) as reported by the Yang group (Scheme 4.10.b).[36] The relevant substrate was prepared and subjected to the reported conditions, but no reaction

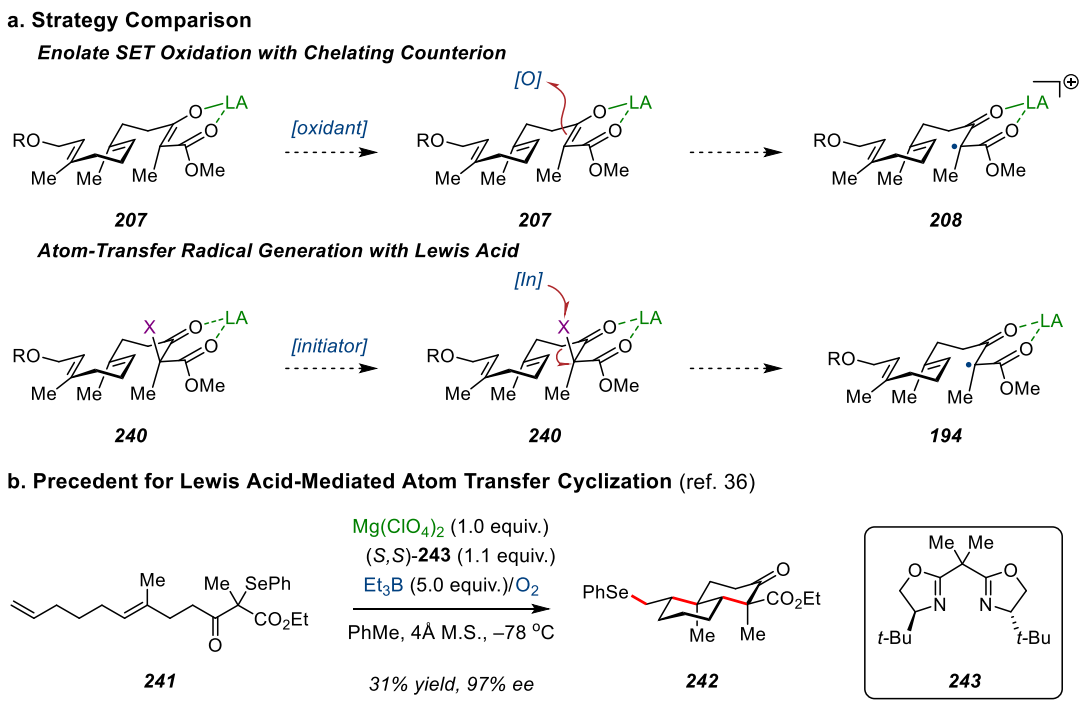

Scheme 4.10 Chelated atom-transfer radical cyclization.

occurred (Table 4.8, Entry 1). The reaction was slowly allowed to warm from –78 °C to rt, but only starting material remained. Eventually, heating the reaction to 70 °C consumed the substrate, but the crude NMR revealed that the substrate had decomposed. The Yang group also reported a chelated atom-transfer cyclization of α-bromo β-keto esters,[37] along with a method for generating the requisite brominated starting material.[38] Using the reported conditions for α-bromination provided an intractable mixture. Ultimately, treatment of the sodium enolate with NBS successfully yielded the desired bromide. At this stage, traditional atom-transfer cyclization conditions were employed with the aim of replicating the Mn^{III}-mediated result before attempting to introduce a chelating Lewis acid (Entries 2-5). Unfortunately, a brief survey was unsuccessful, yielding starting material or complex mixtures of products.

Table 4.8 Attempts at using atom-transfer to promote radical cyclizations (unchelated).

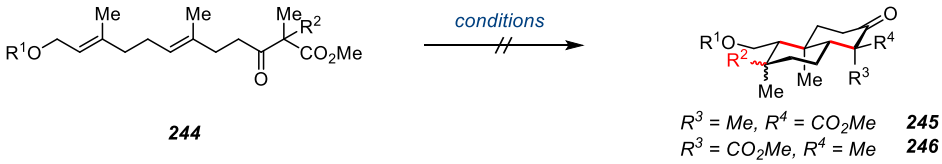

244

R^3 = Me, R^4 = CO_2Me **245**

R^3 = CO_2Me, R^4 = Me **246**

Entry	Substrate (R^1, R^2)	Solvent	Lewis acid (equiv.)	Initiator (equiv.)	Temp (°C)	Time	Result
1	Ac, SePh	THF	$Mg(ClO_4)_2$ (1.1)	Et_3B (5.0) /O_2	-78 to 70	48h	decomp.
2	TBS, Br	PhH	—	AIBN (0.1)	75	4h	no rxn.
3	TBS, Br	PhH	—	$Bu_3SnSnBu_3$ (0.1)/hν	rt	2h	inseperable mixture
4	TBS, Br	THF	—	$Bu_3SnSnBu_3$ (0.1)/hν	rt	4h	complex mixture
5	H, Br	PhH	—	$Bu_3SnSnBu_3$ (0.1)/hν	rt	1.5h	no rxn.

A modification to the atom-transfer cyclization was also explored, entailing generation of a chelated β-hydroxy ester followed by initiation of the desired radical cyclization. Guindon and coworkers have extensively examined the effects of various Lewis acids on β-hydroxy and β-alkoxy esters under radical reduction conditions.[39-44] They found that monodentate Lewis acids lead to the formation of one diastereomer, while bidentate Lewis acids produce the opposite diastereomer. $AlMe_3$ is commonly employed as the bidentate Lewis acid for β-hydroxy ester substrates (such as **247**), leading to excellent diastereoselectivity (Scheme 4.11.a).[43] These conditions led to the expected chelation-controlled reduction product **250**, implying that the aluminum alkoxy effectively coordinates to the ester to make cyclic chelated radical **249**. In the present case, it was anticipated that an atom-transfer cyclization could be induced if the reductant was omitted. Further support for this strategy comes from the successful allylation of aluminum chelated radicals (Scheme 4.11.b),[42] and the successful reductive cyclization of aluminum chelated radicals

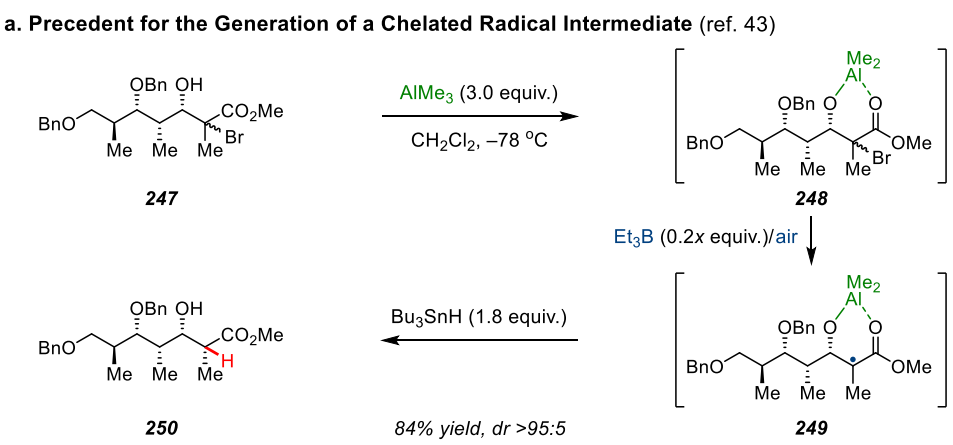

Scheme 4.11 Atom-transfer cyclizations with α-bromo β-hydroxy esters.

(generated from the α-seleno β-hydroxy ester, not shown).[45] Confusingly, when α-bromo β-hydroxy ester **253** was subjected to the reported reaction conditions without Bu_3SnH, no reaction occurred (Table 4.9, Entry 1). Even

Table 4.9 Atom-transfer cyclizations with α-bromo β-hydroxy esters.

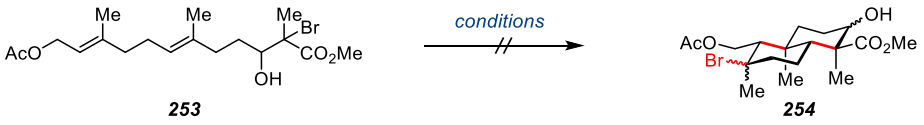

Entry	*Solvent*	*Lewis acid (equiv.)*	*Initiator (equiv.)*	*Base (equiv.)*	*Temp (°C)*	*Time*	*Result*
1	CH_2Cl_2	$AlMe_3$ (1.1)	Et_3B (5.0) /O_2	—	-78	48h	complex mixture (mostly sm)
2	CH_2Cl_2	$AlMe_3$ (1.1)	Et_3B (10.0) /O_2	—	rt	19h	complex mixture (mostly sm)
3	CH_2Cl_2	$EtAlCl_2$ (2.0)	Et_3B (5.0) /O_2	—	-5	20h	inseparable mixture
4	CH_2Cl_2	$AlMe_3$ (1.1)	$Ru(bpy)_3Cl_2$•$6H_2O$ (5 mol%)	—	-78 to rt	21h	no rxn.
5	THF	$AlMe_3$ (1.2)	$Ru(bpy)_3Cl_2$•$6H_2O$ (5 mol%)	2,4,6-tri-*t* Bupyr. (2.0)	rt	3h	no rxn.

elevated temperature failed to consume the starting material (Entry 2). Use of the more electrophilic $EtAlCl_2$ instead of $AlMe_3$ induced a reaction, but the result was a complex mixture of products (Entry 3). Attempts using the photoredox catalyst $Ru(bpy)_3Cl_2•6H_2O$ failed to consume starting material (Entries 4-5).

F. Investigation of a Truncated Model System

Considering the mechanism of the atom-transfer cyclization, it seemed possible that the complex mixtures were a result of the many possible products under the conditions employed (Figure 4.1). Even a successful cyclization could produce a mixture of bromide diastereomers (**255** & **256**), in addition to three possible olefin isomers (**257**), with further complications arising from monocyclic products (**258**, **259**, & **260**). It seemed prudent to optimize the cyclization on a model system that would facilitate analysis. Cutting a prenyl unit out of the original substrate would leave allylic acetate **264** as a model system that would accurately model both the initiation and termination of the cyclization (Scheme 4.12). The substrate was synthesized starting from prenyl alcohol **261**, which was acetylated. The allylic oxidation catalyzed by SeO_2 yielded allylic alcohol

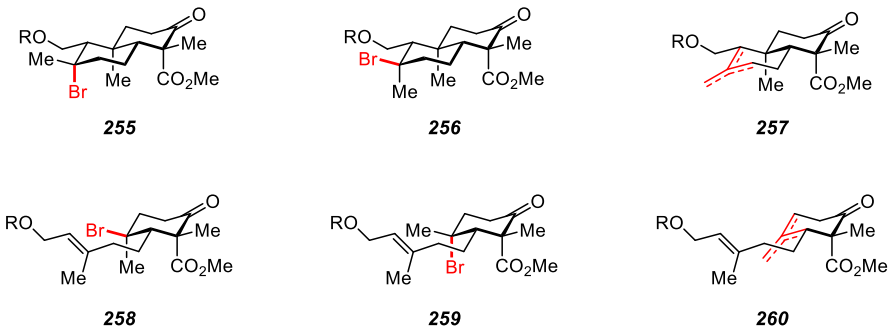

Figure 4.1 Possible products arising from atom-transfer cyclization.

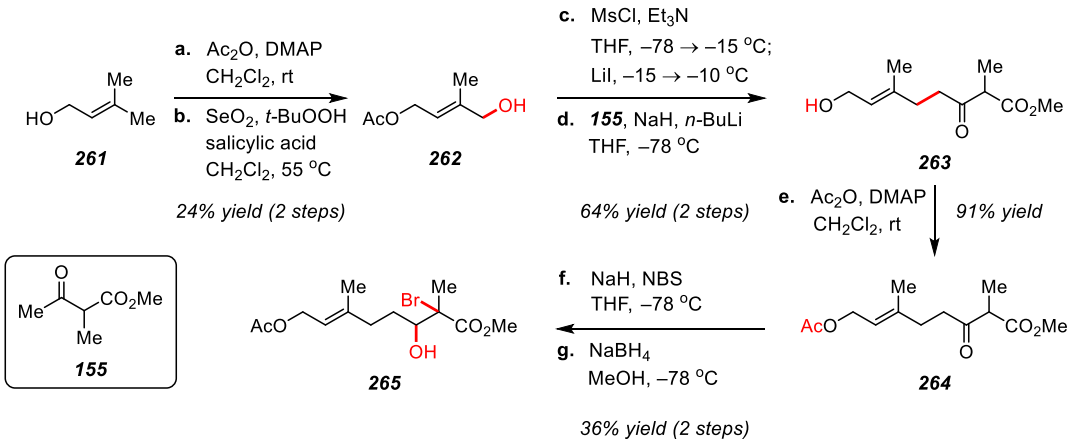

Scheme 4.12 Synthesis of a truncated model system.

262, albeit in low yield (26%), presumably because the olefin is electron deficient due to the acetate (which is the basis for the regioselectivity when conducting the same reaction on geranyl acetate). Conversion to the iodide, and alkylation using the dianion derived from methyl 2-methyl-3-oxobutanoate (**155**) yielded model allylic alcohol **263**.

Model allylic alcohol **263** was subjected to the standard Mn^{III}-mediated oxidative radical cyclization conditions in an attempt to obtain the free-radical cyclization product as a standard (Table 4.10, Entries

Table 4.10 Initial cyclization attempts on truncated model system **264**.

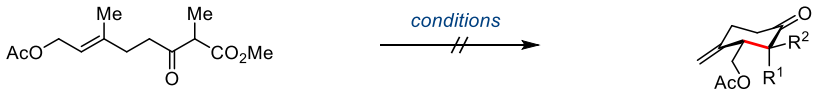

Entry	Substrate (R)	Solvent	Oxidant (equiv.)	Additive (equiv.)	Base (equiv.)	Temp (°C)	Time	Result
1	Ac	AcOH	$Mn(OAc)_3$ (2.2)	$Cu(OAc)_2$ (1.0)	—	rt	7.5h	complex mixture
2	H	AcOH	$Mn(OAc)_3$ (2.2)	$Cu(OAc)_2$ (1.0)	—	rt	6.5h	complex mixture
3	Ac	CH_2Cl_2	$V(O)Cl_2$(OTFE) (3.0)	TMSOTf (3.0)	2,4,6-tri-t Bupyr. (4.5)	-78 to -10	7.5h	inseparable mix. (mostly sm)

1-2). Surprisingly, these reactions yielded a complex mixture of products that resisted characterization. Model allylic acetate **264** was also treated with the oxo-vanadium oxidant in the presence of TMSOTf as an activator, but the reaction yielded mostly starting material (Entry 3).

The model system **265** was also used to probe the aluminum chelated radical cyclization strategy. Accordingly, the model α-bromo β-hydroxy ester **265** was prepared (Scheme 4.12, **264** to **265**). When the presumed aluminum complex was treated with Et_3B/O_2, no reaction occurred (Table 4.11, Entry 1). Using $EtAlCl_2$ to generate the aluminum complex resulted in decomposition of the starting material (Entry 2). To determine if the desired radical was being formed, Bu_3SnH was added to the reaction to see if reduction or reductive cyclization would occur. Interestingly, the reduction product **269** was formed in 41% yield, but no cyclization products were observed (Entry 3). This indicates that the desired radical was forming, but was not cyclizing. It was surprising that an intermolecular process was

Table 4.11 Cyclization attempts on truncated model system **265**. [A] Added with syringe pump.

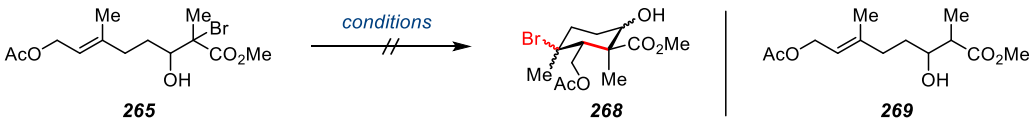

265 ***268*** ***269***

Entry	*Solvent*	*Lewis acid / counterion (equiv.)*	*Initiator (equiv.)*	*Additive (equiv.)*	*Temp (°C)*	*Time*	*Result*
1	CH_2Cl_2	$AlMe_3$ (3.0)	Et_3B (5.0)[A] /O_2	—	-78	4h	no rxn.
2	CH_2Cl_2	Et_2AlCl (2.0)	Et_3B (5.0)[A] /O_2	—	-5	4h	decomp.
3	CH_2Cl_2	$AlMe_3$ (3.0)	Et_3B (2.0)[A] /O_2	Bu_3SnH (1.8)	-40	4h	**269** (41%)
4	CH_2Cl_2	$AlMe_3$ (3.0)	Et_3B (1.0)[A] /O_2	Bu_3SnH (1.8)	0	2h	inseparable mixture (approx. half sm)
5	PhMe	$AlMe_3$ (3.0)	CuI (0.2) / 1,10-phen (0.4)	—	-70 to rt	22h	inseparable mixture (mostly sm)

outcompeting an intramolecular process. It is possible that the nucleophilicity of the olefin in **265** is significantly attenuated by the acetate, preventing cyclization onto the electrophilic radical.

G. Exploration of a Truncated Model System Lacking the Allylic Acetate

To improve the nucleophilicity of the olefin and more closely model the first cyclization, a second model system was devised. The only difference between the second model system and the first is the omission of the allylic acetate. Synthesis of the second model system **272** was relatively straightforward (Scheme 4.13). Commercial *trans*-2-methyl-2-butenal (**270**) was reduced to yield allylic alcohol **271**, which was converted to the iodide and coupled with the dianion derived from methyl 2-methyl-3-oxobutanoate (**155**) to yield model β-keto ester **272**. The bromide **273** was produced in the usual manner, and subsequent reduction afforded model α-bromo β-hydroxy ester **274**. The chelated aluminum intermediate was generated in the usual way, and fluorinated phenols (3,5-CF_3-PhOH and F_5PhOH) were added to generate a more electrophilic aluminum species,

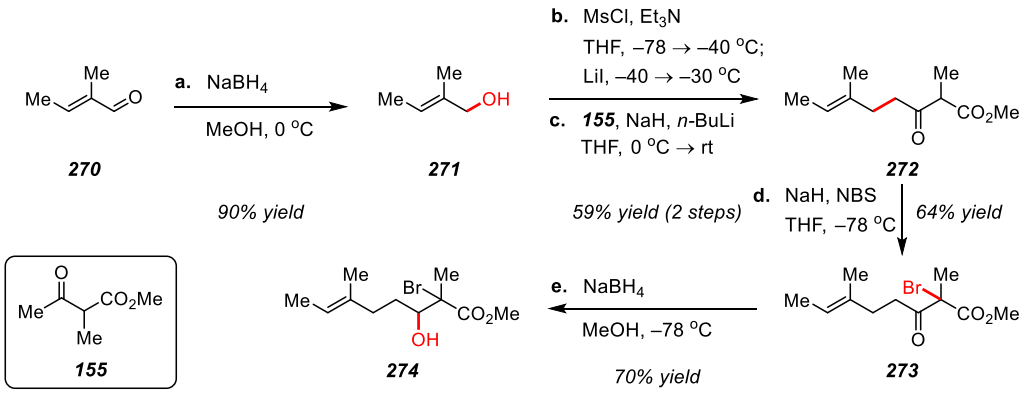

Scheme 4.13 Synthesis of a truncated model system lacking the allylic acetate.

Table 4.12 Atom-transfer experiments on truncated model system **274**. [A] Syringe pump.

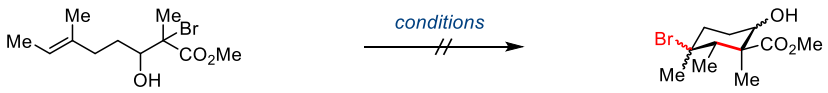

274 **275**

Entry	Solvent	Lewis acid / counterion (equiv.)	Initiator (equiv.)	Additive (equiv.)	Temp (°C)	Time	Result
1	CH_2Cl_2	$AlMe_3$ (1.1)	Et_3B (2.0)[A] /O_2	pentafluorophenol (2.2)	-70	2.5h	no rxn.
2	CH_2Cl_2	$AlMe_3$ (1.1)	Et_3B (1.0)[A] /O_2	3,5-CF_3-PhOH (2.2)	-70	3h	no rxn.
3	CH_2Cl_2	$AlMe_3$ (1.1)	Et_3B (2.0)[A] /O_2	3,5-CF_3-PhOH (2.2)	rt	3h	complex mixture (mostly sm)
4	CH_2Cl_2	$AlMe_3$ (1.1)	$Bu_3SnSnBu_3$ (0.2)/ hν	3,5-CF_3-PhOH (2.2)	rt	4h	complex mixture
5	CH_2Cl_2	$AlMe_3$ (1.1)	*fac*-Ir(ppy)$_3$ (2.5 mol%)	3,5-CF_3-PhOH (2.2) / *p*-MeOPhNPh_2 (2.0)	rt	12h	complex mixture
6	PhMe	$AlMe_3$ (1.1)	CuBr (10 mol%) / PMDA (1.0)	3,5-CF_3-PhOH (2.2) / TBABr (0.5)	rt	22.5h	opposite diastereomer

increasing the electrophilicity of the resultant radical and increasing reactivity. Reactions conducted in this manner failed to consume starting material, whether conducted at –70 °C or room temperature (Table 4.12, Entries 1-3). Using ultraviolet light and $Bu_3SnSnBu_3$ initiated a reaction, but the crude material was a complex mixture of products (Entry 4). Similarly, using the photoredox catalyst *fac*-Ir(ppy)$_3$ consumed starting material, but yielded a complex mixture (Entry 5). Cu^I-mediated radical initiation yielded what appeared to be the opposite diastereomer of the starting material, though this has not been rigorously determined (Entry 6).

H. Photoredox Catalyzed Radical Cyclization

Although several previous experiments had employed photoredox catalysts, a more thorough investigation seemed warranted. Thankfully, the

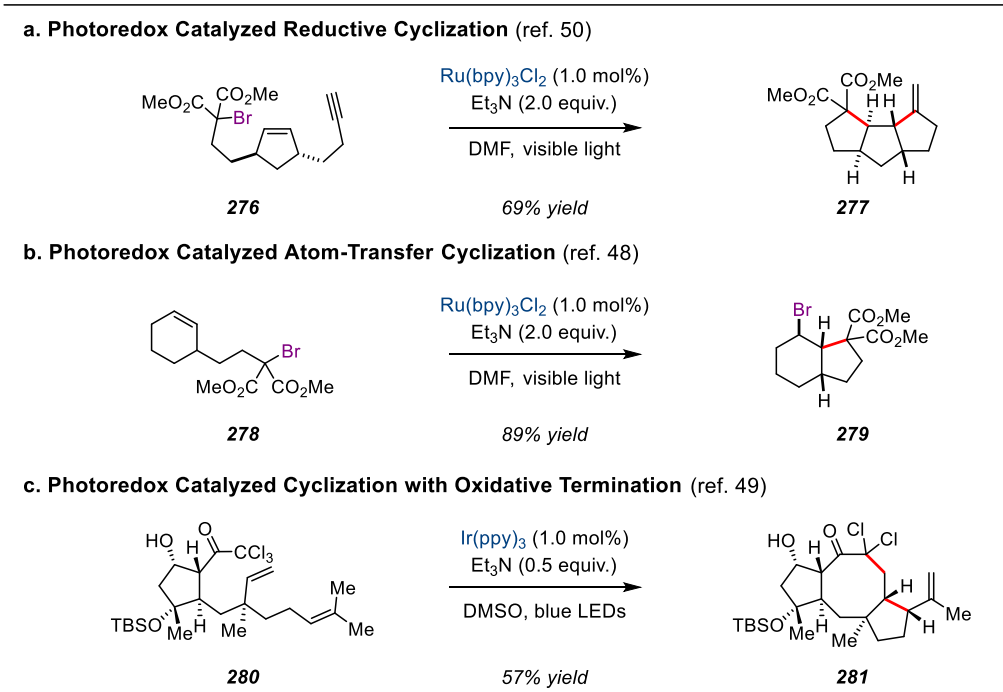

Scheme 4.14 Precedent for various termination modes for photoredox-catalyzed radical cyclizations.

recent explosion of interest in iridium- and ruthenium-based photocatalysts[46-49] has extended into intramolecular radical cyclizations of α-bromo β-dicarbonyls (Scheme 4.14a–4.14.b).[50-52] Prior work has demonstrated that three termination modes are possible: 1) reductive (Scheme 4.14.a), 2) atom-transfer (Scheme 4.14.b), or 3) oxidative (Scheme 4.14.c), depending on the substrate and conditions used. At the outset, it was unclear which termination pathway would prevail, but it was hoped that the tertiary radical would be oxidized to the cation *en route* to the desired exocyclic olefin. Initial experiments were focused on conducting cyclizations without the presence of a chelating Lewis acid so that other parameters could be optimized before attempting to reverse the diastereoselectivity. The first attempt utilized $Ru(bpy)_3(PF_6)_2$, which did not have a reduction potential high enough to cleave the C-Br bond (Table 4.13,

Table 4.13 Optimization of photoredox-catalyzed radical cyclization of truncated model system **273** to produce lactone **282**.

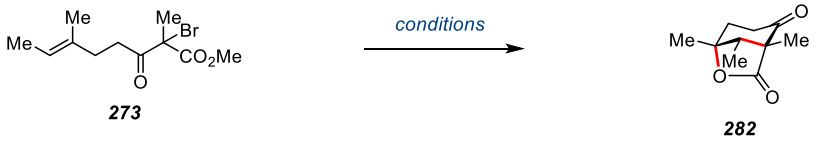

273 **282**

Entry	Solvent	Catalyst (equiv.)	Base (equiv.)	Time	Notes	282
1	CH_2Cl_2	$Ru(bpy)_2(PF_6)_2$ (2.5 mol%)	2,6-lutidine (1.1)	24h	–	0% (no rxn.)
2	CH_2Cl_2	*fac*-Ir(ppy)$_3$ (2.5 mol%)	2,6-lutidine (2.0)	1h	–	10%
3	CH_2Cl_2	*fac*-Ir(ppy)$_3$ (2.5 mol%)	Et_3N (2.0)	2h	–	8%
4	CH_2Cl_2	*fac*-Ir(ppy)$_3$ (2.5 mol%)	DBU (2.0)	2h	–	0%
5	CH_2Cl_2	*fac*-Ir(ppy)$_3$ (2.5 mol%)	*p*-MeOPhNPh$_2$ (2.0)	2h	–	0%
6	CH_2Cl_2	*fac*-Ir(ppy)$_3$ (2.5 mol%)	(*p*-BrPh)$_3$N (2.0)	2h	–	3%
7	CH_2Cl_2	*fac*-Ir(ppy)$_3$ (2.5 mol%)	DABCO (2.0)	2h	–	10%
8	CH_2Cl_2	*fac*-Ir(ppy)$_3$ (2.5 mol%)	DABCO (2.0)	1.5h	–	8%
9	CH_2Cl_2	*fac*-Ir(ppy)$_3$ (2.5 mol%)	DABCO (2.0)	1.5h	after rxn, added HCl (4.0), 0.5h	17%
10	CH_2Cl_2	*fac*-Ir(ppy)$_3$ (2.5 mol%)	DABCO (2.0)	1.5h	freeze-pump-thawed 3x	10%
11	CH_2Cl_2	*fac*-Ir(ppy)$_3$ (2.5 mol%)	Et_3N (2.0)	1h	after rxn, added HCl (4.0), 18h	17%
12	CH_2Cl_2	*fac*-Ir(ppy)$_3$ (2.5 mol%)	*i*-Pr$_2$NEt (2.0)	1h	after rxn, added HCl (4.0), 18h	15%
13	CH_2Cl_2	*fac*-Ir(ppy)$_3$ (2.5 mol%)	DABCO (2.0)	1h	after rxn, added HCl (4.0), 18h	28%
14	CH_2Cl_2	*fac*-Ir(ppy)$_3$ (2.5 mol%)	4-MeOpyridine (2.0)	1h	after rxn, added HCl (4.0), 21h	13%
15	CH_2Cl_2	*fac*-Ir(ppy)$_3$ (2.5 mol%)	DMAP (2.0)	1h	after rxn, added HCl (4.0), 21h	12%
16	CH_2Cl_2	*fac*-Ir(ppy)$_3$ (2.5 mol%)	PMDA (2.0)	1h	after rxn, added HCl (4.0), 21h	7%
17	CH_2Cl_2	*fac*-Ir(ppy)$_3$ (2.5 mol%)	imidazole (2.0)	1h	after rxn, added HCl (4.0), 21h	14%
18	CH_2Cl_2	*fac*-Ir(ppy)$_3$ (2.5 mol%)	piperidine (2.0)	1h	after rxn, added HCl (4.0), 21h	9%
19	CH_2Cl_2	*fac*-Ir(ppy)$_3$ (2.5 mol%)	TMEDA (2.0)	1h	after rxn, added HCl (4.0), 20h	11%
20	CH_2Cl_2	*fac*-Ir(ppy)$_3$ (2.5 mol%)	*t*-BuNH$_2$ (2.0)	1h	after rxn, added HCl (4.0), 20h	14%
21	CH_2Cl_2	*fac*-Ir(ppy)$_3$ (2.5 mol%)	(EtO)$_3$N (2.0)	1h	after rxn, added HCl (4.0), 20h	12%
22	CH_2Cl_2	*fac*-Ir(ppy)$_3$ (2.5 mol%)	2-aminopyridine (2.0)	1h	after rxn, added HCl (4.0), 20h	17%

Entry 1). Further examination of the literature revealed that tertiary bromides such as **273** are difficult substrates for photoredox catalysis, typically requiring the strongest reducing catalyst *fac*-Ir(ppy)$_3$.[53] Gratifyingly, irradiation of *fac*-Ir(ppy)$_3$ with blue LEDs in the presence of

model bromide **273** yielded lactone **282** in 10% isolated yield (Entry 2). Several bases were surveyed, with DABCO providing the best result as determined analysis of the crude NMR (Entry 7, internal standard: 0.02M 1,3,5-trimethoxybenzene in $CDCl_3$). Before attempting further optimization, the mechanism of the reaction was considered (Scheme 4.15.a). First, the photoredox catalyst is excited by the visible light from $[Ir^{III}]$ to $[Ir^{III}]^*$. The excited catalyst reductively cleaves tertiary bromide **273** to yield free radical **283**, which undergoes a 6-*endo* cyclization to yield tertiary radical **284**. During this process, the catalyst is oxidized from $[Ir^{III}]^*$ to $[Ir^{IV}]$. The oxidized catalyst produces the carbocation **285** from tertiary radical **284**. The resultant cation can form three possible olefins **286** or lactone **282**. Alternatively, a radical chain mechanism may be operant, in which the initiation is the same, but tertiary radical **284** abstracts bromine from tertiary bromide **273** to propagate the chain. The resultant tertiary bromide could be readily eliminated to form **286**, which could then be converted to lactone **282** through the action of the conjugate acid of the base. This mechanism seems unlikely in this case because it involves the direct interaction of a tertiary radical with a tertiary bromide, a highly congested transition state.

The NMR of the crude product revealed several vinyl protons, implying that olefins **286** were forming from the reaction. The mixture of olefins could not be separated, so other techniques were sought to better determine the cyclization yield. It was anticipated that addition of HCl at the end of the reaction could converge the olefins **286** to lactone **282** (Scheme 4.15.b). Re-protonation of the olefin could regenerate the cation **285**, and then allow for capture by the proximal ester to form lactone **282**.

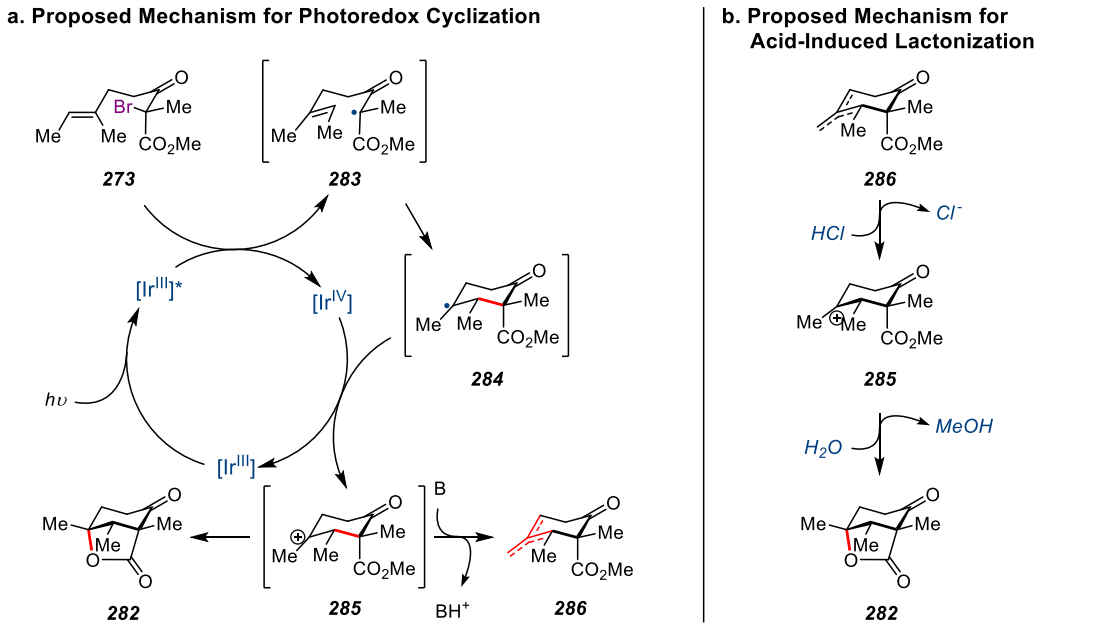

Scheme 4.15 Proposed mechanism for the photoredox-catalyzed cyclization of truncated model system **273**.

Indeed, addition of HCl increased the yield of lactone **282**, and allowed for a more thorough analysis of the cyclization. A variety of bases were screened with the additional HCl step, and it was found that DABCO was optimal, yielding 28% of lactone **282** (Entry 13).

During experiments with model bromide **273**, several experiments were conducted towards the double cyclization (**287** to **288**/**289**, Table 4.14). Initial experiments on acetate protected linear precursor **287** were unsuccessful with both $Ru(bpy)_3Cl_2 \bullet 6H_2O$ and *fac*-$Ir(ppy)_3$ in the presence or absence of Lewis acid additives (Entries 1-9). When the linear alcohol **290** was used instead of its acetate protected congener, the desired cyclization to bicycle **162** occurred (Table 4.15, as determined by the crude NMR, internal standard: 0.02M 1,3,5-trimethoxybenzene in $CDCl_3$). Initial experiments probed the effect of concentration, revealing that more dilute reactions increased the yield of **162** (Entries 1-3). This is expected for an

Table 4.14 Initial attempts at the photoredox-catalyzed cyclization of acetate **287**.

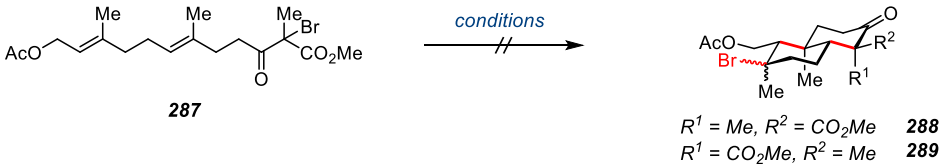

287

R^1 = Me, R^2 = CO_2Me **288**
R^1 = CO_2Me, R^2 = Me **289**

Entry	Solvent	Lewis acid (equiv.)	Catalyst (equiv.)	Base (equiv.)	Time	Result
1	MeCN	—	$Ru(bpy)_3Cl_2•6H_2O$ (5 mol%)	—	0.5h	complex mixture
2	MeCN	—	$Ru(bpy)_3Cl_2•6H_2O$ (5 mol%)	2,4,6-tri-*t*-Bupyr. (1.2)	0.5h	complex mixture
3	MeCN	$Sc(OTf)_3$ (1.0)	$Ru(bpy)_3Cl_2•6H_2O$ (5 mol%)	—	1h	decomp.
4	MeCN	$Sc(OTf)_3$ (0.1)	$Ru(bpy)_3Cl_2•6H_2O$ (5 mol%)	2,4,6-tri-*t*-Bupyr. (2.0)	24h	complex mixture
5	MeCN	$Yb(OTf)_3$ (0.1)	$Ru(bpy)_3Cl_2•6H_2O$ (5 mol%)	2,4,6-tri-*t*-Bupyr. (2.0)	24h	complex mixture
6	CH_2Cl_2	—	*fac*-$Ir(ppy)_3$ (2.5 mol%)	2,6-lutidine (2.0)	1h	complex mixture
7	CH_2Cl_2	—	*fac*-$Ir(ppy)_3$ (0.5 mol%)	DABCO (2.0)	0.5h	decomp.
8	CH_2Cl_2	—	*fac*-$Ir(ppy)_3$ (1.5 mol%)	DABCO (2.0)	0.5h	decomp.
9	CH_2Cl_2	—	*fac*-$Ir(ppy)_3$ (2.5 mol%)	DABCO (2.0)	0.5h	decomp.

intramolecular process, as increasing dilution decreases the probability of destructive intermolecular interactions. Next, equivalents of base were varied, revealing that less than one equivalent was detrimental (Entries 4-8). Various solvents were explored, with polar solvents retarding the reaction rate (Entries 10-17). The solvent appeared to have little impact on yield, so MeCN was chosen for future reactions as it was better able to solubilize photocatalyst salts. Exploration of photocatalysts revealed that $Ru(bpy)_3(PF_6)_2$ was optimal (Entries 18 to 22). The catalyst loading was explored, with the hope that lower catalyst loadings would decrease the rate of oxidation of the alkyl radicals, decreasing the amount of premature oxidation (Entries 23-27). These experiments were inconclusive. Impressively, the reaction proceeded efficiently when 0.01 mol% of catalyst was used (Entry 27). The yields slowly decreased over time, presumably

Table 4.15 Photoredox-catalyzed cyclization of **290**.

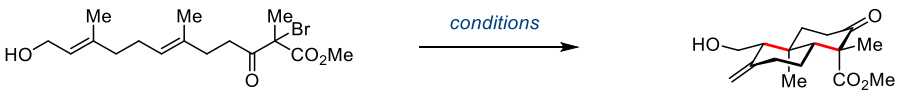

290 ***162***

Entry	*Solvent*	*Catalyst (equiv.)*	*Base (equiv.)*	*Time*	*162*	*290*
1	CH_2Cl_2 (0.1M)	*fac*-Ir(ppy)$_3$ (0.5 mol%)	DABCO (2.0)	1.5h	7.4%	–
2	CH_2Cl_2 (0.05M)	*fac*-Ir(ppy)$_3$ (0.5 mol%)	DABCO (2.0)	1.5h	8.1%	–
3	CH_2Cl_2 (0.02M)	*fac*-Ir(ppy)$_3$ (0.5 mol%)	DABCO (2.0)	1.5h	13.7%	–
4	CH_2Cl_2 (0.02M)	*fac*-Ir(ppy)$_3$ (0.5 mol%)	DABCO (0.5)	0.5h	8.0%	–
5	CH_2Cl_2 (0.02M)	*fac*-Ir(ppy)$_3$ (0.5 mol%)	DABCO (1.0)	0.5h	12.0%	–
6	CH_2Cl_2 (0.02M)	*fac*-Ir(ppy)$_3$ (0.5 mol%)	DABCO (2.0)	0.5h	11.4%	–
7	CH_2Cl_2 (0.02M)	*fac*-Ir(ppy)$_3$ (0.5 mol%)	DABCO (4.0)	0.5h	12.0%	–
8	CH_2Cl_2 (0.02M)	*fac*-Ir(ppy)$_3$ (0.5 mol%)	DABCO (8.0)	0.5h	11.6%	–
9	CH_2Cl_2 (0.02M)	*fac*-Ir(ppy)$_3$ (0.5 mol%)	DABCO (2.0)	0.5h	12.0%	–
10	PhMe (0.02M)	*fac*-Ir(ppy)$_3$ (0.5 mol%)	DABCO (2.0)	0.5h	4.9%	–
11	MeCN (0.02M)	*fac*-Ir(ppy)$_3$ (0.5 mol%)	DABCO (2.0)	0.5h	6.5%	30.0%
12	DMF (0.02M)	*fac*-Ir(ppy)$_3$ (0.5 mol%)	DABCO (2.0)	0.5h	4.2%	43.0%
13	THF (0.02M)	*fac*-Ir(ppy)$_3$ (0.5 mol%)	DABCO (2.0)	0.5h	3.4%	23.0%
14	DMSO (0.02M)	*fac*-Ir(ppy)$_3$ (0.5 mol%)	DABCO (2.0)	0.5h	3.5%	43.0%
15	MeCN (0.02M)	*fac*-Ir(ppy)$_3$ (0.5 mol%)	DABCO (2.0)	3.5h	13.0%	–
16	DMF (0.02M)	*fac*-Ir(ppy)$_3$ (0.5 mol%)	DABCO (2.0)	3.5h	8.4%	–
17	DMSO (0.02M)	*fac*-Ir(ppy)$_3$ (0.5 mol%)	DABCO (2.0)	3.5h	11.4%	–
18	MeCN (0.02M)	*fac*-Ir(ppy)$_3$ (1.0 mol%)	DABCO (2.0)	0.5h	8.1%	–
19	MeCN (0.02M)	Ir(ppy)$_2$(dtbpy)PF$_6$ (1.0 mol%)	DABCO (2.0)	0.5h	9.9%	–
20	MeCN (0.02M)	Ir(dF-ppy)$_3$ (1.0 mol%)	DABCO (2.0)	0.5h	8.1%	–
21	MeCN (0.02M)	Ir(dF-ppy)$_2$(dtbpy)PF6 (1.0 mol%)	DABCO (2.0)	0.5h	9.9%	–
22	MeCN (0.02M)	Ru(bpy)$_3$(PF$_6$)$_2$ (1.0 mol%)	DABCO (2.0)	0.5h	11.6%	–
23	MeCN (0.02M)	Ru(bpy)$_3$(PF$_6$)$_2$ (1.0 mol%)	DABCO (2.0)	0.5h	12.6%	–
24	MeCN (0.02M)	Ru(bpy)$_3$(PF$_6$)$_2$ (0.5 mol%)	DABCO (2.0)	0.5h	11.5%	–
25	MeCN (0.02M)	Ru(bpy)$_3$(PF$_6$)$_2$ (0.1 mol%)	DABCO (2.0)	0.5h	11.4%	–
26	MeCN (0.02M)	Ru(bpy)$_3$(PF$_6$)$_2$ (0.05 mol%)	DABCO (2.0)	0.5h	7.3%	–
27	MeCN (0.02M)	Ru(bpy)$_3$(PF$_6$)$_2$ (0.01 mol%)	DABCO (2.0)	0.5h	10.4%	–

Table 4.16 Attempted Photoredox-catalyzed cyclization of **290** in the presence of copper co-oxidants (continued on next page).

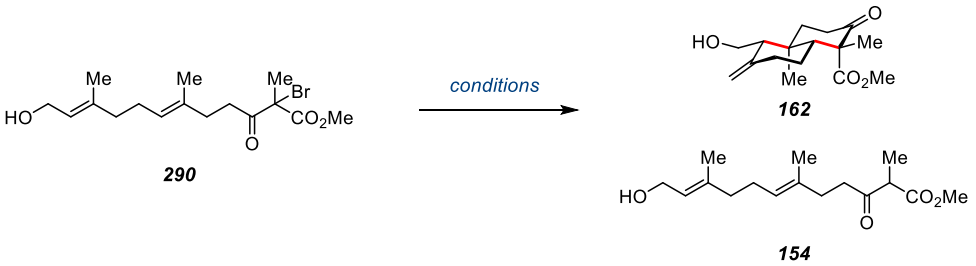

290 **162** **154**

Entry	Solvent	Catalyst (equiv.)	Additive (equiv.)	Base (equiv.)	Time	162	290	154
1	MeCN (0.02M)	*fac*-Ir(ppy)$_3$ (0.5 mol%)	CuOAc (20 mol%)	DABCO (2.0)	6h	–	–	–
2	MeCN (0.02M)	*fac*-Ir(ppy)$_3$ (0.5 mol%)	[(MeCN)$_4$Cu]PF$_6$ (20 mol%)	DABCO (2.0)	6h	–	–	–
3	MeCN (0.02M)	Ru(bpy)$_3$(PF$_6$)$_2$ (4.0 mol%)	Cu(OTf)$_2$ (1.0)	DABCO (2.0)	3.5h	–	–	–
4	MeCN (0.02M)	Ru(bpy)$_3$(PF$_6$)$_2$ (4.0 mol%)	Cu(OAc)$_2$ (1.0)	DABCO (2.0)	3.5h	–	–	–
5	MeCN (0.02M)	Ru(bpy)$_3$(PF$_6$)$_2$ (4.0 mol%)	Cu(2-ethylhexanoate)$_2$ (1.0)	DABCO (2.0)	3.5h	–	–	–
6	MeCN (0.02M)	Ru(bpy)$_3$(PF$_6$)$_2$ (4.0 mol%)	CuCl$_2$ (1.0)	DABCO (2.0)	3.5h	–	–	–
7	MeCN (0.02M)	Ru(bpy)$_3$(PF$_6$)$_2$ (4.0 mol%)	Cu(hfacac)$_2$ (1.0)	DABCO (2.0)	3.5h	–	–	–
8	CH$_2$Cl$_2$ (0.02M)	Ru(bpy)$_3$(PF$_6$)$_2$ (7.5 mol%)	Cu(2-ethylhexanoate)$_2$ (1.0)	DABCO (2.0)	18h	–	49.0%	–
9	CH$_2$Cl$_2$ (0.02M)	Ru(bpy)$_3$(PF$_6$)$_2$ (7.5 mol%)	Cu(2-ethylhexanoate)$_2$ (1.0) / 2,2'-bpy (1.0)	DABCO (2.0)	18h	–	56.0%	–
10	CH$_2$Cl$_2$ (0.02M)	Ru(bpy)$_3$(PF$_6$)$_2$ (7.5 mol%)	Cu(2-ethylhexanoate)$_2$ (1.0) / 1,10-phen (1.0)	DABCO (2.0)	18h	–	53.0%	–
11	CH$_2$Cl$_2$ (0.02M)	Ru(bpy)$_3$(PF$_6$)$_2$ (7.5 mol%)	Cu(2-ethylhexanoate)$_2$ (1.0) / terpyridine (1.0)	DABCO (2.0)	18h	–	–	–
12	CH$_2$Cl$_2$ (0.02M)	Ru(bpy)$_3$(PF$_6$)$_2$ (7.5 mol%)	Cu(2-ethylhexanoate)$_2$ (1.0) / 3,4,7,8-Mephen (1.0)	DABCO (2.0)	18h	–	–	–
13	CH$_2$Cl$_2$ (0.02M)	Ru(bpy)$_3$(PF$_6$)$_2$ (2.5 mol%)	Cu(2-ethylhexanoate)$_2$ (0.5)	DABCO (2.0)	22h	–	50.0%	–
14	CH$_2$Cl$_2$ (0.02M)	Ru(bpy)$_3$(PF$_6$)$_2$ (2.5 mol%)	Cu(2-ethylhexanoate)$_2$ (0.2)	DABCO (2.0)	22h	–	53.0%	–
15	CH$_2$Cl$_2$ (0.02M)	Ru(bpy)$_3$(PF$_6$)$_2$ (2.5 mol%)	Cu(2-ethylhexanoate)$_2$ (0.1)	DABCO (2.0)	22h	–	55.0%	–
16	CH$_2$Cl$_2$ (0.02M)	Ru(bpy)$_3$(PF$_6$)$_2$ (2.5 mol%)	Cu(2-ethylhexanoate)$_2$ (0.05)	DABCO (2.0)	22h	–	56.0%	–

Table 4.16 Attempted Photoredox-catalyzed cyclization of **290** in the presence of copper co-oxidants.

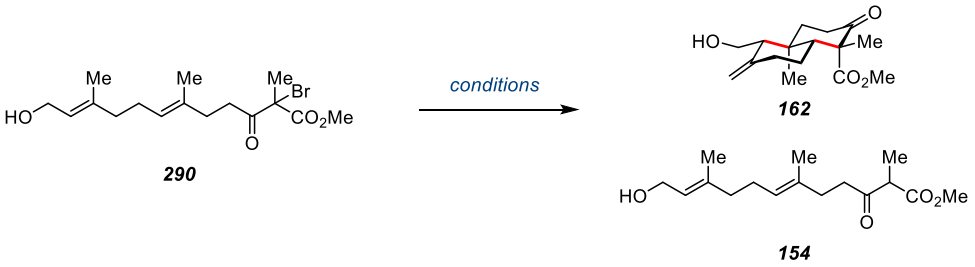

Entry	Solvent	Catalyst (equiv.)	Additive (equiv.)	Base (equiv.)	Time	162	290	154
17	CH_2Cl_2 (0.02M)	$Ru(bpy)_3(PF_6)_2$ (2.5 mol%)	$Cu(2\text{-ethylhexanoate})_2$ (0.01)	DABCO (2.0)	22h	–	45.0%	–
18	MeCN/THF (0.012M)	$Ru(bpy)_3(PF_6)_2$ (2.5 mol%)	$Cu(2\text{-ethylhexanoate})_2$ (0.5) / 2,2'-bpy (0.5)	DABCO (2.0)	20.5h	–	–	–
19	MeCN/THF (0.012M)	$Ru(bpy)_3(PF_6)_2$ (2.5 mol%)	$Cu(2\text{-ethylhexanoate})_2$ (0.2) / 2,2'-bpy (0.2)	DABCO (2.0)	20.5h	–	–	13.0%
20	MeCN/THF (0.012M)	$Ru(bpy)_3(PF_6)_2$ (2.5 mol%)	$Cu(2\text{-ethylhexanoate})_2$ (0.1) / 2,2'-bpy (0.1)	DABCO (2.0)	20.5h	1.0%	–	9.0%
21	MeCN/THF (0.012M)	$Ru(bpy)_3(PF_6)_2$ (2.5 mol%)	$Cu(2\text{-ethylhexanoate})_2$ (0.05) / 2,2'-bpy (0.05)	DABCO (2.0)	20.5h	–	9.0%	3.0%
22	MeCN/THF (0.012M)	$Ru(bpy)_3(PF_6)_2$ (2.5 mol%)	$Cu(2\text{-ethylhexanoate})_2$ (0.01) / 2,2'-bpy (0.01)	DABCO (2.0)	20.5h	–	17.0%	–
23	DMF (0.02M)	$Ru(bpy)_3(PF_6)_2$ (1.0 mol%)	CuOAc (20 mol%)	K_2CO_3 (1.1)	19h	–	–	–
24	DMF (0.02M)	$Ru(bpy)_3(PF_6)_2$ (1.0 mol%)	CuOAc (20 mol%)	2,6-lutidine (1.1)	19h	–	–	–
25	DMF (0.02M)	$Ru(bpy)_3(PF_6)_2$ (1.0 mol%)	CuOAc (20 mol%)	$NaH_2PO_4 \cdot 2H_2O$ (1.1)	19h	–	–	–
26	DMF (0.02M)	$Ru(bpy)_3(PF_6)_2$ (1.0 mol%)	CuOAc (20 mol%)	Na_2HPO_4 (1.1)	19h	–	–	–
27	DMF (0.02M)	$Ru(bpy)_3(PF_6)_2$ (1.0 mol%)	CuOAc (20 mol%)	NaOAc (1.1)	19h	–	–	–

because the starting material is sensitive, and was slowly decomposing over time.

Addition of Cu^{I} and Cu^{II} co-oxidants was explored in an attempt to improve the reaction (Table 4.16). These experiments failed to produce any of the desired bicycle **162** (except Entry 20, 1% yield). Instead, the copper salts significantly retarded the reaction, often returning large amounts of

starting **290**. Interestingly, loadings as low as 1 mol% of Cu(2-ethylhexanoate)$_2$ were sufficient to shut down the reaction (Entries 17 and 22). Various ligands were explored to modulate reactivity and increase solubility, but to no avail.

Ultimately, time constraints prevented further exploration of photoredox catalyzed radical cyclizations, but these initial results seem to be a promising avenue for further study.

I. Retrospective Analysis

Unfortunately, none of the strategies employed were able to produce isolable amounts of the desired *trans*-decalin associated with xiamycin A. In retrospect, it would have been helpful to commit more time to the isolation and characterization of reaction products. Specifically, more time could have been spent analyzing experiments labeled as 'inseparable mixture,' as they had interesting crude NMR spectra. Standard SiO_2-based methods were consistently employed, but proved to be insufficient. Perhaps normal-phase HPLC techniques would have been more effective.

REFERENCES

[1] Yang, D., Ye, X. Y., Xu, M., Pang, K. W., & Cheung, K. K., Investigation of Mn(III)-based oxidative free-radical cyclization reactions toward the synthesis of triptolide: The effects of lanthanide triflates and substituents on stereoselectivity. *J. Am. Chem. Soc.* **2000,** *122*, 1658–1663.

[2] Curran, D. P., Morgan, T. M., Schwartz, C. E., Snider, B. B., & Dombroski, M. A., Cyclizations of unsaturated •$CR(COX)_2$ radicals. Manganese(III) acetate oxidative cyclizations of unsaturated acetoacetates and atom-transfer cyclizations of unsaturated haloacetoacetates give the same radicals. *J. Am. Chem. Soc.* **1991,** *113*, 6607–6617.

[3] Barrero, A. F., Herrador, M. M., Quílez del Moral, J. F., & Valdivia, M. V., A convenient synthesis of A-ring-functionalized podolactones. Revision of the structure of wentilactone B. *Org. Lett.* **2002,** *4*, 1379–1382.

[4] Connelly, N. G., & Geiger, W. E., Chemical redox agents for organometallic chemistry. *Chem. Rev.* **1996,** *96*, 877–910.

[5] Jahn, U., Highly efficient generation of radicals from ester enolates by the ferrocenium ion. Application to selective α-oxygenation and dimerization reactions of esters. *J. Org. Chem.* **1998,** *63*, 7130-7131.

[6] Jahn, U., & Hartmann, P., Electron transfer-induced sequential transformations of malonates by the ferrocenium ion. *Chem. Commun.* **1998,** 209–210.

[7] Jahn, U., Müller, M., & Aussieker, S., The combination of anionic and radical reactions to oxidative tandem processes exemplified by the synthesis of functionalized pyrrolidines. *J. Am. Chem. Soc.* **2000,** *122*, 5212–5213.

[8] Jahn, U., Hartmann, P., Dix, I., & Jones, Peter G., Lithium malonate enolates as precursors for radical reactions – convenient induction of radical cyclizations with either radical or cationic termination. *Eur. J. Org. Chem.* **2001,** *2001*, 3333–3355.

[9] Jahn, U., Tandem anionic Michael addition/radical cyclizations: a new and efficient strategy for the synthesis of functionalized cyclopentanes. *Chem. Commun.* **2001,** 1600–1601.

[10] Jahn, U., & Hartmann, P., Oxidative radical cyclizations of malonate enolates induced by the ferrocenium ion - a remarkable influence of enolate counterion and additives. *J. Chem. Soc., Perkin Trans. 1* **2001,** 2277–2282.

[11] Jahn, U., Hartmann, P., Dix, I., & Jones, Peter G., Oxidative enolate cyclizations of 6,8-nonadienoates: Towards the synthesis of prostanes. *Eur. J. Org. Chem.* **2002,** *2002*, 718–735.

[12] Jahn, U., Hartmann, P., & Kaasalainen, E., Efficient oxidative radical cyclizations of ester enolates with carbocation desilylation as termination: Synthesis of cyclopentanoid monoterpenes and analogues. *Org. Lett.* **2004,** 6, 257–260.

[13] Jahn, U., & Dinca, E., Total synthesis of 15-F_{2t}-isoprostane by using a new oxidative cyclization of distonic radical anions as the key step. *Chem. Eur. J.* **2009,** 15, 58–62.

[14] Khobragade, D. A., Mahamulkar, S. G., Pospíšil, L., Císařová, I., Rulíšek, L., & Jahn, U., Acceptor-substituted ferrocenium salts as strong, single-electron oxidants: Synthesis, electrochemistry, theoretical investigations, and initial synthetic application. *Chem. Eur. J.* **2012,** 18, 12267–12277.

[15] Jagtap, P. R., Ford, L., Deister, E., Pohl, R., Císařová, I., Hodek, J., Weber, J., Mackman, R., Bahador, G., & Jahn, U., Highly functionalized and potent antiviral cyclopentane derivatives formed by a tandem process consisting of organometallic, transition-metal-catalyzed, and radical reaction steps. *Chem. Eur. J.* **2014,** 20, 10298–10304.

[16] Kafka, F., Holan, M., Hidasová, D., Pohl, R., Císařová, I., Klepetářová, B., & Jahn, U., Oxidative catalysis using the stoichiometric oxidant as a reagent: An efficient strategy for single-electron-transfer-induced tandem anion–radical reactions. *Angew. Chem. Int. Ed.* **2014,** 53, 9944–9948.

[17] Amatov, T., Pohl, R., Císařová, I., & Jahn, U., Synthesis of bridged diketopiperazines by using the persistent radical effect and a formal synthesis of bicyclomycin. *Angew. Chem. Int. Ed.* **2015,** 54, 12153–12157.

[18] Chen, P., Cao, L., Tian, W., Wang, X., & Li, C., Total synthesis and absolute configuration determination of (+)-subincanadine F. *Chem. Commun.* **2010,** 46, 8436–8438.

[19] Carney, M. J., Lesniak, J. S., Likar, M. D., & Pladziewicz, J. R., Ferrocene derivatives as metalloprotein redox probes: Electron-transfer reactions of ferrocene and ferricenium ion derivatives with cytochrome c. *J. Am. Chem. Soc.* **1984,** 106, 2565–2569.

[20] Guo, F., Clift, M. D., & Thomson, R. J., Oxidative coupling of enolates, enol silanes, and enamines: Methods and natural product synthesis. *Eur. J. Org. Chem.* **2012,** 2012, 4881–4896.

[21] Blanchette, M. A., Choy, W., Davis, J. T., Essenfeld, A. P., Masamune, S., Roush, W. R., & Sakai, T., Horner–Wadsworth–Emmons reaction: Use of lithium chloride and an amine for base-sensitive compounds. *Tetrahedron Lett.* **1984,** 25, 2183–2186.

[22] Schmittel, M., & Söllner, R., First characterization of a titanium enolate radical cation in solution: Carbon–carbon bond formation and the kinetics of the mesolytic Ti–O bond cleavage. *Angew. Chem. Int. Ed.* **1996,** 35, 2107–2109.

[23] Schmittel, M., & Söllner, R., Electroactive protecting groups and reaction units, 6. Titanium enolate radical cations in solution: Generation, characterization, and their reactions. *Chem. Ber.* **1997,** 130, 771–777.

[24] Schmittel, M., Burghart, A., Malisch, W., Reising, J., & Söllner, R., Diastereoselective enolate coupling through redox umpolung in silicon and titanium bisenolates: A novel concept based on intramolecularization of carbon–carbon bond formation. *J. Org. Chem.* **1998,** 63, 396–400.

[25] Schmittel, M., Burghart, A., Werner, H., Laubender, M., & Söllner, R., Probing M–O bond cleavage in silicon and titanium bisenolate radical cations. *J. Org. Chem.* **1999,** 64, 3077–3085.

[26] Schmittel, M., & Haeuseler, A., One-electron oxidation of metal enolates and metal phenolates. *J. Organomet. Chem.* **2002,** 661, 169–179.

[27] Schmittel, M., Lal, M., Lal, R., Röck, M., Langels, A., Rappoport, Z., Basheer, A., Schlirf, J., Deiseroth, H.-J., Flörke, U., & Gescheidt, G., A comprehensive picture of the one-electron oxidation chemistry of enols, enolates and α-carbonyl radicals: Oxidation potentials and characterization of radical intermediates. *Tetrahedron* **2009,** 65, 10842-10855.

[28] Li, Q., Hurley, P., Ding, H., Roberts, A. G., Akella, R., & Harran, P. G., Exploring symmetry-based logic for a synthesis of palau'amine. *J. Org. Chem.* **2009,** 74, 5909–5919.

[29] Moreira, I. d. P. R., Bofill, J. M., Anglada, J. M., Solsona, J. G., Nebot, J., Romea, P., & Urpí, F., Unconventional biradical character of titanium enolates. *J. Am. Chem. Soc.* **2008,** 130, 3242–3243.

[30] Hirao, T., Fujii, T., Miyata, S., & Ohshiro, Y., Oxovanadium(V)-induced oxidative transformations of cyclobutanones. *J. Org. Chem.* **1991,** 56, 2264–2266.

[31] Hirao, T., Fujii, T., Tanaka, T., & Ohshiro, Y., Oxovanadium(V)-induced tandem nucleophilic addition and oxidative ring-opening transformation. *Synlett* **1994,** 1994, 845–846.

[32] Hirao, T., Sakaguchi, M., Ishikawa, T., & Ikeda, I., Oxovanadium-induced or-catalyzed oxidative allylation of 1,3-dicarbonyl compounds with allylsilanes. *Synth. Commun.* **1995,** 25, 2579–2585.

[33] Hirao, T., Vanadium in modern organic synthesis. *Chem. Rev.* **1997,** 97, 2707–2724.

[34] Ryter, K., & Livinghouse, T., Dichloro(2,2,2-trifluoroethoxy)oxovanadium(V). A remarkably effective reagent for promoting one-electron oxidative cyclization and unsymmetrical coupling of silyl enol ethers. *J. Am. Chem. Soc.* **1998,** 120, 2658–2659.

[35] Hirao, T., Mori, M., & Ohshiro, Y., Versatile dehydrogenative aromatization of α , β -unsaturated cyclohexenones with $VO(OEt)Cl_2$-Me_3SiOTf. *Chem. Lett.* **1991,** 20, 783–784.

[36] Yang, D., Zheng, B. F., Gao, Q., Gu, S., & Zhu, N. Y., Enantioselective PhSe-group-transfer tandem radical cyclization reactions catalyzed by a chiral Lewis acid. *Angew. Chem. Int. Ed.* **2005,** 45, 255–258.

[37] Yang, D., Gu, S., Yan, Y. L., Zhao, H. W., & Zhu, N. Y., Atom-transfer tandem radical cyclization reactions promoted by Lewis acids. *Angew. Chem. Int. Ed.* **2002,** 41, 3014–3017.

[38] Yang, D., Yan, Y.-L., & Lui, B., Mild α-halogenation reactions of 1,3-dicarbonyl compounds catalyzed by Lewis acids. *J. Org. Chem.* **2002,** 67, 7429–7431.

[39] Guindon, Y., Lavallee, J. F., Llinas-Brunet, M., Horner, G., & Rancourt, J., Stereoselective chelation-controlled reduction of α -iodo- β -alkoxy esters under radical conditions. *J. Am. Chem. Soc.* **1991,** *113*, 9701–9702.

[40] Guindon, Y., Guérin, B., Chabot, C., & Ogilvie, W., Stereoselective radical carbon–carbon bond forming reactions of β -alkoxy esters: Atom and group transfer allylations under bidentate chelation controlled conditions. *J. Am. Chem. Soc.* **1996,** *118*, 12528–12535.

[41] Guindon, Y., & Rancourt, J., The use of Lewis acids in radical chemistry. Chelation-controlled radical reductions of substituted α -bromo- β -alkoxy esters and chelation-controlled radical addition reactions. *J. Org. Chem.* **1998,** 63, 6554–6565.

[42] Cardinal-David, B., Guérin, B., & Guindon, Y., Synthesis of tertiary and quaternary stereogenic centers: A diastereoselective tandem reaction sequence combining Mukaiyama and free radical-based allylation. *J. Org. Chem.* **2005,** 70, 776–784.

[43] Brazeau, J.-F., Mochirian, P., Prévost, M., & Guindon, Y., Stereopentads derived from a sequence of Mukaiyama aldolization and free radical reduction on α -methyl- β -alkoxy aldehydes: A general strategy for efficient polypropionate synthesis. *J. Org. Chem.* **2009,** 74, 64–74.

[44] Denissova, I., Maretti, L., Wilkes, B. C., Scaiano, J. C., & Guindon, Y., Raising the ceiling of diastereoselectivity in hydrogen transfer on acyclic radicals. *J. Org. Chem.* **2009,** 74, 2438–2446.

[45] Renaud, P., Andrau, L., & Schenk, K., First example of chelation control during radical cascade reactions of β -hydroxyester derivatives. *Synlett* **1999,** 1999, 1462-1464.

[46] Nicewicz, D. A., & MacMillan, D. W. C., Merging photoredox catalysis with organocatalysis: The direct asymmetric alkylation of aldehydes. *Science* **2008,** 322, 77–80.

[47] Furst, L., Matsuura, B. S., Narayanam, J. M. R., Tucker, J. W., & Stephenson, C. R. J., Visible light-mediated intermolecular C–H functionalization of electron-rich heterocycles with malonates. *Org. Lett.* **2010,** 12, 3104–3107.

[48] Wallentin, C.-J., Nguyen, J. D., Finkbeiner, P., & Stephenson, C. R. J., Visible light-mediated atom transfer radical addition via oxidative and reductive quenching of photocatalysts. *J. Am. Chem. Soc.* **2012,** 134, 8875–8884.

[49] Brill, Z. G., Grover, H. K., & Maimone, T. J., Enantioselective synthesis of an ophiobolin sesterterpene via a programmed radical cascade. *Science* **2016,** 352, 1078–1082.

[50] Tucker, J. W., Nguyen, J. D., Narayanam, J. M. R., Krabbe, S. W., & Stephenson, C. R. J., Tin-free radical cyclization reactions initiated by visible light photoredox catalysis. *Chem. Commun.* **2010,** 46, 4985–4987.

[51] Ju, X., Liang, Y., Jia, P., Li, W., & Yu, W., Synthesis of oxindoles via visible light photoredox catalysis. *Org. Biomol. Chem.* **2012,** 10, 498–501.

[52] Alpers, D., Brasholz, M., & Rehbein, J., Photoredox-induced radical 6-exo-trig cyclizations onto the indole nucleus: Aromative versus dearomative pathways. *Eur. J. Org. Chem.* **2017,** 2017, 2186–2193.

[53] Swift, E. C., Williams, T. M., & Stephenson, C. R. J., Intermolecular photocatalytic C–H functionalization of electron-rich heterocycles with tertiary alkyl halides. *Synlett* **2016,** 27, 754–758.

Chapter 5. Future Directions

A. Future Directions for the Xiamycin Family

It would be worthwhile to synthesize the 'dioridamycins' and compare their biological activity to the dixiamycins (Scheme 5.1). The only difference would be a single epimeric stereocenter on each monomer, leading to a minimal difference in overall structure. It is possible that the biological activity could be comparable to the natural dimers.

To synthesize 'dioridamycin A/B' (**291/292**) the electrochemical dimerization developed by Baran could be employed directly on oridamycin A (**26**) to produce the unnatural N-N linked dimers.[1] Baran and coworkers observed only one of the two possible atropisomers in their synthesis of dixiamycin B (**39**), so it is possible that only one atropisomer of 'dioridamycin' would be formed under identical conditions.

Synthesis of 'dioridamycin C' (**295**) would require a simple modification to the previously reported synthesis (Scheme 5.1.b). Namely, a Grignard reagent could be employed that would introduce the desired functional handle at C6 to allow for late-stage Buchwald–Hartwig C-N cross coupling to produce the desired dimeric compound **295**. A similar strategy was previously employed by Li *et al* in their synthesis of dixiamycin C (**42**).[2]

The synthesis of 'dioridamycin D/E' (**301/302**) would require more development (Scheme 5.1.c). Hydroboration/oxidation of **296** could produce the primary alcohol **297**. Elimination of the secondary alcohol and oxidation/functionalization of the primary alcohol would generate **298**. A Friedel–Crafts acylation could produce the desired fused carbazole **299**

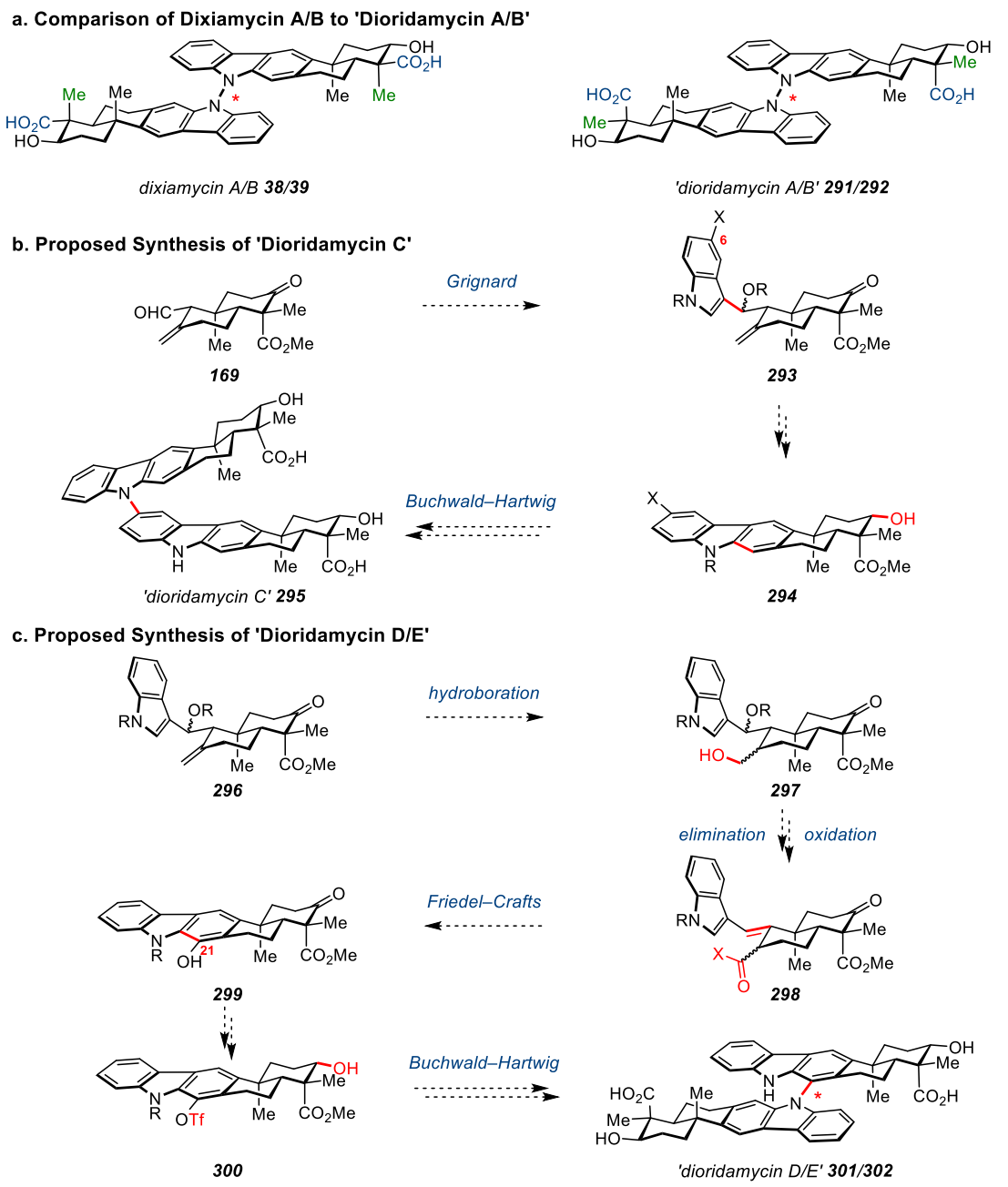

Scheme 5.1 Proposed syntheses of the 'dioridamycins.'

harboring a functional handle at C21. Triflation would precede a C–N cross coupling to form 'dioridamycin D/E' (**301/302**).

Future experiments could also be directed at producing xiamycin A (**28**, Scheme 5.2). Due to significant difficulties encountered when

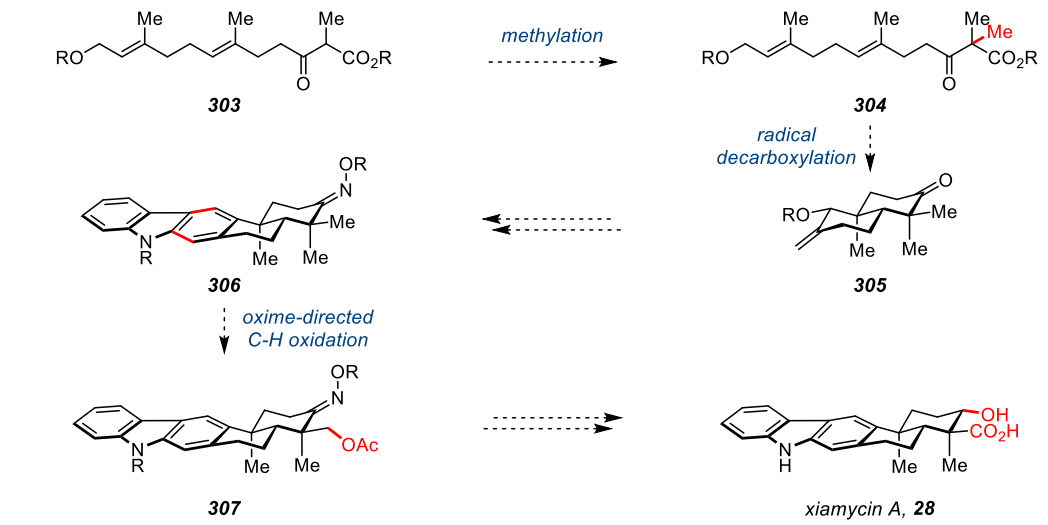

Scheme 5.2 Alternate synthetic strategy for xiamycin A (**28**).

attempting to generate the chelated radical intermediate, a mechanistically distinct strategy was sought. Starting with common synthetic precursor **303**, methylation and transesterification could produce *gem*-dimethyl **304**. The ester would be transformed into a photoactivatable substituent, such that upon irradiation with visible light in the presence of a photocatalyst substrate **304** would undergo a radical decarboxylation, followed by radical cyclization to produce *gem*-dimethyl bicycle **305**.[3-4] The carbazole **306** would be produced in the usual manner, and a C-H oxidation would produce the desired oxidized product through selective engagement of the equatorial methyl to produce **307**. Further manipulations would lead to xiamycin A (**28**).

B. Future Directions for Organic Chemistry

The current culture surrounding organic chemistry seems to favor applied research over basic research. Certainly, many great advances have

come from applying synthetic organic chemistry to myriad other fields, including biology, materials science, medicinal chemistry, and inorganic chemistry. That said, it seems as though excitement for basic research on organic chemistry has diminished, with proclamations that the era of "molecules" is over.[5] There is a push to reduce funding for classic organic chemistry, but findings in basic research are the fuel for translational research—applications of organic chemistry require a strong foundation of basic understanding. That is not to say that all funding should be focused on basic research rather than translational research. Both areas must push forward simultaneously.

A stronger emphasis on physical organic chemistry and mechanistic understanding is necessary to advance the field. The principles behind chemical reactivity must be honed in order to rationally construct complex molecules. Otherwise we are groping in the dark. Funding for basic research in organic chemistry can be discontinued when every reaction reliably produces the desired product.

Another promising future direction for organic chemistry is the blending of computational and organic chemistry. This collaboration could lead to a deeper understanding of the complex interactions at play in organic chemistry, aiding in the design and development of complex molecules. Furthermore, once a more robust understanding of chemical interactions is achieved, computational resources could be directed at predicting the outcomes of reactions, which would significantly accelerate research progress in organic chemistry and related fields.

Finally, it seems apparent that modularity will play an increasingly important role as organic chemistry matures. Nature has repeatedly demonstrated the power of modularity through DNA, proteins, and oligosaccharides. Presumably, the prevalence of cross coupling in drug discovery is due to its modular nature, allowing for high variability within a synthetic route. Modular methods are needed that produce a wider range of chemical motifs to battle the overwhelming tendency to produce flat, sp^2-rich compounds. The field must expand the repertoire of 'click chemistry' to include more methods that generate chiral centers, expanding the range of readily accessible chemical space.[6]

Another potential application of modularity could be in catalyst design. A catalyst domain that specifically binds to a particular substrate could be generated, and then various reactive functional units could be attached in a modular fashion to the binding domain. In this way, a target substrate could be selectively modified at various positions using catalysts readily synthesized from a common binding domain precursor.

REFERENCES

[1] Rosen, B. R., Werner, E. W., O'Brien, A. G., & Baran, P. S., Total synthesis of dixiamycin B by electrochemical oxidation. *J. Am. Chem. Soc.* **2014,** 136, 5571–5574.

[2] Meng, Z., Yu, H., Li, L., Tao, W., Chen, H., Wan, M., Yang, P., Edmonds, D. J., Zhong, J., & Li, A., Total synthesis and antiviral activity of indolosesquiterpenoids from the xiamycin and oridamycin families. *Nat. Commun.* **2015,** 6, 6096.

[3] Okada, K., Okamoto, K., Morita, N., Okubo, K., & Oda, M., Photosensitized decarboxylative Michael addition through N-(acyloxy)phthalimides via an electron-transfer mechanism. *J. Am. Chem. Soc.* **1991,** 113, 9401–9402.

[4] Schnermann, M. J., & Overman, L. E., A concise synthesis of (–)-aplyviolene facilitated by a strategic tertiary radical conjugate addition. *Angew. Chem. Int. Ed.* **2012,** 51, 9576–9580.

[5] Whitesides, G. M., Reinventing chemistry. *Angew. Chem. Int. Ed.* **2015,** 54, 3196–3209.

[6] Kolb, H. C., Finn, M., & Sharpless, K. B., Click chemistry: Diverse chemical function from a few good reactions. *Angew. Chem. Int. Ed.* **2001,** 40, 2004–2021.

Appendix I. Experimental Details and Tabulated Data

General Information. All commercial reagents (Aldrich, Alfa-Aesar, Acros Organics, Fluka) were used without further purification. All solvents were reagent or HPLC grade (Fisher). Anhydrous solvents were purchased from Sigma-Aldrich and were used without further purification. All reactions were carried out under an argon atmosphere unless otherwise noted. Analytical thin-layer chromatography (TLC) was performed using EMD Millipore silica gel 60 F_{254} plates (250 μm thickness) and visualized by UV fluorescence quenching and $KMnO_4$ staining. Preparative thin-layer chromatography (PTLC) separations were performed with EMD Millipore silica gel 60 F_{254} plates (1000 μm or 500 μm thickness). Flash column chromatography was performed using Silicycle silica gel 60 (40-63 μm). Yields refer to chromatographically and spectroscopically pure compounds. Infrared measurements were performed on a JASCO FT/IR 6100 spectrometer. ^{1}H NMR and ^{13}C NMR spectra were recorded on a Bruker Avance DRX-600 MHz at ambient temperature unless otherwise stated. Chemical shifts are reported in parts per million relative to residual solvent $CDCl_3$ (^{1}H, 7.26 ppm, ^{13}C, 77.16 ppm) or CD_3OD (^{1}H, 3.31 ppm, ^{13}C, 49.00 ppm). Multiplicities are reported as follows: s = singlet, d = doublet, dd = doublet of doublets, t = triplet, td = triplet of doublets, tt = triplet of triplets, m = multiplet, q = quartet, app. = apparent, br. s = broad singlet. Diastereomeric ratio (*dr*) was determined by ^{1}H NMR analysis. High-resolution mass spectral analyses were performed by the MSKCC core facility staff.

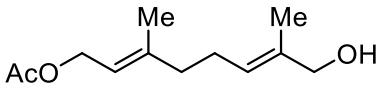

156

Allylic Alcohol **156**. SeO_2 (15.5 g, 140 mmol, 0.7 equiv.) was added to a solution of geranyl acetate (**157**, 39.2 g, 200 mmol, 1.0 equiv.) in anhydrous EtOH (500 mL) and was heated under a reflux condenser (oil bath = 105 °C) for 24 h. After cooling to room temperature, the solution was filtered through a celite pad and condensed. The resultant orange oil was dissolved in EtOH (100 mL) and Et_2O (360 mL) and cooled to 0 °C. Next, solid $NaBH_4$ (7.6 g, 200 mmol, 1.0 equiv.) was added in three equal portions and the solution was allowed to stir for 1 h at 0 °C. More $NaBH_4$ (3.0g, 79 mmol, 0.39 equiv.) was added, and the solution was allowed to stir 3 h at 0 °C. Upon completion, ice cold H_2O (300 mL) was slowly added to quench the reaction, which was allowed to slowly warm to room temperature and was stirred overnight. Saturated aq. $NaHCO_3$ was added, the layers were separated, and the aqueous layer was extracted with Et_2O (3 x 100 mL). The combined organic layers were washed with H_2O (2 x 100 mL) and brine (1 x 100 mL), dried over $MgSO_4$, filtered, and condensed to yield a yellow oil that was distilled (1.0 mbar, product in fraction collected between oil bath temperatures 175 °C → 205 °C) to yield the allylic alcohol **156** as a pale-yellow oil (23.3 g, 55 % yield).

156: The spectroscopic data matched the literature[1]; ^1H NMR (600 MHz, $CDCl_3$) δ 5.38 – 5.26 (m, 2H), 4.56 (d, *J* = 7.1 Hz, 2H), 3.96 (s, 2H), 2.18 – 2.11 (m, 2H), 2.09 – 2.04 (m, 2H), 2.03 (s, 3H), 1.68 (s, 2H), 1.64 (s, 3H);

^{13}C NMR (150 MHz, $CDCl_3$) δ 171.3, 141.8, 135.4, 125.3, 118.7, 68.9, 61.5, 39.2, 25.8, 21.1, 16.5, 13.8.

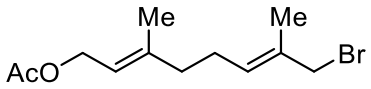

158

Allylic Bromide **158**. A solution of allylic alcohol **156** (9.88 g, 46.6 mmol, 1.0 equiv.) in anhydrous THF (150 mL) was cooled to -40 °C in a dry ice/acetone bath. MsCl (4.7 mL, 60.6 mmol, 1.3 equiv.) was added in one portion, followed by dropwise addition of Et_3N (12.9 mL, 93.2 mmol, 2.0 equiv.) and the contents were allowed to slowly warm to -20 °C over the course of 1 h. Next, a solution of LiBr (16.2g, 186.4 mmol, 4.0 equiv.) in THF (50 mL) was slowly added and the solution was slowly allowed to warm to 0 °C over the course of 1.5 h. After stirring at 0 °C for 1 h, the solution was quenched with H_2O (100 mL), the aqueous was extracted with Et_2O (3 x 100 mL), the combined organics were washed with sat. aq. $NaHCO_3$ (1 x 100 mL), brine (1 x 100 mL), dried over $MgSO_4$, filtered, and condensed to yield pure allylic bromide **158** as an orange-yellow oil (11.52 g, 90% yield).

158: Spectroscopic data was in agreement with the literature[2]; ^{1}H NMR (600 MHz, $CDCl_3$) δ 5.55 (t, *J* = 7.1 Hz, 1H), 5.32 (tq, *J* = 7.1, 1.3 Hz, 1H), 4.57 (d, *J* = 7.1 Hz, 2H), 3.95 (s, 2H), 2.15 (q, *J* = 7.3 Hz, 2H), 2.07 (t, *J* = 7.8 Hz, 2H), 2.04 (s, 3H), 1.74 (s, 3H), 1.69 (s, 3H); ^{13}C NMR (150 MHz, $CDCl_3$) δ 171.2, 141.4, 132.6, 130.5, 119.0, 61.4, 41.7, 38.7, 26.5, 21.2, 16.5, 14.8.

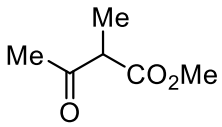

155

Methyl 2-Methyl-3-oxobutanoate **155**. Methyl acetoacetate (54 mL, 500 mmol, 1.0 equiv.) and iodomethane (31 mL, 500 mmol, 1.0 equiv.) were cooled to 0 °C. Then K_2CO_3 (104 g, 750 mmol, 1.5 equiv.) was added in four equal portions over the course of 30 min. The reaction was vigorously stirred for 18 h (vigorous stirring is vital!) and allowed to slowly reach room temperature. Then, the contents were diluted with Et_2O (~150 mL), filtered, the precipitate was washed with Et_2O (6 x 100 mL), then the filtrate was condensed and distilled (1.0 mbar, 44 °C vapor temperature) to yield methyl 2-methyl-3-oxobutanoate **155** as a clear oil (54.3 g, 84% yield).

155: Spectroscopic data was in agreement with the literature[3]; ^{1}H NMR (600 MHz, $CDCl_3$) δ 3.74 (s, 3H), 3.52 (q, *J* = 7.2 Hz, 1H), 2.23 (s, 3H), 1.35 (d, *J* = 7.2 Hz, 3H); ^{13}C NMR (150 MHz, $CDCl_3$) δ 203.7, 171.1, 53.6, 52.6, 28.6, 12.9.

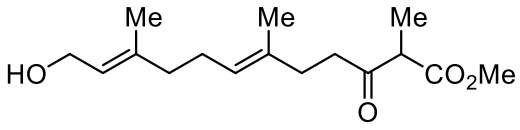

154

Linear Alcohol **154**. NaH (60 wt%/mineral oil, 9.3 g, 234 mmol, 5.0 equiv.) was added to a flame-dried flask, followed by the addition of anhydrous THF (540 mL) and HMPA (15 mL) and the solution was cooled to

0 °C. Next, neat **155** (30.3 g, 234 mmol, 5.0 equiv.) was added slowly, causing the gas evolution and the grey suspension to thicken. The solution was stirred at 0 °C for 30 min. A solution of *n*-BuLi (2.37M in hexanes, 98 mL, 234 mmol, 5.0 equiv.) was added dropwise at 0 °C, and the suspension became soluble and turned orange. Crude allylic bromide **158** (12.8 g, 46.7 mmol, 1.0 equiv.) in THF (50 mL) was then added rapidly in one portion. The reaction was allowed to slowly warm to room temperature and was stirred for 16 h. Upon completion, the reaction was quenched with sat. aq. NH_4Cl (300 mL), the aqueous layer was extracted with CH_2Cl_2 (3 x 150 mL), dried over $MgSO_4$, filtered, and condensed. The resultant orange oil was purified via flash column chromatography (silica gel, gradient of hexanes/EtOAc 20/3 → 4/1 → 3/1 → 20/7) to yield linear alcohol **154** as a pale orange oil (10.73 g, 82% yield).

154: Spectroscopic data was in agreement with the literature[4]; ^{1}H NMR (600 MHz, $CDCl_3$) δ 5.38 – 5.26 (m, 2H), 4.56 (d, *J* = 7.1 Hz, 2H), 3.96 (s, 2H), 2.18 – 2.11 (m, 2H), 2.09 – 2.04 (m, 2H), 2.03 (s, 3H), 1.68 (s, 2H), 1.64 (s, 3H); ^{13}C NMR (150 MHz, $CDCl_3$) δ 205.6, 171.2, 139.3, 133.7, 124.7, 123.8, 59.5, 52.8, 52.5, 40.1, 39.4, 33.2, 26.2, 16.3, 16.2, 12.9.

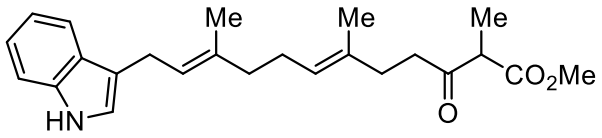

159

Linear Indole **159**. Linear alcohol **154** (1.35 g, 4.79 mmol, 1.0 equiv.) was dissolved in 48 mL Et_2O and cooled to 0 °C. PBr_3 (226 μL, 2.39 mmol, 0.5 equiv.) was added and the solution was allowed to stir at 0 °C for 25 min. Upon completion, the reaction was quenched with ice water, followed by cold sat. aqueous $NaHCO_3$ (0 °C). The aqueous layer was extracted 2x with EtOAc, and the combined organic layers were washed with sat. aqueous $NaHCO_3$, brine, dried over $MgSO_4$, filtered, and condensed. The resultant material was used directly in the next step without further purification. A suspension of $Zn(OTf)_2$ (2.1 g, 5.75 mmol, 1.2 equiv.), TBAI (1.77 g, 4.79 mmol, 1.0 equiv.), indole (1.12 g, 9.58 mmol, 2.0 equiv.), and *i*-Pr_2NEt (1.8 mL, 10.54 mmol, 2.2 equiv.) in 28 mL of PhMe was created, to which crude bromide **158** was added as a solution in PhMe. The resultant suspension was stirred at room temperature for 1 h, and was quenched with sat. aqueous NH_4Cl. The aqueous layer was extracted 3x with EtOAc, and the combined organic layers were washed with H_2O, dried over $MgSO_4$, filtered, and condensed. The resultant material was purified via flash column chromatography (silica gel, 20% Et_2O/hexanes) to produce linear indole **159** as a yellow oil (1.28 g, 70% yield).

159: R_f = 0.27 (silica gel, 20% acetone/hexanes); IR (film): ν_{max} 3404, 2984, 2912, 1739, 1710, 1454, 1433, 1336, 1203, 1089, 740 cm^{-1}; ^1H NMR

(600 MHz, $CDCl_3$) δ 8.05 (s, 1H), 7.59 (d, J = 7.7 Hz, 1H), 7.35 (d, J = 8.1 Hz, 1H), 7.21 – 7.16 (m, 1H), 7.13 – 7.06 (m, 1H), 6.97 – 6.90 (m, 1H), 5.45 (t, J = 7.1 Hz, 1H), 5.13 (d, J = 6.7 Hz, 1H), 3.72 (s, 3H), 3.52 (q, J = 7.2 Hz, 1H), 3.47 (d, J = 7.2 Hz, 2H), 2.66 – 2.50 (m, 2H), 2.24 (t, J = 7.7 Hz, 2H), 2.13 (q, J = 7.2 Hz, 2H), 2.10 – 2.05 (m, 2H), 1.75 (s, 3H), 1.59 (s, 3H), 1.32 (d, J = 7.2 Hz, 4H); ^{13}C NMR (150 MHz, $CDCl_3$) δ 205.7, 171.3, 136.6, 135.4, 133.5, 127.6, 125.1, 123.3, 122.0, 121.4, 119.2, 119.1, 116.2, 111.2, 52.8, 52.6, 40.3, 39.6, 33.4, 26.5, 24.1, 16.3, 16.1, 13.0; HRMS (ESI, m/z) calcd for $C_{24}H_{32}NO_3$ $[M+H]^+$ 382.2382, found 382.2367.

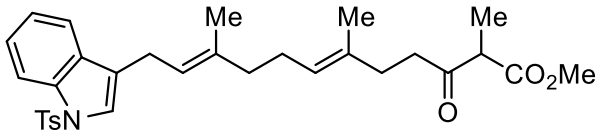

160

Linear Tosyl-Indole **160**. A suspension of NaH (60% dispersion in mineral oil, 52 mg, 1.31 mmol, 1.0 equiv.) in 13 mL THF was prepared at room temperature, and subsequently cooled to 0 °C. A solution of linear indole **159** (500 mg, 1.31 mmol, 1.0 equiv.) in THF was added and stirred for 20 min, followed by slow addition of *n*-BuLi (2.04M/hexanes, 640 μL, 1.31 mmol, 1.0 equiv.). The solution was stirred for an additional 20 min at 0 °C, and *p*-TsCl (274 mg, 1.44 mmol, 1.1 equiv.) was added. The reaction was stirred at for 1 h at 0 °C, and was quenched with sat. aqueous NH_4Cl. The aqueous layer was extracted 3x with CH_2Cl_2, and the combined organic layers were dried over $MgSO_4$, filtered, and condensed. The resultant material was purified via flash column chromatography (silica gel, 5% acetone, 45%

PhMe, 50% hexanes) to produce linear tosyl-indole **160** as a yellow oil (375 mg, 53% yield).

160: R_f = 0.28 (silica gel, 20% acetone/hexanes); IR (film): ν_{max} 3431, 2928, 1716, 1446, 1368, 1173, 1120, 973, 744, 670, 578 cm^{-1}; ^1H NMR (600 MHz, $CDCl_3$) δ 7.96 (d, J = 8.3 Hz, 1H), 7.73 (d, J = 8.4 Hz, 2H), 7.45 (d, J = 7.6 Hz, 1H), 7.32 – 7.28 (m, 1H), 7.27 – 7.26 (m, 1H), 7.23 – 7.18 (m, 3H), 5.35 (t, J = 7.1 Hz, 1H), 5.12 (t, J = 6.9 Hz, 1H), 3.72 (s, 3H), 3.54 (q, J = 7.2 Hz, 1H), 3.34 (d, J = 7.0 Hz, 2H), 2.69 – 2.52 (m, 2H), 2.33 (s, 3H), 2.25 (t, J = 7.6 Hz, 2H), 2.12 (q, J = 7.2 Hz, 2H), 2.09 – 2.03 (m, 2H), 1.71 (s, 3H), 1.60 (s, 3H), 1.33 (d, J = 7.2 Hz, 3H); ^{13}C NMR (150 MHz, $CDCl_3$) δ 205.7, 171.2, 144.8, 137.3, 135.6, 135.5, 133.7, 131.2, 129.9, 126.9, 124.9, 124.7, 123.1, 122.9, 122.8, 121.0, 119.7, 113.9, 52.8, 52.6, 40.3, 39.6, 33.4, 26.6, 24.0, 21.7, 16.4, 16.3, 13.0; HRMS (ESI, m/z) calcd for $C_{31}H_{37}NO_5NaS$ $[M+Na]^+$ 558.2290, found 558.2277.

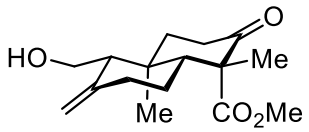

162

Bicyclic Alcohol **162**. Linear alcohol **154** (2.82 g, 10.0 mmol, 1.0 equiv.) was dissolved in PhMe (~100 mL) and trace water was removed via azeotropic distillation, then it was dissolved in acetic acid (110 mL) and degassed with two freeze-pump-thaw cycles (Note: as has been previously noted for related transformations, it was vital to thoroughly degass the solution prior to cyclization to obtain reasonable yields).[5] Next, $Mn(OAc)_3•2H_2O$ (5.9 g, 22 mmol, 2.2 equiv.) and $Cu(OAc)_2•H_2O$ (2.0 g,

10 mmol, 1.0 equiv.) were added simultaneously, and the dark brown suspension was stirred at room temperature under an Argon atmosphere for 16 h. The suspension was condensed, then taken up in EtOAc (~100 mL), to which H_2O (~100 mL) and sat. $NaHSO_3$ (~100 mL) were added. The phases were separated and the aqueous layer was extracted with EtOAc (2 x 50 mL). The combined organic layers were washed brine (2 x 50 mL), then dried over Na_2SO_4, filtered, and condensed. The orange oil was purified via flash column chromatography (silica gel, hexanes/Et_2O 3/7) to yield bicyclic alcohol **162** as a crystalline white solid (1.41 g, 50% yield).

162: R_f = 0.67 (silica gel, Et_2O); IR (film): ν_{max} 3444, 2951, 1711, 1457, 1223, 1024, 891 cm^{-1}; ^1H NMR (600 MHz, $CDCl_3$) δ 5.04 (s, 1H), 4.73 (s, 1H), 3.85 (d, *J* = 6.7 Hz, 2H), 3.66 (s, 3H), 2.95 (td, *J* = 14.8, 6.3 Hz, 1H), 2.52 – 2.43 (m, 2H), 2.09 (ddd, *J* = 13.3, 6.4, 2.7 Hz, 1H), 2.03 – 1.91 (m, 4H), 1.67 (td, *J* = 14.1, 4.3 Hz, 1H), 1.63 – 1.54 (m, 1H), 1.43 (d, *J* = 5.8 Hz, 1H), 1.37 (s, 3H), 0.85 (s, 3H); ^{13}C NMR (150 MHz, $CDCl_3$) δ 208.2, 173.9, 146.1, 107.9, 58.9, 57.6, 57.3, 52.3, 39.1, 38.8, 37.8, 37.1, 26.0, 21.4, 13.4; HRMS (ESI, m/z) calcd for $C_{16}H_{24}O_4Na$ $[M+Na]^+$ 303.1572, found 303.1572.

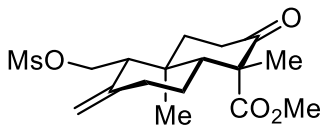

A1

Mesylate **A1**. Bicyclic alcohol **162** (26 mg, 92 μmol, 1.0 equiv.) was dissolved in 1 mL CH_2Cl_2 and cooled to -78 °C. Et_3N (25 μL, 184 μmol,

2.0 equiv.) was added and the solution was stirred for 10 min. MsCl (10 μL, 120 μmol, 1.3 equiv.) was added, and the solution was removed from the cold bath and stirred for 25 min before being quenched with sat. aqueous $NaHCO_3$. The solution was further diluted with Et_2O and H_2O, the aqueous layer was extracted 3x with Et_2O, and the combined organic layers were washed with sat. aqueous $NaHCO_3$, 2x with H_2O, 2x with sat. aqueous NH_4Cl, and brine, dried over $MgSO_4$, filtered, and condensed. The resultant material was used (and characterized) without further purification, yielding mesylate **A1** as a yellow oil (28 mg, 85% yield).

A1: R_f = 0.31 (silica gel, 40% ethyl acetate/hexanes); IR (film): ν_{max} 3350, 2939, 1712, 1354, 1225, 1173, 951, 733 cm^{-1}; ^1H NMR (600 MHz, $CDCl_3$) δ 5.01 (s, 1H), 4.70 (s, 1H), 4.47 (dd, J = 10.2, 4.1 Hz, 1H), 4.40 (dd, J = 10.2, 8.3 Hz, 1H), 3.66 (s, 3H), 3.00 (s, 3H), 2.95 (td, J = 14.8, 6.2 Hz, 1H), 2.54 – 2.45 (m, 2H), 2.16 (dd, J = 8.3, 4.0 Hz, 1H), 2.11 (ddd, J = 13.3, 6.2, 2.7 Hz, 1H), 2.04 – 1.88 (m, 3H), 1.71 (td, J = 14.1, 4.6 Hz, 1H), 1.61 (dd, J = 10.5, 4.7 Hz, 1H), 1.37 (s, 3H), 0.89 (s, 3H); ^{13}C NMR (150 MHz, $CDCl_3$) δ 207.6, 173.6, 144.1, 109.2, 77.4, 77.2, 77.0, 65.9, 57.6, 57.0, 53.7, 52.3, 39.3, 38.7, 37.8, 37.4, 36.9, 25.7, 21.4, 13.3; HRMS (ESI, m/z) calcd for $C_{17}H_{27}O_6S$ $[M+H]^+$ 359.1528, found 359.1528.

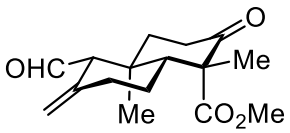

169

Bicyclic Aldehyde **169**. Bicyclic alcohol **162** (1.31 g, 4.7 mmol, 1.0 equiv.) was dissolved in anhydrous CH_2Cl_2 (50 mL) and cooled to 0 °C. Dess–Martin periodinane[6-7] (3.97 g, 9.4 mmol, 2.0 equiv.) was added and the cloudy white suspension was stirred at 0 °C for 30 min. The reaction was quenched with 1:1 sat. aqueous $NaHCO_3$: sat. aqueous $Na_2S_2O_3$ (~50 mL) at 0 °C, then removed from the ice bath and allowed to stir at room temperature until both layers were transparent. The aqueous layer was extracted with CH_2Cl_2 (3 x 25 mL), and the combined organic layers were washed with 1:1 sat. aqueous $NaHCO_3$: sat. aqueous $Na_2S_2O_3$ (1 x 25 mL), and brine (1 x 25 mL), then dried over $MgSO_4$, filtered, and condensed. The resultant yellow oil was purified via flash column chromatography (silica gel, hexanes/acetone 85/15) to yield bicyclic aldehyde **169** as a crystalline white solid (0.95 g, 73% yield).

169: R_f = 0.48 (silica gel, hexanes/Et_2O 1/1); IR (film): ν_{max} 2953, 1717, 1457, 1223, 1143, 1097, 896 cm^{-1}; ^1H NMR (600 MHz, $CDCl_3$) δ 9.88 (d, *J* = 4.0 Hz, 1H), 5.03 (s, 1H), 4.59 (s, 1H), 3.69 (s, 3H), 2.98 (td, *J* = 14.9, 6.1 Hz, 1H), 2.53 – 2.48 (m, 2H), 2.45 (ddd, *J* = 14.8, 4.5, 2.7 Hz, 1H), 2.07 – 1.93 (m, 3H), 1.62 – 1.55 (m, 2H), 1.49 (dd, *J* = 11.7, 3.2 Hz, 1H), 1.38 (s, 3H), 1.21 (s, 3H); ^{13}C NMR (150 MHz, $CDCl_3$) δ 207.5, 203.2, 173.6, 143.1, 110.9, 66.1, 57.6, 56.4, 52.4, 38.9, 38.7, 36.9, 36.7, 25.2, 21.4, 13.9; HRMS (ESI, m/z) calcd for $C_{16}H_{23}O_4$ $[M+H]^+$ 279.1596, found 279.1583.

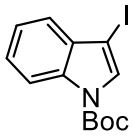

A2

Tert-butyl 3-iodoindole-1-carboxylate **A2**. KOH (2.39 g, 42.7 mmol, 2.5 equiv.) was added to a solution of indole (2 g, 17.1 mmol, 1.0 equiv.) in anhydrous DMF (35 mL) at room temperature under air. A solution of I_2 (4.38 g, 17.2 mmol, 1.0 equiv.) in anhydrous DMF (5 mL) was added and the resultant solution was stirred at room temperature for 50 min. Upon completion, the solution was poured into ice water (400 mL), the precipitate was collected via filtration, washed with H_2O (~30 mL), and dried via azeotropic distillation with PhMe. The resultant material was immediately used in the next step due to its instability. The resultant beige powder was dissolved in anhydrous CH_2Cl_2 (90 mL) at room temperature. Et_3N (7.2 mL, 51.3 mmol, 3.0 equiv.) was added and the solution was cooled to 0 °C. Then, Boc_2O (7.9 mL, 34.2 mmol, 2.0 equiv.) was added, followed by a catalytic amount of DMAP (~ 10 mg). The solution was removed from the ice bath and stirred at room temperature overnight (16 h). The reaction was quenched with H_2O (~150 mL), the aqueous layer was extracted with CH_2Cl_2 (3 x 75 mL), the combined organic layers were washed with H_2O (1 x 100 mL), brine (1 x 100 mL), dried over $MgSO_4$, filtered, and condensed. The crude material was purified via flash column chromatography (silica gel, hexanes/EtOAc 19/1) to yield *tert*-butyl 3-iodoindole-1-carboxylate **A2** as a dark brown oil (5.27 g, 90% yield over two steps).

A2: Spectroscopic data was in agreement with the literature[8]; ^{1}H NMR (600 MHz, $CDCl_3$) δ 8.15 (d, *J* = 6.4 Hz, 1H), 7.75 (s, 1H), 7.42 (d, *J* = 8.0 Hz, 1H), 7.39 (t, *J* = 7.8 Hz, 1H), 7.33 (t, *J* = 7.3 Hz, 1H), 1.69 (s, 9H); ^{13}C NMR (150 MHz, $CDCl_3$) δ 148.8, 134.9, 132.2, 130.2, 125.4, 123.4, 121.59, 115.2, 84.38, 65.6, 28.3.

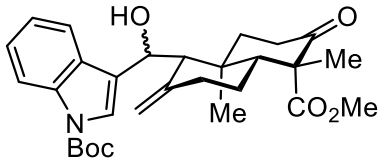

171

Secondary Alcohol **171**. Trace water was removed from *tert*-butyl 3-iodoindole-1-carboxylate **A2** (5.87 g, 17.1 mmol, 5.0 equiv.) via azeotropic distillation with PhMe. Then, it was dissolved in anhydrous THF (90 mL) and cooled to 0 °C. A solution of EtMgBr (3.0 M in Et_2O, 5.6 mL, 16.9 mmol, 4.95 equiv.) was added dropwise. The solution was stirred at 0 °C for 20 min, then it was removed from the ice bath and stirred at room temperature for 35 min. During this time, a solution of aldehyde **169** (0.95 g, 3.42 mmol, 1.0 equiv.) was prepared as follows: Trace water was removed from aldehyde **169** via azeotropic distillation with PhMe. Then it was dissolved in THF (60 mL) and cooled to 0 °C. The solution of *tert*-butyl 3-iodoindole-1-carboxylate **A1** and EtMgBr was re-cooled to 0 °C, then cannulated dropwise into the solution containing aldehyde **169** over the course of 15 min at 0 °C. The resulting solution was allowed to stir at 0 °C for 30 min before being quenched with sat. NH_4Cl (~100 mL). The aqueous layer was extracted with EtOAc (3 x 75 mL), and the combined organic layers were dried over $MgSO_4$, filtered, and condensed. The orange-yellow oil was purified via flash column

chromatography (silica gel, hexanes/acetone 4/1) to yield secondary alcohol **171** as a pale-yellow powder (1.68 g, 99% yield). The diastereomers were not separated and were characterized together (approximate *dr* = 4:1).

171: R_f = 0.45 (silica gel, hexanes/Et_2O 1/1); IR (film): ν_{max} 3535, 2982, 2951, 1711, 1454, 1367, 1252, 1223, 1155, 735 cm^{-1}; ^1H NMR (600 MHz, $CDCl_3$): Selected Peaks, *Major Diastereomer* δ 7.53 (s, 1H), 7.49 (d, *J* = 7.8 Hz, 1H), 5.51 (t, *J* = 3.7 Hz, 1H), 5.28 (s, 1H), 5.06 (s, 1H), 3.01 (td, *J* = 14.7, 6.1 Hz, 1H), 2.41 (ddd, *J* = 14.7, 4.5, 2.8 Hz, 1H), 1.24 (s, 3H). *Minor Diastereomer*: δ 7.57 (d, *J* = 7.8 Hz, 1H), 7.46 (s, 1H), 5.40 (dd, *J* = 7.5, 3.4 Hz, 1H), 4.83 (s, 1H), 4.58 (s, 1H), 2.83 (ddd, *J* = 13.8, 6.1, 2.8 Hz, 1H), 2.54 (d, *J* = 7.4 Hz, 1H), 1.20 (s, 3H); ^{13}C NMR (150 MHz, $CDCl_3$) *Both Diastereomers*: δ 208.9, 208.5, 173.9, 173.8, 149.8, 147.2, 144.2, 135.7, 128.8, 125.6, 124.7, 124.5, 124.0, 123.8, 122.8, 122.7, 122.6, 119.5, 115.6, 115.6, 111.7, 110.3, 83.9, 68.3, 66.6, 58.9, 58.3, 58.2, 58.2, 58.0, 57.6, 52.2, 52.2, 42.0, 40.6, 39.9, 39.1, 38.9, 38.2, 37.4, 37.2, 28.3, 28.3, 26.5, 26.4, 21.6, 21.4, 14.6, 13.7; HRMS (ESI, m/z) calcd for $C_{29}H_{37}NO_6Na$ $[M+Na]^+$ 518.2519, found 518.2521.

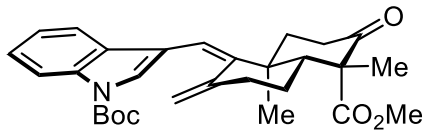

175

Triene **175**. Secondary alcohol **171** (25 mg, 50 μmol, 1.0 equiv.) was dissolved in 1 mL CH_2Cl_2 and cooled to 0 °C. TFA (8 μL, 100 μmol, 2.0 equiv.) was added dropwise, and the solution was stirred for 40 min at 0 °C. The

reaction was removed from the ice bath and allowed to warm to room temperature over 2h. The reaction was diluted with EtOAc and H_2O, and the aqueous layer was extracted 3x with EtOAc. The combined organic layers were washed with brine, dried over $MgSO_4$, filtered, and condensed. The resultant material was purified via flash column chromatography (silica gel, 10% EtOAc/hexanes) to yield triene **175** as a clear oil (20 mg, 83% yield).

175: R_f = 0.25 (silica gel, 10% ethyl acetate/hexanes); IR (film): ν_{max} 1727, 1453, 1370, 1224, 1155, 1082, 907, 732 cm^{-1}; ^1H NMR (600 MHz, $CDCl_3$) δ 8.07 (s, 1H), 7.71 (s, 1H), 7.49 (d, J = 7.7 Hz, 1H), 7.29 (t, J = 7.8 Hz, 1H), 7.22 (t, J = 7.6 Hz, 1H), 6.20 (s, 1H), 5.02 (s, 1H), 4.80 (s, 1H), 3.71 (s, 3H), 3.13 (td, J = 14.8, 5.8 Hz, 1H), 2.69 – 2.54 (m, 2H), 2.25 – 2.00 (m, 5H), 1.74 (dd, J = 12.2, 3.3 Hz, 1H), 1.66 (s, 10H), 1.40 (s, 3H), 1.21 (s, 3H); ^{13}C NMR (150 MHz, $CDCl_3$) δ 208.3, 173.7, 152.1, 145.2, 124.4, 123.3, 122.5, 119.2, 117.3, 115.3, 114.2, 109.8, 57.9, 56.2, 52.3, 41.7, 37.5, 37.2, 36.8, 28.4, 25.6, 21.6, 18.6; HRMS (ESI, m/z) calcd for $C_{29}H_{36}NO_5$ $[M+H]^+$ 478.2593, found 478.2574.

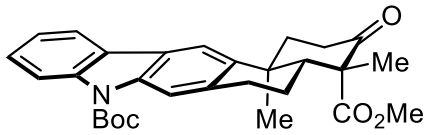

176

Boc-Carbazole **176**. *Preparation 1.* Triene **175** (17 mg, 36 μmol, 1.0 equiv.) was dissolved in 600 μL PhMe and transferred to a pressure tube. The solution was heated to 140 °C for 2 h and 20 min before being condensed. The crude material was purified via flash column

chromatography (silica gel, 12% to 15% EtOAc/hexanes) to yield Boc-carbazole **176** as a pale-yellow oil (11.3 mg, 66% yield).

Boc-Carbazole **176**. *Preparation 2.* Secondary alcohol **171** (260 mg, 0.52 mmol, 1.0 equiv.) was dissolved in anhydrous CH_2Cl_2 (9 mL) and cooled to 0 °C (no effort was made to maintain an inert atmosphere). TFA (80μL, 1.05 mmol, 2.0 equiv.) was added in one portion, and the solution was stirred at 0 °C for 20 min. The flask was removed from the ice bath and was allowed to warm to room temperature, and was stirred at room temperature for 2.5 h. The solvent was removed under reduced pressure, then azeotropically distilled with PhMe, dissolved in anhydrous PhMe (9 mL), and heated to 140 °C for 2 h and 20 min. Upon completion, the reaction was condensed to yield a brown foam, which was purified by flash column chromatography (silica gel, hexanes/acetone 9/1) to yield **176** as a beige foam (168 mg, 68% yield).

176: R_f = 0.22 (silica gel, hexanes/acetone 9/1); IR (film): ν_{max} 2976, 1723, 1456, 1359, 1226, 1156, 769 cm^{-1}; ^1H NMR (600 MHz, $CDCl_3$) δ 8.22 (d, *J* = 8.4 Hz, 1H), 8.04 (s, 1H), 7.92 (d, *J* = 7.3 Hz, 1H), 7.87 (s, 1H), 7.42 (ddd, *J* = 8.4, 7.3, 1.3 Hz, 1H), 7.32 (td, *J* = 7.5, 1.0 Hz, 1H), 3.73 (s, 3H), 3.24 – 3.16 (m, 2H), 3.09 – 3.00 (m, 1H), 2.78 (ddd, *J* = 13.3, 6.3, 2.5 Hz, 1H), 2.64 (ddd, *J* = 14.7, 4.5, 2.4 Hz, 1H), 2.29 – 2.21 (m, 2H), 1.95 – 1.85 (m, 2H), 1.75 (s, 9H), 1.50 (s, 3H), 1.41 (s, 3H); ^{13}C NMR (150 MHz, $CDCl_3$) δ 208.1, 174.2, 151.3, 141.6, 138.8, 137.3, 134.7, 126.9, 125.9, 124.5, 123.1, 119.4, 116.4, 116.4, 116.2, 84.0, 57.7, 54.2, 52.4, 39.8, 38.4,

37.7, 32.9, 28.5, 23.4, 21.8, 21.1; HRMS (ESI, m/z) calcd for $C_{29}H_{33}NO_5Na$ $[M+Na]^+$ 498.2256, found 498.2239.

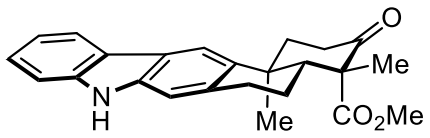

177

Carbazole **177**. *Preparation 1.* Boc-carbazole **173** (11.3 mg, 24 μmol, 1.0 equiv.) was dissolved in 400 μL CH_2Cl_2. TFA (18 μL, 240 μmol, 10.0 equiv.) was added, and the solution was heated to 45 °C for 2.5 h. The solution was condensed and the resultant material was purified via flash column chromatography (silica gel, 15% acetone/hexanes) to yield carbazole **177** as a white foam (5.5 mg, 61% yield).

Carbazole **177**. *Preparation 2.* Secondary alcohol **171** (1.42 g, 2.87 mmol, 1.0 equiv.) was dissolved in anhydrous CH_2Cl_2 (48 mL) and cooled to 0 °C. TFA (440 μL, 5.74 mmol, 2.0 equiv.) was added dropwise, and the solution was allowed to stir at 0° C for 10 min, at which point it was removed from the ice bath and allowed to warm to room temperature. The solution was stirred at room temperature for 3 h, then it was condensed, azeotropically distilled with PhMe to remove trace TFA and H_2O, dissolved in anhydrous PhMe (48 mL), transferred to a pressure tube, heated to 135 °C, and stirred for 2 h. The solution was allowed to cool to room temperature, then TFA (2.2 mL, 28.7 mmol, 10.0 equiv.) was added dropwise, the solution was heated to 45 °C, and the mixture was stirred for 2.5 h. The solution was condensed and the resultant brown oil was purified by flash column

chromatography (silica gel, acetone/hexanes 4/1) to yield carbazole **177** as a brown foam (561 mg, 52% yield).

177: R_f = 0.63 (silica gel, hexanes/EtOAc 2/1); IR (film): ν_{max} 3410, 2956, 1705, 1467, 1322, 1239, 1097, 735 cm^{-1}; ^1H NMR (600 MHz, $CDCl_3$) δ 8.00 (d, *J* = 7.8 Hz, 1H), 7.98 (s, 1H), 7.87 (s, 1H), 7.37 (d, *J* = 3.5 Hz, 1H), 7.20 (dt, *J* = 8.0, 3.8 Hz, 1H), 7.11 (s, 1H), 3.73 (s, 3H), 3.25 – 3.12 (m, 2H), 3.08 – 2.99 (m, 1H), 2.82 (ddd, *J* = 13.3, 6.3, 2.5 Hz, 1H), 2.64 (ddd, *J* = 14.7, 4.6, 2.4 Hz, 1H), 2.31 – 2.19 (m, 2H), 1.94 (td, *J* = 14.0, 4.5 Hz, 1H), 1.89 (dd, *J* = 11.4, 2.7 Hz, 1H), 1.50 (s, 3H), 1.43 (s, 3H); ^{13}C NMR (150 MHz, $CDCl_3$) δ 208.4, 174.3, 140.2, 138.5, 138.3, 133.6, 125.8, 123.5, 122.4, 120.1, 119.4, 116.9, 110.7, 110.0, 57.7, 54.5, 52.3, 40.1, 38.4, 37.8, 32.7, 23.6, 21.8, 21.2; HRMS (ESI, m/z) calcd for $C_{24}H_{26}NO_3$ $[M+H]^+$ 376.1913, found 376.1913.

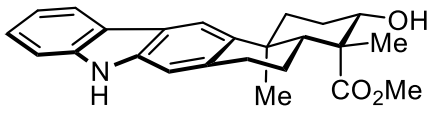

178

Alcohol **178**. Carbazole **177** (100 mg, 0.27 mmol, 1.0 equiv.) was azeotropically distilled with PhMe to remove trace H_2O, then dissolved in anhydrous MeOH (6 mL) and cooled to 0 °C. $NaBH_4$ (31 mg, 0.80 mmol, 3.0 equiv.) was added in one portion, and the reaction was stirred for 3 h. Upon completion, the reaction was quenched with with H_2O (~10 mL), then diluted with EtOAc (~10 mL). The aqueous phase was extracted with EtOAc (3 x 10 mL), and the combined organic layers were dried over $MgSO_4$, filtered, and condensed. The resultant oil was purified by flash column

chromatography (silica gel, EtOAc/hexanes 3/7) to yield alcohol **178** as a pink foam (72 mg, 72% yield).

178: R_f = 0.42 (silica gel, hexanes/EtOAc 7/3); IR (film): ν_{max} 3410, 2951, 1701, 1467, 1236, 1027, 735 cm^{-1}; ^1H NMR (600 MHz, $CDCl_3$) δ 8.02 (d, *J* = 7.8 Hz, 1H), 7.97 (s, 1H), 7.92 (s, 1H), 7.38 (t, *J* = 7.4 Hz, 1H), 7.32 (d, *J* = 8.0 Hz, 1H), 7.21 (t, *J* = 7.6 Hz, 1H), 7.00 (s, 1H), 3.72 (s, 3H), 3.65 (d, *J* = 11.9 Hz, 1H), 3.24 (td, *J* = 11.9, 4.4 Hz, 1H), 3.10 (dd, *J* = 16.6, 4.3 Hz, 1H), 3.05 – 2.95 (m, 1H), 2.56 (dt, *J* = 13.3, 3.6 Hz, 1H), 2.34 – 2.20 (m, 2H), 2.11 – 2.01 (m, 2H), 1.64 (td, *J* = 13.6, 4.1 Hz, 1H), 1.56 (s, 3H), 1.18 (s, 3H); ^{13}C NMR (150 MHz, $CDCl_3$) δ 178.7, 140.2, 139.6, 138.3, 133.7, 125.6, 123.6, 122.3, 120.1, 119.3, 117.2, 110.6, 109.8, 78.3, 53.0, 51.4, 49.2, 39.1, 38.5, 33.2, 29.4, 23.9, 23.8, 21.5; HRMS (ESI, m/z) calcd for $C_{24}H_{28}NO_3$ $[M+H]^+$ 378.2069, found 378.2057.

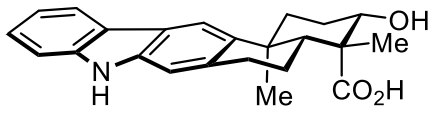

Oridamycin A (**26**)

Oridamycin A (**26**). Alcohol **178** (50 mg, 0.135 mmol, 1.0 equiv.) was dissolved in DMSO (3 mL) and solid NaCN (132 mg, 2.7 mmol, 20.0 equiv.) was added in one portion (no effort was made to maintain an inert atmosphere). The resulting solution was heated to 120 °C and stirred for 2 h and 40 min before it was allowed to cool to room temperature. The amber solution was diluted with EtOAc (~20 mL), washed with a solution of 5:3 brine:1M HCl (4 x 15 mL) (Beware! Forms HCN, highly toxic! Keep in fume hood!), dried over $MgSO_4$, filtered, and condensed. The resultant amber

solid was found to be pure Oridamycin A (**26**) (42 mg, 86% yield) and no further purification was necessary.

Oridamycin A (**26**): IR (film): ν_{max} 3411, 2962, 1693, 1611, 1466, 1321, 1243, 1026, 937, 737 cm^{-1}; ^{1}H NMR (600 MHz, CD_3OD) δ 7.98 – 7.94 (m, 2H), 7.34 (d, *J* = 8.1 Hz, 1H), 7.28 (t, *J* = 7.6 Hz, 1H), 7.08 (t, *J* = 7.6 Hz, 1H), 7.05 (s, 1H), 3.24 (dd, *J* = 12.2, 4.6 Hz, 1H), 3.07 (ddd, *J* = 16.9, 5.5, 1.9 Hz, 1H), 3.00 – 2.92 (m, 1H), 2.58 (dt, *J* = 13.2, 3.6 Hz, 1H), 2.32 (dq, *J* = 13.6, 3.6 Hz, 1H), 2.26 – 2.19 (m, 1H), 2.13 (dt, *J* = 12.9, 5.4 Hz, 1H), 1.96 – 1.90 (m, 1H), 1.59 (dt, *J* = 13.6, 3.9 Hz, 1H), 1.52 (d, 12.3 Hz, 1H), 1.49 (s, 3H), 1.27 (s, 3H); ^{13}C NMR (150 MHz, CD_3OD) δ 181.0, 142.0, 140.3, 140.1, 134.5, 126.1, 124.6, 123.2, 120.6, 119.3, 117.5, 111.4, 110.7, 79.1, 54.1, 48.7, 40.0, 39.6, 34.0, 30.3, 24.8, 24.6, 22.5; HRMS (ESI, m/z) calcd for $C_{23}H_{25}NO_3Na$ $[M+Na]^+$ 386.1732, found 386.1724.

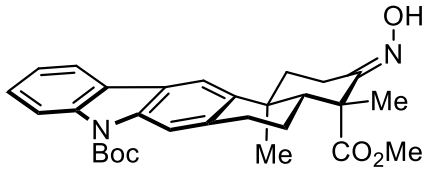

186

Oxime **186**. Boc-carbazole **176** (70 mg, 150 μmol, 1.0 equiv.) was dissolved in 1 mL pyridine, and NH_2OH•HCl (14 mg, 200 μmol, 1.35 equiv.) was added. The solution was heated to 80 °C and stirred for 40 min before being cooled to room temperature and diluted with EtOAc. The solution was washed 3x with 20% aqueous AcOH, sat. aqueous $NaHCO_3$, brine, dried over $MgSO_4$, filtered, and condensed. The resultant material was purified via

flash column chromatography (silica gel, 20% EtOAc/hexanes) to yield oxime **186** as a yellow oil (58 mg, 78% yield).

186: R_f = 0.27 (silica gel, 20% ethyl acetate/hexanes); IR (film): ν_{max} 3462, 3272, 2977, 1720, 1358, 1325, 1225, 1153, 941, 766, 733 cm^{-1}; ^1H NMR (600 MHz, $CDCl_3$) δ 8.22 (d, J = 8.3 Hz, 1H), 8.01 (s, 1H), 7.92 (d, J = 7.3 Hz, 1H), 7.86 (s, 1H), 7.45 – 7.39 (m, 2H), 7.32 (t, J = 7.5 Hz, 1H), 3.72 (s, 3H), 3.59 (ddd, J = 15.0, 4.7, 2.5 Hz, 1H), 3.16 (dd, J = 16.8, 4.7 Hz, 1H), 3.07 – 2.98 (m, 1H), 2.61 (ddd, J = 13.1, 5.5, 2.6 Hz, 1H), 2.43 (td, J = 14.8, 5.4 Hz, 1H), 2.31 (dd, J = 13.8, 6.2 Hz, 1H), 2.21 – 2.10 (m, 1H), 1.80 (dd, J = 12.2, 1.9 Hz, 1H), 1.75 (s, 9H), 1.65 (td, J = 13.5, 4.8 Hz, 1H), 1.57 (s, 3H), 1.28 (s, 3H); ^{13}C NMR (150 MHz, $CDCl_3$) δ 175.6, 161.5, 151.3, 142.4, 138.8, 137.2, 135.0, 126.8, 126.1, 124.4, 123.0, 119.4, 116.4, 116.3, 83.9, 54.1, 52.3, 50.8, 38.6, 38.6, 33.0, 28.5, 23.4, 22.4, 21.4, 19.8; HRMS (ESI, m/z) calcd for $C_{29}H_{35}N_2O_5$ $[M+H]^+$ 491.2546, found 491.2547.

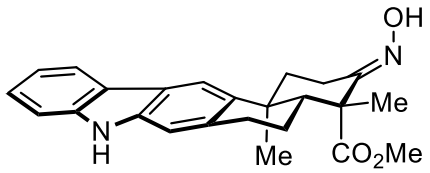

A3

Oxime **A3**. Carbazole **177** (50 mg, 130 μmol, 1.0 equiv.) was dissolved in 500 μL pyridine, to which NH_2OH•HCl (13 mg, 180 μmol, 1.35 equiv.) was added. The solution was heated to 80 °C and stirred for 45 min before being cooled to room temperature and diluted with EtOAc. The solution was washed 3x with 20% aqueous AcOH, 3x with sat. aqueous $NaHCO_3$, dried

over $MgSO_4$, filtered, and condensed. The resultant material was purified via flash column chromatography (silica gel, 30% acetone/hexanes) to yield oxime **A3** as a beige powder (43 mg, 85% yield).

A3: R_f = 0.27 (silica gel, 30% ethyl acetate/hexanes); IR (film): ν_{max} 3405, 2951, 1719, 1465, 1320, 1239, 1106, 906, 729 cm^{-1}; ^1H NMR (600 MHz, $CDCl_3$) δ 8.00 (d, J = 7.8 Hz, 1H), 7.97 (s, 1H), 7.83 (s, 1H), 7.38 – 7.35 (m, 2H), 7.24 (s, 1H), 7.21 – 7.17 (m, 1H), 7.09 (s, 1H), 3.71 (s, 3H), 3.58 (ddd, J = 15.0, 4.7, 2.6 Hz, 1H), 3.14 (dd, J = 16.6, 5.2 Hz, 1H), 3.06 – 2.98 (m, 1H), 2.65 (ddd, J = 13.1, 5.5, 2.6 Hz, 1H), 2.44 (td, J = 14.8, 5.4 Hz, 1H), 2.31 (ddt, J = 13.7, 6.3, 1.8 Hz, 1H), 2.22 – 2.15 (m, 1H), 1.82 (dd, J = 12.2, 1.9 Hz, 1H), 1.67 (td, J = 13.7, 4.7 Hz, 1H), 1.57 (s, 3H), 1.30 (s, 3H); ^{13}C NMR (150 MHz, $CDCl_3$) δ 175.7, 161.7, 140.2, 139.1, 138.4, 133.9, 125.7, 123.6, 122.4, 120.1, 119.4, 117.0, 110.6, 109.9, 54.3, 52.2, 50.8, 38.9, 38.7, 32.8, 23.6, 22.5, 21.5, 19.9; HRMS (ESI, m/z) calcd for $C_{24}H_{27}N_2O_3$ $[M+H]^+$ 391.2022, found 391.2022.

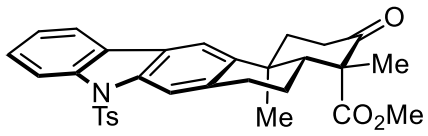

A4

Tosyl-Carbazole **A4**. Carbazole **177** (30 mg, 80 μmol, 1.0 equiv.) was dissolved in 800 μL DMF and degassed with Ar for 10 min. NaH (60% dispersion in mineral oil, 3.5 mg, 90 μmol, 1.1 equiv.) was added and the solution was stirred at room temperature for 1 h. *p*-TsCl (30 mg, 160 μmol, 2.0 equiv.) was added, and the solution was heated to 50 °C and stirred for 6 h. The solution was removed from heat, diluted with EtOAc, and quenched

with sat. aqueous NH_4Cl. The aqueous layer was extracted 3x with EtOAc, and the combined organic layers were washed 3x with brine, dried over $MgSO_4$, filtered and condensed. The resultant material was purified using PTLC (silica gel, 0.5mm thickness, 5% acetone, 45% hexanes, 50% PhMe) to yield tosyl-carbazole **A4** as a clear oil (16 mg, 38% yield).

A4: R_f = 0.27 (silica gel, 25% ethyl acetate/hexanes); IR (film): ν_{max} 2952, 1713, 1451, 1368, 1171, 1092, 995, 812, 747, 658 cm^{-1}; ^1H NMR (600 MHz, $CDCl_3$) δ 8.25 (d, J = 8.3 Hz, 1H), 8.00 (s, 1H), 7.83 (d, J = 7.7 Hz, 1H), 7.79 (s, 1H), 7.72 – 7.68 (m, 2H), 7.46 – 7.41 (m, 1H), 7.32 (td, J = 7.5, 1.0 Hz, 1H), 7.12 (d, J = 8.0 Hz, 2H), 3.73 (s, 3H), 3.22 (dt, J = 16.7, 3.5 Hz, 1H), 3.17 (td, J = 14.7, 6.3 Hz, 1H), 3.10 – 3.01 (m, 1H), 2.71 (ddd, J = 13.2, 6.2, 2.5 Hz, 1H), 2.62 (ddd, J = 14.7, 4.6, 2.4 Hz, 1H), 2.28 (s, 3H), 2.27 – 2.21 (m, 2H), 1.90 – 1.84 (m, 1H), 1.49 (s, 3H), 1.38 (s, 3H); ^{13}C NMR (150 MHz, $CDCl_3$) δ 207.9, 174.1, 144.9, 142.5, 138.7, 137.1, 135.3, 135.3, 129.8, 127.2, 126.7, 126.5, 124.9, 123.9, 119.7, 116.7, 115.2, 115.0, 57.7, 54.0, 52.4, 39.7, 38.4, 37.6, 32.9, 23.4, 21.7, 21.7, 21.1; HRMS (ESI, m/z) calcd for $C_{31}H_{32}NO_5S$ $[M+H]^+$ 530.2001, found 530.1992.

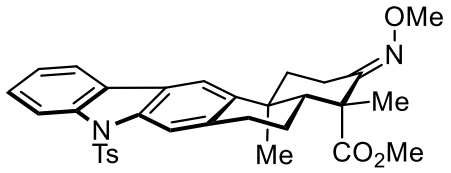

187

O-Methyloxime **187**. Tosyl-carbazole **A4** (29 mg, 50 μmol, 1.0 equiv.) was dissolved in 250 μL pyridine. $MeONH_2$•HCl (7 mg, 80 μmol, 1.5 equiv.)

was added, and the solution was stirred at room temperature for 21 h. The solution was diluted with EtOAc and added to 20% aqueous AcOH. The organic layer was washed 3x with 20% aqueous AcOH, 3x with sat. aqueous $NaHCO_3$, dried over $MgSO_4$, filtered and condensed. The resultant material was purified via flash column chromatography (silica gel, 20% EtOAc/hexanes) to yield O-methyloxime **187** as a pale-yellow oil (29 mg, 95% yield).

187: R_f = 0.25 (silica gel, 20% ethyl acetate/hexanes); IR (film): ν_{max} 3421, 2936, 1727, 1453, 1370, 1238, 1173, 1115, 1049, 907, 732, 666, 582 cm^{-1}; ^1H NMR (600 MHz, $CDCl_3$) δ 8.28 (d, J = 8.3 Hz, 1H), 8.00 (s, 1H), 7.86 (d, J = 7.6 Hz, 1H), 7.79 (s, 1H), 7.72 (d, J = 8.5 Hz, 2H), 7.48 – 7.42 (m, 1H), 7.34 (td, J = 7.5, 1.0 Hz, 1H), 7.14 (d, J = 8.0 Hz, 2H), 3.89 (s, 3H), 3.73 (s, 3H), 3.48 (dq, J = 15.0, 4.6, 2.5 Hz, 1H), 3.22 (dd, J = 16.8, 5.2 Hz, 1H), 3.11 – 3.01 (m, 1H), 2.72 (s, 0H), 2.53 (dq, J = 13.0, 5.4, 2.6 Hz, 1H), 2.48 – 2.32 (m, 2H), 2.30 (s, 3H), 2.22 – 2.12 (m, 1H), 1.80 (dd, J = 12.3, 1.8 Hz, 1H), 1.60 (s, 4H), 1.26 (s, 3H); ^{13}C NMR (150 MHz, $CDCl_3$) δ 175.8, 159.6, 144.9, 143.4, 138.7, 136.9, 135.6, 135.3, 129.8, 127.1, 126.7, 124.8, 123.9, 119.7, 116.8, 115.2, 114.8, 61.6, 54.0, 52.2, 50.6, 38.7, 38.6, 33.0, 23.3, 22.4, 21.7, 21.4, 20.5; HRMS (ESI, m/z) calcd for $C_{32}H_{35}N_2O_5S$ $[M+H]^+$ 559.2267, found 559.2250.

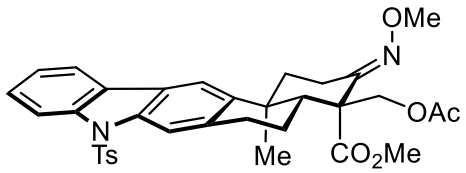

189

Acetoxymethyl **189**. *O*-Methyloxime **187** (9.4 mg, 17 μmol, 1.0 equiv.) was dissolved in 200 μL of 1:1 AcOH: Ac_2O at room temperature. $PhI(OAc)_2$ (11 mg, 34 μmol, 2.0 equiv.) and $Pd(OAc)_2$ (376 μg, 1.68 μmol, 10 mol%) were added, and the solution was heated to 80 °C for 4 h. The solution was cooled, diluted with EtOAc, washed 2x with sat. aq. $NaHCO_3$, brine, dried over $MgSO_4$, filtered, and condensed. The resultant crude material was purified via PTLC (silica gel, 25% EtOAc/hexanes) to yield acetoxymethyl **189** as a white foam (3.9 mg, 37% yield).

189: R_f = 0.29 (silica gel, 25% ethyl acetate/hexanes); IR (film): ν_{max} 3414, 2945, 1731, 1368, 1225, 1171, 1045, 908, 729, 664 cm^{-1}; ^1H NMR (600 MHz, $CDCl_3$) δ 8.25 (d, J = 8.4 Hz, 1H), 7.98 (s, 1H), 7.85 (d, J = 7.6 Hz, 1H), 7.80 (s, 1H), 7.71 (d, J = 8.3 Hz, 2H), 7.47 – 7.41 (m, 1H), 7.32 (t, J = 7.5 Hz, 1H), 7.13 (d, J = 8.2 Hz, 2H), 4.66 (d, J = 10.7 Hz, 1H), 4.55 (d, J = 10.7 Hz, 1H), 3.84 (s, 3H), 3.74 (s, 3H), 3.28 – 3.21 (m, 1H), 3.17 (dd, J = 17.0, 5.4 Hz, 1H), 3.08 – 3.00 (m, 1H), 2.59 – 2.49 (m, 2H), 2.28 (s, 3H), 2.18 – 2.10 (m, 2H), 2.06 – 1.97 (m, 4H), 1.67 – 1.58 (m, 1H), 1.27 (s, 3H); ^{13}C NMR (150 MHz, $CDCl_3$) δ 172.5, 170.8, 156.0, 144.9, 143.0, 138.6, 137.0, 135.3, 135.2, 129.8, 127.2, 126.7, 126.5, 124.8, 123.9, 119.7, 116.7, 115.1, 114.9, 65.7, 62.0, 54.4, 52.4, 46.8, 38.1, 36.7, 32.3, 23.5, 21.7, 21.2, 21.2, 20.8; HRMS (ESI, m/z) calcd for $C_{34}H_{37}N_2O_7S$ $[M+H]^+$ 617.2321, found 617.2298.

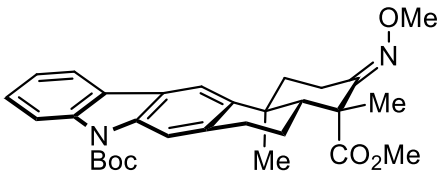

190

O-Methyloxime **190.** Boc-carbazole **176** (168 mg, 0.35 mmol, 1.0 equiv.) was dissolved in anhydrous pyridine (6 mL), to which $MeONH_2$•HCl (73 mg, 0.88 mmol, 2.5 equiv.) was added in one portion. The reaction was heated to 70 °C and stirred at that temperature for 3.5 h (no effort was made to maintain an inert atmosphere). Upon completion, the mixture was diluted with EtOAc (~25 mL), washed with sat. NH_4Cl (4 x 15 mL), washed with 1M HCl (1 x 15 mL), dried over $MgSO_4$, filtered, and condensed. The resulting yellow oil was purified by flash chromatography (silica gel, hexanes/acetone 19/1) to yield O-methyloxime **190** as a yellow foam (160 mg, 90% yield).

190: R_f = 0.40 (silica gel, hexanes/acetone 9/1); IR (film): ν_{max} 2976, 1725, 1490, 1359, 1228, 1158, 1049, 769, 736 cm^{-1}; ^1H NMR (600 MHz, $CDCl_3$) δ 8.22 (d, *J* = 8.3 Hz, 1H), 8.01 (s, 1H), 7.91 (d, *J* = 7.5 Hz, 1H), 7.84 (s, 1H), 7.41 (ddd, *J* = 8.5, 7.3, 1.3 Hz, 1H), 7.31 (td, *J* = 7.5, 1.0 Hz, 1H), 3.87 (s, 3H), 3.71 (s, 3H), 3.48 (ddd, *J* = 15.0, 4.7, 2.5 Hz, 1H), 3.15 (dd, *J* = 16.9, 4.3 Hz, 1H), 3.02 (ddd, *J* = 17.4, 12.6, 6.2 Hz, 1H), 2.57 (ddd, *J* = 13.0, 5.5, 2.6 Hz, 1H), 2.40 (td, *J* = 14.8, 5.3 Hz, 1H), 2.31 (dd, *J* = 13.8, 6.1 Hz, 1H), 2.14 (qd, *J* = 12.9, 5.3 Hz, 1H), 1.79 (dd, *J* = 12.3, 1.8 Hz, 1H), 1.75 (s, 10H), 1.68 – 1.61 (m, 1H), 1.58 (s, 3H), 1.26 (s, 3H); ^{13}C NMR (150 MHz, $CDCl_3$) δ 175.8, 159.8, 151.3, 142.5, 138.8, 137.1, 135.0, 126.8, 126.1,

124.4, 123.0, 119.4, 116.4, 116.3, 116.2, 83.9, 61.6, 54.2, 52.2, 50.6, 38.7, 38.6, 33.0, 28.6, 28.5, 23.4, 22.4, 21.4, 20.5; HRMS (ESI, m/z) calcd for $C_{30}H_{37}N_2O_5$ $[M+H]^+$ 505.2702, found 505.2706.

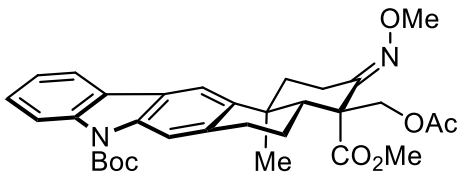

192

Acetoxymethyl **192**. O-Methyloxime **190** (152 mg, 0.3 mmol, 1.0 equiv) was dissolved in 1:1 Ac_2O: AcOH (3 mL). $PhI(OAc)_2$ (193 mg, 0.6 mmol, 2.0 equiv.) and $Pd(OAc)_2$ (7 mg, 0.03 mmol, 0.1 equiv.) were added sequentially and the contents were heated to 70 °C and stirred at that temperature for 16 h (no effort was made to maintain an inert atmosphere). Upon completion, the mixture was diluted with EtOAc (~30 mL), washed with sat. aqueous $NaHCO_3$ (3 x 20 mL), dried over $MgSO_4$, filtered, and condensed. The resultant brown oil was purified by flash chromatography (silica gel, hexanes/acetone 20/3) to yield acetoxymethyl **192** as a yellow oil (116 mg, 69% yield).

192: R_f = 0.42 (silica gel, hexanes/acetone 4/1); IR (film): ν_{max} 2973, 1727, 1491, 1360, 1227, 1154, 1051, 769, 736 cm^{-1}; ^1H NMR (600 MHz, $CDCl_3$) δ 8.23 (d, *J* = 8.3 Hz, 1H), 8.02 (s, 1H), 7.93 (d, *J* = 7.6 Hz, 1H), 7.88 (s, 1H), 7.42 (t, *J* = 7.4 Hz, 1H), 7.32 (t, *J* = 7.2 Hz, 1H), 4.67 (d, *J* = 10.7 Hz, 1H), 4.56 (d, *J* = 10.7 Hz, 1H), 3.85 (s, 3H), 3.74 (s, 3H), 3.32 – 3.24 (m, 1H), 3.14 (dd, *J* = 16.9,

5.4 Hz, 1H), 3.03 (ddd, *J* = 17.4, 12.3, 6.4 Hz, 1H), 2.62 – 2.52 (m, 2H), 2.18 (d, *J* = 11.5 Hz, 1H), 2.12 (dd, *J* = 13.3, 6.2 Hz, 1H), 2.05 – 1.96 (m, 4H), 1.75 (s, 9H), 1.69 – 1.61 (m, 1H), 1.30 (s, 3H); ^{13}C NMR (150 MHz, $CDCl_3$) δ 172.5, 170.7, 156.1, 151.3, 142.2, 138.9, 137.2, 134.7, 126.9, 126.0, 124.4, 123.1, 119.4, 116.4, 116.4, 116.2, 83.9, 65.7, 62.0, 54.4, 52.4, 46.9, 38.0, 36.8, 32.4, 28.5, 23.5, 21.2, 21.1, 20.8; HRMS (ESI, m/z) calcd for $C_{32}H_{39}N_2O_7$ $[M+H]^+$ 563.2757, found 563.2762.

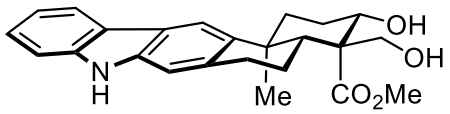

193

Diol **193**. Acetoxymethyl **192** (20 mg, 0.036 mmol, 1.0 equiv.) was dissolved in acetone (540 µL) and aq. 1M HCl (180 µL) was added (no effort was made to maintain an inert atmosphere). The contents were heated to 80 °C and maintained at that temperature for 13 h. Upon completion, the reaction mixture was diluted with CH_2Cl_2 (10 mL), washed with H_2O (1 x 5 mL) and sat. aq. $NaHCO_3$ (1 x 5 mL), dried over Na_2SO_4, filtered, and condensed. The crude material was immediately taken up in MeOH (720 µL) and cooled to 0 °C. $NaBH_4$ (4 mg, 0.11 mmol, 3.0 equiv.) was added, and the solution was stirred at 0 °C for 40 min. The reaction was diluted with EtOAc (500 µL), quenched by addition of aq. 1M HCl (500 µL), and stirred at room temperature for 15 min to quench excess reagent. Additional H_2O (5 mL) and EtOAc (5 mL) were added, the aqueous was extracted with EtOAc (2 x 5 mL), the combined organic layers were washed with sat. aqueous $NaHCO_3$ (2 x 5 mL), dried over Na_2SO_4, filtered, and condensed. The resultant material

was purified via flash column chromatography (silica gel, hexanes/acetone 5/2) to yield diol **193** as a brown foam (4.0 mg, 25% yield).

193: R_f = 0.35 (silica gel, hexanes/acetone 3/2); IR (film): 3408, 2926, 1706, 1492, 1240, 1071, 735 ν_{max} cm^{-1}; ^1H NMR (600 MHz, $CDCl_3$) δ 7.99 (d, *J* = 7.7 Hz, 1H), 7.95 (s, 1H), 7.83 (s, 1H), 7.37 (d, *J* = 3.9 Hz, 2H), 7.20 (dq, *J* = 8.0, 4.4 Hz, 1H), 7.07 (s, 1H), 4.38 (t, *J* = 10.6 Hz, 1H), 3.96 (d, *J* = 10.4 Hz, 1H), 3.84 – 3.81 (m, 2H), 3.80 (s, 4H), 3.69 (td, *J* = 12.0, 4.6 Hz, 1H), 3.09 (dd, *J* = 16.5, 5.3 Hz, 1H), 3.05 – 2.95 (m, 1H), 2.59 (dt, *J* = 13.4, 3.6 Hz, 1H), 2.35 (qd, *J* = 13.2, 3.9 Hz, 1H), 2.14 (dd, *J* = 14.0, 6.0 Hz, 1H), 2.08 – 1.99 (m, 2H), 1.70 – 1.63 (m, 2H), 1.22 (s, 3H); ^{13}C NMR (150 MHz, $CDCl_3$) δ 176.4, 140.2, 139.2, 138.3, 133.5, 125.7, 123.6, 122.4, 120.1, 119.4, 117.1, 110.6, 109.8, 79.6, 72.0, 53.4, 51.9, 47.5, 38.8, 38.3, 32.7, 29.4, 24.2, 21.3; HRMS (ESI, m/z) calcd for $C_{24}H_{28}NO_4$ $[M+H]^+$ 394.2018, found 394.2006.

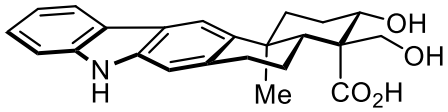

Oridamycin B (**27**)

Oridamycin B (**27**). Diol **193** (1.3 mg, 3.3 μmol, 1.0 equiv.) was dissolved in DMSO (70 μL) and solid NaCN (3.2 mg, 70 μmol, 21 equiv.) was added in one portion (no effort was made to maintain an inert atmosphere). The reaction was heated to 120 °C and was stirred at that temperature for 2 h. Upon completion, the amber solution was diluted with EtOAc (~20 mL), washed with a solution of 5:3 brine:1M HCl (4 x 15 mL) (Beware! Forms HCN,

highly toxic! Keep in fume hood!), dried over Na_2SO_4, filtered, and condensed. The crude material was purified by semi-preparative HPLC (7 injections, Varian Microsorb 300-5 C18 column, 5µm, 250 x 4.6 mm) using MeCN/H_2O (30/70 to 80/20, 0.6 mL/min) as eluent to give pure oridamycin B (**27**), as a white powder (t_R = 10.39 min, 0.30 mg, 24% yield). NOTE: While the ^{1}H NMR spectrum of purified **27** corroborated the proposed structure (splitting, J values, relative chemical shifts, etc.), notable differences were found in the chemical shift of several protons relative to the isolated material. However, it was found that upon treatment with excess TFA the ^{1}H NMR spectrum matched that of the natural isolate, and the tabulated data from both spectra are provided below.

Oridamycin B (**27**): IR (film): 3391, 2931, 2856, 1695, 1607, 1494, 1340, 1266, 1026, 740 ν_{max} cm^{-1}; ^{1}H NMR (600 MHz, CD_3OD) δ 7.97 (s, 1H), 7.96 (d, *J* = 7.9 Hz, 1H), 7.33 (d, *J* = 8.0 Hz, 1H), 7.27 (dt, *J* = 7.6, 1.3 Hz, 1H), 7.07 (dt, *J* = 7.6, 1.2 Hz, 1H), 7.05 (s, 1H), 4.04 (d, *J* = 10.9 Hz, 1H), 3.95 (d, *J* = 10.9 Hz, 1H), 3.61 (dd, *J* = 12.1, 4.7 Hz, 1H), 3.06 – 2.99 (m, 2H), 2.55 (dt, *J* = 13.0, 3.6 Hz, 1H), 2.45 (dq, *J* = 12.5, 3.9 Hz, 1H), 2.27 – 2.22 (m, 2H), 1.95 – 1.88 (m, 1H), 1.84 – 1.78 (m, 1H), 1.55 (td, *J* = 13.4, 3.7 Hz, 1H), 1.36 (s, 3H), 1.34 – 1.27 (m, 1H); ^{13}C NMR (150 MHz, CD_3OD) δ 180.6,[A] 142.0, 141.2, 140.0, 135.2, 125.9, 124.7, 123.0, 120.5, 119.2, 117.6, 111.3, 110.6, 73.1, 64.7, 56.1, 46.9, 40.3, 39.5, 34.0, 30.8, 25.7, 22.6; HRMS (ESI, m/z) calcd for $C_{23}H_{25}NO_4$ $[M-H]^-$ 378.1705, found 378.1723.

[A] Assigned from HMBC data.

Oridamycin B (**27**): *with TFA (excess)*: ^{1}H NMR (600 MHz, CD_3OD) δ 7.97 (s, 1H), 7.96 (d, *J* = 8.0 Hz, 1H), 7.35 (d, *J* = 8.0 Hz, 1H), 7.28 (dt, *J* = 7.7, 1.2 Hz, 1H), 7.08 (d, *J* = 7.7 Hz, 1H), 7.07 (s, 1H), 4.11 (d, *J* = 10.9 Hz, 1H), 3.93 (d, *J* = 10.9 Hz, 1H), 3.77 (dd, *J* = 12.2, 4.5, 1H), 3.05 (m, 2H), 2.62 (dt, *J* = 13.5, 3.6, 1H), 2.43 (dq, *J* = 13.2, 3.7, 1H), 2.23-2.17 (m, 1H), 2.08 (m, 1H), 1.99-1.92 (m, 2H), 1.62 (dt, *J* = 13.7, 3.8, 1H), 1.32 (s, 3H).

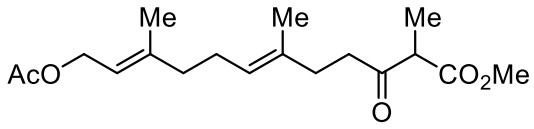

237

Linear Acetate **237**. Linear alcohol **154** (2.9 g, 10.4 mmol, 1.0 equiv.) was dissolved in 70 mL CH_2Cl_2 at room temperature. Pyridine (2.0 mL, 25.0 mmol, 2.4 equiv.) was added, followed by Ac_2O (1.47 mL, 15.6 mmol, 1.5 equiv.). The solution was allowed to stir for 21 h at room temperature. DMAP (9 mg, 73 μmol, 0.7 mol%) was added, and the solution was allowed to stir for an additional 5 h. Upon completion, the reaction mixture was diluted with CH_2Cl_2, and quenched with sat. aqueous $NaHCO_3$. The layers were separated and the organic layer was washed with H_2O and brine, then dried over Na_2SO_4, filtered, and condensed. The resultant material was purified via flash column chromatography (silica gel, 15% EtOAc/hexanes) to yield linear acetate **237** as a pale-yellow oil (2.52 g, 75% yield).

237: R_f = 0.58 (silica gel, 20% ethyl acetate/hexanes); IR (film): ν_{max} 2916, 1739, 1716, 1437, 1368, 1232, 1070, 1024 cm^{-1}; ^{1}H NMR (600 MHz, $CDCl_3$) δ 5.33 (t, J = 7.0 Hz, 1H), 5.10 (t, J = 6.3 Hz, 1H), 4.58 (d, J = 7.1 Hz, 2H), 3.73 (s,

3H), 3.54 (q, J = 7.2 Hz, 1H), 2.71 – 2.55 (m, 2H), 2.26 (t, J = 7.7 Hz, 2H), 2.14 – 2.08 (m, 2H), 2.05 (s, 3H), 2.05 – 1.99 (m, 2H), 1.70 (s, 3H), 1.59 (s, 3H), 1.34 (d, J = 7.1 Hz, 3H); ^{13}C NMR (150 MHz, $CDCl_3$) δ 205.6, 171.3, 171.2, 142.1, 134.0, 124.6, 118.6, 61.5, 52.9, 52.5, 40.3, 39.5, 33.4, 26.3, 21.2, 16.6, 16.2, 13.0; HRMS (ESI, m/z) calcd for $C_{18}H_{28}O_5Na$ $[M+Na]^+$ 347.1834, found 347.1820.

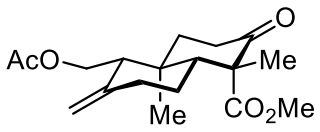

A5

Bicyclic Acetate **A5**. Bicyclic alcohol **162** (150 mg, 540 μmol, 1.0 equiv.) was dissolved in 5.4 mL Ac_2O/pyridine (1/1) and stirred at room temperature for 19 h. The mixture was diluted with EtOAc, and then added to sat. aqueous $NaHCO_3$. The layers were separated and the organic layer was washed with sat. aqueous $NaHCO_3$, H_2O, and brine. The resultant solution was dried over $MgSO_4$, filtered, and condensed. The resultant material was purified via flash column chromatography (silica gel, 20% EtOAc/hexanes) to yield bicyclic acetate **A5** as a pale-yellow oil (126 mg, 72% yield).

A5: R_f = 0.32 (silica gel, 20% EtOAc/hexanes); IR (film): ν_{max} 2952, 2855, 1713, 1364, 1228, 1095, 1031, 891, 733 cm^{-1}; ^{1}H NMR (600 MHz, $CDCl_3$) δ 4.95 (s, 1H), 4.61 (s, 1H), 4.33 (dd, J = 11.4, 4.0 Hz, 1H), 4.25 (dd, J = 11.4, 8.5 Hz, 1H), 3.66 (s, 3H), 2.96 (td, J = 14.8, 6.2 Hz, 1H), 2.52 – 2.43 (m, 2H), 2.12 (ddd, J = 13.4, 6.3, 2.7 Hz, 1H), 2.09 – 2.04 (m, 1H), 2.02 (s, 3H), 2.01 – 1.90 (m, 2H), 1.68 (td, J = 14.1, 4.6 Hz, 1H), 1.62 – 1.57 (m, 1H), 1.55 (s, 1H), 1.37 (s, 3H), 0.88 (s, 3H); ^{13}C

NMR (150 MHz, $CDCl_3$) δ 200.5, 171.3, 169.1, 142.2, 133.8, 124.9, 118.6, 62.7, 61.5, 54.0, 39.5, 37.1, 34.4, 26.3, 25.6, 21.2, 16.6, 16.2; HRMS (ESI, m/z) calcd for $C_{18}H_{26}O_5Na$ $[M+Na]^+$ 345.1678, found 345.1665.

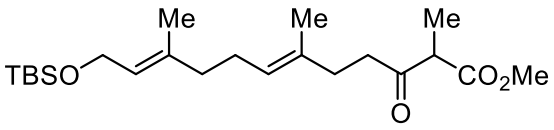

A6

Linear Silyl Ether **A6**. Linear alcohol **154** (1.5 g, 5.3 mmol, 1.0 equiv.) was dissolved in 25 mL DMF. TBSCl (964 mg, 6.4 mmol, 1.2 equiv.) and imidazole (645 mg, 9.5 mmol, 1.8 equiv.) were added and the solution was stirred at room temperature for 17 h. The reaction was diluted with Et_2O and H_2O. The aqueous layer was extracted 3x with Et_2O, and the combined organic layers were washed 3x with brine, dried over $MgSO_4$, filtered, and condensed. The resultant material was purified via flash column chromatography (silica gel, 2% acetone/hexanes) to yield linear silyl ether **A6** as a yellow oil (1.33 g, 63% yield).

A6: R_f = 0.29 (silica gel, 5% ethyl acetate/hexanes); IR (film): ν_{max} 2930, 2855, 1752, 1716, 1462, 1254, 1200, 1064, 833, 772, 737 cm^{-1}; ^1H NMR (600 MHz, $CDCl_3$) δ 5.29 (t, J = 6.4 Hz, 1H), 5.11 (t, J = 7.0 Hz, 1H), 4.19 (d, J = 6.6 Hz, 2H), 3.73 (s, 3H), 3.59 – 3.50 (m, 1H), 2.71 – 2.47 (m, 2H), 2.25 (t, J = 7.7 Hz, 2H), 2.09 (q, J = 7.4 Hz, 2H), 2.03 – 1.95 (m, 2H), 1.61 (s, 3H), 1.59 (s, 3H), 1.34 (d, J = 7.1 Hz, 3H), 0.90 (s, 9H), 0.07 (s, 6H);^{13}C NMR (150 MHz, $CDCl_3$) δ 205.6, 171.2, 136.8, 133.7, 125.0, 124.7, 60.5, 52.8, 52.5, 40.3, 39.5, 33.4, 26.4, 26.2, 18.6, 16.5, 16.2,

13.0, -4.9; HRMS (ESI, m/z) calcd for $C_{22}H_{39}O_4Si$ [M−H]$^-$ 395.2618, found 395.2622.

211

Bicyclic Silyl Ether **211**. Bicyclic alcohol **162** (634 mg, 2.26 mmol, 1.0 equiv.) was dissolved in 11 mL DMF. TBSCl (410 mg, 2.72 mmol, 1.2 equiv.) and imidazole (308 mg, 4.53 mmol, 2.0 equiv.) were added, and the solution as allowed to stir at room temperature for 48 h. The solution was diluted with Et_2O and H_2O. The aqueous layer was extracted 3x with Et_2O, and the combined organic layers were washed 4x with brine, dried over $MgSO_4$, filtered, and condensed. The resultant material was purified via flash column chromatography (silica gel, 5% EtOAc/hexanes) to yield bicyclic silyl ether **211** as a yellow oil (653 mg, 73% yield).

211: R_f = 0.52 (silica gel, 10% ethyl acetate/hexanes); IR (film): ν_{max} 2952, 2930, 2855, 1739, 1713, 1451, 1250, 1095, 837, 776 cm^{-1}; ^{1}H NMR (600 MHz, $CDCl_3$) δ 4.89 (s, 1H), 4.66 (s, 1H), 3.83 (dd, J = 5.9, 1.9 Hz, 2H), 3.66 (s, 3H), 2.96 (td, J = 14.7, 6.1 Hz, 1H), 2.47 – 2.39 (m, 2H), 2.20 (ddd, J = 13.6, 6.1, 2.7 Hz, 1H), 2.02 – 1.96 (m, 1H), 1.93 – 1.88 (m, 2H), 1.83 (t, J = 5.3 Hz, 1H), 1.66 (td, J = 14.2, 4.4 Hz, 1H), 1.59 – 1.56 (m, 1H), 1.55 (s, 3H), 1.36 (s, 3H), 0.89 (s, 3H), 0.86 (s, 9H), 0.03 (s, 6H); ^{13}C NMR (150 MHz, $CDCl_3$) δ 208.8, 174.0, 146.4, 108.4, 60.4, 57.8, 56.8, 52.2, 39.3, 39.2, 37.9, 37.4, 26.0, 26.0, 21.4, 18.3, 13.4, -5.3, -5.3; HRMS (ESI, m/z) calcd for $C_{22}H_{37}O_4Si$ [M−H]$^-$ 393.2461, found 393.2457.

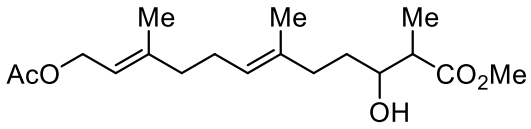

A7

Linear β-Hydroxy Ester **A7**. Linear acetate **237** (755 mg, 2.33 mmol, 1.0 equiv.) was dissolved in 24 mL MeOH and cooled to -78 °C. $NaBH_4$ (106 mg, 2.80 mmol, 1.2 equiv.) was added and the solution was stirred for 3.5 h before being diluted with EtOAc and H_2O, followed by quenching with sat. aqueous $NaHCO_3$. The aqueous layer was extracted 3x with EtOAc, and the combined organic layers were washed with sat. aqueous $NaHCO_3$, brine, dried over $MgSO_4$, filtered, and condensed. The resultant material was purified via flash column chromatography (silica gel, 20% EtOAc/hexanes) to yield linear β-hydroxy ester **A7** as a pale-yellow oil (514 mg, 68% yield).

A7: R_f = 0.45 (silica gel, 30% ethyl acetate/hexanes); IR (film): ν_{max} 3435, 2932, 1727, 1439, 1368, 1231, 1025, 914, 729 cm^{-1}; ^1H NMR (600 MHz, $CDCl_3$) δ *Major Diastereomer*: 3.67 – 3.61 (m, 1H), 1.20 (d, J = 7.2 Hz, 3H), *Minor Diastereomer*: 3.86 (ddd, J = 8.4, 4.1 Hz, 1H), 1.19 (d, J = 7.2 Hz, 3H), *Shared Peaks*: 5.34 (t, J = 7.1 Hz, 1H), 5.14 (t, J = 6.8 Hz, 1H), 4.58 (d, J = 7.1 Hz, 2H), 3.71 (s, 3H), 2.59 – 2.47 (m, 2H), 2.21 – 1.99 (m, 9H), 1.70 (s, 3H), 1.60 (s, 3H), 1.56 – 1.44 (m, 1H); ^{13}C NMR (150 MHz, $CDCl_3$) δ 176.6, 176.5, 171.3, 142.2, 135.2, 135.1, 124.5, 124.4, 118.6, 73.2, 71.6, 61.6, 51.9, 51.9, 45.4, 44.5, 39.6, 36.2, 35.8, 32.9, 32.1, 26.3, 26.2, 21.2, 16.6, 16.1, 14.4, 11.0; HRMS (ESI, m/z) calcd for $C_{18}H_{30}O_5Na$ $[M+Na]^+$ 349.1991, found 349.1996.

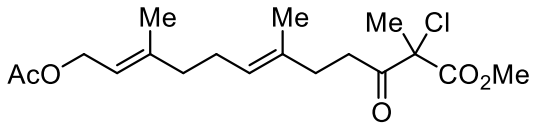

239

α-Chlorinated Product **239.** Linear acetate **237** (50 mg, 150 μmol, 1.0 equiv.) was dissolved in 16 mL PhMe, to which 2,4,6-tri-*tert*-butylpyridine (148 mg, 600 μmol, 4.0 equiv.) and $Cu(OTf)_2$ (163 mg, 45 μmol, 3.0 equiv.) were added. The solution was freeze-pump-thawed 3x to remove trace O_2. The reaction was cooled to -55 °C and $V(O)Cl_2$(OTFE) was added (prepared according to the literature[9]). The solution was stirred and slowly allowed to warm to -25 °C over the course of 2.5 h, at which point the reaction was diluted with EtOAc and quenched with aqueous 1M HCl. The aqueous layer was extracted 2x with EtOAc, and the combined organic layers were washed with sat. aqueous NH_4Cl, sat. aqueous $NaHCO_3$, brine, dried over $MgSO_4$, filtered, and condensed. The resultant material was purified via flash column chromatography (silica gel, 10% EtOAc/hexanes) to yield α-chlorinated product **239** as a clear oil (30 mg, 56% yield).

239: R_f = 0.26 (silica gel, 10% ethyl acetate/hexanes); IR (film): ν_{max} 2923, 2855, 1735, 1447, 1372, 1232, 1117, 1027, 733 cm^{-1}; ^1H NMR (600 MHz, $CDCl_3$) δ 5.33 (t, J = 7.0 Hz, 1H), 5.13 (t, J = 7.0 Hz, 1H), 4.58 (d, J = 7.1 Hz, 2H), 3.82 (s, 3H), 2.92 – 2.84 (m, 1H), 2.77 – 2.69 (m, 1H), 2.28 (t, J = 7.7 Hz, 2H), 2.11 (q, J = 7.4 Hz, 2H), 2.07 – 2.02 (m, 5H), 1.83 (s, 3H), 1.70 (s, 3H), 1.61 (s, 3H); ^{13}C NMR (150 MHz, $CDCl_3$) δ 201.1, 171.3, 168.8, 142.1, 133.7, 124.9, 118.6, 70.9, 61.5,

53.90, 39.5, 36.5, 33.9, 26.3, 24.7, 21.2, 16.6, 16.2; HRMS (ESI, m/z) calcd for $C_{18}H_{27}O_6ClNa$ $[M+Na]^+$ 381.1445, found 381.1440.

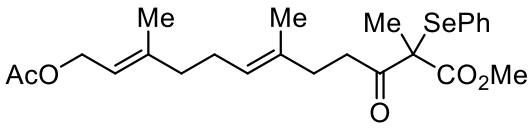

A8

Linear α-Seleno Acetate **A8**. Linear acetate **237** (50 mg, 150 μmol, 1.0 equiv.) was dissolved in 1.5 mL THF and cooled to -78 °C. *t*-BuOK (26 mg, 230 μmol, 1.5 equiv.) was added and the solution was stirred at -78 °C for 50 min. PhSeCl (44 mg, 230 μmol, 1.5 equiv.) was added, and the solution was stirred at -78 °C for 3.5 h. The reaction was diluted with EtOAc and quenched with sat. aqueous NH_4Cl. The aqueous layer was extracted 3x with EtOAc, and the combined organic layers were dried over $MgSO_4$, filtered, and condensed. The resultant material was purified via flash column chromatography (silica gel, 5% acetone/hexanes) to yield linear α-seleno acetate **A8** as a clear oil (71 mg, 98% yield).

A8: R_f = 0.24 (silica gel, 10% acetone/hexanes); IR (film): ν_{max} 3450, 2942, 1737, 1700, 1633, 1303, 1233, 1104, 917, 737, 692 cm^{-1}; ^1H NMR (600 MHz, $CDCl_3$) δ 7.57 – 7.51 (m, 2H), 7.27 – 7.24 (m, 3H), 5.30 (t, J = 7.1 Hz, 1H), 4.55 (qd, J = 12.5, 7.0 Hz, 2H), 3.67 (s, 3H), 3.10 – 2.98 (m, 3H), 2.52 – 2.43 (m, 1H), 2.31 – 2.19 (m, 2H), 2.09 (ddd, J = 12.8, 9.2, 7.9 Hz, 1H), 2.05 (s, 3H), 1.97 (ddd, J = 12.8, 8.8, 5.7 Hz, 1H), 1.72 (t, J = 1.6 Hz, 3H), 1.70 – 1.63 (m, 4H), 1.42 (s, 3H); ^{13}C NMR (150 MHz, $CDCl_3$) δ 171.2, 169.9, 169.8, 141.2, 134.0, 130.9, 129.4, 127.7,

119.6, 97.4, 92.0, 61.4, 55.3, 51.0, 38.0, 35.8, 31.2, 29.4, 22.0, 21.2, 16.4, 11.5; HRMS (ESI, m/z) calcd for $C_{24}H_{33}O_5Se$ $[M+H]^+$ 481.1493, found 481.1482.

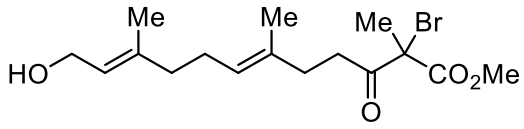

290

Linear α-Bromo Alcohol **290**. Linear alcohol **154** (250 mg, 890 μmol, 1.0 equiv.) was dissolved in 18 mL THF and cooled to 0 °C. NaH (60 % dispersion in mineral oil, 35 mg, 890 μmol, 1.0 equiv.) was added and the solution was stirred for 2h at 0 °C. The solution was cooled to -78 °C and NBS (173 mg, 980 μmol, 1.1 equiv.) was added. The solution was stirred for 1 h at -78 °C before being diluted with Et_2O and quenched with sat. aqueous $NaHCO_3$. The aqueous layer was extracted 3x with Et_2O, and the combined organic layers were washed 2x with H_2O, brine, dried over $MgSO_4$, filtered, and condensed. The resultant material was used without further purification, yielding linear α-bromo alcohol **290** as a yellow oil (320 mg, 99% yield).

290: R_f = 0.29 (silica gel, 30% ethyl acetate/hexanes); IR (film): ν_{max} 3391, 2921, 1723, 1442, 1250, 1119, 994, 736 cm^{-1}; ^1H NMR (600 MHz, $CDCl_3$) δ 5.40 (t, J = 7.0 Hz, 1H), 5.14 (t, J = 6.7 Hz, 1H), 4.15 (d, J = 6.9 Hz, 2H), 3.82 (s, 3H), 2.97 – 2.89 (m, 1H), 2.81 – 2.74 (m, 1H), 2.30 (t, J = 7.5 Hz, 2H), 2.11 (q, J = 7.3 Hz, 2H), 2.06 – 2.01 (m, 2H), 1.99 (s, 4H), 1.67 (s, 3H), 1.61 (s, 3H); ^{13}C NMR (150 MHz, $CDCl_3$) δ 200.5, 169.1, 139.5, 133.6, 125.1, 123.8, 62.7, 59.6, 54.0, 39.4,

36.96, 34.3, 26.3, 25.6, 16.4, 16.2; HRMS (ESI, m/z) calcd for $C_{16}H_{25}O_4NaBr$ $[M+Na]^+$ 383.0834, found 383.0846.

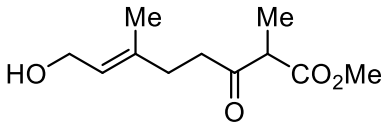

263

Truncated Linear Alcohol **263.** Allylic alcohol **262** (see Scheme 4.12 [pg. 107], prepared according to the literature[10], 3.57g, 24.8 mmol, 1.0 equiv.) was azeotropically distilled with PhMe to remove trace water, and was subsequently dissolved in 83 mL THF. The solution was cooled to -78 °C and MsCl (2.5 mL, 32.2 mmol, 1.3 equiv.) and Et_3N (6.9 mL, 49.6 mmol, 2.0 equiv.) were added. The solution was slowly allowed to warm to -15 °C over 3 h. A solution of LiI (13.3 g, 99.2 mmol, 4.0 equiv.) in 50 mL THF was added, and the resultant solution was stirred for 50 min, slowly warming from -15 °C to -10 °C. The resultant solution was diluted with Et_2O, quenched with sat. aqueous $NaHCO_3$, extracted 3x with Et_2O, washed with 10% aqueous $NaHSO_3$, sat. aqueous NH_4Cl, H_2O, and brine. The combined organic layers were dried over $MgSO_4$, filtered, and condensed to yield the corresponding allylic iodide (5.2 g, 83% yield). The resultant crude material was used directly in the next step.

A suspension of NaH (60% dispersion in mineral oil, 4.1 g, 102.5 mmol, 5.0 equiv.) in 256 mL THF was cooled to 0 °C, and neat methyl 2-methyl-3-oxobutanoate **155** (13.3 g, 102.5 mmol, 5.0 equiv.) was slowly added and the solution was allowed to stir for 35 min. *n*-BuLi (2.28M/hexanes, 45 mL,

102.5 mmol, 5.0 equiv.) was slowly added at 0 °C and the solution was allowed to stir for 45 min before being cooled to -78 °C. A solution of the allylic iodide (5.2 g, 20.5 mmol, 1.0 equiv.) in 40 mL THF was slowly added and the solution was stirred for 45 min. The resultant solution was diluted with EtOAc, and quenched with H_2O and sat. aqueous NH_4Cl. The aqueous layer was extracted 3x with EtOAc, and the combined organic layers were washed with brine, dried over $MgSO_4$, filtered, and condensed. The resultant crude material was purified via flash column chromatography (silica gel, 10% to 15% to 25% to 35% to 50% EtOAc/hexanes) to yield truncated linear alcohol **263** as a yellow oil (2.82 g, 64% yield). Truncated linear acetate **264** was also isolated as a yellow oil (500 mg, 10% yield).

263: R_f = 0.19 (silica gel, 40% ethyl acetate/hexanes); IR (film): ν_{max} 3418, 2920, 1739, 1710, 1437, 1268, 1207, 1070, 999 cm^{-1}; ^1H NMR (600 MHz, $CDCl_3$) δ 5.40 (t, J = 6.9 Hz, 1H), 4.15 (d, J = 6.9 Hz, 2H), 3.74 (s, 3H), 3.55 (q, J = 7.2 Hz, 1H), 2.77 – 2.69 (m, 1H), 2.68 – 2.60 (m, 1H), 2.31 (d, J = 7.5 Hz, 2H), 1.68 (s, 3H), 1.35 (d, J = 7.1 Hz, 3H);^{13}C NMR (150 MHz, $CDCl_3$) δ 205.2, 171.1, 138.1, 124.2, 59.4, 52.9, 52.6, 39.7, 33.0, 16.6, 13.0; HRMS (ESI, m/z) calcd for $C_{11}H_{18}O_4Na$ $[M+Na]^+$ 237.1103, found 237.1096.

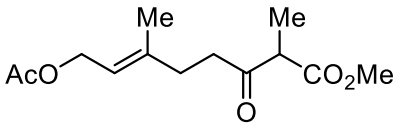

264

Truncated Linear Acetate **264**. Truncated linear alcohol **263** (1.44 g, 5.6 mmol, 1.0 equiv.) was dissolved in 5.6 mL CH_2Cl_2 at room temperature. Ac_2O (1.32 mL, 14 mmol, 2.5 equiv.) was added, followed by DMAP (17 mg, 140 μmol, 2.5 mol%), and the solution was stirred at room temperature for 1.25 h before MeOH was added. After stirring for an additional 10 min, the solution was added to H_2O/hexanes, and the layers were separated. The organic layer was washed 2x with H_2O, 2x with sat. aqueous $NaHCO_3$, brine, dried over $MgSO_4$, filtered, and condensed to yield truncated linear acetate **264** as a pale-yellow oil (1.57 g, 91% yield). The resultant material was pure enough to be used in subsequent operations without purification.

264: R_f = 0.26 (silica gel, 20% ethyl acetate/hexanes); IR (film): ν_{max} 3336, 2923, 1739, 1716, 1454, 1433, 1368, 1232, 1024, 610 cm^{-1}; ^1H NMR (600 MHz, $CDCl_3$) δ 5.33 (t, J = 7.0 Hz, 1H), 4.57 (d, J = 7.1 Hz, 2H), 3.74 (s, 3H), 3.54 (q, J = 7.0 Hz, 1H), 2.77 – 2.69 (m, 1H), 2.67 – 2.60 (m, 1H), 2.33 (t, J = 7.7 Hz, 2H), 2.05 (s, 3H), 1.71 (s, 3H), 1.35 (d, J = 7.2 Hz, 3H); ^{13}C NMR (150 MHz, $CDCl_3$) δ 205.0, 171.2, 171.1, 140.6, 119.2, 61.3, 52.9, 52.6, 39.6, 33.0, 21.2, 16.8, 13.0; HRMS (ESI, m/z) calcd for $C_{13}H_{20}O_5Na$ $[M+Na]^+$ 279.1208, found 279.1196.

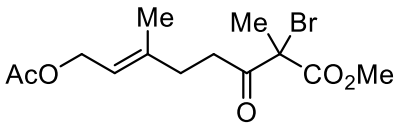

A9

Truncated α-Bromo Acetate **A9**. Truncated linear acetate **264** (1.57 g, 6.13 mmol, 1.0 equiv.) was azeotropically distilled 2x with PhMe to remove trace H_2O, dissolved in 125 mL THF, and cooled to 0 °C. NaH (60% dispersion in mineral oil, 270 mg, 6.74 mmol, 1.1 equiv.) was added, and the solution was stirred for 1.17 h at 0 °C. The solution was cooled to -78 °C and NBS (1.2 g, 6.74 mmol, 1.1 equiv.) was added. The solution was stirred at -78 °C for 1 h before being diluted with EtOAc and quenched with aqueous. 1M HCl. The aqueous layer was exracted 3x with EtOAc, and the combined organic layers were washed with sat. aqueous $NaHCO_3$, brine, and dried over $MgSO_4$, filtered, and condensed. The resultant material was purified via flash column chromatography (silica gel, 15% EtOAc/hexanes) to yield truncated α-bromo acetate **A9** as a pale-yellow oil (1.53 g, 75% yield).

A9: R_f = 0.50 (silica gel, 20% ethyl acetate/hexanes); IR (film): ν_{max} 1728, 1443, 1367, 1230, 1118, 1073, 1022, 957, 736, 607 cm^{-1}; ^1H NMR (600 MHz, $CDCl_3$) δ 5.36 (t, J = 7.0 Hz, 1H), 4.58 (d, J = 7.0 Hz, 2H), 3.83 (s, 3H), 3.03 – 2.94 (m, 1H), 2.88 – 2.79 (m, 1H), 2.37 (t, J = 7.7 Hz, 2H), 2.05 (s, 3H), 1.99 (s, 3H), 1.72 (s, 3H); ^{13}C NMR (150 MHz, $CDCl_3$) δ 200.2, 171.2, 169.0, 140.3, 119.4, 62.4, 61.3, 54.0, 36.5, 34.1, 25.6, 21.2, 16.7; HRMS (ESI, m/z) calcd for $C_{13}H_{19}O_5NaBr$ $[M+Na]^+$ 357.0314, found 357.0311.

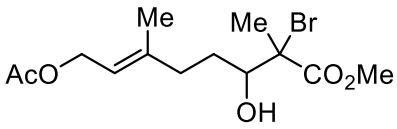

265

α-Bromo β-Hydroxy Ester **265.** Truncated α-bromo acetate **A9** (270 mg, 810 μmol, 1.0 equiv.) was azeotropically distilled 2x with PhMe to remove trace H_2O, and was then dissolved in 16 mL MeOH. The solution was cooled to -78 °C, and $NaBH_4$ (61 mg, 1.61 mmol, 2.0 equiv.) was added. The solution was stirred for 50 min before being diluted with EtOAc and quenched with aqueous 1M HCl. The aqueous layer was extracted 3x with EtOAc, and the combined organic layers were washed with sat. aqueous $NaHCO_3$, brine, dried over $MgSO_4$, filtered, and condensed. The resultant material was purified via flash column chromatography (silica gel, 15% EtOAc/hexanes) to yield α-bromo β-hydroxy ester **265** as a pale-yellow oil (130 mg, 48% yield).

265: R_f = 0.23 (silica gel, 20% ethyl acetate/hexanes); IR (film): ν_{max} 3497, 2959, 2934, 1739, 1713, 1447, 1383, 1232, 1114, 1052, 1020, 737, 625 cm^{-1}; ^1H NMR (600 MHz, $CDCl_3$) δ 5.42 (t, J = 7.2 Hz, 1H), 4.60 (dd, J = 7.1, 3.0 Hz, 2H), 4.07 (ddd, J = 10.6, 6.1, 1.6 Hz, 1H), 3.83 (s, 3H), 2.53 (d, J = 6.0 Hz, 1H), 2.38 – 2.31 (m, 1H), 2.20 – 2.14 (m, 1H), 2.06 (s, 3H), 2.04 – 1.98 (m, 1H), 1.87 (s, 3H), 1.74 (s, 3H); ^{13}C NMR (150 MHz, $CDCl_3$) δ 171.9, 171.3, 141.5, 119.3, 75.2, 63.1, 61.5, 53.5, 36.4, 29.0, 22.0, 21.2, 16.6; HRMS (ESI, m/z) calcd for $C_{13}H_{21}O_5NaBr$ $[M+Na]^+$ 359.0470, found 359.0458.

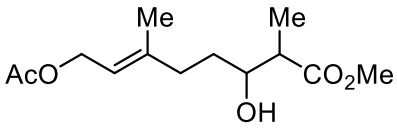

269

Truncated β-Hydroxy Ester **269**. *Preparation 1.* α-Bromo β-hydroxy ester **265** (25 mg, 74 μmol, 1.0 equiv.) was azeotropically distilled 2x with PhMe to remove trace water, and was subsequently dissolved in 3.7 mL of CH_2Cl_2 and cooled to -45 °C under an O_2 balloon. $AlMe_3$ (2M/hexanes, 111 μL, 222 μmol, 3.0 equiv.) was added and the solution was stirred for 35 min. Bu_3SnH (36 μL, 133 μmol, 1.8 equiv.) was added, and syringe pump addition (0.08 mL/h) of Et_3B (1M/hexanes, 148 μL, 148 μmol, 2.0 equiv.) was initiated. After stirring for 4 h, the solution was diluted with EtOAc, and quenched with H_2O, aqueous 1M HCl, and solid potassium sodium tartrate tetrahydrate. The solution was allowed to stir for 30 min before sat. aqueous $NaHCO_3$ was added until the layers were clear. The aqueous layer was extracted 3x with EtOAc, and the combined organic layers were washed with sat. aqueous $NaHCO_3$, brine, dried over $MgSO_4$, filtered, and condensed. The resultant crude material was purified via flash column chromatography (silica gel, 25% EtOAc/hexanes) to yield truncated β-hydroxy ester **269** as a clear oil (7.8 mg, 41% yield).

Truncated β-Hydroxy Ester **269**. *Preparation 2.* Truncated linear acetate **264** (80 mg, 240 μmol, 1.0 equiv.) was dissolved in 5 mL MeOH and cooled to 0 °C. $NaBH_4$ (18 mg, 480 μmol, 2.0 equiv.) was added, and the solution was stirred at 0 °C for 25 min before being diluted with EtOAc and

quenched with aqueous 1M HCl. The aqueous layer was extracted 3x with EtOAc, and the combined organic layers were washed with sat. aqueous $NaHCO_3$, brine, dried over $MgSO_4$, filtered, and condensed. The resultant material was purified via flash column chromatography (silical gel, gradient: 20% to 25% EtOAc/hexanes) to yield truncated β-hydroxy ester **269** as a clear oil (57 mg, 70% yield).

269: R_f = 0.29 (silica gel, 30% ethyl acetate/hexanes); IR (film): ν_{max} 3467, 2947, 1731, 1439, 1368, 1231, 1025 cm^{-1}; ^1H NMR (600 MHz, $CDCl_3$) δ *Major Diastereomer*: 3.67 – 3.61 (m, 1H), 1.22 (d, J = 7.2 Hz, 3H), *Minor Diastereomer*: 3.86 (ddd, J = 8.4, 4.0 Hz, 1H), 1.19 (d, J = 7.3 Hz, 1H), *Shared Peaks*: 5.37 (t, J = 7.2 Hz, 1H), 4.58 (d, J = 7.1 Hz, 2H), 3.71 (s, 3H), 2.60 (d, J = 6.8 Hz, 1H), 2.58 – 2.52 (m, 1H), 2.51 (d, J = 4.7 Hz, 0H), 2.30 – 2.22 (m, 1H), 2.17 – 2.06 (m, 1H), 2.05 (s, 3H), 1.71 (s, 3H), 1.68 – 1.47 (m, 3H); ^{13}C NMR (150 MHz, $CDCl_3$) δ 176.6, 176.5, 171.3, 142.0, 141.9, 118.9, 118.8, 73.1, 71.5, 61.5, 61.4, 52.0, 51.9, 45.3, 44.5, 36.0, 35.6, 32.8, 31.8, 21.2, 16.6, 16.6, 14.5, 11.0; HRMS (ESI, m/z) calcd for $C_{13}H_{22}O_5Na$ $[M+Na]^+$ 281.1365, found 281.1363.

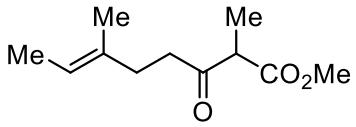

272

Truncated β-Keto Ester **272**. *Trans*-2-methyl-2-butenal **270** (see Scheme 4.13 [pg. 109], 2 g, 23.8 mmol, 1.0 equiv.) was dissolved in 240 mL MeOH and cooled to -10 °C. $NaBH_4$ (995 mg, 26.2 mmol, 1.1 equiv.) was added

and the solution was allowed to stir for 35 min. The reaction was diluted with CH_2Cl_2 and quenched with sat. aqueous $NaHCO_3$. Brine was added, along with solid potassium sodium tartrate tetrahydrate and H_2O. The solution was removed from the cold bath and allowed to stir for 30 min before the aqueous layer was extracted 3x with CH_2Cl_2. The combined organic layers were dried over $MgSO_4$, filtered, and condensed to yield allylic alcohol **271** as a pale-yellow oil (1.84 g, 90% yield, spectroscopic data matched the literature). The crude material was used directly in the next step without further purification.

Allylic alcohol **271** (1.84 g, 21.4 mmol, 1.0 equiv.) was dissolved in 72 mL THF and cooled to -78 °C. MsCl (2.2 mL, 27.8 mmol, 1.3 equiv.) and Et_3N (6.0 mL, 42.8 mmol, 2.0 equiv.) were added and the solution was slowly allowed to warm to -40 °C over the course of 3.5 h. A solution of LiI (11.5 g, 85.6 mmol, 4.0 equiv.) in 36 mL THF was added, and the resultant solution was stirred for 1 h. The reaction was diluted with Et_2O and quenched with sat. aqueous $NaHCO_3$, H_2O, and 10% aqueous $NaHSO_3$. The aqueous layer was extracted 3x with Et_2O, and the combined organic layers were washed with sat. aqueous NH_4Cl, H_2O, and brine. The organic layers were dried over $MgSO_4$, filtered, and condensed (rotovap bath temperature = 0 °C) to yield the corresponding iodide, which was used without further purification in the next step.

A suspension of NaH (60% dispersion in mineral oil, 2.57 g, 64.2 mmol, 3.0 equiv.) in 250 mL THF was cooled to 0 °C, and neat methyl 2-methyl-3-oxobutanoate **155** (8.35 g, 64.2 mmol, 3.0 equiv.) was slowly added, and the resultant solution was allowed to stir for 30 min. *n*-BuLi (2.28M/hexanes, 28 mL, 64.2 mmol, 3.0 equiv.) was slowly added, and the resultant solution

was allowed to stir for 35 min. A solution of the allylic iodide (assuming quantitative yield from previous step, 21.4 mmol, 1.0 equiv.) in 40 mL THF was added, and the reaction was removed from the cold bath and allowed to stir at room temperature for 2.5 h. The resultant solution was diluted with EtOAc and quenched with sat. aqueous NH_4Cl, H_2O, and 10% aqueous $NaHSO_3$. The aqueous layer was extracted 3x with EtOAc, and the combined organic layers were washed with brine, dried over $MgSO_4$, filtered, and condensed. The resultant crude material was purified via flash column chromatography (silica gel, 2.5% to 5% to 7.5% Et_2O/hexanes) to yield truncated β-keto ester **272** as a pale-yellow oil (2.5 g, 59% yield over 2 steps).

272: R_f = 0.44 (silica gel, 10% ethyl acetate/hexanes); IR (film): ν_{max} 2948, 1745, 1713, 1437, 1200, 1174, 1120, 1070 cm^{-1}; ^1H NMR (600 MHz, $CDCl_3$) δ 5.20 (q, J = 6.6 Hz, 1H), 3.73 (s, 3H), 3.54 (q, J = 7.1 Hz, 1H), 2.70 – 2.54 (m, 2H), 2.26 (t, J = 7.7 Hz, 2H), 1.59 (s, 3H), 1.56 (s, 3H), 1.33 (d, J = 7.1 Hz, 3H); ^{13}C NMR (150 MHz, $CDCl_3$) δ 205.7, 171.2, 134.2, 119.4, 52.9, 52.5, 40.3, 33.4, 15.8, 13.5, 13.0; HRMS (ESI, m/z) calcd for $C_{11}H_{17}O_3$ $[M-H]^-$ 197.1178, found 197.1185.

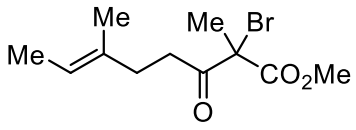

273

Truncated α-Bromo β-Keto Ester **273.** Truncated β-keto ester **272** (300 mg, 1.52 mmol, 1.0 equiv.) was azeotropically distilled 2x with PhMe to remove trace H_2O, then dissolved in 30 mL MeOH and cooled to 0 °C. NaH

(60% dispersion in mineral oil, 67 mg, 1.67 mmol, 1.1 equiv.) was added and the solution was allowed to stir for 35 min at 0 °C. The solution was cooled to -78 °C, then NBS (297 mg, 1.67 mmol, 1.1 equiv.) was added and the solution was allowed to stir for 40 min at -78 °C. Upon completion, the solution was diluted with EtOAc and quenched with aqueous 1M HCl. The aqueous layer was extracted 3x with EtOAc, and the combined organic layers were washed with sat. aqueous $NaHCO_3$, brine, dried over $MgSO_4$, filtered, and condensed. The resultant material was purified via flash column chromatography (silica gel, gradient: 2% to 3% to 4% EtOAc/hexanes) to yield truncated α-bromo β-keto ester **273** as a clear oil (270 mg, 64% yield). NOTE: This compound is unstable at room temperature and should be stored in a freezer.

273: R_f = 0.63 (silica gel, 10% ethyl acetate/hexanes); IR (film): ν_{max} 2959, 2920, 2862, 1760, 1724, 1443, 1268, 1117, 1074, 974, 737 cm^{-1}; ^1H NMR (600 MHz, $CDCl_3$) δ 5.25 (q, J = 6.6 Hz, 1H), 3.82 (s, 3H), 2.97 – 2.89 (m, 1H), 2.82 – 2.73 (m, 1H), 2.30 (t, J = 7.6 Hz, 2H), 1.99 (s, 4H), 1.61 (s, 3H), 1.57 (d, J = 6.6 Hz, 3H); ^{13}C NMR (150 MHz, $CDCl_3$) δ 200.6, 169.1, 134.0, 119.7, 62.8, 54.0, 37.1, 34.4, 25.6, 15.8, 13.5; HRMS (ESI, m/z) calcd for $C_{11}H_{18}O_3Br$ $[M+H]^+$ 277.0439, found 277.0436.

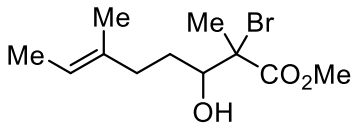

274

Truncated α-Bromo β-Hydroxy Ester **274**. Truncated α-bromo β-keto ester **273** (270 mg, 980 μmol, 1.0 equiv.) was dissolved in 20 mL MeOH and cooled to -78 °C. $NaBH_4$ (75 mg, 1.96 mmol, 2.0 equiv.) was added and the solution was stirred at -78 °C for 40 min. Another portion of $NaBH_4$ (37 mg, 980 μmol, 1.0 equiv.) was added and the solution was stirred for 20 min at -78 °C. The reaction was diluted with EtOAc, and quenched with aqueous 1M HCl. The aqueous layer was extracted 3x with EtOAc, and the combined organic layers were washed with sat. aqueous $NaHCO_3$, brine, dried over $MgSO_4$, filtered, and condensed. The resultant material was purified via flash column chromatography (silica gel, gradient: 5% to 10% EtOAc/hexanes) to yield truncated α-bromo β-hydroxy ester **274** as a clear oil (190 mg, 70% yield).

274: R_f = 0.32 (silica gel, 15% ethyl acetate/hexanes); IR (film): ν_{max} 3439, 2925, 1727, 1446, 1268, 1119, 1057, 910, 736 cm^{-1}; ^1H NMR (600 MHz, $CDCl_3$) δ 5.30 (q, J = 6.8 Hz, 1H), 4.07 (ddd, J = 10.5, 6.1, 1.6 Hz, 1H), 3.82 (s, 3H), 2.47 (d, J = 6.2 Hz, 1H), 2.31 – 2.23 (m, 1H), 2.16 – 2.08 (m, 1H), 2.02 – 1.94 (m, 1H), 1.86 (s, 3H), 1.63 (s, 3H), 1.59 (d, J = 6.7, 1.1 Hz, 3H), 1.53 – 1.44 (m, 1H); ^{13}C NMR (150 MHz, $CDCl_3$) δ 171.9, 135.1, 119.6, 75.4, 63.4, 53.4, 36.6, 29.3, 22.2, 15.7, 13.5; HRMS (ESI, m/z) calcd for $C_{11}H_{20}O_3Br$ $[M+H]^+$ 279.0596, found 279.0586.

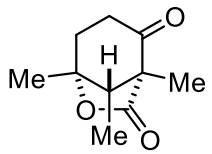

282

Bicyclic Lactone **282**. Truncated α-Bromo β-Keto Ester **273** (58 mg, 210 μmol, 1.0 equiv.) was dissolved in 2.1 mL CH_2Cl_2, and 2,6-lutidine (49 μL, 420 μmol, 2.0 equiv.) and *fac*-Ir(ppy)$_3$ (3.4 mg, 5.3 μmol, 2.5 mol%) were added at room temperature. Two strips of blue LEDs were turned on (purchased from Creative Lighting Solutions, creativelightings.com, Product Code: CL-FRS5050-12WP-12V, Model: Sapphire Blue LED Flex Strip) and the reaction was stirred for 1 h at room temperature. Upon completion, the solution was condensed and purified via PTLC (silica gel, 25% EtOAc/hexanes) to yield bicyclic lactone **282** as a clear oil (3.8 mg, 10% yield).

282: R_f = 0.39 (silica gel, 30% ethyl acetate/hexanes); IR (film): ν_{max} 2926, 1778, 1720, 1451, 1383, 1243, 1146, 1056, 927, 740 cm^{-1}; ^{1}H NMR (600 MHz, $CDCl_3$) δ 2.72 – 2.59 (m, 2H), 2.35 (qd, J = 13.9, 8.8, 1.4 Hz, 1H), 2.29 (q, J = 7.0 Hz, 1H), 1.99 (ddd, J = 14.1, 10.4, 8.0 Hz, 1H), 1.49 (s, 3H), 1.22 (s, 3H), 1.03 (d, J = 7.1 Hz, 3H).; ^{13}C NMR (150 MHz, $CDCl_3$) δ 201.5, 175.0, 84.4, 63.0, 48.6, 36.5, 35.4, 21.3, 11.1, 10.6; HRMS (ESI, m/z) calcd for $C_{10}H_{14}O_3Na$ $[M+Na]^+$ 205.0841, found 205.0847.

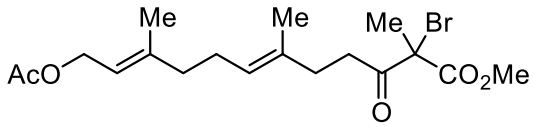

287

Linear α-Bromo Acetate **287**. Linear acetate **237** (960 mg, 2.96 mmol, 1.0 equiv.) was azeotropically distilled 2x with PhMe to remove trace H_2O, dissolved in 60 mL THF, and cooled to -78 °C. NaH (60% dispersion in mineral oil, 130 mg, 3.26 mmol, 1.1 equiv.) was added, and the solution was removed from the cold bath and allowed to warm to room temperature over the course of 1.17 h. The solution was re-cooled to -78 °C and NBS (632 mg, 3.55 mmol, 1.2 equiv.) was added. The solution was allowed to stir for 40 min at -78 °C before being diluted with EtOAc and quenched with a 1/1 solution of brine/aqueous 1M HCl. The aqueous layer was extracted 3x with EtOAc, and the combined organic layers were washed with sat. aqueous $NaHCO_3$, brine, dried over $MgSO_4$, filtered, and condensed. The resultant material was purified via flash column chromatography (silica gel, gradient: 5% to 7.5% EtOAc/hexanes) to yield linear α-bromo acetate **287** as a pale-yellow oil (877 mg, 74 % yield).

287: R_f = 0.26 (silica gel, 10% ethyl acetate/hexanes); IR (film): ν_{max} 2920, 2851, 1731, 1443, 1379, 1228, 1117, 1024, 737 cm^{-1}; ^1H NMR (600 MHz, $CDCl_3$) δ 5.33 (t, J = 7.1 Hz, 1H), 5.14 (t, J = 6.1 Hz, 1H), 4.58 (d, J = 7.1 Hz, 2H), 3.82 (s, 3H), 2.98 – 2.88 (m, 1H), 2.83 – 2.74 (m, 1H), 2.30 (t, J = 7.7 Hz, 2H), 2.15 – 2.08 (m, 2H), 2.07 – 2.03 (m, 5H), 1.99 (s, 3H), 1.70 (s, 3H), 1.61 (s, 3H); ^{13}C NMR (150 MHz, $CDCl_3$) δ 200.5, 171.3, 169.1, 142.2, 133.8, 124.9, 118.6, 62.7, 61.5,

54.0, 39.5, 37.1, 34.4, 26.3, 25.6, 21.2, 16.6, 16.2; HRMS (ESI, m/z) calcd for $C_{18}H_{27}NaBrO_5$ $[M+Na]^+$ 425.0940, found 425.0921.

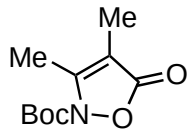

A10

N-Boc-3,4-Dimethyl-5-Isoxazolone **A10**. Methyl 2-methyl-3-oxobutanoate **155** (500 mg, 3.85 mmol, 1.0 equiv.) was dissolved in 10 mL EtOH and 2.5 mL H_2O. NaOAc (347 mg, 4.23 mmol, 1.1 equiv.) and NH_2OH•HCl (296 mg, 4.23 mmol, 1.1 equiv.) were added and the reaction was heated to 100 °C and stirred at that temperature for 1.5 h. The solution was diluted with CH_2Cl_2 and H_2O, extracted 3x with CH_2Cl_2, dried over $MgSO_4$, filtered, and condensed. The crude reaction products were purified via flash column chromatography (silica gel, 20% to 30% acetone/hexanes) to yield 3,4-dimethyl-5-isozazolone as a yellow oil (characterization data not acquired, mixture of tautomers, 266 mg, 61% yield).

3,4-Dimethyl-5-isoxazolone (66 mg, 580 μmol, 1.0 equiv.) was dissolved in 3 mL CH_2Cl_2 and was cooled to 0 °C. Et_3N (161 μL, 1.16 mmol, 2.0 equiv.) and Boc_2O (200 μL, 870 μmol, 1.5 equiv.) were added, and the solution was stirred at 0 °C for 50 min. The reaction was removed from the cold bath and allowed to stir at room temperature for 1.5 h. The reaction was quenched with sat. aqueous NH_4Cl, extracted 3x with CH_2Cl_2, dried over $MgSO_4$, filtered, and condensed. The crude reaction products were purified via flash column chromatography (silica gel, 10% acetone/hexanes) to yield

N-Boc-3,4-dimethyl-5-isoxazolone **A10** as an orange-yellow oil (78 mg, 63% yield).

A10: Rf = 0.36 (silica gel, 20% ethyl acetate/hexanes); IR (film): νmax 3366, 2979, 2929, 1745, 1632, 1366, 1330, 1256, 1147, 947, 845, 725, 685, 582 cm^{-1}; ^{1}H NMR (600 MHz, $CDCl_3$) δ 2.44 (s, 3H), 1.82 (s, 3H), 1.57 (s, 9H); ^{13}C NMR (150 MHz, $CDCl_3$) δ 168.2, 154.0, 146.2, 101.7, 86.0, 28.2, 13.6, 6.7.

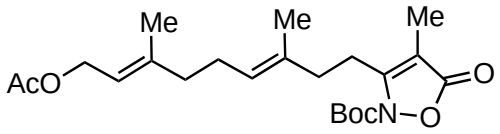

A11

Linear Boc-Isoxazolone **A11**. N-Boc-3,4-dimethyl-5-isozazolone **A10** (40 mg, 190 µL, 1.0 equiv.) was dissolved in 1.9 mL THF and 100 µL HMPA and cooled to -70 °C. KHMDS (0.5M/PhMe, 420 µL, 210 µmol, 1.1 equiv.) was added, and the solution was stirred at -70 °C for 20 min. Allylic bromide **158** (52 mg, 190 µmol, 1.0 equiv.) was added as a solution in 400 µL THF, and the reaction was allowed to slowly warm to 0 °C over the course of 5.5 h. Upon completion, the solution was quenched with sat. aqueous NH_4Cl, extracted 3x with CH_2Cl_2, dried over $MgSO_4$, filtered, and condensed. The resultant crude product mixture was purified via flash column chromatography (silica gel, 10% acetone/hexanes) to yield linear Boc-isoxazolone **A11** as a clear oil (46 mg, 59% yield).

A11: Rf = 0.38 (silica gel, 20% ethyl acetate/hexanes); IR (film): νmax 2980, 2930, 1764, 1727, 1631, 1333, 1232, 1143, 1027, 844, 737 cm^{-1}; ^1H NMR (600 MHz, $CDCl_3$) δ 5.33 (t, J = 7.2 Hz, 1H), 5.13 (t, J = 6.9 Hz, 1H), 4.58 (d, J = 7.1 Hz, 2H), 2.98 - 2.90 (m, 2H), 2.26 (t, J = 7.7 Hz, 2H), 2.14 - 2.08 (m, 2H), 2.06 - 2.01 (m, 5H), 1.80 (s, 3H), 1.69 (d, J = 2173.8 Hz, 3H), 1.66 (s, 3H); 13C NMR (150 MHz, $CDCl_3$) δ 171.2, 168.3, 157.8, 145.8, 142.0, 133.4, 125.9, 118.6, 101.8, 86.0, 61.5, 39.4, 37.5, 28.2, 28.2, 28.2, 26.4, 26.1, 21.2, 16.6, 16.1, 6.7.

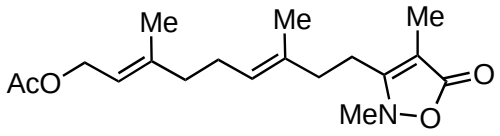

A12

Linear Methyl Isoxazolone **A12**. Methyl 2-methyl-3-oxobutanoate **155** (500 mg, 3.85 mmol, 1.0 equiv.) was dissolved in 7.7 mL AcOH. NaOAc (350 mg, 4.23 mmol, 1.1 equiv.) and MeNHOH•HCl (355 mg, 4.23 mmol, 1.1 equiv.) were added and the solution was stirred at room temperature for 1.5 h. The reaction was heated to 85 °C and stirred for 1 h before being diluted with CH_2Cl_2 and H_2O, extracted 3x with CH_2Cl_2, dried over $MgSO_4$, filtered, and condensed. The crude reaction mixture was purified via flash column chromatography (silica gel, 30% acetone/hexanes) to yield 3,4,5-trimethyl-5-isoxazolone as a clear oil (^1H NMR data matched the literature[11], 380 mg, 78% yield).

3,4,5-Trimethyl-5-isoxazolone (100 mg, 790 μmol, 1.0 equiv.) was dissolved in 6 mL THF and 400 μL HMPA and was cooled to 0 °C. *n*-BuLi

(2.37M/hexanes, 350 μL, 830 μmol, 1.05 equiv.) was added and the reaction was stirred for 25 min. A solution of allylic bromide **158** (216 mg, 790 μmol, 1.0 equiv.) in 2 mL THF was added, and the solution was stirred at 0 °C for 2.25 h. The reaction was quenched with sat. aqueous NH_4Cl, diluted with Et_2O and H_2O, extracted 3x with CH_2Cl_2, dried over $MgSO_4$, filtered, and condensed. The crude mixture was purified via flash column chromatography (silica gel, 20% acetone/hexanes) to yield linear methyl isoxazolone **A12** as a pale-yellow liquid (174 mg, 69% yield).

A12: Rf = 0.34 (silica gel, 50% ethyl acetate/hexanes); IR (film): νmax 2923, 1731, 1631, 1441, 1379, 1232, 1120, 1024, 754 cm^{-1}; ^1H NMR (600 MHz, $CDCl_3$) δ 5.33 (t, J = 7.2 Hz, 1H), 5.15 (t, J = 7.0 Hz, 1H), 4.59 (d, J = 7.1 Hz, 2H), 3.20 (s, 3H), 2.56 - 2.46 (m, 2H), 2.21 (d, J = 8.2 Hz, 2H), 2.16 - 2.09 (m, 2H), 2.08 - 2.01 (m, 5H), 1.77 (s, 3H), 1.70 (s, 3H), 1.66 (s, 3H); ^{13}C NMR (150 MHz, $CDCl_3$) δ 172.1, 171.2, 165.6, 141.9, 133.0, 126.2, 118.8, 99.5, 61.5, 39.3, 38.8, 37.3, 26.3, 24.6, 21.2, 16.6, 16.2, 7.0; HRMS (ESI, m/z) calcd for $C_{18}H_{28}NO_4$ [M+H]+ 322.2018, found 322.2018.

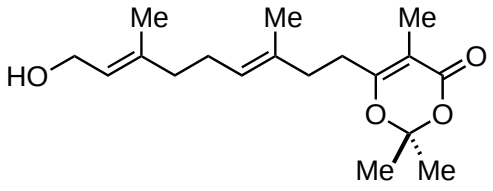

A13

Linear Acetonide **A13**. *Tert*-butyl 2-methyl-3-oxobutanoate (2.06 g, 12 mmol, 1.0 equiv.) was dissolved in 3.4 mL Ac_2O and 1.75 mL acetone and

cooled to 0 °C. Concentrated aqueous H_2SO_4 (700 µL, 12 mmol, 1.0 equiv.) was added dropwise and the solution was slowly allowed to warm to room temperature over the course of 15 h. The solution was diluted with CH_2Cl_2 and H_2O, extracted 5x with CH_2Cl_2, dried over Na_2SO_4, filtered, and condensed. The crude reaction products were purified via flash column chromatography (silica gel, 15% acetone/hexanes) to yield 2,2,5,6-tetramethyl-4H-1,3-dioxin-4-one as an orange liquid (^{1}H NMR data matched the literature[12], 1.3 g, 69% yield).

A solution consisting of *i*-Pr_2NH (93 µL, 670 µmol, 1.05 equiv.) in 2.5 mL THF was prepared and cooled to 0 °C. *n*-BuLi (2.37M/hexanes, 280 µL, 670 µmol, 1.05 equiv.) was added and the solution was stirred for 20 min. HMPA (300 µL) was added, followed by dropwise addition of a solution of 2,2,5,6-tetramethyl-4H-1,3-dioxin-4-one (100 mg, 640 µmol, 1.0 equiv.) in 2 mL THF. The solution was stirred for 30 min before a solution of allylic bromide **158** (175 mg, 640 µmol, 1.0 equiv.) in 2 mL THF was slowly added. The reaction was stirred at 0 °C for 2.75 h before being quenched with sat. aqueous NH_4Cl, diluted with Et_2O and H_2O, extracted 3x with CH_2Cl_2, dried over $MgSO_4$, filtered, and condensed. The crude reaction mixture was purified via flash column chromatography (silica gel, 10% acetone/hexanes) to yield linear acetonide **A13** as a clear oil (76 mg, 39% yield).

A13: Rf = 0.38 (silica gel, 20% ethyl acetate/hexanes); IR (film): νmax 2926, 1724, 1645, 1372, 1232, 1143, 1024 cm^{-1}; ^{1}H NMR (600 MHz, $CDCl_3$) δ 5.34 (t, J = 7.2 Hz, 1H), 5.14 (t, J = 6.6 Hz, 1H), 4.59 (d, J = 7.1 Hz, 2H), 2.40 - 2.33 (m,

2H), 2.19 (t, J = 7.8 Hz, 2H), 2.12 (q, J = 7.1 Hz, 2H), 2.08 - 2.02 (m, 5H), 1.82 (s, 3H), 1.70 (s, 3H), 1.64 (s, 6H); ^{13}C NMR (150 MHz, CDCl3) δ 171.2, 165.7, 163.0, 142.0, 133.7, 125.3, 118.7, 104.8, 100.4, 61.5, 39.4, 35.9, 30.0, 26.3, 25.3, 21.2, 16.6, 16.1, 10.3.

Representative Photoredox-Catalyzed Cyclization

Linear α-bromo alcohol **290** (26 mg, 72 μmol, 1.0 equiv.) was dissolved in 3.6 mL CH_2Cl_2 (no effort was made to exclude O_2 or H_2O). DABCO (16 mg, 145 μmol, 2.0 equiv.) and *fac*-Ir(ppy)$_3$ (240 μg, 360 nmol, 0.5 mol%) were added, and two strips of blue LEDs were turned on (purchased from Creative Lighting Solutions, creativelightings.com, Product Code: CL-FRS5050-12WP-12V, Model: Sapphire Blue LED Flex Strip). After 1.5 h the lights were turned off, the reaction was diluted with Et_2O, several drops of aqueous 1M HCl were added (to precipitate DABCO), the solution was dried over $MgSO_4$, filtered through celite, and condensed. The crude product mixture was analyzed using an internal standard (0.02M 1,3,5-trimethoxybenzene in $CDCl_3$) revealing bicyclic alcohol **162** (13.7% yield).

REFERENCES

[1] Suhara, Y., Hirota, Y., Nakagawa, K., Kamao, M., Tsugawa, N., & Okano, T., Design and synthesis of biologically active analogues of vitamin K2: Evaluation of their biological activities with cultured human cell lines. *Bioorgan. Med. Chem.* **2008,** *16*, 3108–3117.

[2] Gonzalez, M. A., & Molina-Navarro, S., Attempted synthesis of spongidines by a radical cascade terminating onto a pyridine ring. *J. Org. Chem.* **2007,** *72*, 7462–7465.

[3] Nawrat, C. C., Lewis, W., & Moody, C. J., Synthesis of amino-1,4-benzoquinones and their use in Diels–Alder approaches to the aminonaphthoquinone antibiotics. *J. Org. Chem.* **2011,** *76*, 7872–7881.

[4] Jenny, L., & Borschberg, H. J., Synthesis of the dolabellane diterpene hydrocarbon (±)- δ -araneosene. *Helv. Chim. Acta* **1995,** *78*, 715–731.

[5] Powell, L. H., Docherty, P. H., Hulcoop, D. G., Kemmitt, P. D., & Burton, J. W., Oxidative radical cyclisations for the synthesis of γ-lactones. *Chem. Commun.* **2008,** 2559-2561.

[6] Frigerio, M., Santagostino, M., & Sputore, S., A user-friendly entry to 2-iodoxybenzoic acid (IBX). *J. Org. Chem.* **1999,** *64*, 4537–4538.

[7] Ireland, R. E., & Liu, L., An improved procedure for the preparation of the Dess–Martin periodinane. *J. Org. Chem.* **1993,** *58*, 2899–2899.

[8] Watson, C. G., & Aggarwal, V. K., Asymmetric synthesis of 1-heteroaryl-1-arylalkyl tertiary alcohols and 1-pyridyl-1-arylethanes by lithiation–borylation methodology. *Org. Lett.* **2013,** *15*, 1346–1349.

[9] Ryter, K., & Livinghouse, T., Dichloro(2,2,2-trifluoroethoxy)oxovanadium(V). A remarkably effective reagent for promoting one-electron oxidative cyclization and unsymmetrical coupling of silyl enol ethers. *J. Am. Chem. Soc.* **1998,** *120*, 2658–2659.

[10] Ward, J. L., & Beale, M. H., Synthesis of (2E)-4-hydroxy-3-methylbut-2-enyl diphosphate, a key intermediate in the biosynthesis of isoprenoids. *J. Chem. Soc., Perkin Trans. 1* **2002,** 710–712.

[11] Padwa, A., Bullock, W. H., Kline, D. N., & Perumattam, J., Heterocyclic synthesis via the reaction of nitrones and hydroxylamines with substituted allenes. *J. Org. Chem.* **1989,** 54, 2862-2869.

[12] Prantz, K., & Mulzer, J., Synthesis of (Z)-trisubstituted olefins by decarboxylative Grob-type fragmentations: Epothilone D, discodermolide, and peloruside A. *Chem. Eur. J.* **2010,** 16, 485–506.

Appendix II. Comparison of Natural and Synthetic Oridamycin A and Oridamycin B

1. ^{1}H NMR of Natural Oridamycin A (**26**)[1]

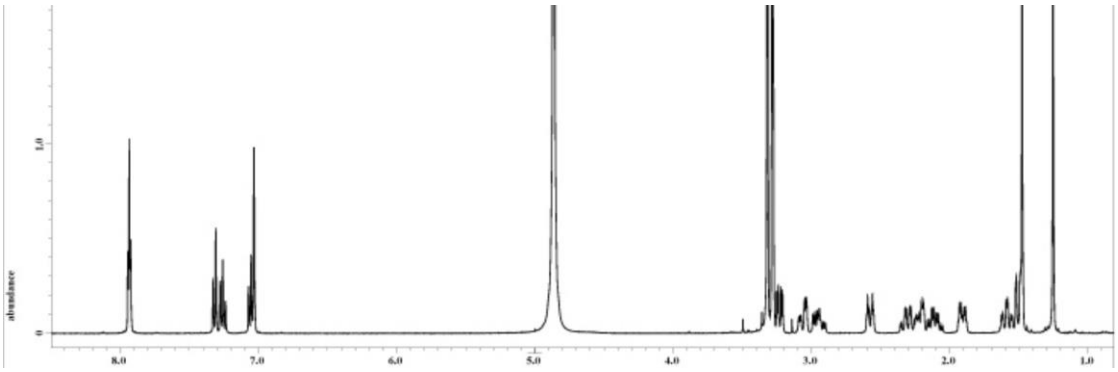

2. ^{1}H NMR of Synthetic Oridamycin A (**26**)

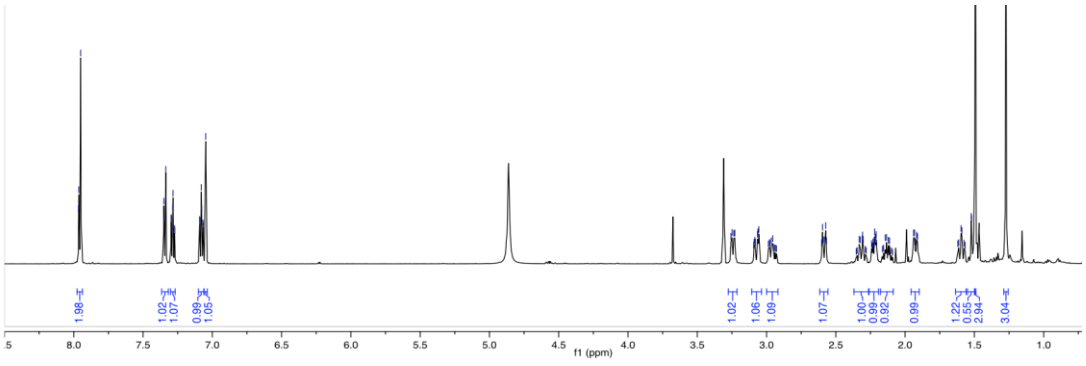

Figure A.1 Comparison of the ^{1}H NMR (CD_3OD) data of natural and synthetic oridamycin A (**26**).

1. ^{13}C NMR of Natural Oridamycin A (**26**)[1]

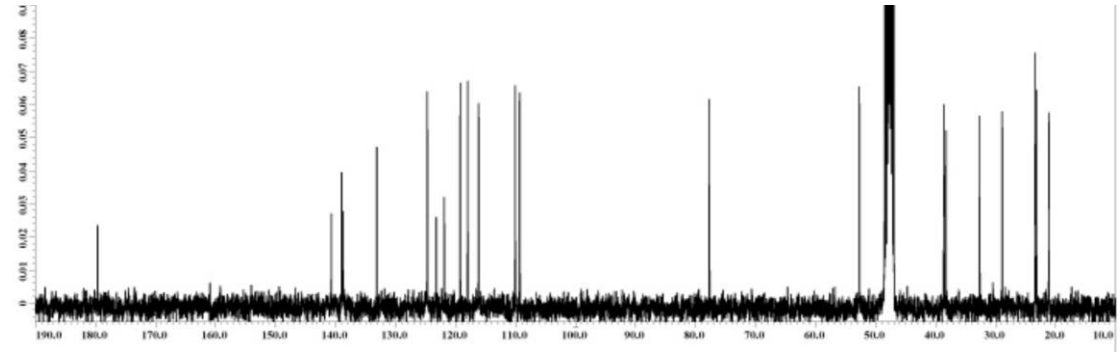

2. ^{13}C NMR of Synthetic Oridamycin A (**26**)

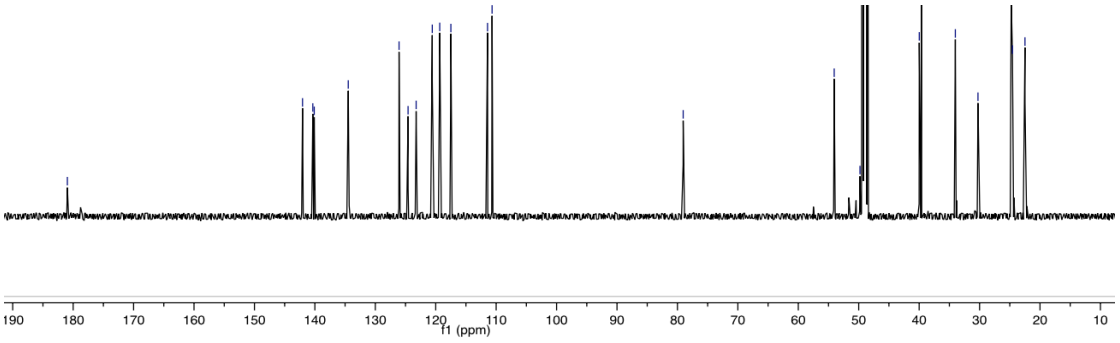

Figure A.2 Comparison of the ^{13}C NMR (CD_3OD) data of natural and synthetic oridamycin A (**26**).

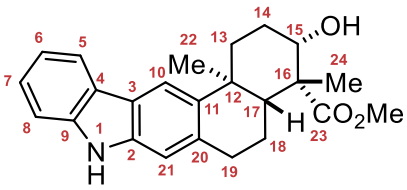

Table A.1 Comparison of the ^{1}H NMR (CD_3OD) of natural and synthetic oridamycin A (**26**).

	Natural		*Synthetic*	
Assigned	δ_H *(ppm)*	*integration, multiplicity, J (Hz)*	δ_H *(ppm)*	*integration, multiplicity, J (Hz)*
5	7.93	1H, d, 8.1	7.96	1H, d, 8.1
10	7.93	1H, s	7.95	1H, s
8	7.32	1H, d, 8.1	7.34	1H, d, 8.1
7	7.25	1H, dt, 8.1, 1.4	7.28	1H, t, 7.6
6	7.05	1H, dt, 8.1, 1.4	7.08	1H, t, 7.6
21	7.03	1H, s	7.05	1H, s
15	3.22	1H, dd, 12.2, 4.6	3.24	1H, dd, 12.2, 4.6
19α	3.06	1H, ddd, 16.3, 5.4, 2.3	3.07	1H, ddd, 16.9, 5.5, 1.9
19β	2.94	1H, ddd, 16.7, 21.7, 2.3	3.00-2.92	1H, m
13α	2.57	1H, dt, 13.6, 3.6	2.58	1H, dt, 13.2, 3.6
14α	2.30	1H, dq, 13.6, 3.6	2.32	1H, dq, 13.6, 3.6
18β	2.23	1H, m	2.26-2.19	1H, m
18α	2.09	1H, dt, 12.7, 5.4	2.13	1H, dt, 12.9, 5.4
14β	1.90	1H, dq, 13.6, 3.6	1.96-1.90	1H, m
13β	1.58	1H, dt, 13.6, 4.1	1.59	1H, dt, 13.6, 3.9
17	1.51	1H, dd, 12.2, 2.3	1.52	1H, d, 12.3
24	1.48	3H, s	1.49	3H, s
22	1.26	3H, s	1.27	3H, s

Table A.2 Comparison of the ^{13}C NMR (CD_3OD) of natural and synthetic oridamycin A (**26**).

	Natural	***Synthetic***
Assigned	δ_C *(ppm)*	δ_C *(ppm)*
23	181.0	181.0
9	142.0	142.0
11	140.3	140.3
2	140.1	140.1
20	134.5	134.5
8	126.1	126.1
4	124.6	124.6
3	123.2	123.2
5	120.6	120.6
6	119.3	119.3
10	117.5	117.5
21	111.4	111.4
7	110.7	110.7
15	79.1	79.1
17	54.1	54.1
16	48.7	48.7
13	40.0	40.0
12	39.6	39.6
19	34.0	34.0
14	30.3	30.3
24	24.8	24.8
22	24.6	24.6
18	22.5	22.5

1. ^{1}H NMR of Natural Oridamycin B (**27**)

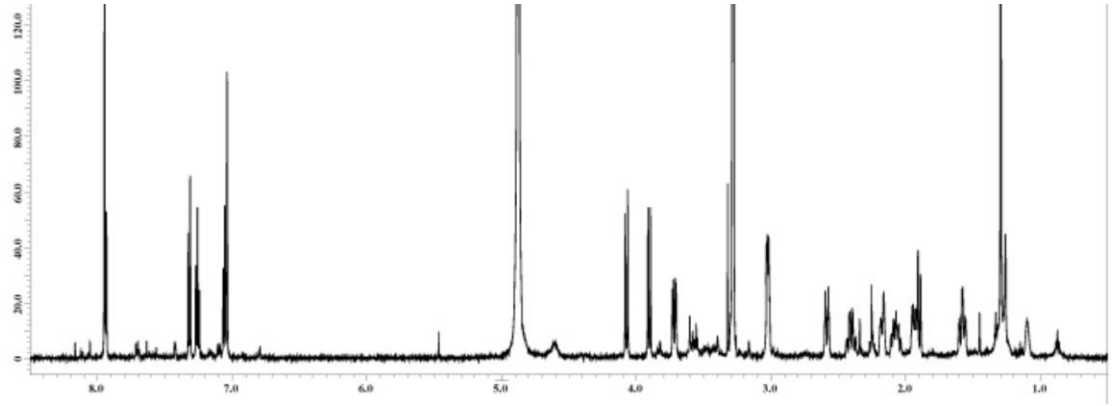

2. ^{1}H NMR of Synthetic Oridamycin B (**27**) (with TFA)

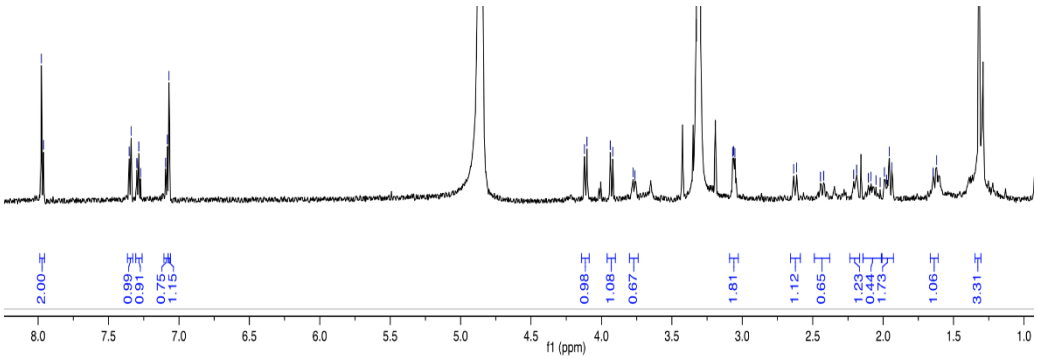

3. ^{1}H NMR of Synthetic Oridamycin B (**27**) (without TFA)

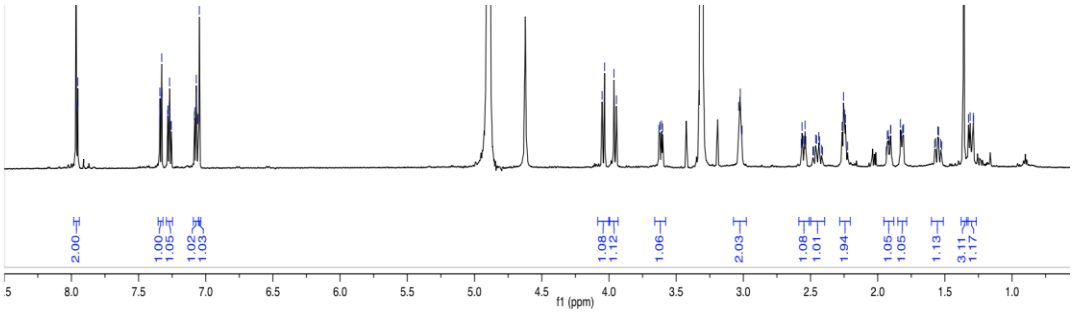

Figure A.3 Comparison of the ^{1}H NMR (CD_3OD) data of natural and synthetic oridamycin B (**27**).

1. ^{13}C NMR of Natural Oridamycin B (**27**)

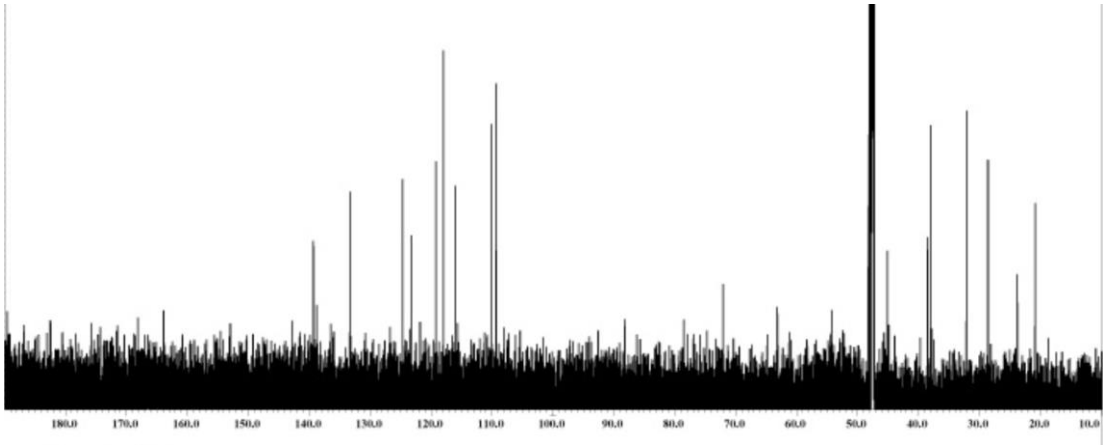

2. ^{13}C NMR of Synthetic Oridamycin B (**27**) (without TFA)

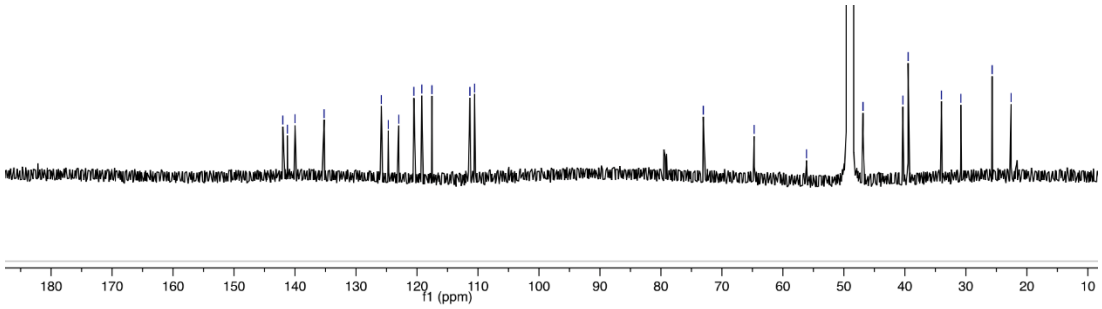

Figure A.4 Comparison of the ^{13}C NMR (CD_3OD) data of natural and synthetic oridamycin B (**27**).

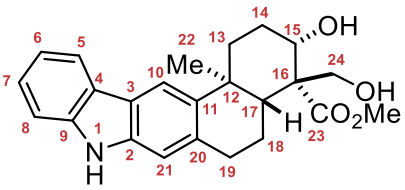

Table A.3 Comparison of the ^{1}H NMR (CD_3OD) of natural and synthetic oridamycin B (**27**) with TFA (*excess*).

	Natural		***Synthetic (with TFA)***	
Assigned	δ_H *(ppm)*	*integration, multiplicity, J (Hz)*	δ_H *(ppm)*	*integration, multiplicity, J (Hz)*
5	7.95	1H, d, 7.9	7.96	1H, d, 8.0
10	7.95	1H, s	7.97	1H, s
8	7.33	1H, d, 7.9	7.35	1H, d, 8.0
7	7.27	1H, dt, 7.9, 1.4	7.28	1H, dt, 7.7, 1.2
6	7.06	1H, dt, 7.9, 1.4	7.08	1H, d, 7.7
21	7.05	1H, s	7.07	1H, s
24b	4.09	1H, d, 11.0	4.11	1H, d, 10.9
24a	3.92	1H, d, 11.0	3.93	1H, d, 10.9
15	3.73	1H, dd, 12.4, 4.8	3.77	1H, dd, 12.2, 4.5
19α/β	3.04	2H, dd, 10.3, 4.1	3.05	2H, m
13α	2.60	1H, dt, 13.0, 3.5	2.62	1H, dt, 13.5, 3.6
14α	2.41	1H, dq, 13.0, 4.1	2.43	1H, dq, 13.2, 3.7
18β	2.17	1H, m	2.23-2.17	1H, m
18α	2.08	1H, m	2.08	1H, m
14β	1.95	1H, m	1.99-1.92	2H, m
17	1.92	1H, dd, 12.2, 2.3		
13β	1.59	1H, m	1.62	1H, dt, 13.7, 3.8
22	1.31	3H, s	1.32	3H, s

Table A.4 Comparison of the ^{1}H NMR (CD_3OD) of natural and synthetic oridamycin B (**27**) without TFA.

	Natural		*Synthetic (without TFA)*	
Assigned	δ_H *(ppm)*	*integration, multiplicity, J (Hz)*	δ_H *(ppm)*	*integration, multiplicity, J (Hz)*
5	7.95	1H, d, 7.9	7.96	1H, d, 7.9
10	7.95	1H, s	7.97	1H, s
8	7.33	1H, d, 7.9	7.33	1H, d, 8.0
7	7.27	1H, dt, 7.9, 1.4	7.27	1H, dt, 7.6, 1.3
6	7.06	1H, dt, 7.9, 1.4	7.07	1H, dt, 7.6, 1.2
21	7.05	1H, s	7.05	1H, s
24b	4.09	1H, d, 11.0	4.04	1H, d, 10.9
24a	3.92	1H, d, 11.0	3.95	1H, d, 10.9
15	3.73	1H, dd, 12.4, 4.8	3.61	1H, dd, 12.1, 4.7
19α/β	3.04	2H, dd, 10.3, 4.1	3.02	2H, m
13α	2.60	1H, dt, 13.0, 3.5	2.55	1H, dt, 13.0, 3.6
14α	2.41	1H, dq, 13.0, 4.1	2.45	1H, dq, 12.5, 3.9
18β	2.17	1H, m	2.27–2.22	2H, m
18α	2.08	1H, m		
14β	1.95	1H, m	1.95–1.88	1H, m
17	1.92	1H, dd, 12.2, 2.3	1.84–1.78	1H, m
13β	1.59	1H, m	1.55	1H, dt, 13.4, 3.7
22	1.31	3H, s	1.36	3H, s

Table A.5 Comparison of the ^{13}C NMR (CD_3OD) of natural and synthetic oridamycin B (**27**) without TFA.

	Natural	*Synthetic*
Assigned	δ_C *(ppm)*	δ_C *(ppm)*
23	179.2	180.6
9	141.9	142.0
11	140.5	141.2
2	140.0	140.0
20	134.5	135.2
8	125.9	125.9
4	124.5	124.7
3	123.2	123.0
5	120.4	120.5
6	119.2	119.2
10	117.2	117.6
7	111.3	111.3
21	110.5	110.6
15	73.3	73.1
24	64.4	64.7
16	55.5	56.1
17	46.3	46.9
13	39.7	40.3
12	39.2	39.5
19	33.3	34.0
14	29.8	30.8
22	25.0	25.7
18	22.1	22.6

REFERENCES

[1] Takada, K., Kajiwara, H., & Imamura, N., Oridamycins A and B, anti-*Saprolegnia parasitica* indolosesquiterpenes isolated from *Streptomyces* sp. KS84. *J. Nat. Prod.* **2010,** 73, 698–701.

Appendix III. ^{1}H and ^{13}C NMR Spectra

^{1}H NMR and ^{13}C NMR spectra were recorded on a Bruker Avance DRX-600 MHz at ambient temperature unless otherwise stated. Chemical shifts are reported in parts per million relative to residual solvent $CDCl_3$ (^{1}H, 7.26 ppm, ^{13}C, 77.16 ppm) or CD_3OD (^{1}H, 3.31 ppm, ^{13}C, 49.00 ppm).

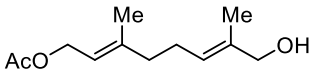

156, 600MHz, $CDCl_3$

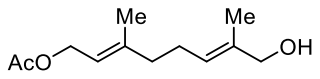

156, 150MHz, $CDCl_3$

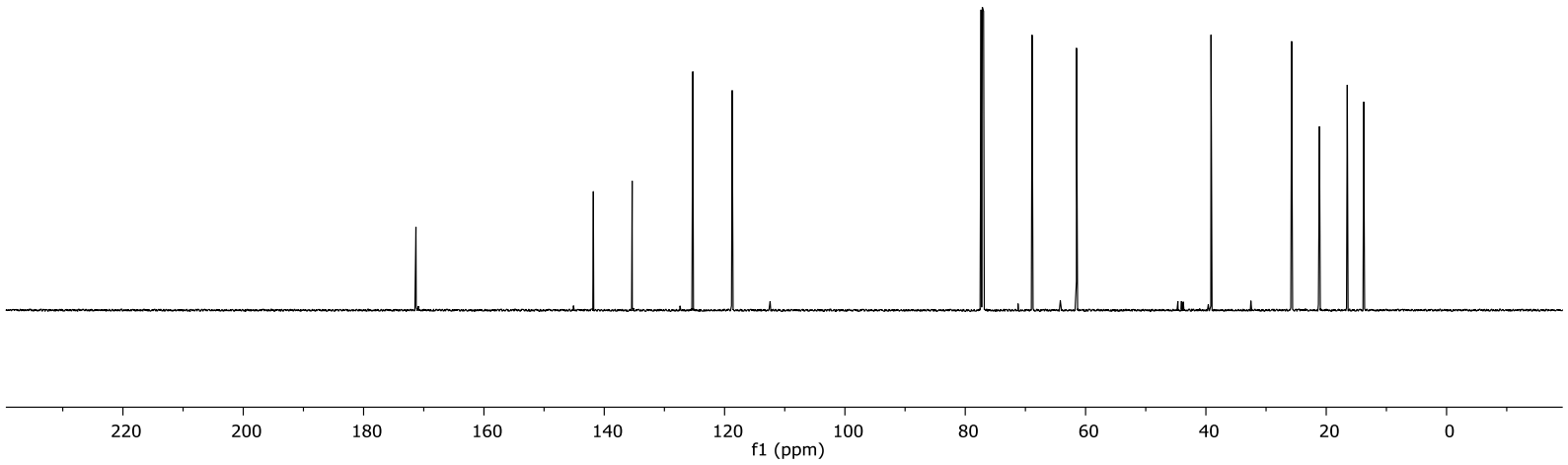

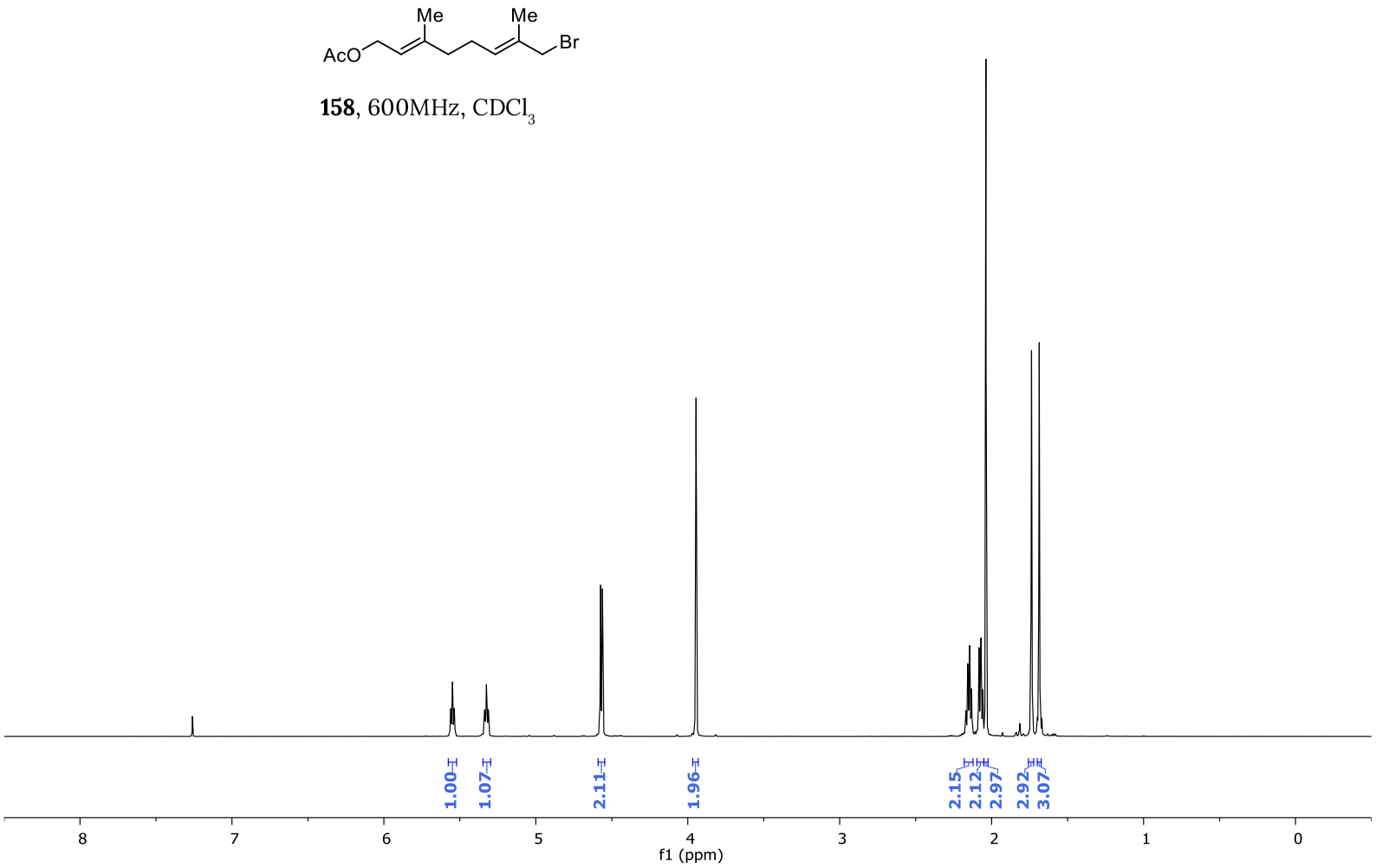
Me
Me
AcO
Br
158, 600MHz, CDCl3
1.00
1.07
2.11
1.96
2.15
2.12
2.97
2.92
3.07
8
7
6
5
4
3
2
1
0
f1 (ppm)

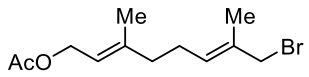

158, 150MHz, $CDCl_3$

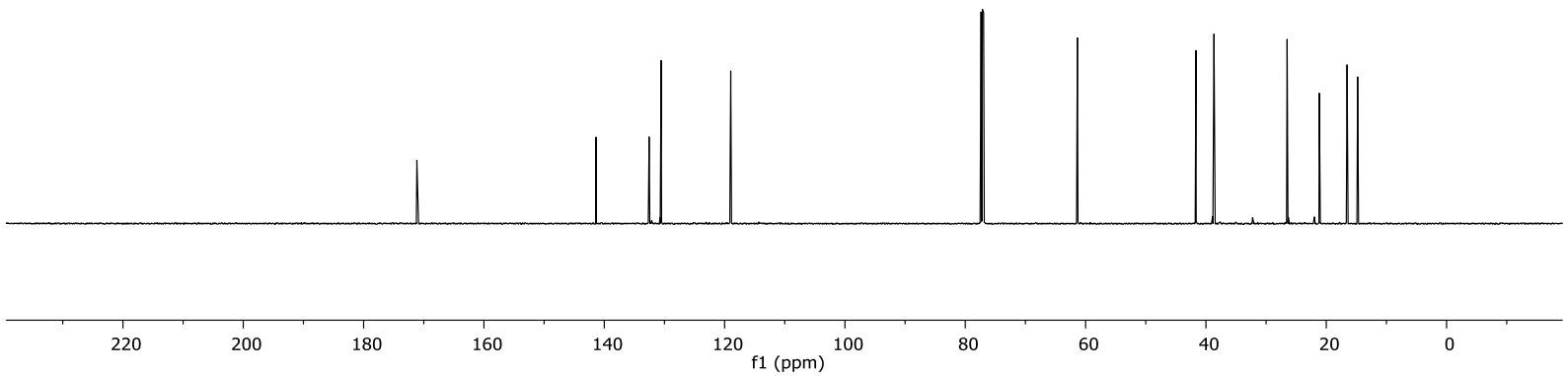

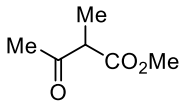

155, 600MHz, $CDCl_3$

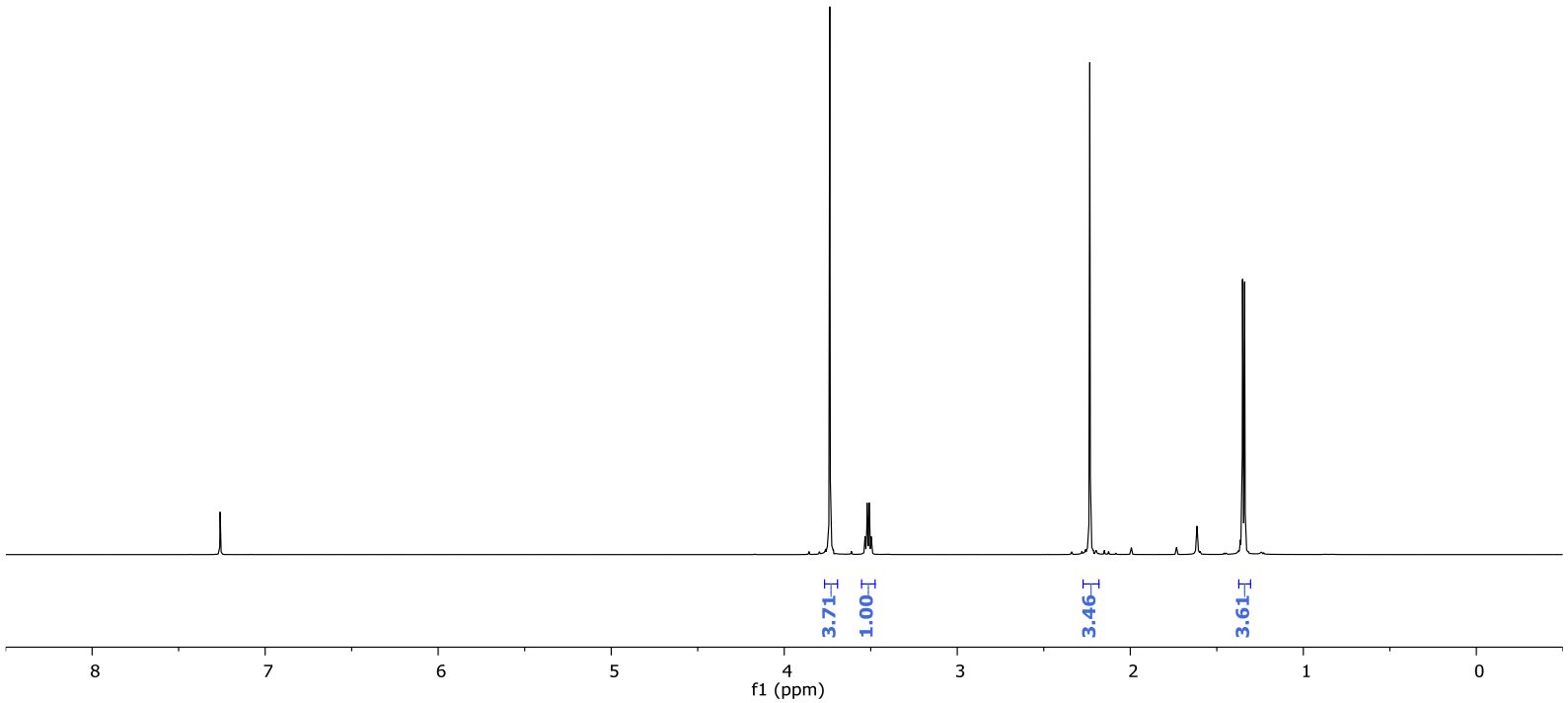

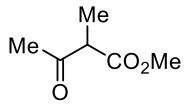

155, 150MHz, $CDCl_3$

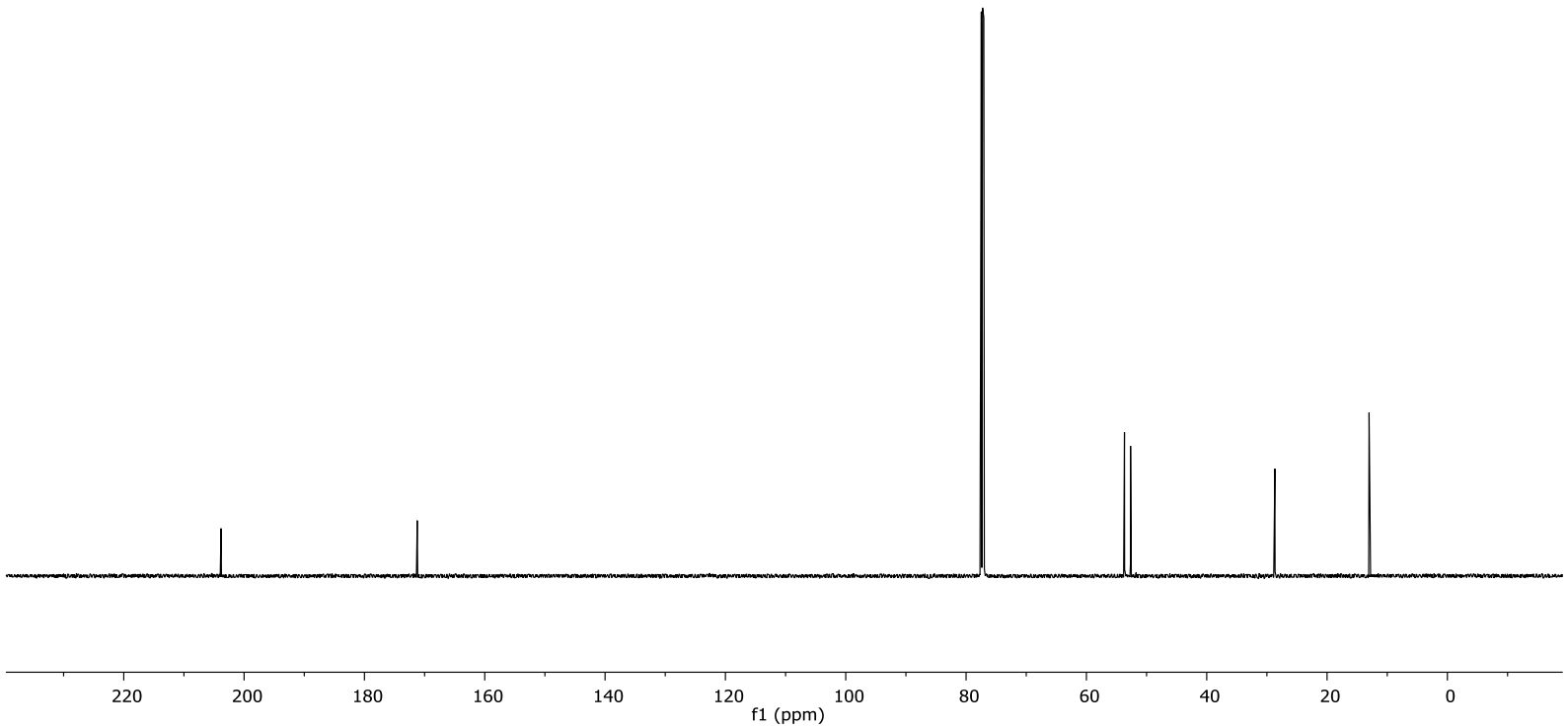

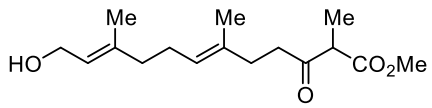

154, 600MHz, $CDCl_3$

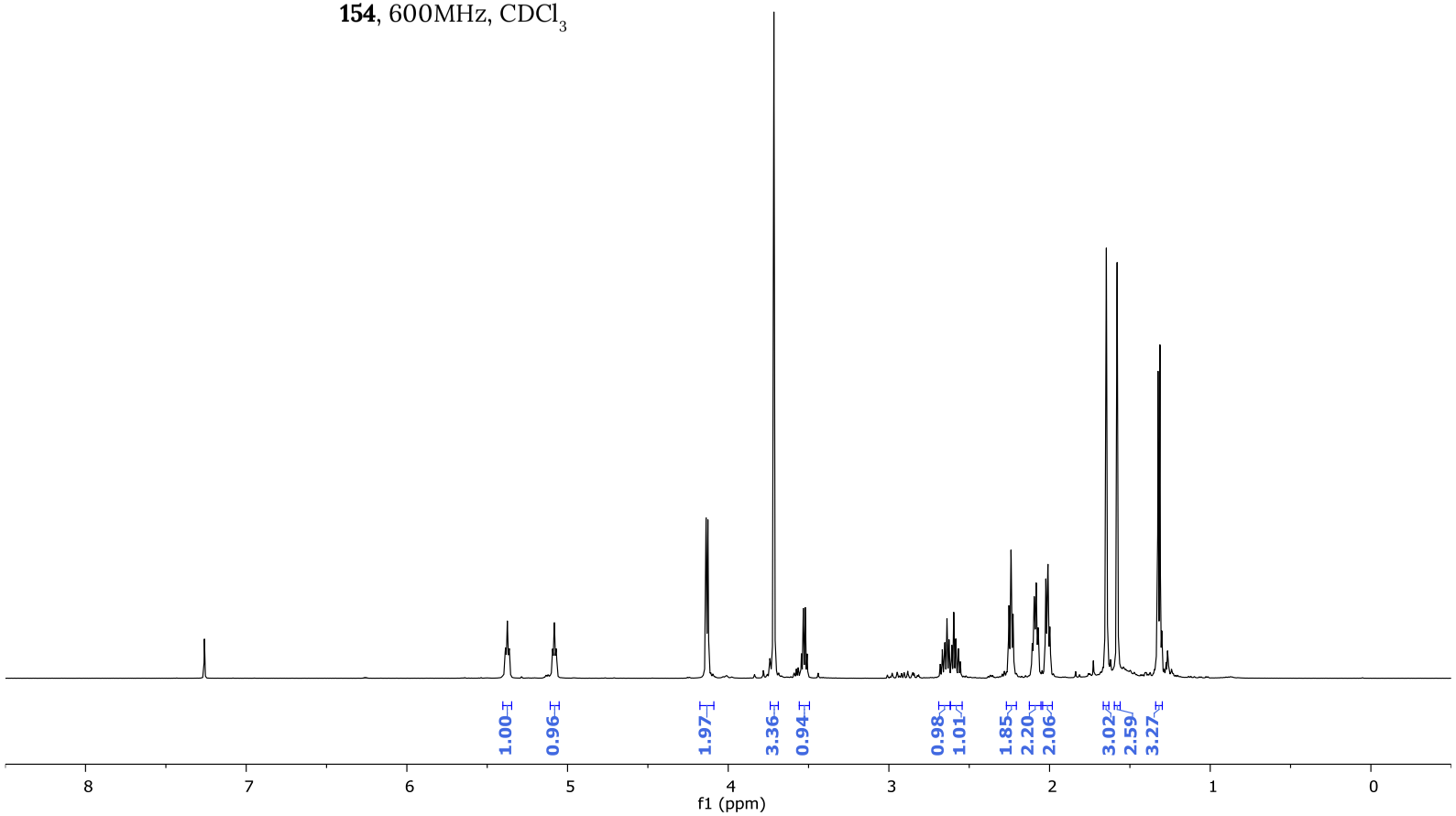

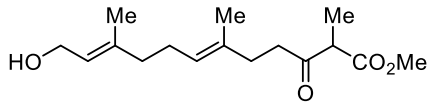

154, 150MHz, $CDCl_3$

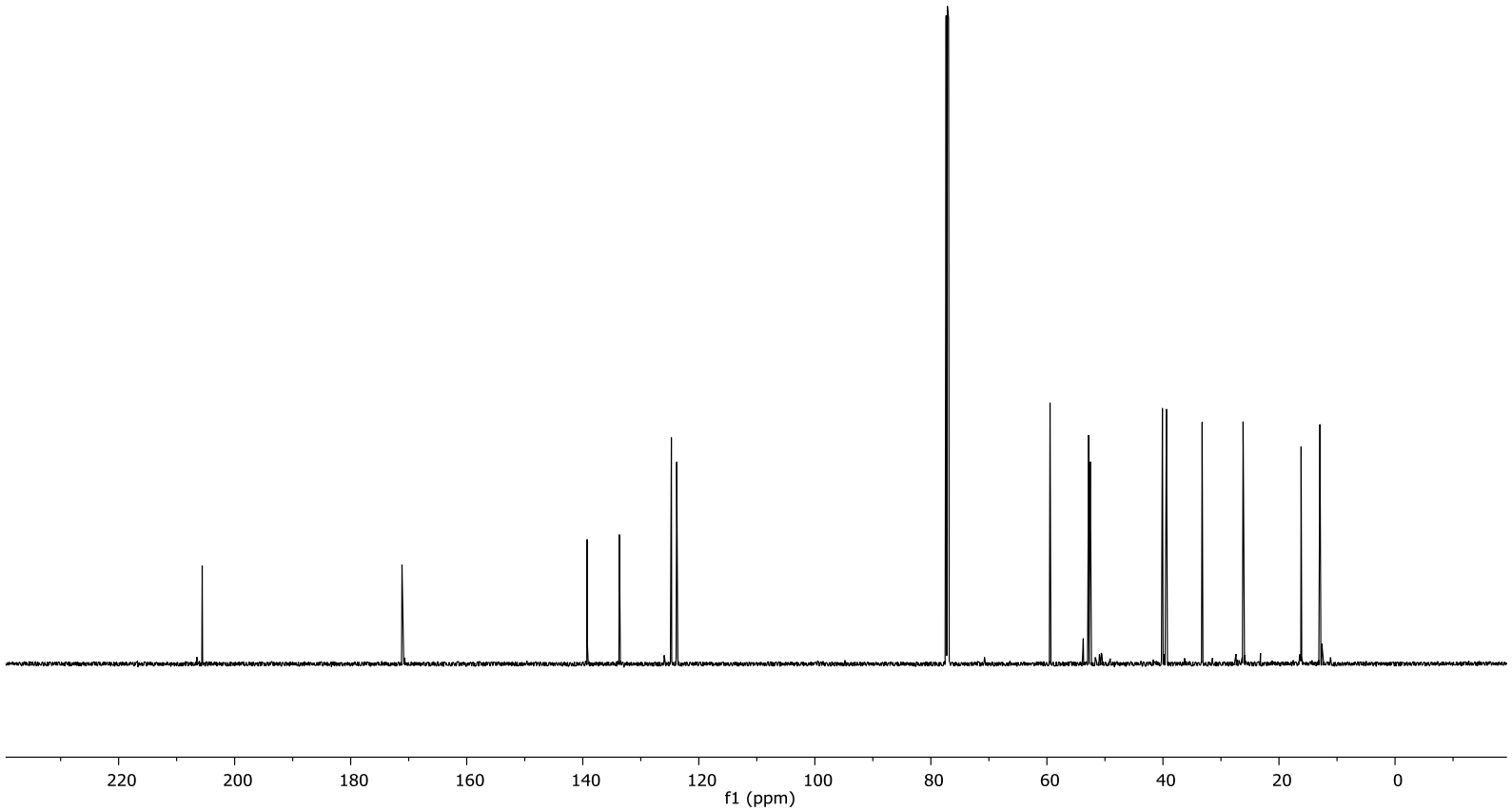

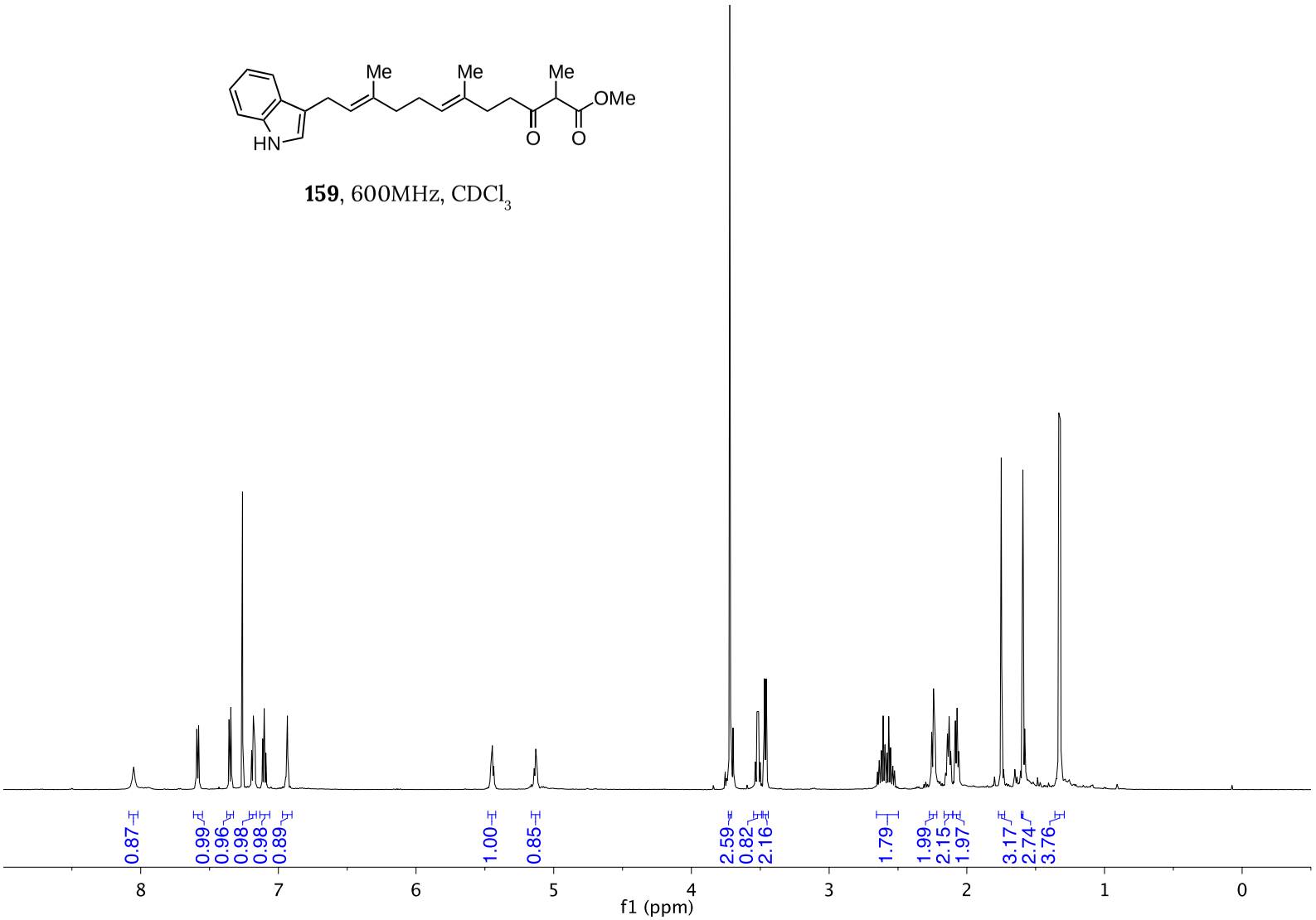

159, 600MHz, $CDCl_3$

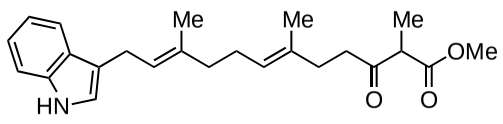

159, 150MHz, $CDCl_3$

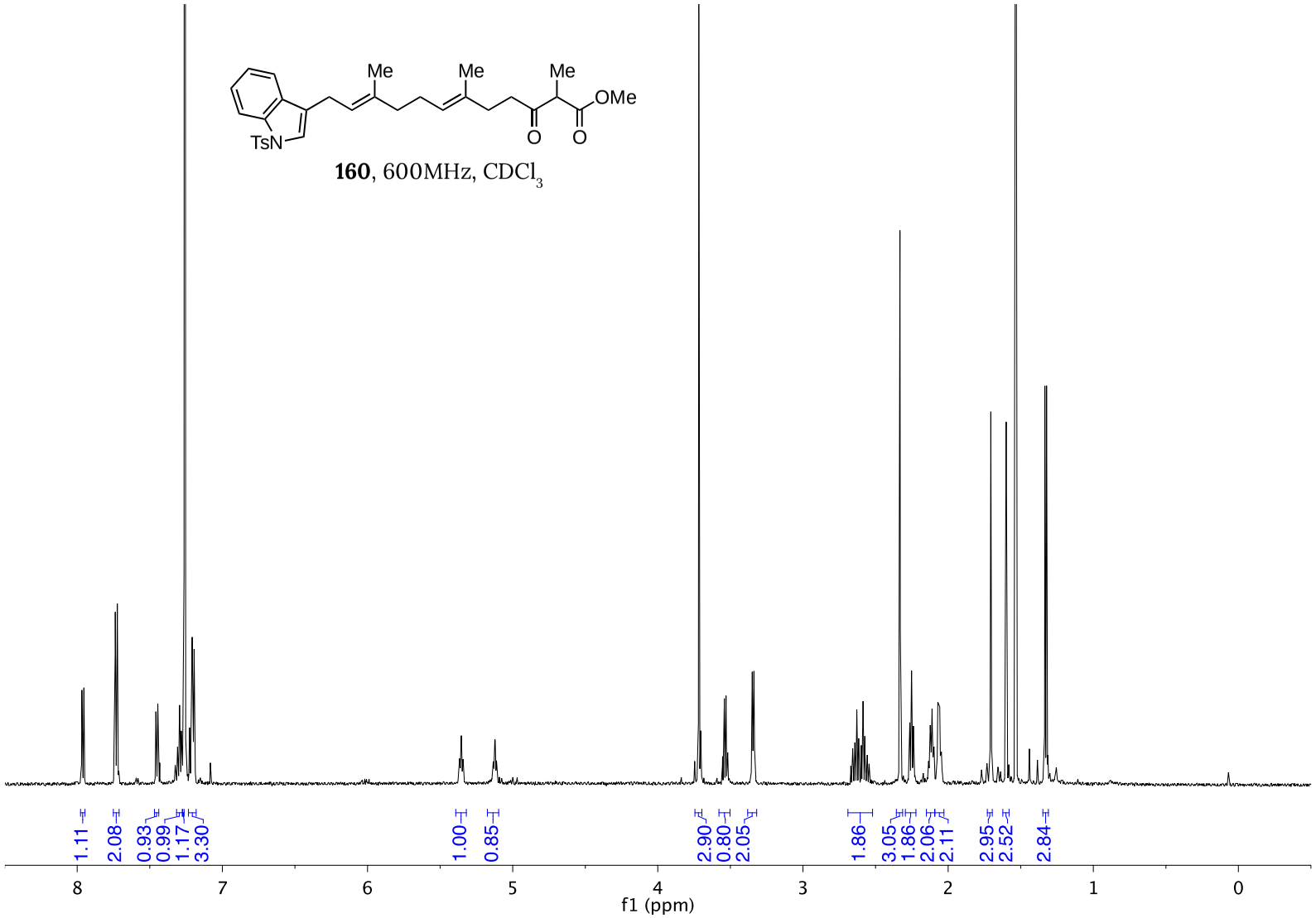
Me
Me
Me
OMe
TsN
O
O
160, 600MHz, CDCl3
1.11
2.08
0.93
0.99
1.17
3.30
1.00
0.85
2.90
0.80
2.05
1.86
3.05
1.86
2.06
2.11
2.95
2.52
2.84
8
7
6
5
4
3
2
1
0
f1 (ppm)

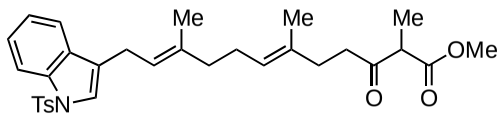

160, 150MHz, $CDCl_3$

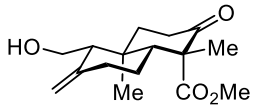

162, 600MHz, $CDCl_3$

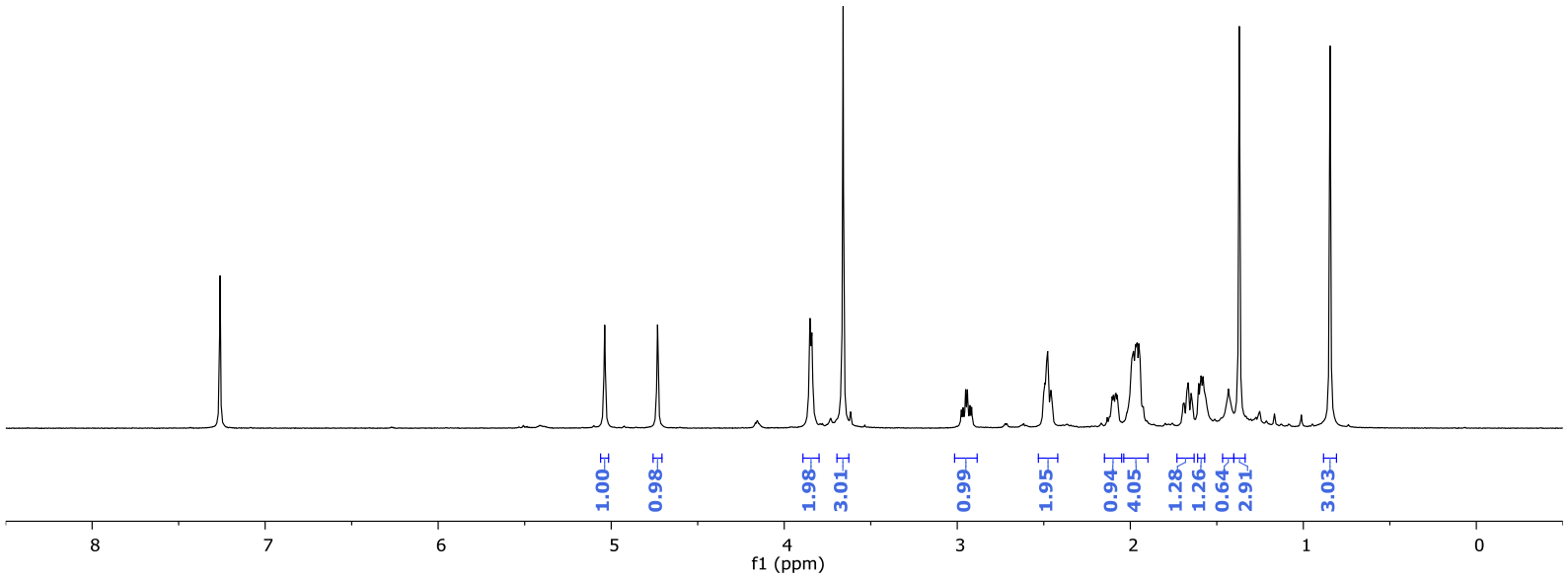

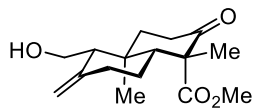

162, 150MHz, $CDCl_3$

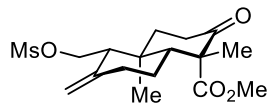

A1, 600MHz, $CDCl_3$

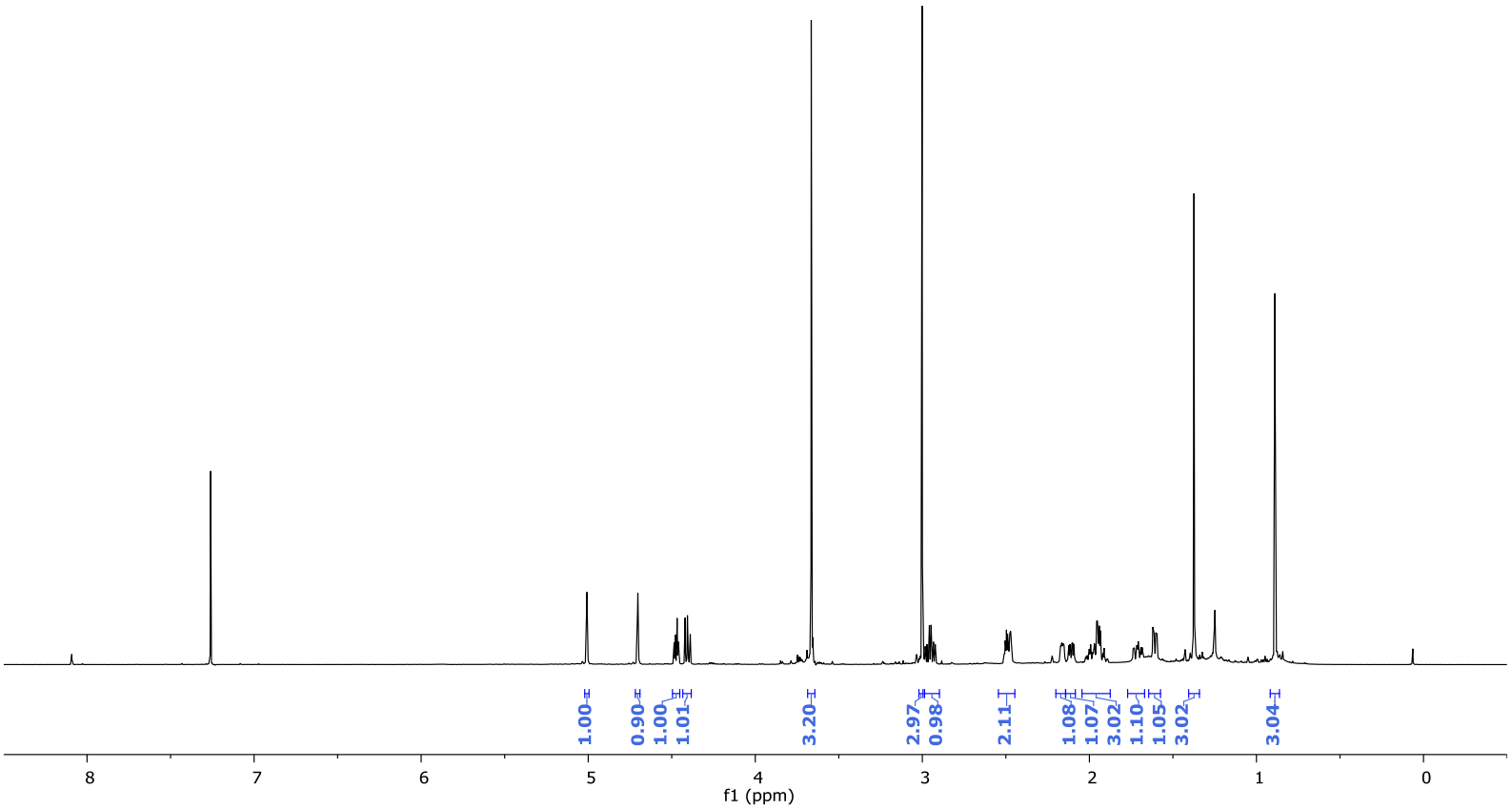

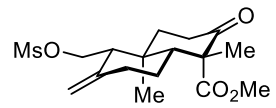

A1, 150MHz, $CDCl_3$

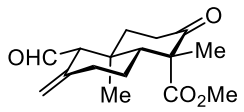

169, 600MHz, $CDCl_3$

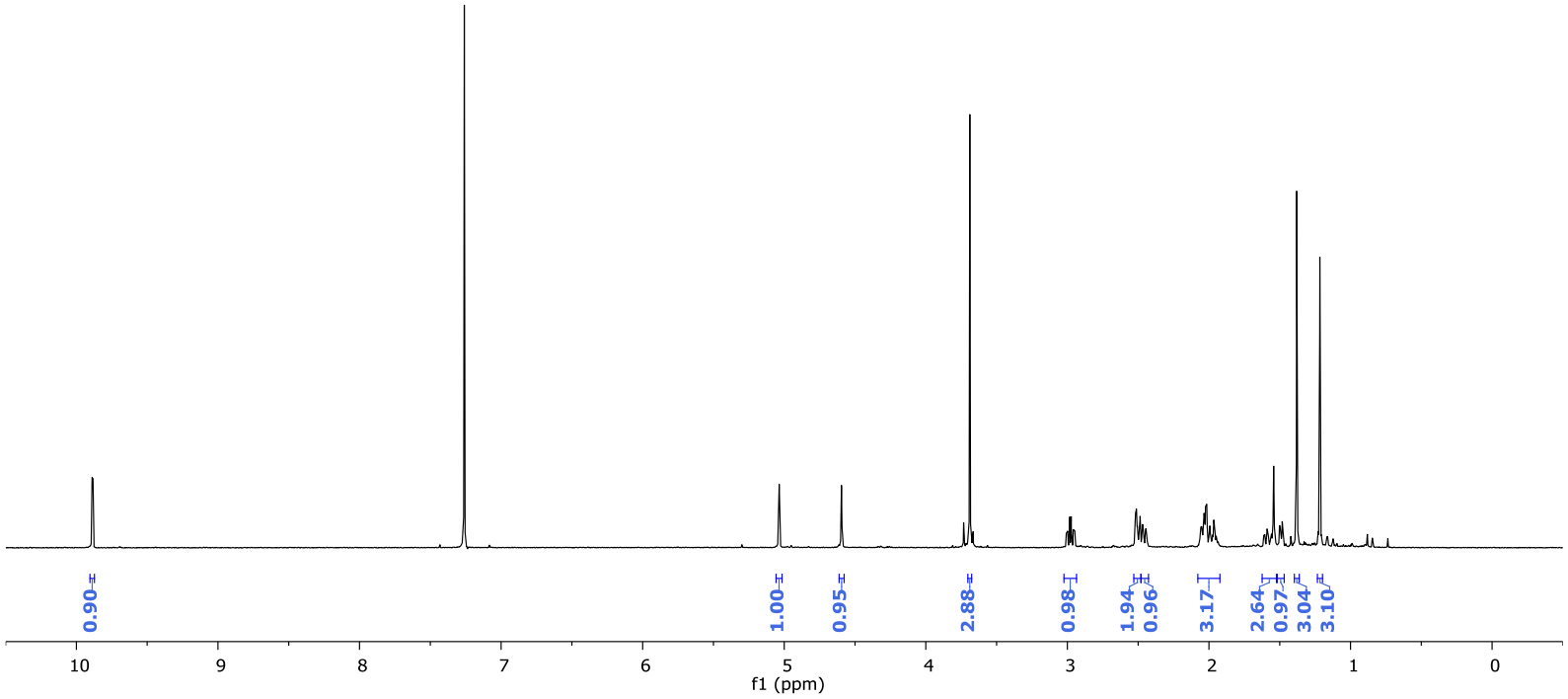

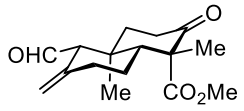

169, 150MHz, $CDCl_3$

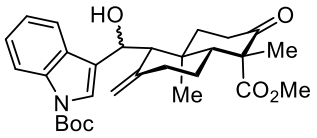

171, 600MHz, $CDCl_3$

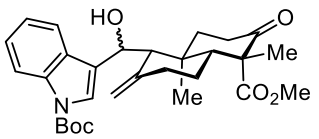

171, 150MHz, $CDCl_3$

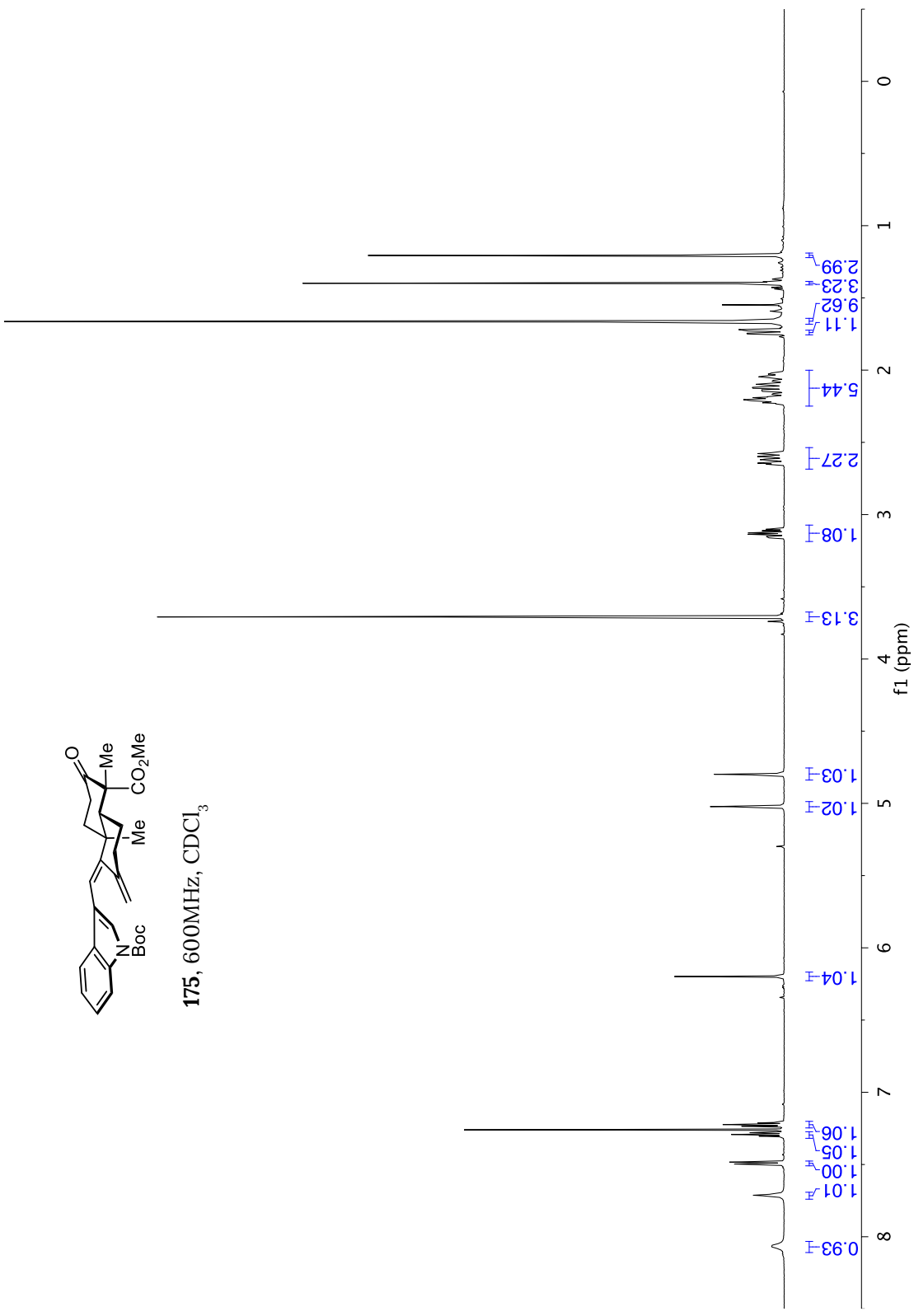

175, 600MHz, $CDCl_3$

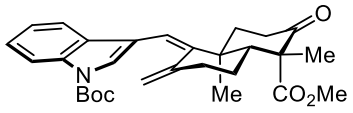

175, 150MHz, $CDCl_3$

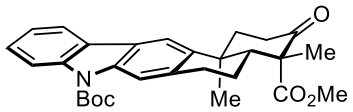

176, 600MHz, $CDCl_3$

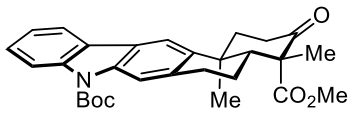

176, 150MHz, $CDCl_3$

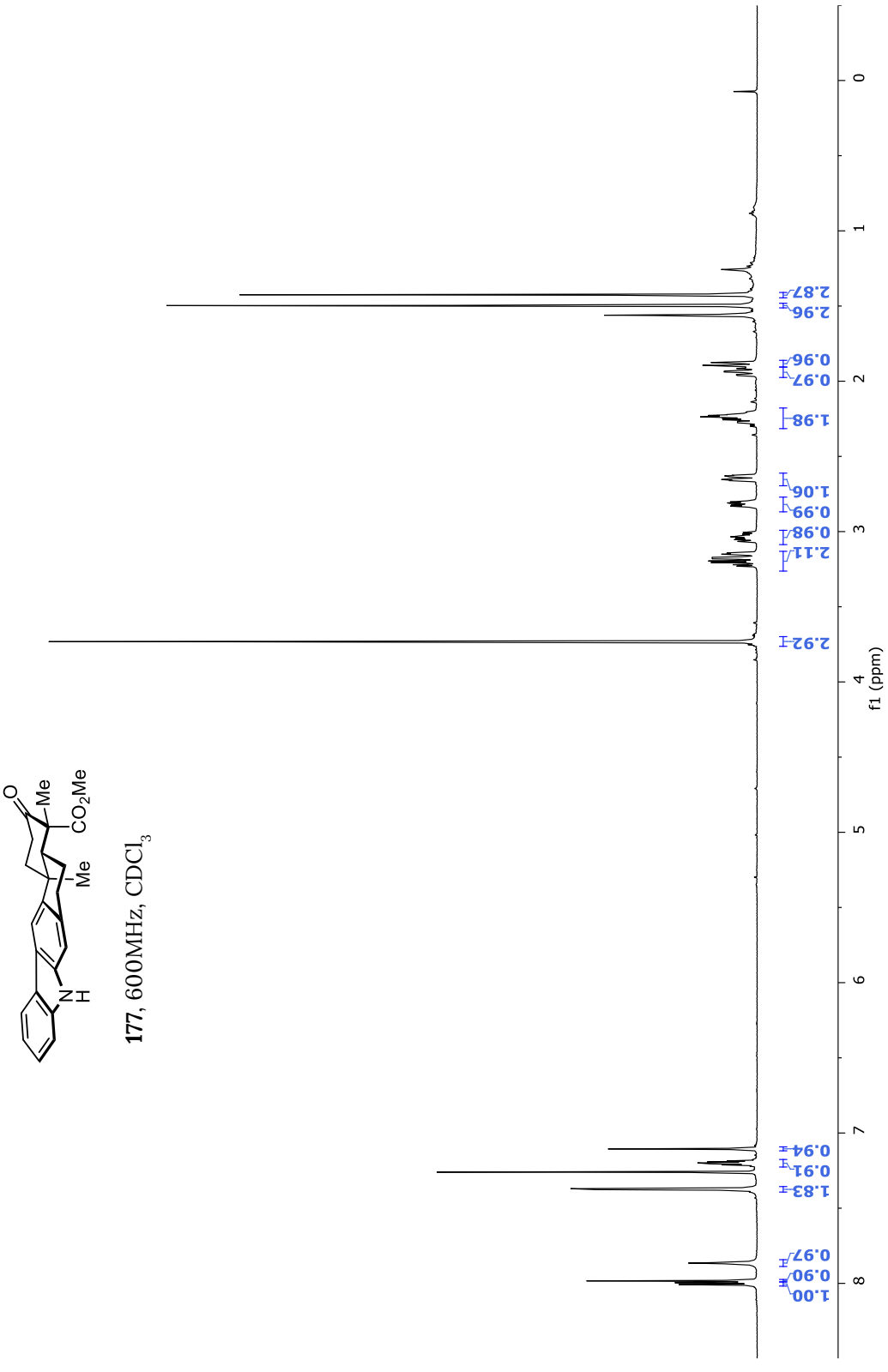

177, 600MHz, $CDCl_3$

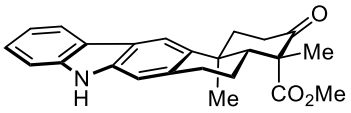

177, 150MHz, $CDCl_3$

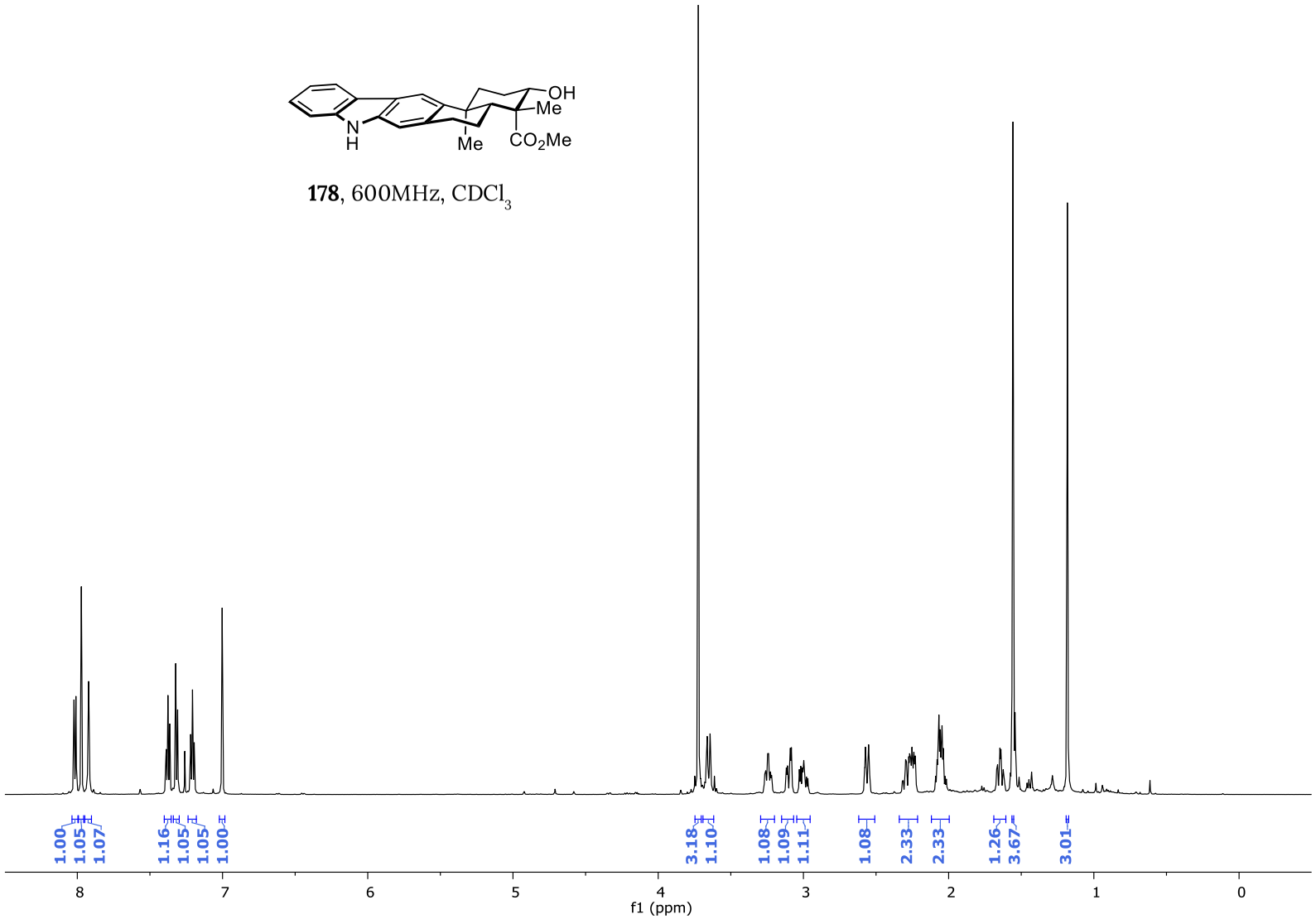
OH
Me
N
H
Me
CO2Me
178, 600MHz, CDCl3
1.00
1.05
1.07
1.16
1.05
1.05
1.00
3.18
1.10
1.08
1.09
1.11
1.08
2.33
2.33
1.26
3.67
3.01
8
7
6
5
4
3
2
1
0
f1 (ppm)

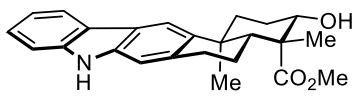

178, 150MHz, $CDCl_3$

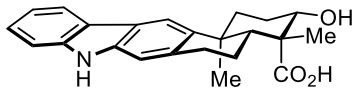

Oridamycin A (**26**), 600MHz, CD_3OD

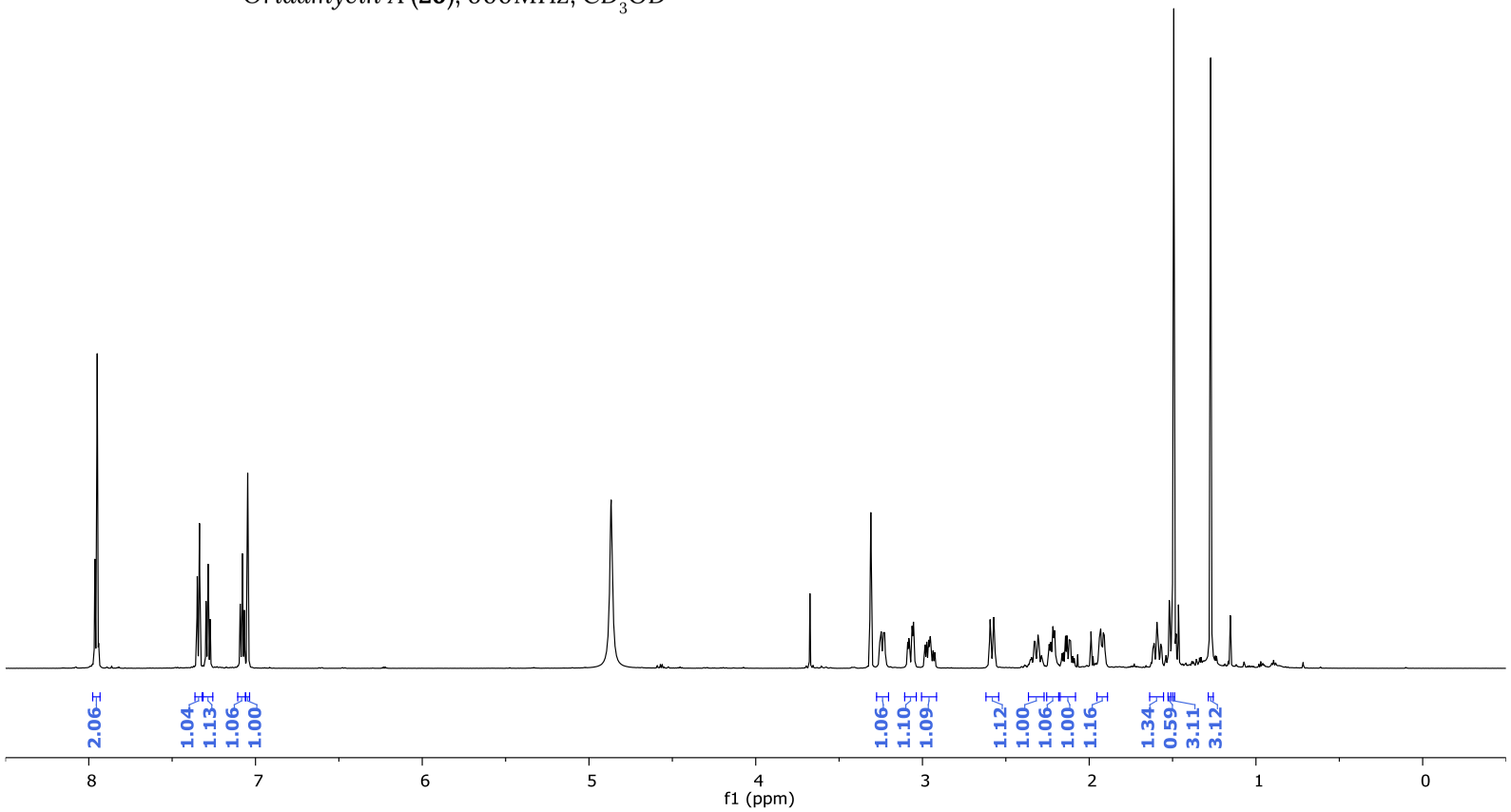

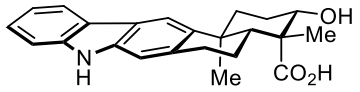

Oridamycin A (**26**), 150MHz, CD_3OD

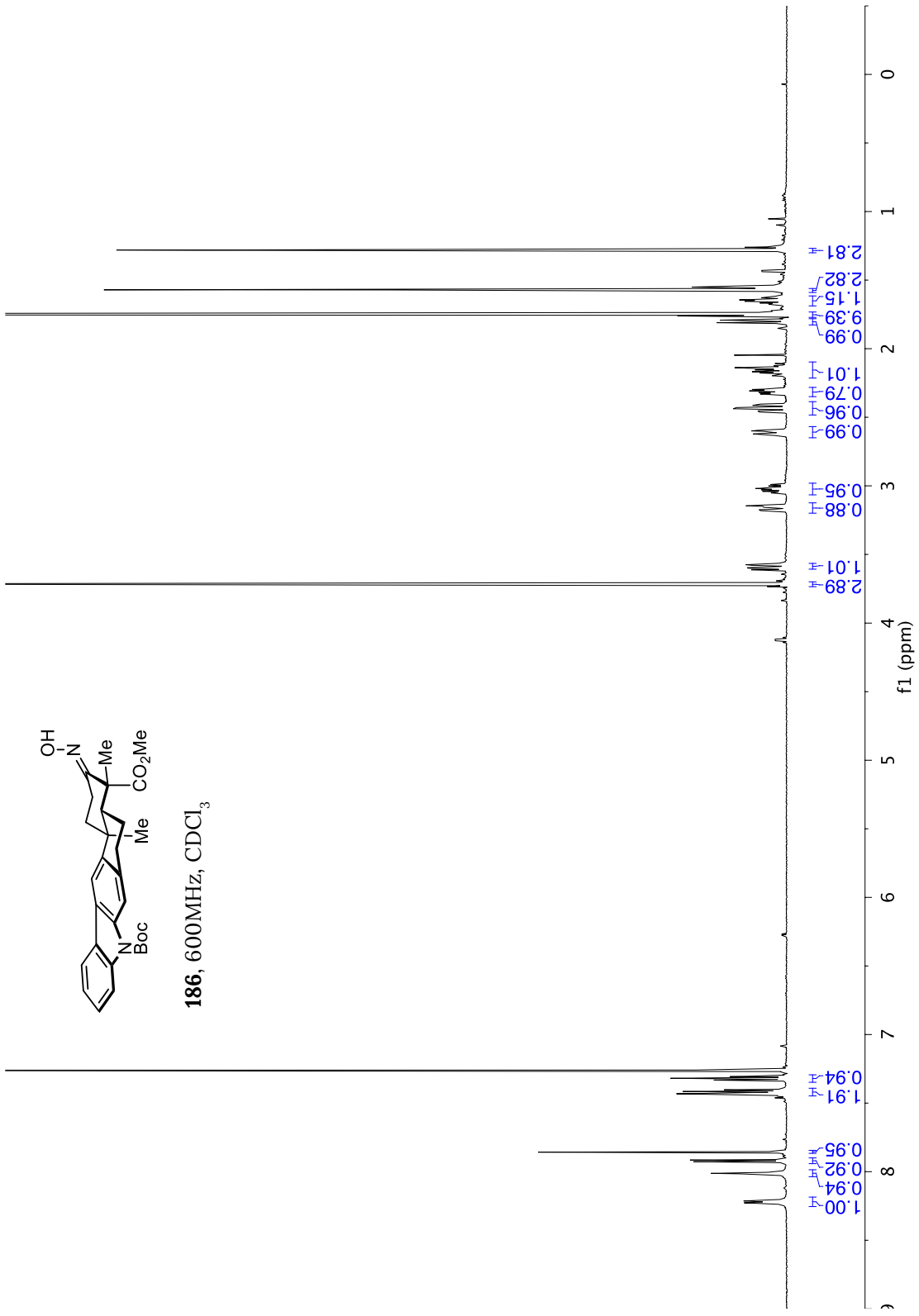
OH
N
Me
CO2Me
Me
N
Boc
186, 600MHz, CDCl3
2.81
2.82
1.15
9.39
0.99
1.01
0.79
0.96
0.99
0.95
0.88
1.01
2.89
1.00
0.94
0.92
0.95
1.91
0.94
f1 (ppm)

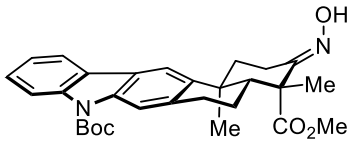

186, 150MHz, $CDCl_3$

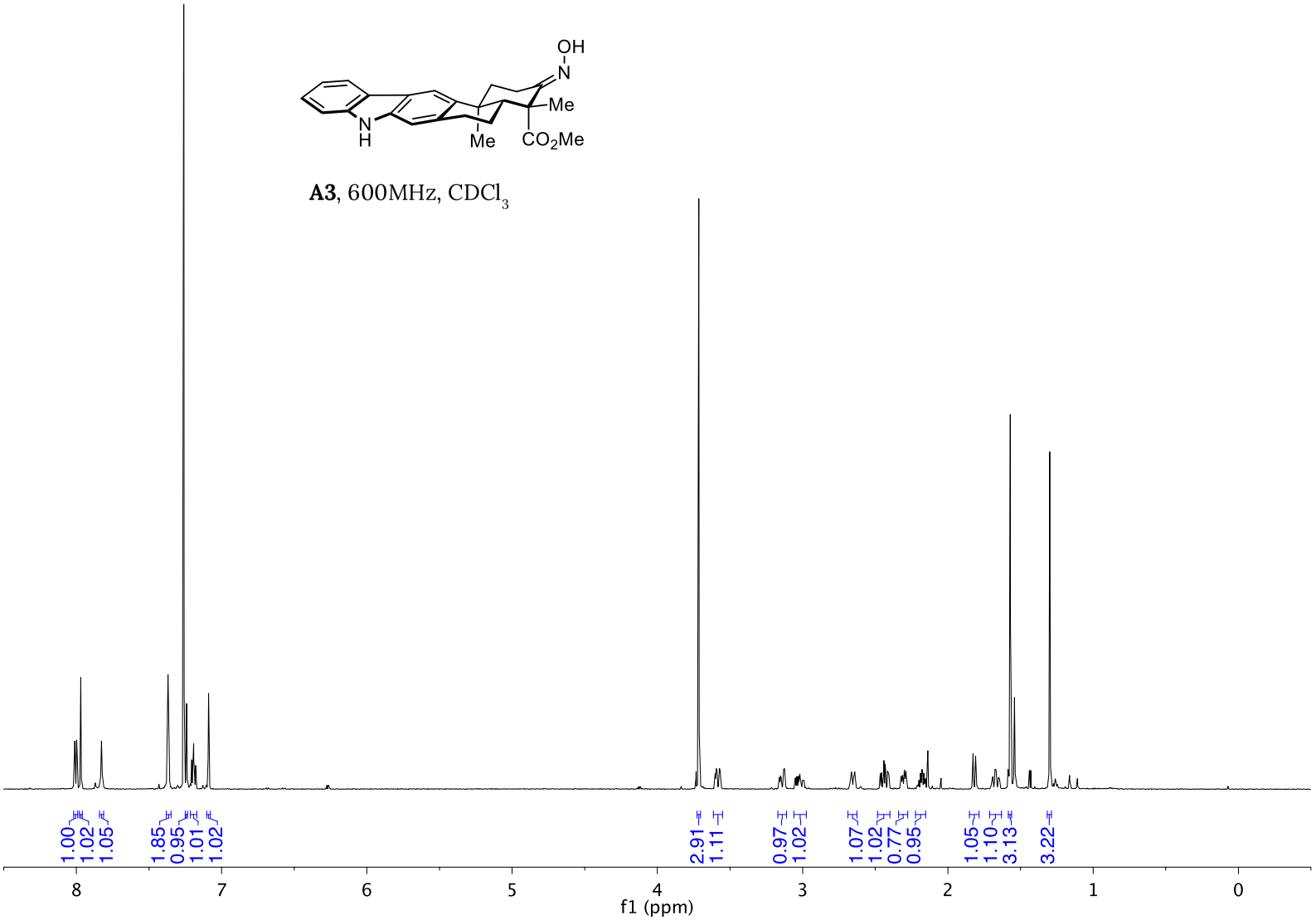

A3, 600MHz, $CDCl_3$

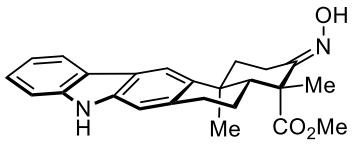

A3, 150MHz, $CDCl_3$

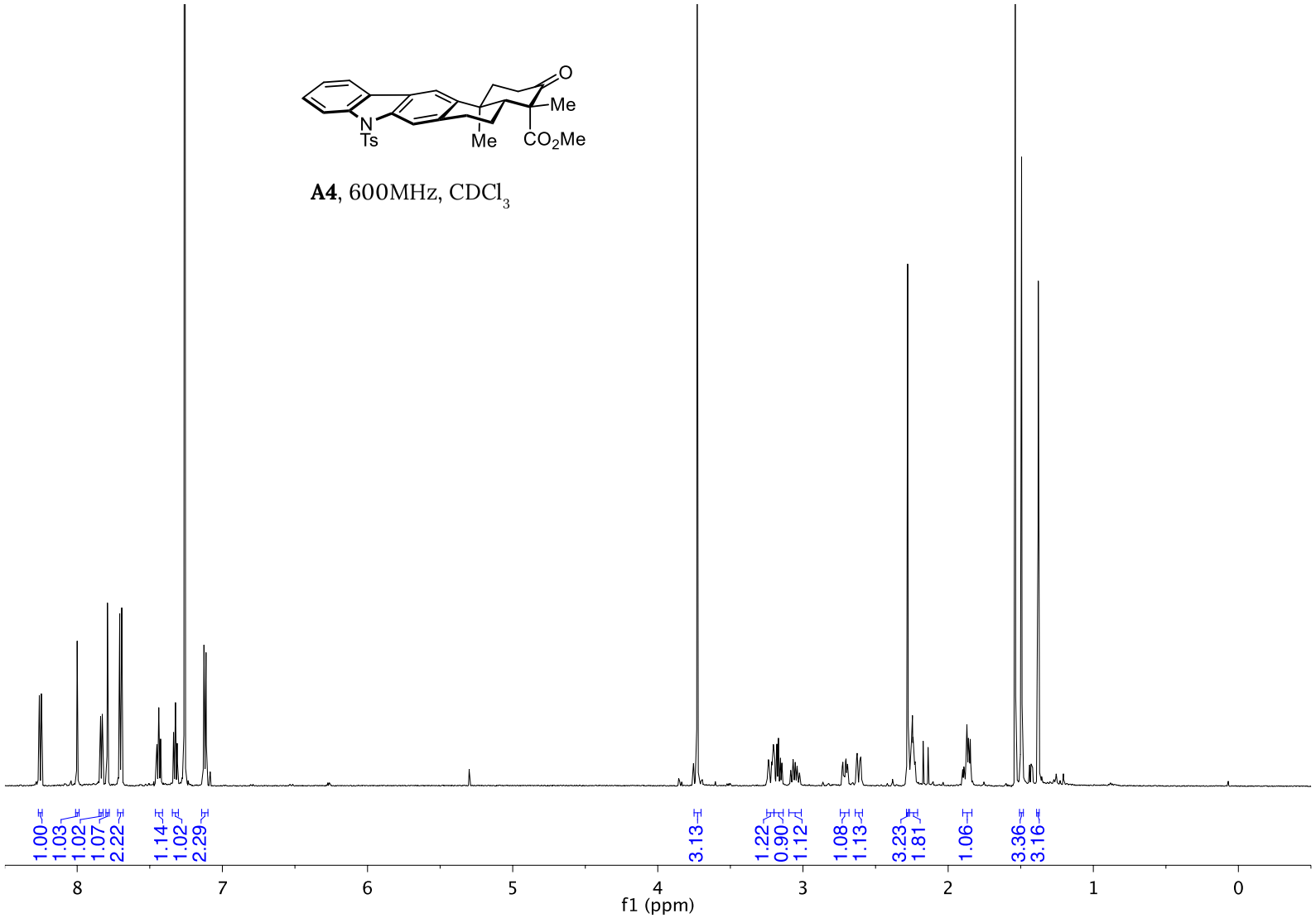
O
Me
N
Ts
Me
CO2Me
A4, 600MHz, CDCl3
1.00
1.03
1.02
1.07
2.22
1.14
1.02
2.29
3.13
1.22
0.90
1.12
1.08
1.13
3.23
1.81
1.06
3.36
3.16
8
7
6
5
4
3
2
1
0
f1 (ppm)

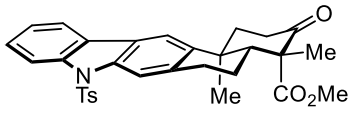

A4, 150MHz, $CDCl_3$

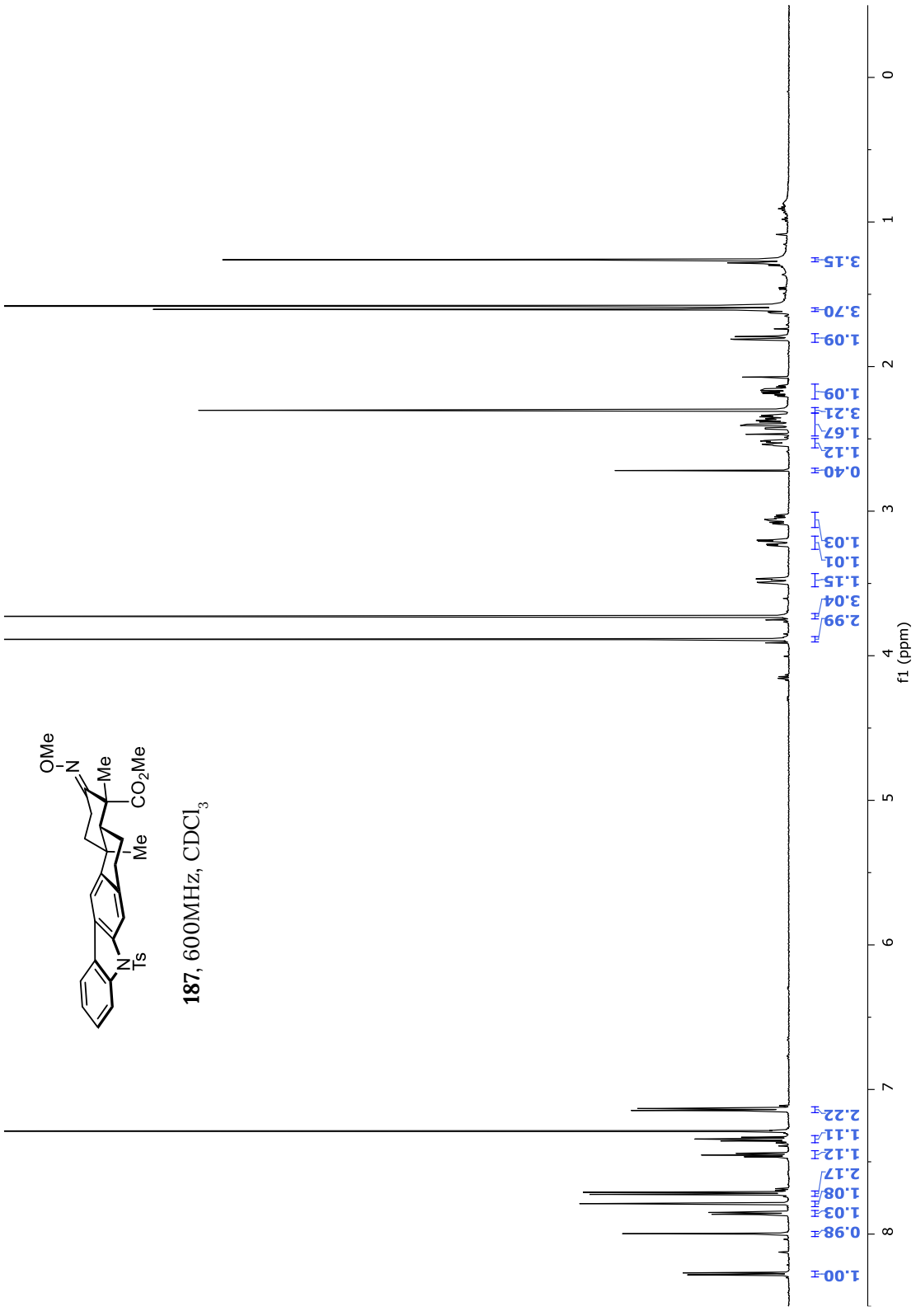
OMe
N
Me
CO2Me
Me
N
Ts
187, 600MHz, CDCl3
1.00
0.98
1.03
1.08
2.17
1.12
1.11
2.22
2.99
3.04
1.15
1.01
1.03
0.40
1.12
1.67
3.21
1.09
1.09
3.70
3.15
f1 (ppm)

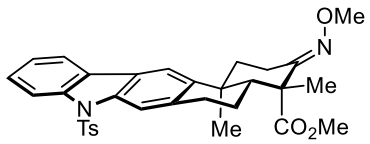

187, 150MHz, $CDCl_3$

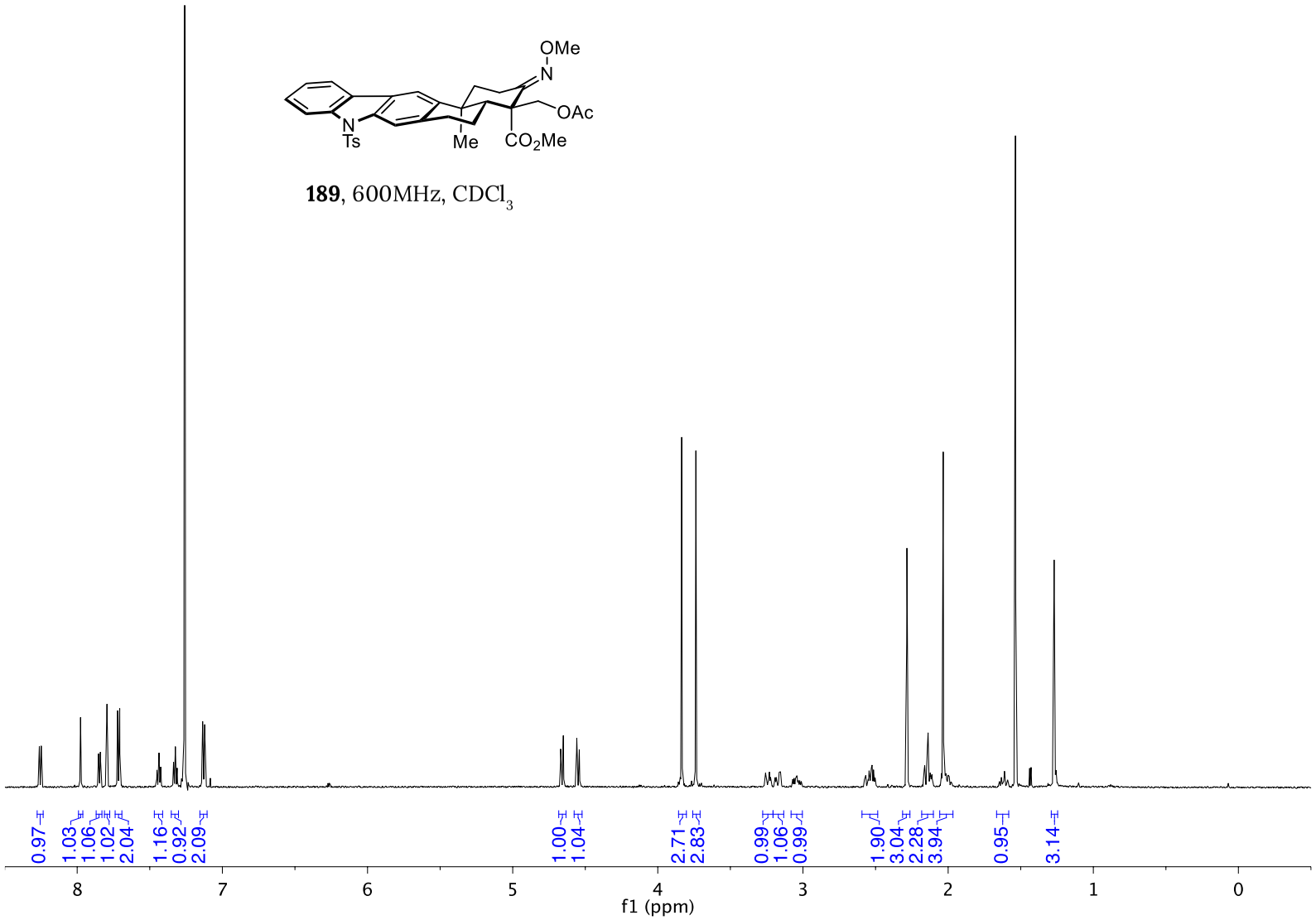
OMe
N
OAc
N
Ts
Me
CO2Me
189, 600MHz, CDCl3
0.97
1.03
1.06
1.02
2.04
1.16
0.92
2.09
1.00
1.04
2.71
2.83
0.99
1.06
0.99
1.90
3.04
2.28
3.94
0.95
3.14
8
7
6
5
4
3
2
1
0
f1 (ppm)

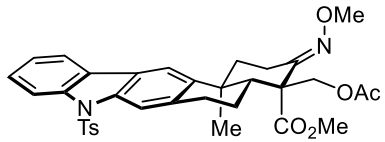

189, 150MHz, $CDCl_3$

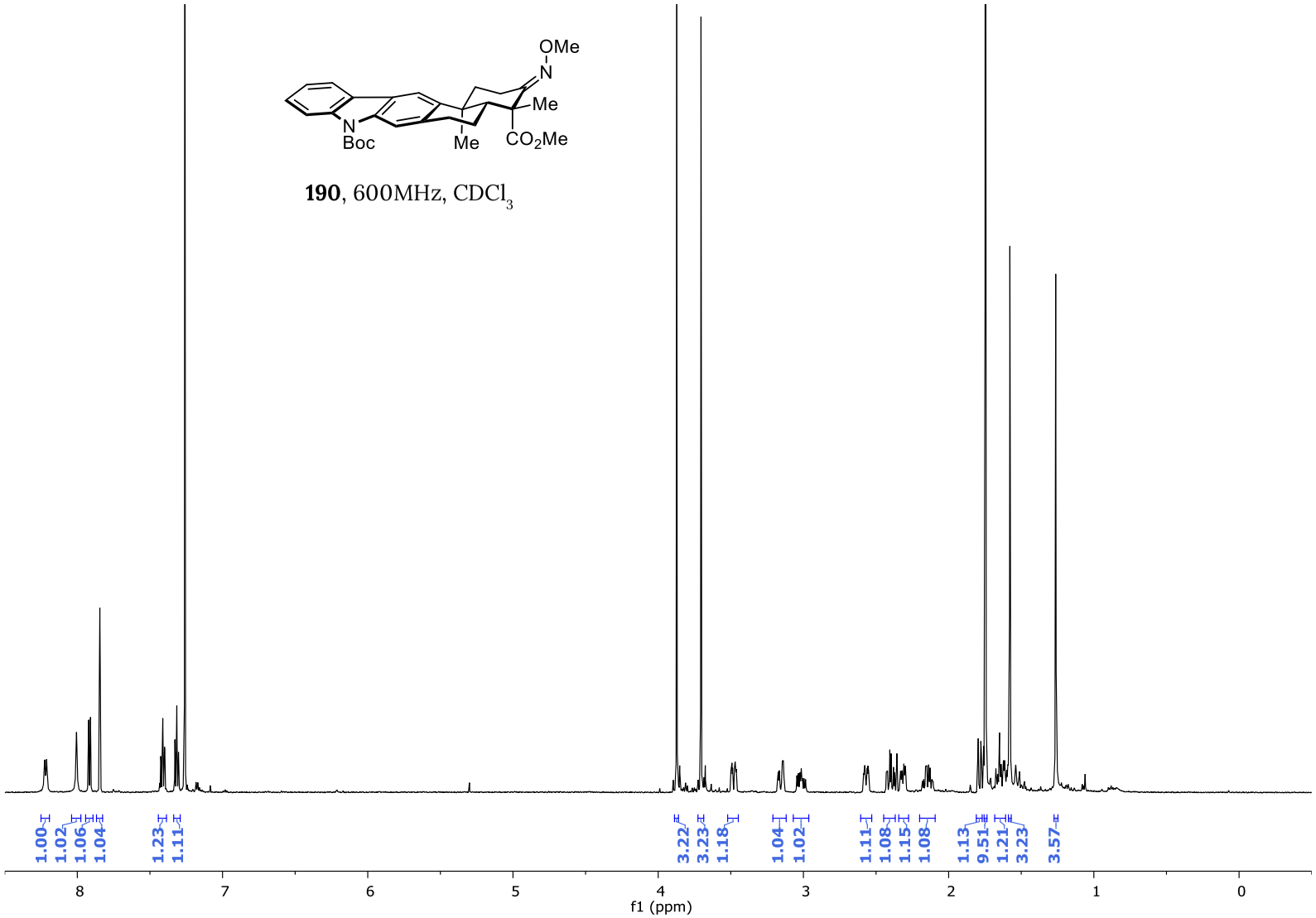
OMe
N
Me
N
Boc
Me
CO2Me
190, 600MHz, CDCl3
1.00
1.02
1.06
1.04
1.23
1.11
3.22
3.23
1.18
1.04
1.02
1.11
1.08
1.15
1.08
1.13
9.51
1.21
3.23
3.57
8
7
6
5
4
3
2
1
0
f1 (ppm)

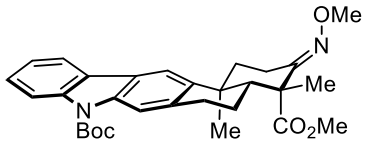

190, 150MHz, $CDCl_3$

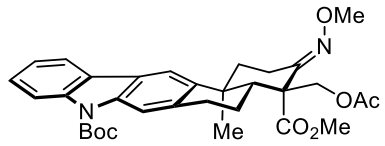

192, 600MHz, $CDCl_3$

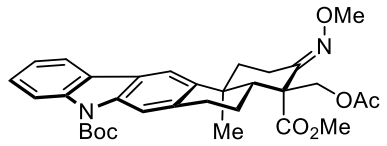

192, 150MHz, $CDCl_3$

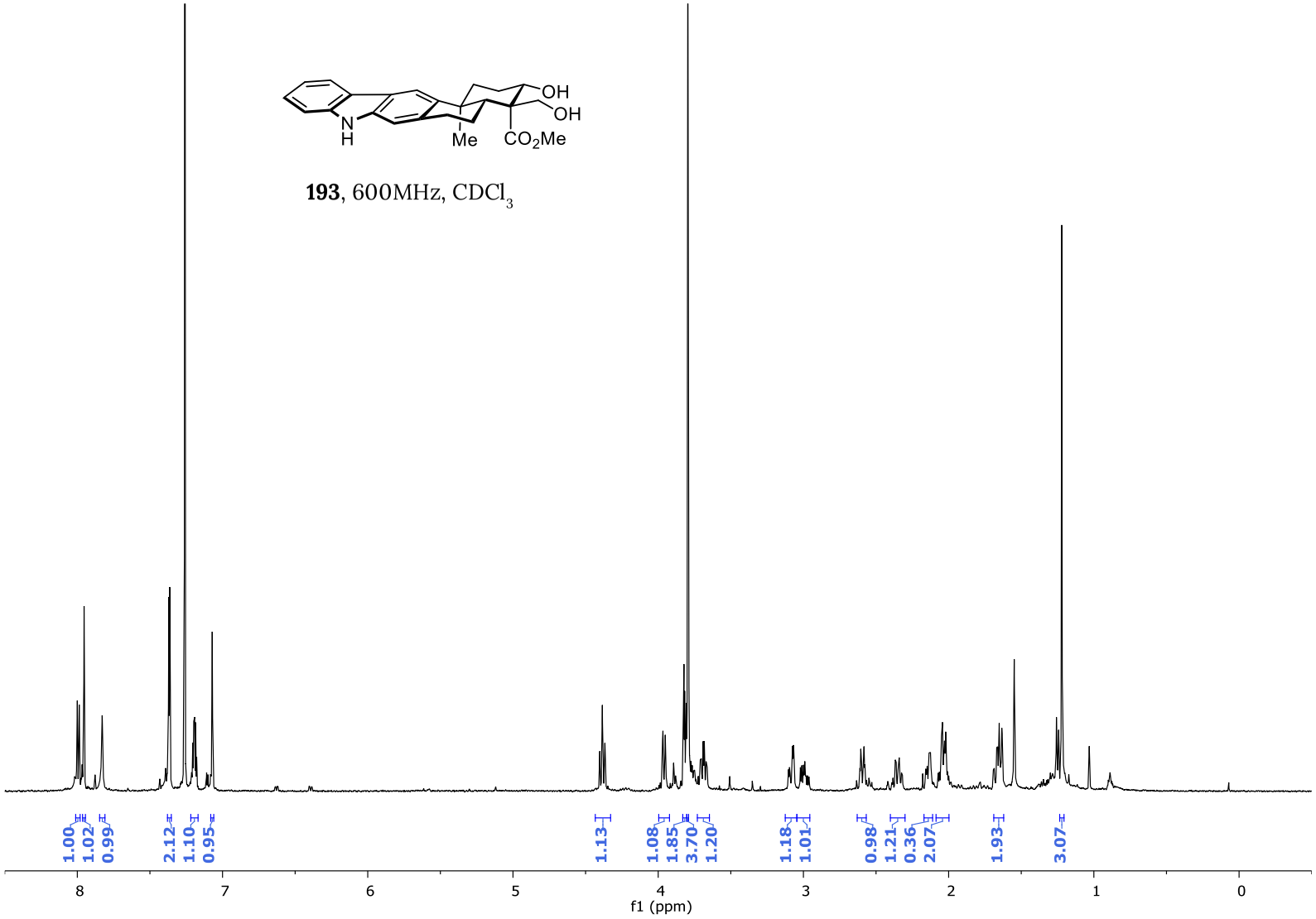
OH
OH
N
H
Me
CO2Me
193, 600MHz, CDCl3
1.00
1.02
0.99
2.12
1.10
0.95
1.13
1.08
1.85
3.70
1.20
1.18
1.01
0.98
1.21
0.36
2.07
1.93
3.07
8
7
6
5
4
3
2
1
0
f1 (ppm)

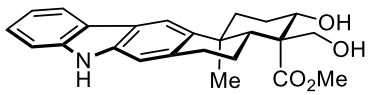

193, 150MHz, $CDCl_3$

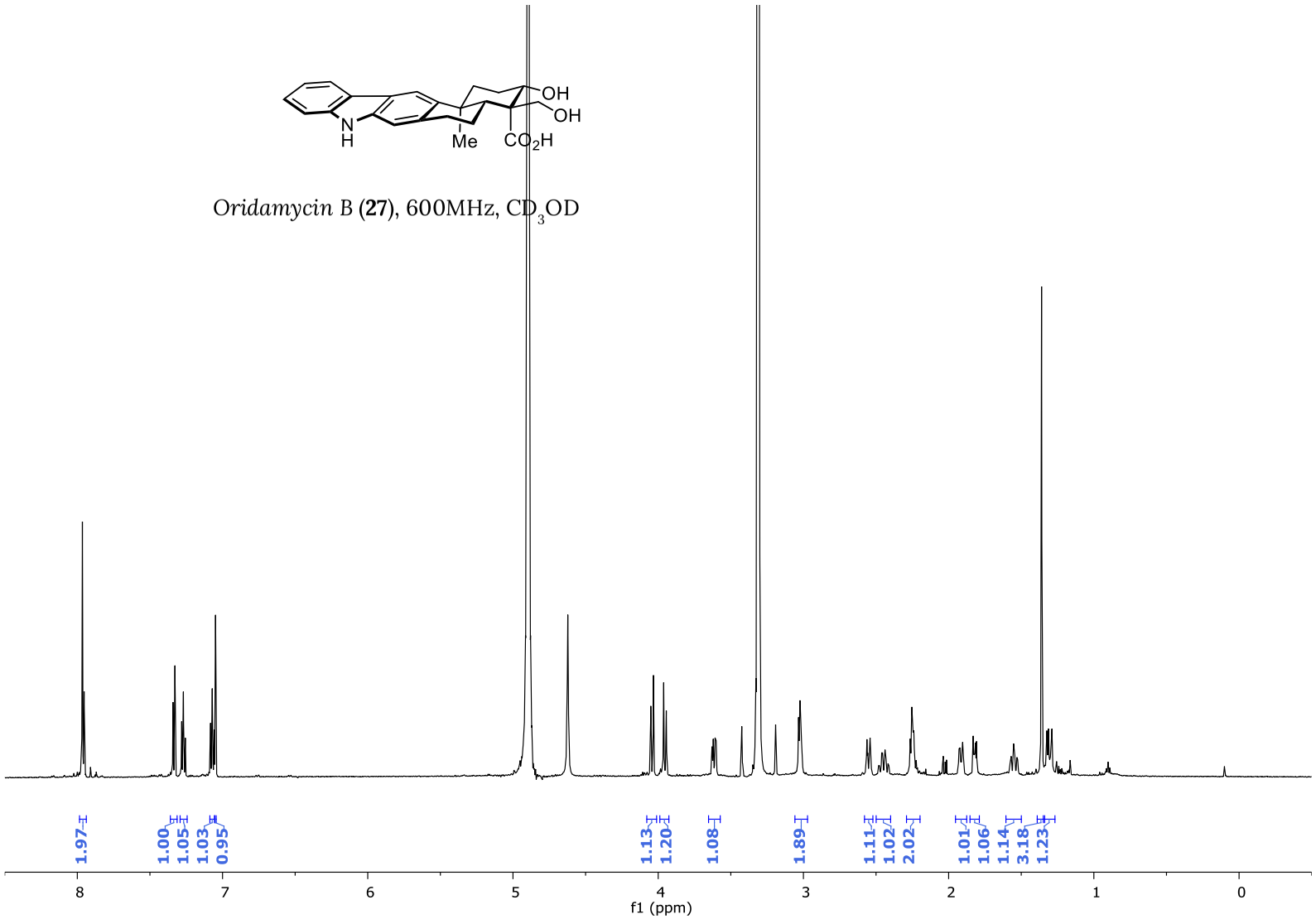

Oridamycin B (**27**), 600MHz, CD_3OD

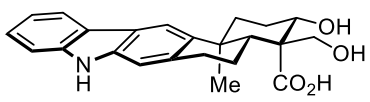

Oridamycin B (**27**), 150MHz, CD_3OD

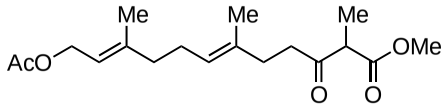

237, 600MHz, $CDCl_3$

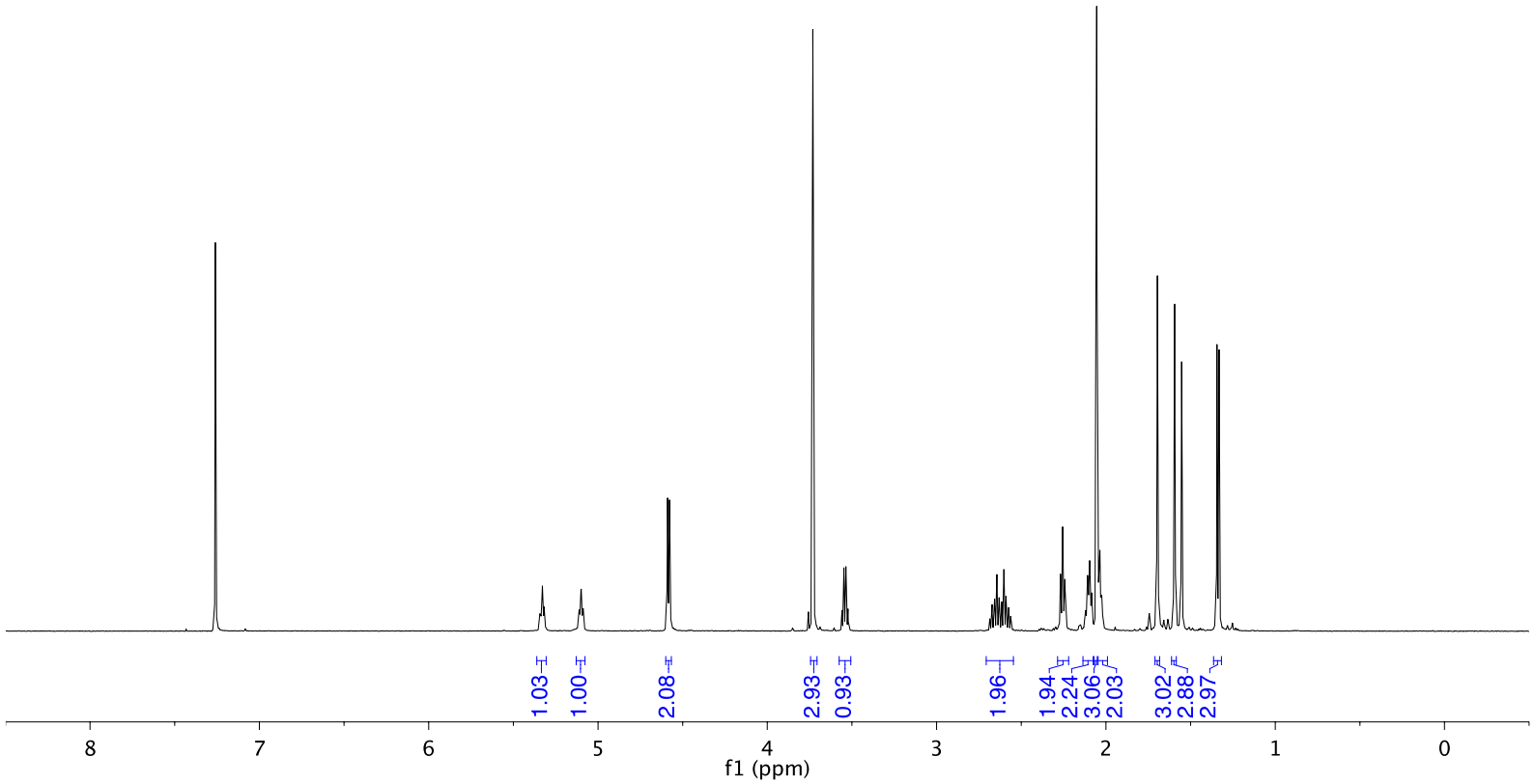

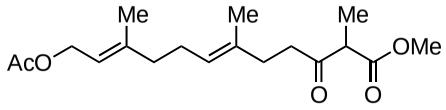

237, 150MHz, $CDCl_3$

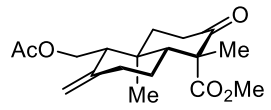

A5, 600MHz, $CDCl_3$

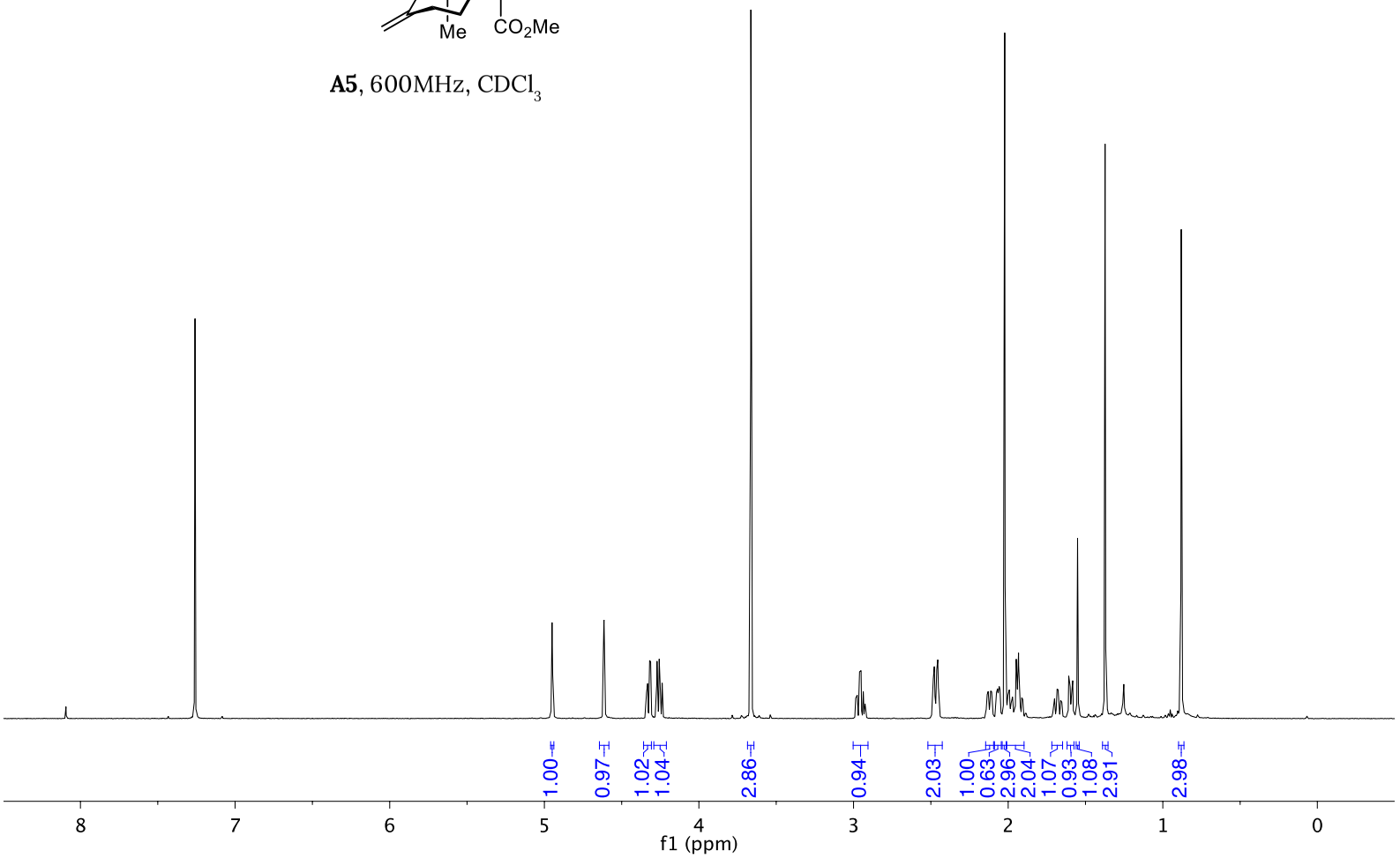

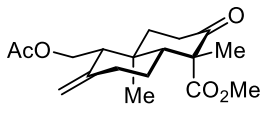

A5, 150MHz, $CDCl_3$

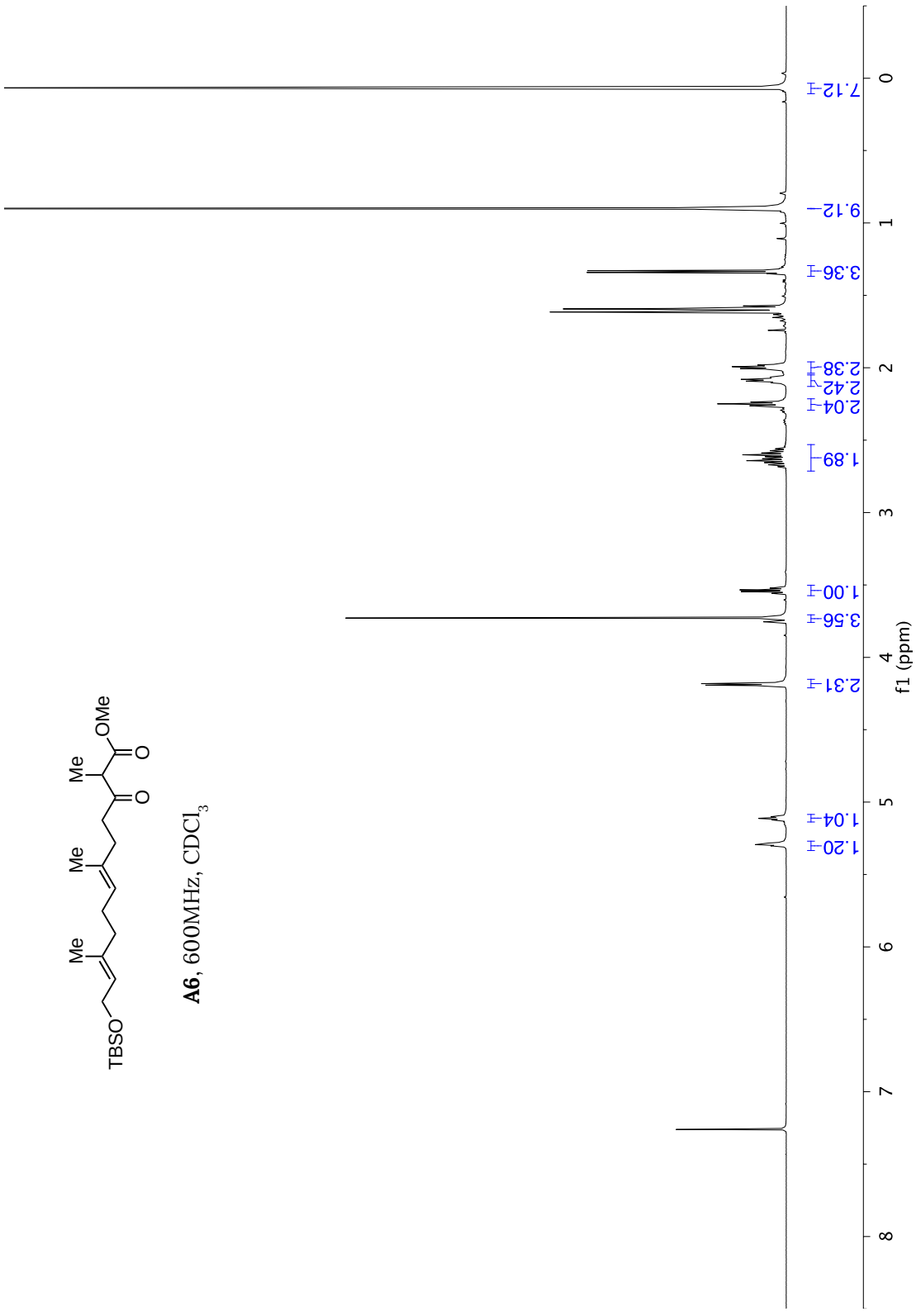
TBSO
Me
Me
Me
O
O
OMe
A6, 600MHz, CDCl3
7.12
9.12
3.36
2.38
2.42
2.04
1.89
1.00
3.56
2.31
1.04
1.20
f1 (ppm)

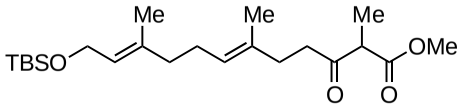

A6, 150MHz, $CDCl_3$

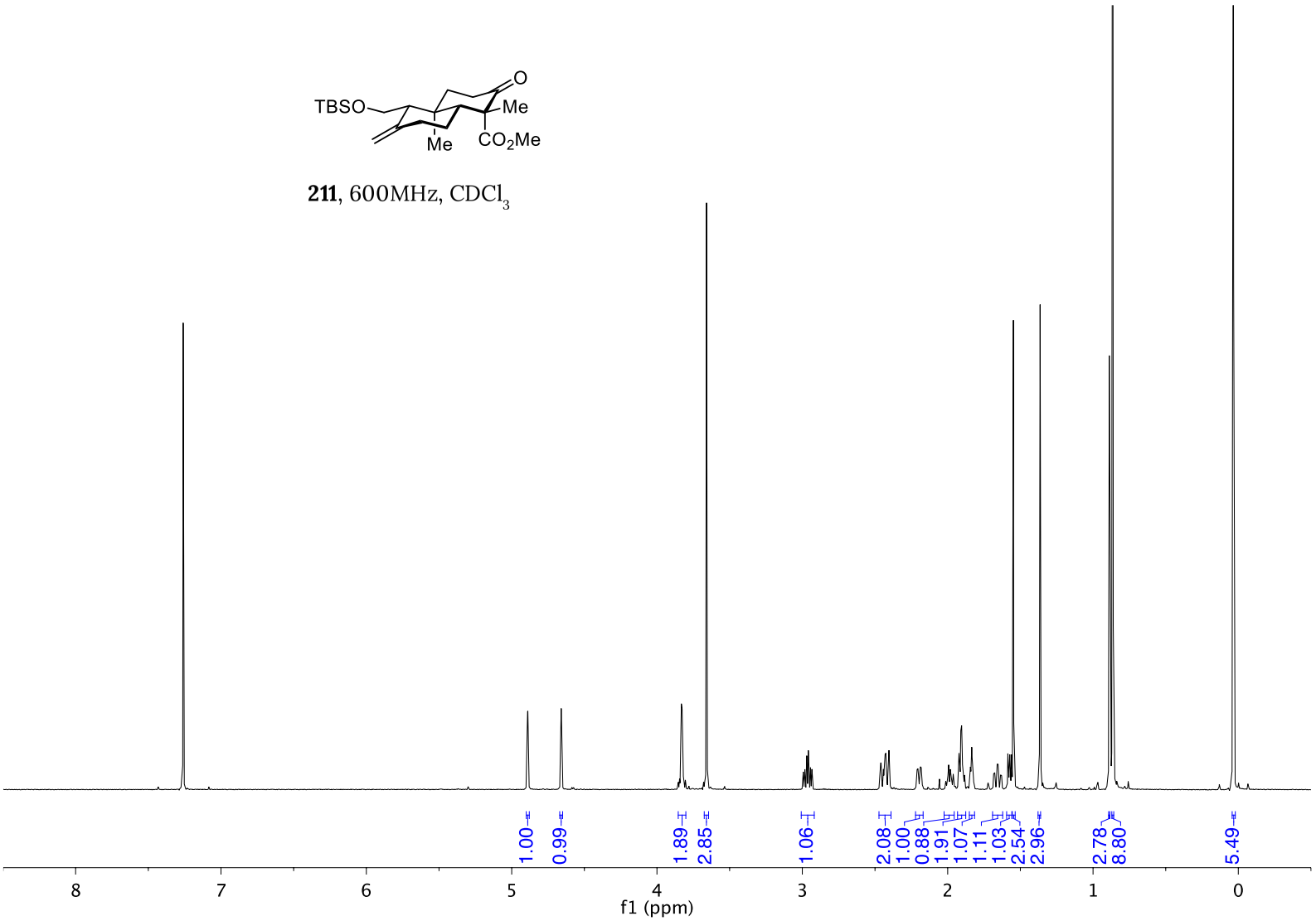
TBSO
O
Me
Me
CO2Me
211, 600MHz, CDCl3
1.00
0.99
1.89
2.85
1.06
2.08
1.00
0.88
1.91
1.07
1.11
1.03
2.54
2.96
2.78
8.80
5.49
8
7
6
5
4
3
2
1
0
f1 (ppm)

211, 150MHz, $CDCl_3$

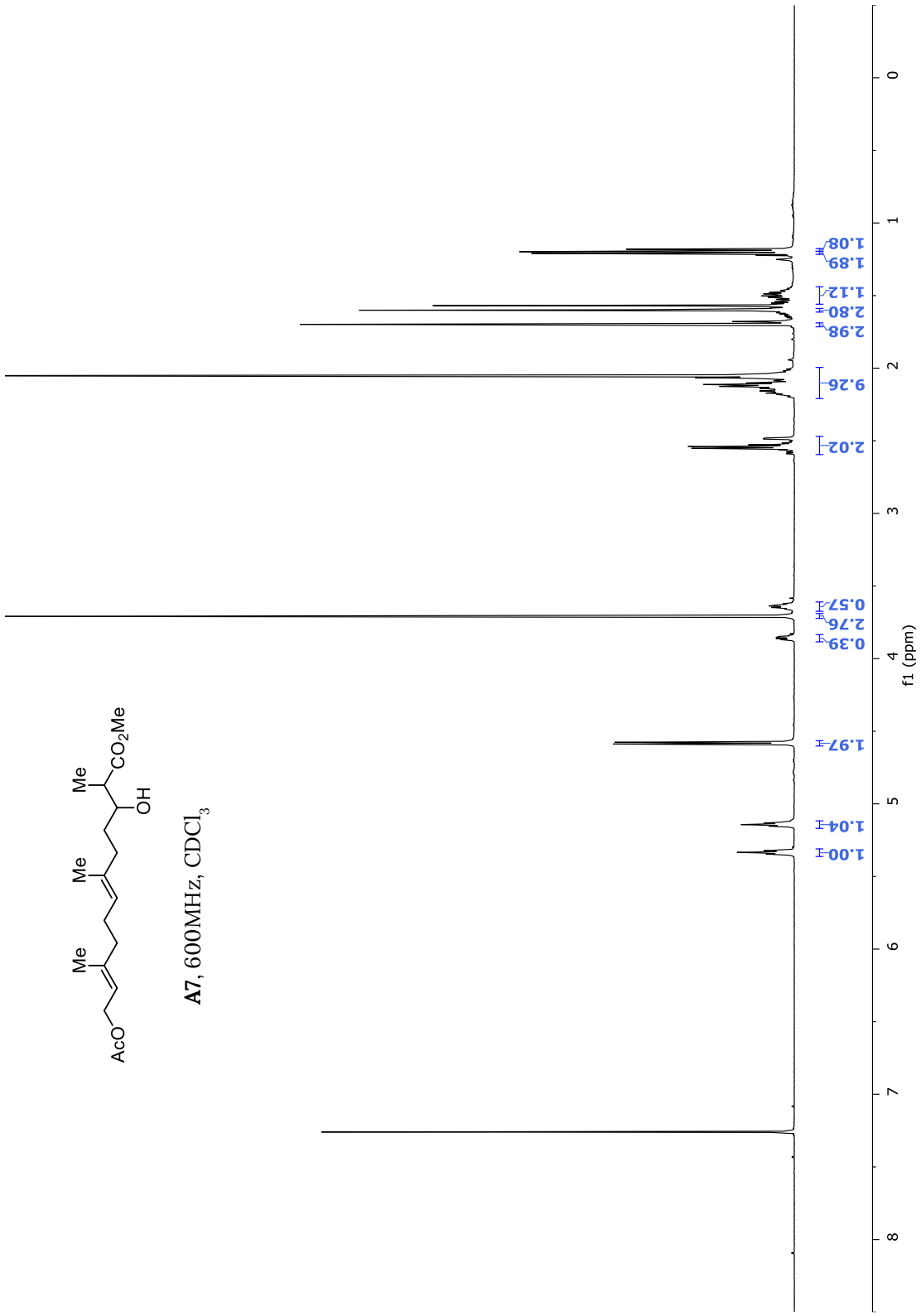
Me
Me
Me
CO2Me
OH
AcO
A7, 600MHz, CDCl3
1.00
1.04
1.97
0.39
2.76
0.57
2.02
9.26
2.98
2.80
1.12
1.89
1.08
f1 (ppm)

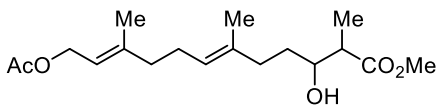

A7, 150MHz, $CDCl_3$

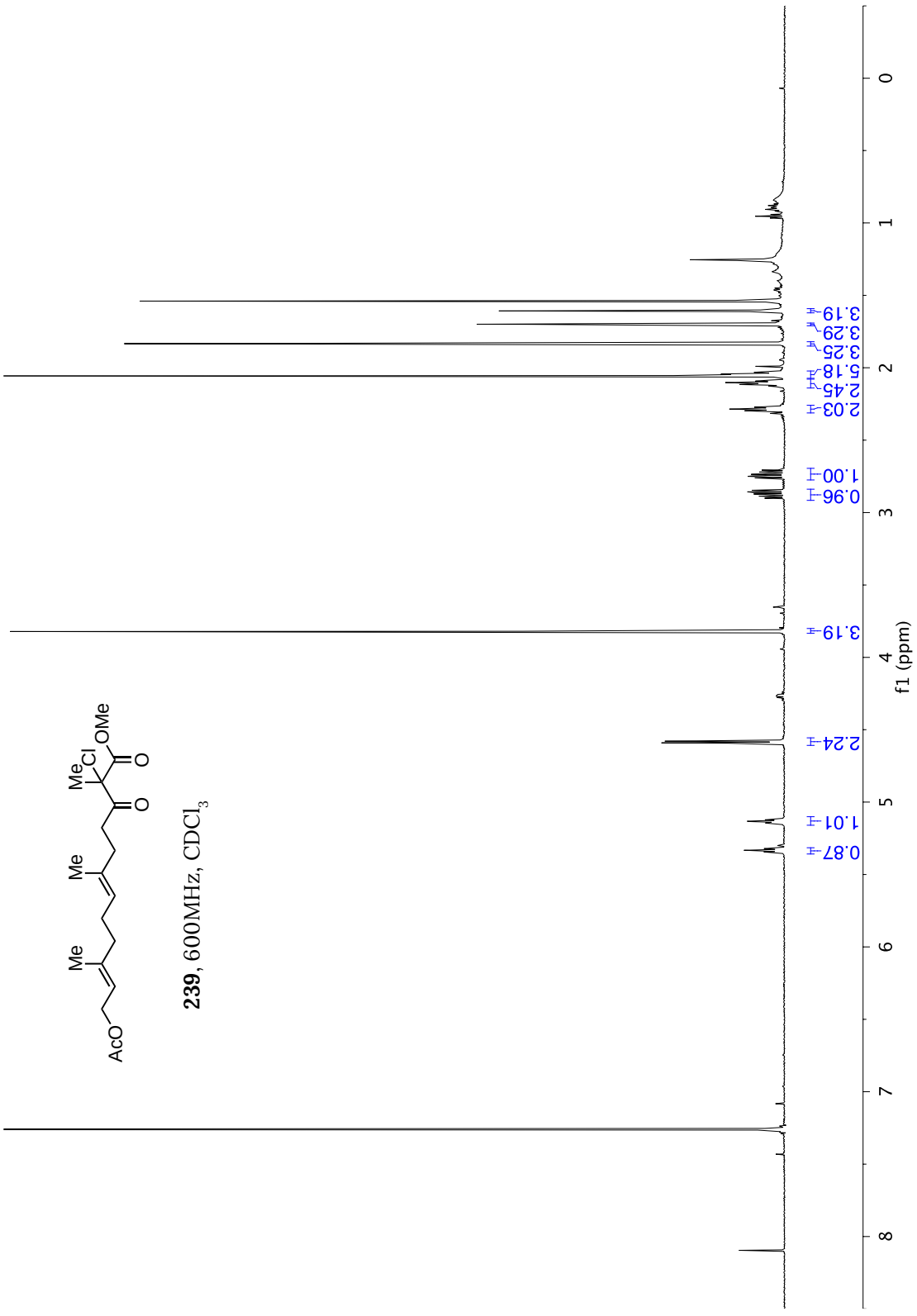
Me
Me
Me
Cl
OMe
O
O
AcO
239, 600MHz, CDCl3
3.19
2.24
1.01
0.87
3.19
3.29
3.25
5.18
2.45
2.03
1.00
0.96
f1 (ppm)

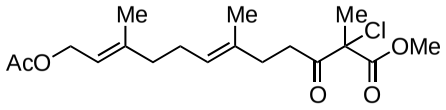

239, 150MHz, $CDCl_3$

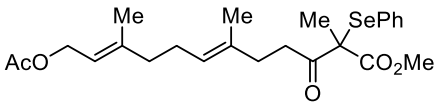

A8, 600MHz, $CDCl_3$

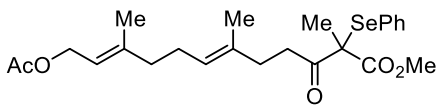

A8, 150MHz, $CDCl_3$

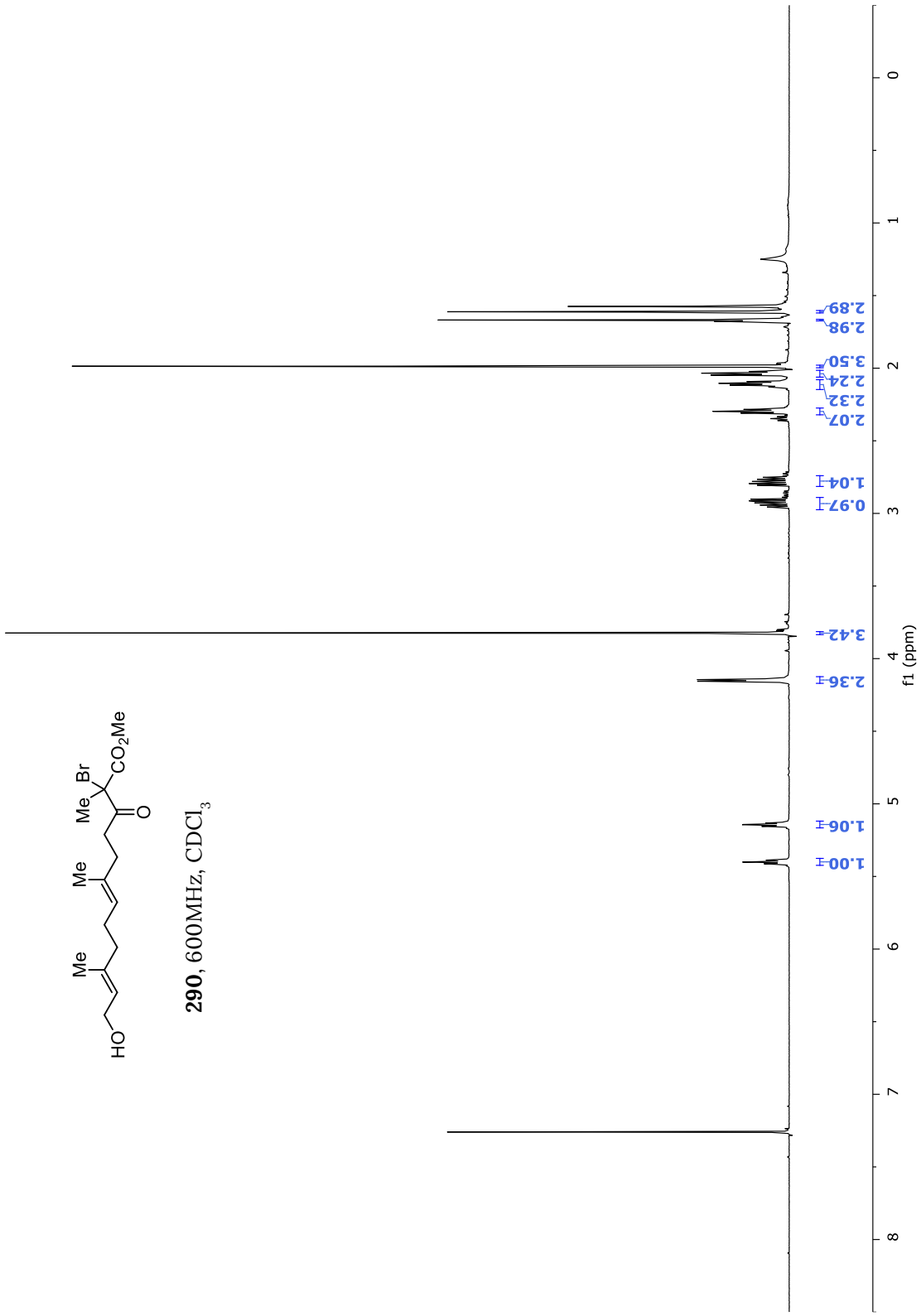

290, 600MHz, $CDCl_3$

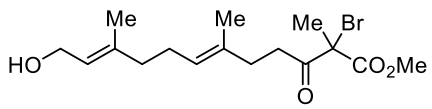

290, 150MHz, $CDCl_3$

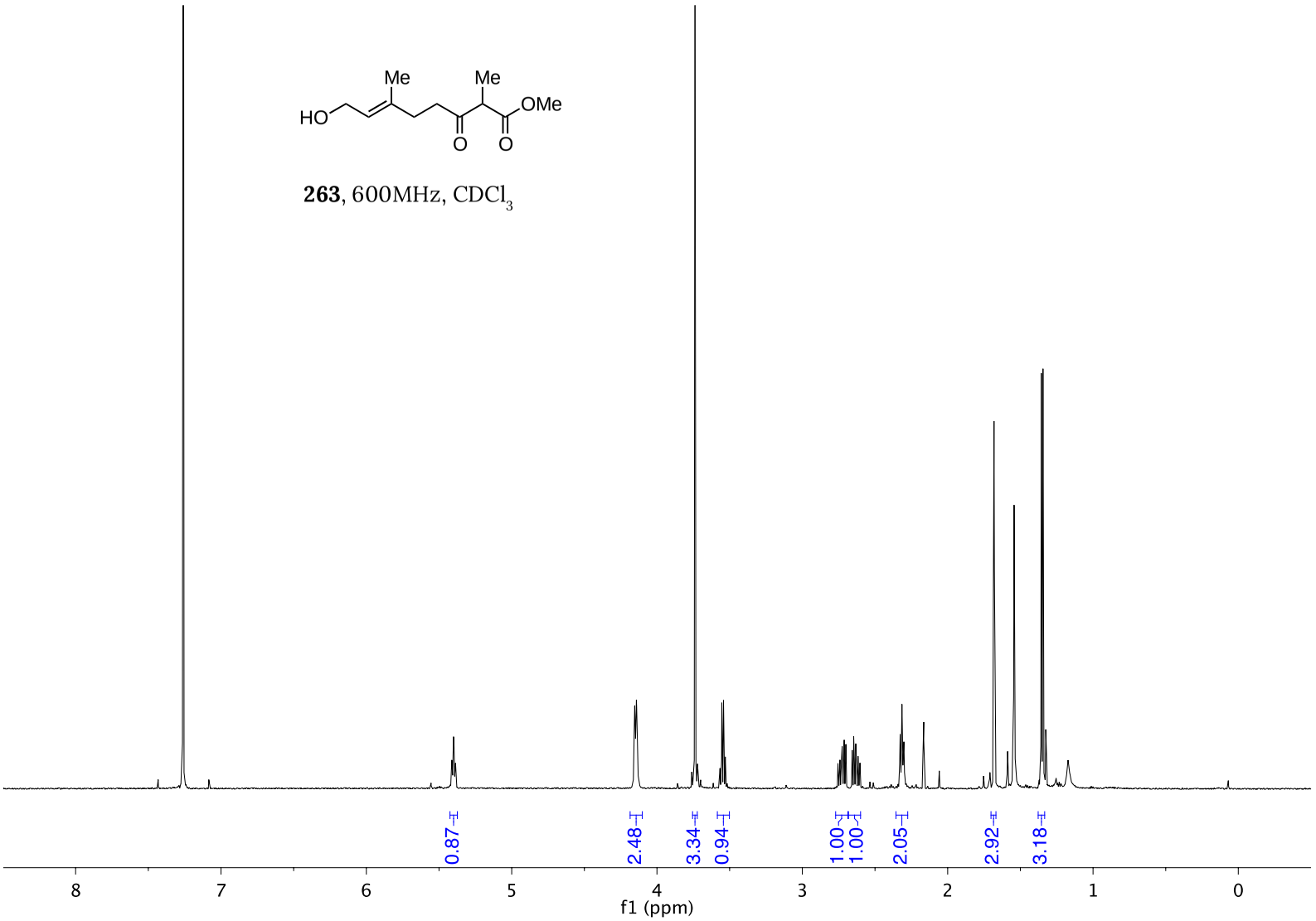

263, 600MHz, $CDCl_3$

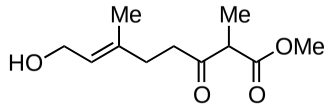

263, 150MHz, $CDCl_3$

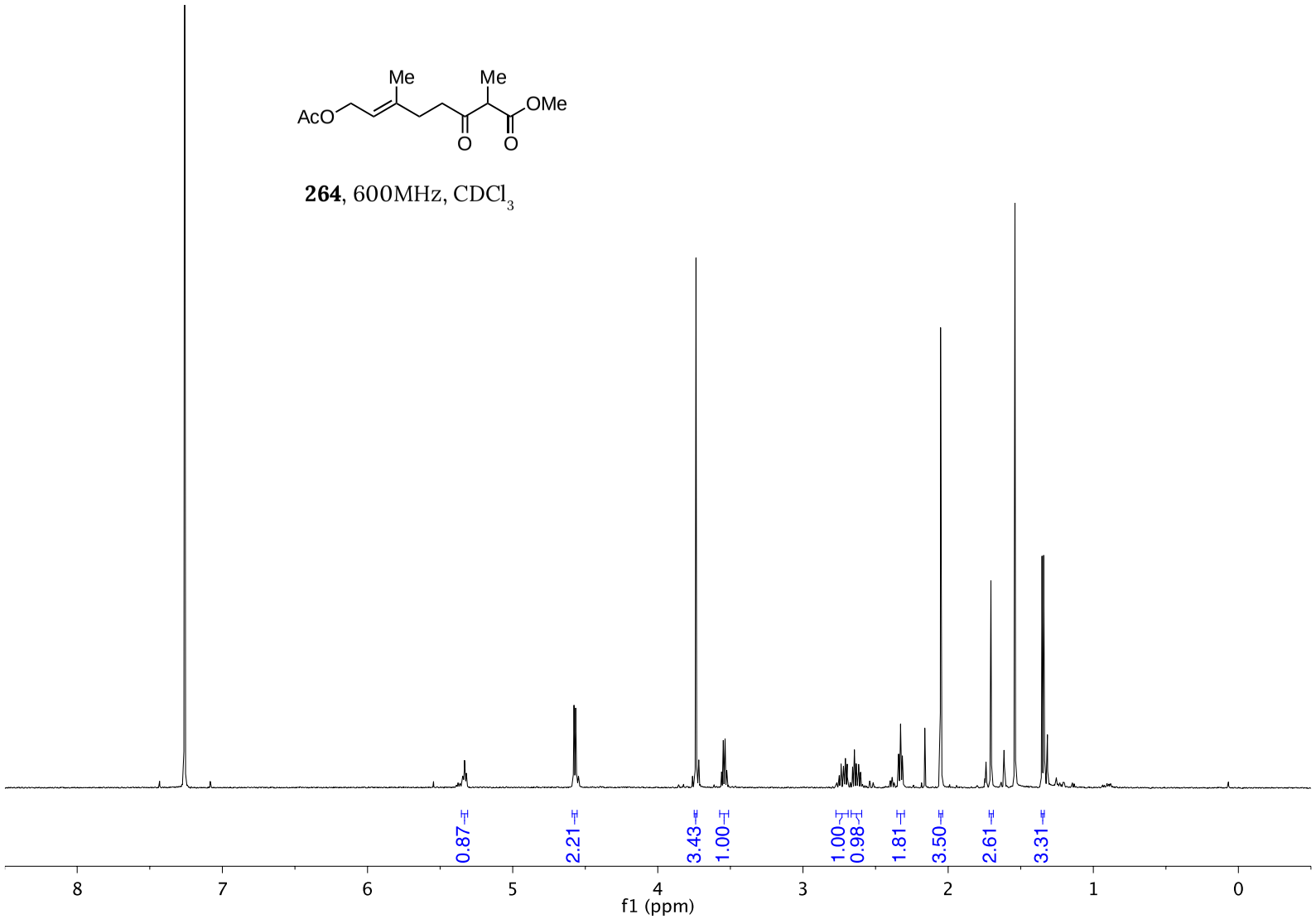

264, 600MHz, $CDCl_3$

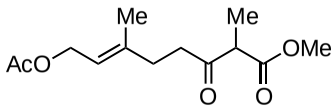

264, 150MHz, $CDCl_3$

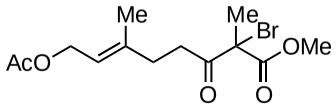

A9, 600MHz, $CDCl_3$

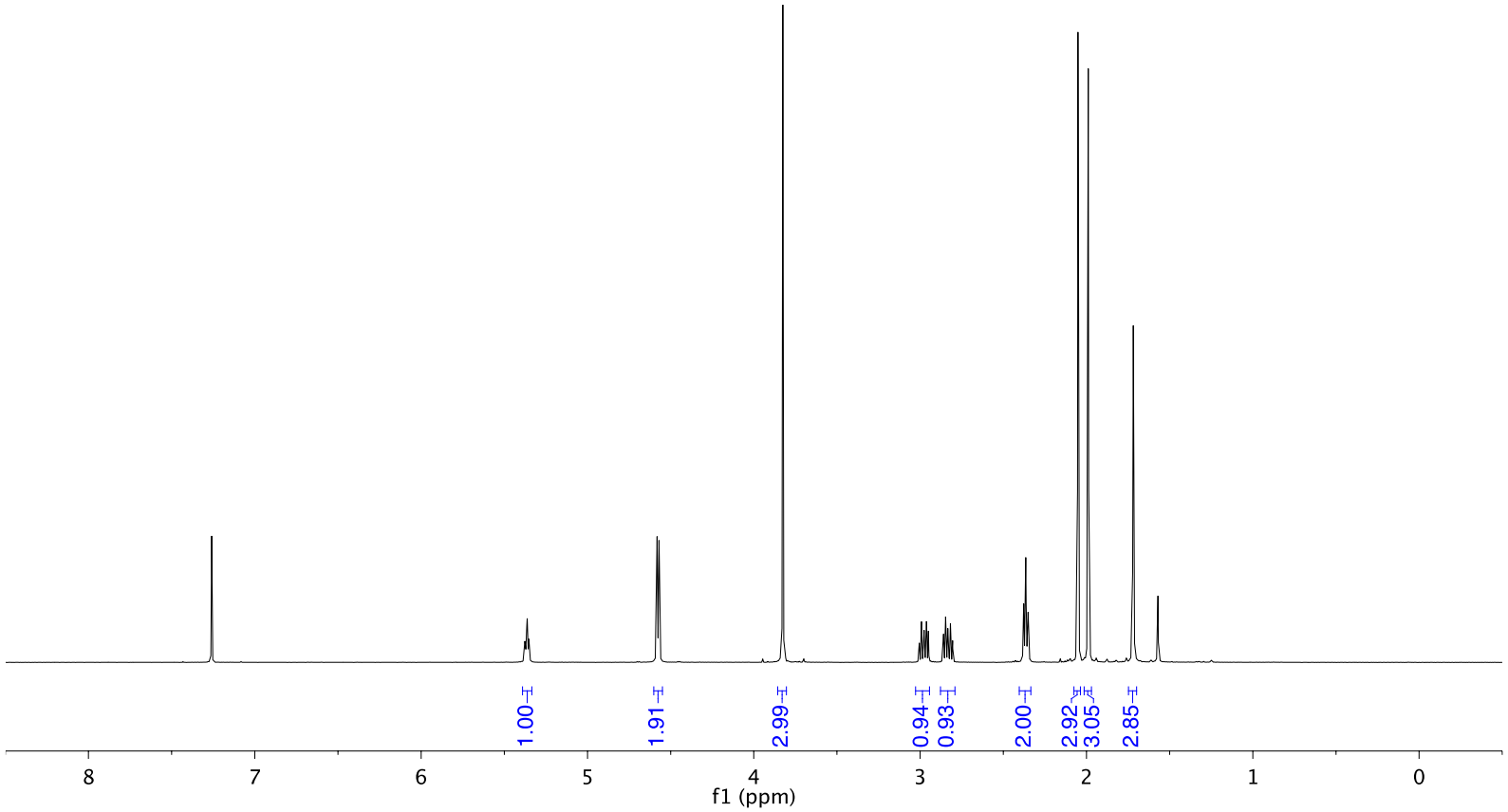

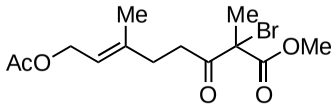

A9, 150MHz, $CDCl_3$

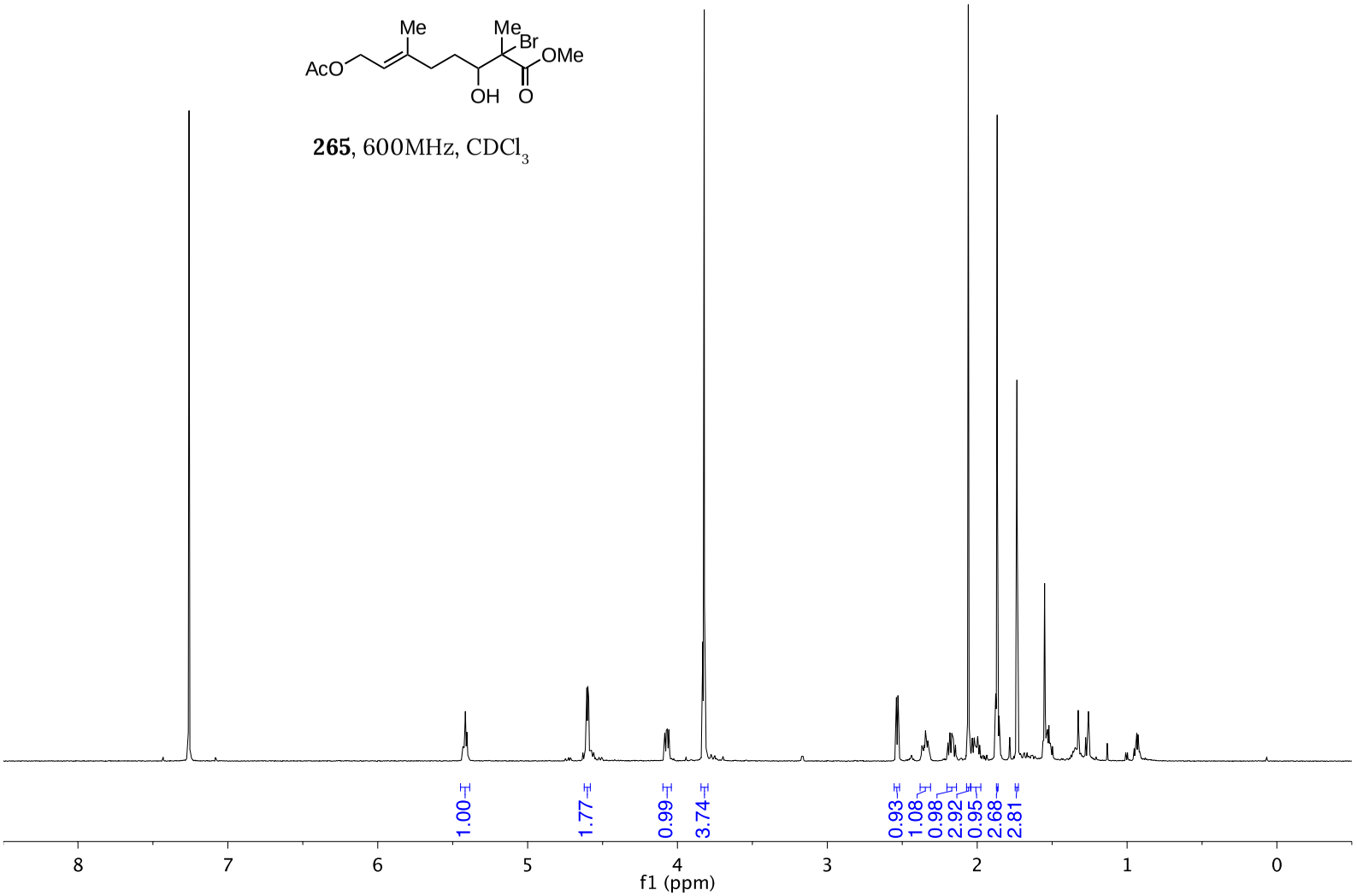
Me
Me
Br
AcO
OMe
OH
O
265, 600MHz, CDCl3
1.00
1.77
0.99
3.74
0.93
1.08
0.98
2.92
0.95
2.68
2.81
8
7
6
5
4
3
2
1
0
f1 (ppm)

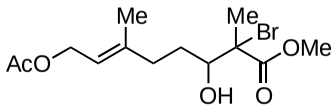

265, 150MHz, $CDCl_3$

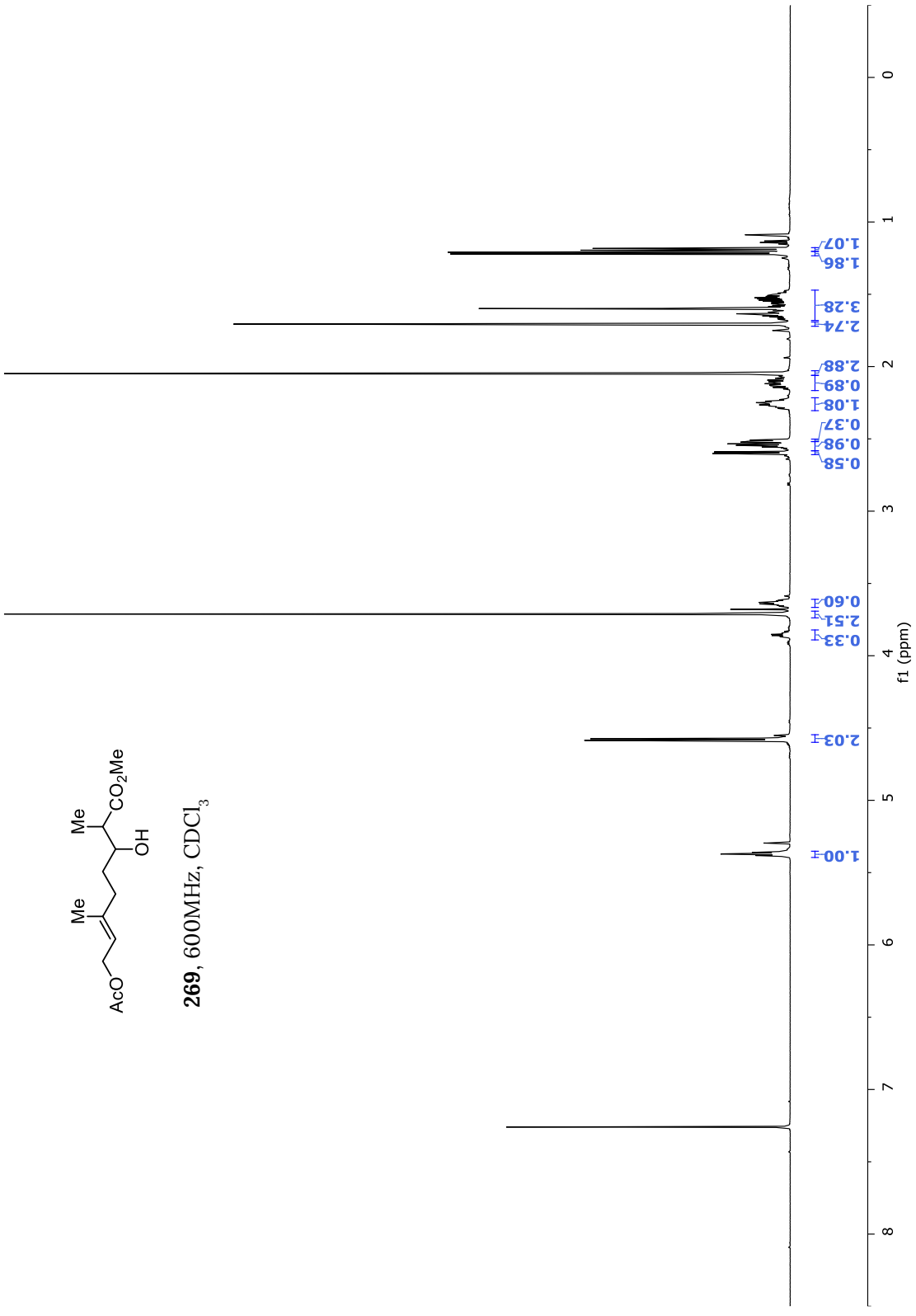
Me
CO2Me
OH
Me
AcO
269, 600MHz, CDCl3
1.00
2.03
0.33
2.51
0.60
0.58
0.98
0.37
1.08
0.89
2.88
2.74
3.28
1.86
1.07
f1 (ppm)

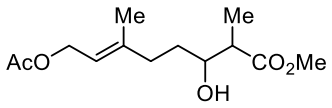

269, 150MHz, $CDCl_3$

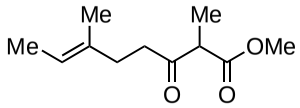

272, 600MHz, $CDCl_3$

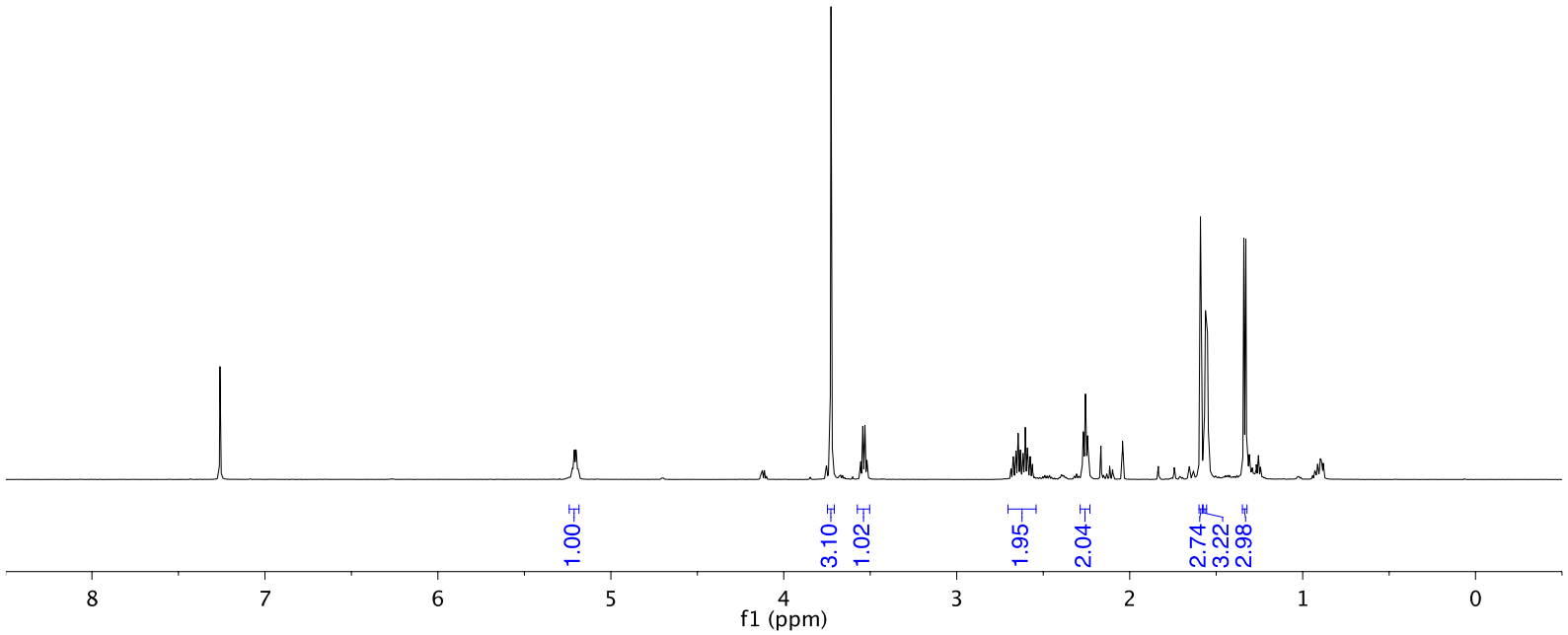

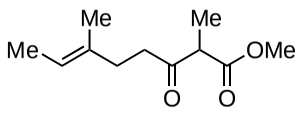

272, 150MHz, $CDCl_3$

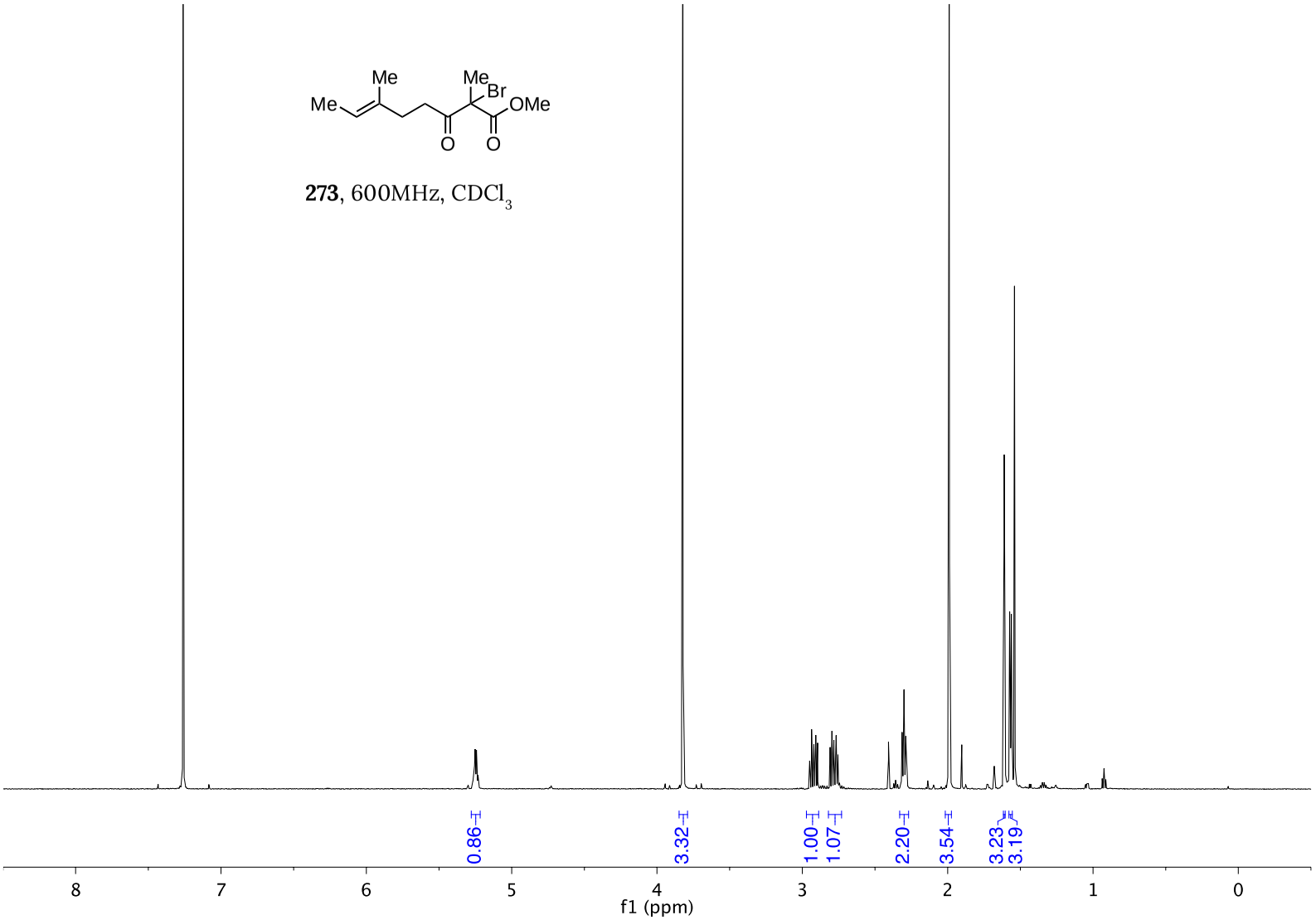
Me
Me
Me
Br
OMe
O
O
273, 600MHz, CDCl3
0.86
3.32
1.00
1.07
2.20
3.54
3.23
3.19
8
7
6
5
4
3
2
1
0
f1 (ppm)

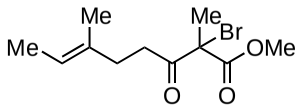

273, 150MHz, $CDCl_3$

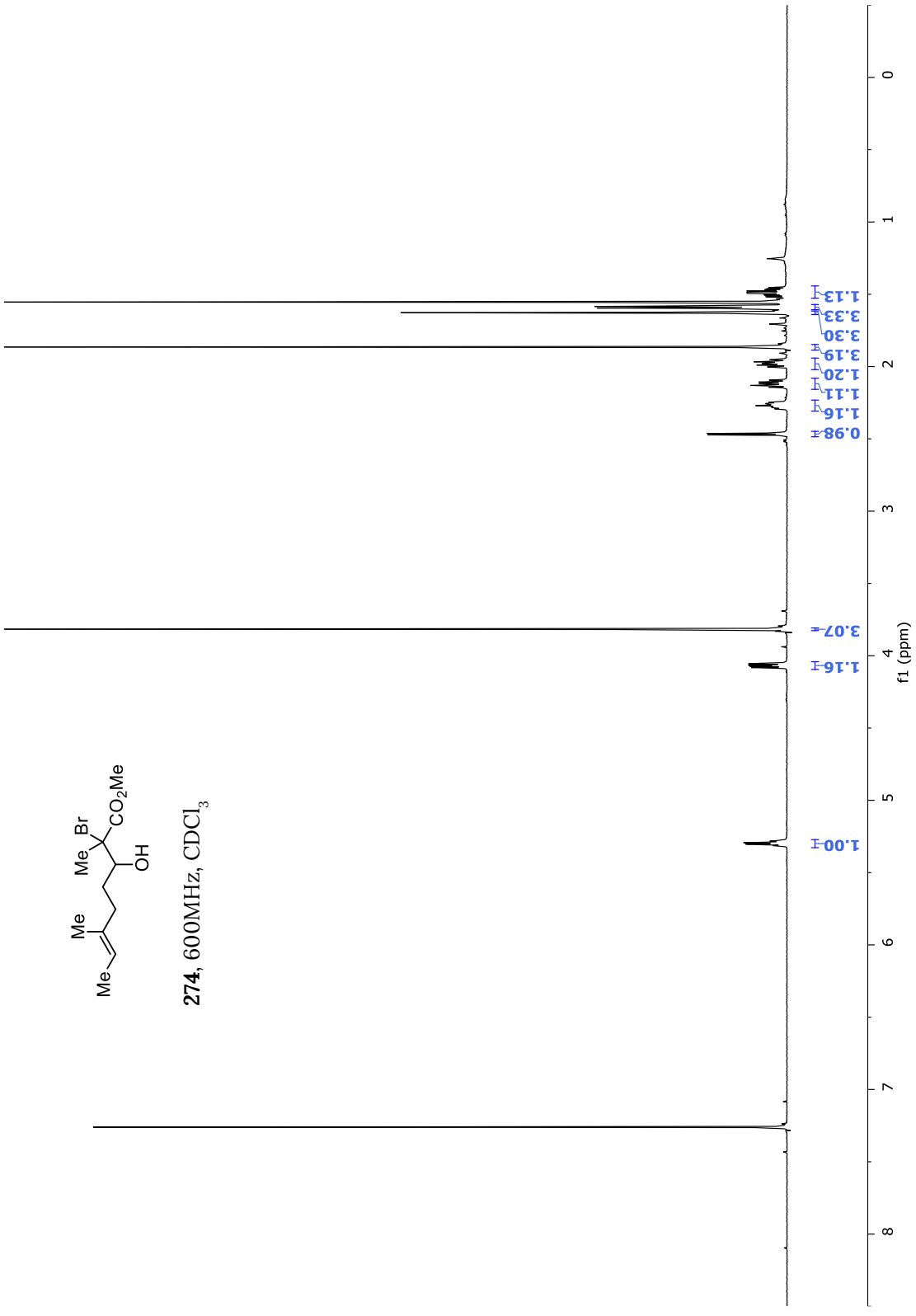
Me
Me
Br
CO2Me
OH
Me
274, 600MHz, CDCl3
1.00
1.16
3.07
0.98
1.16
1.11
1.20
3.19
3.30
3.33
1.13
0
1
2
3
4
5
6
7
8
f1 (ppm)

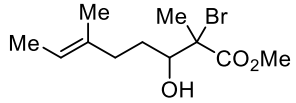

274, 150MHz, $CDCl_3$

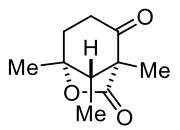

282, 600MHz, $CDCl_3$

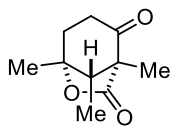

282, 150MHz, $CDCl_3$

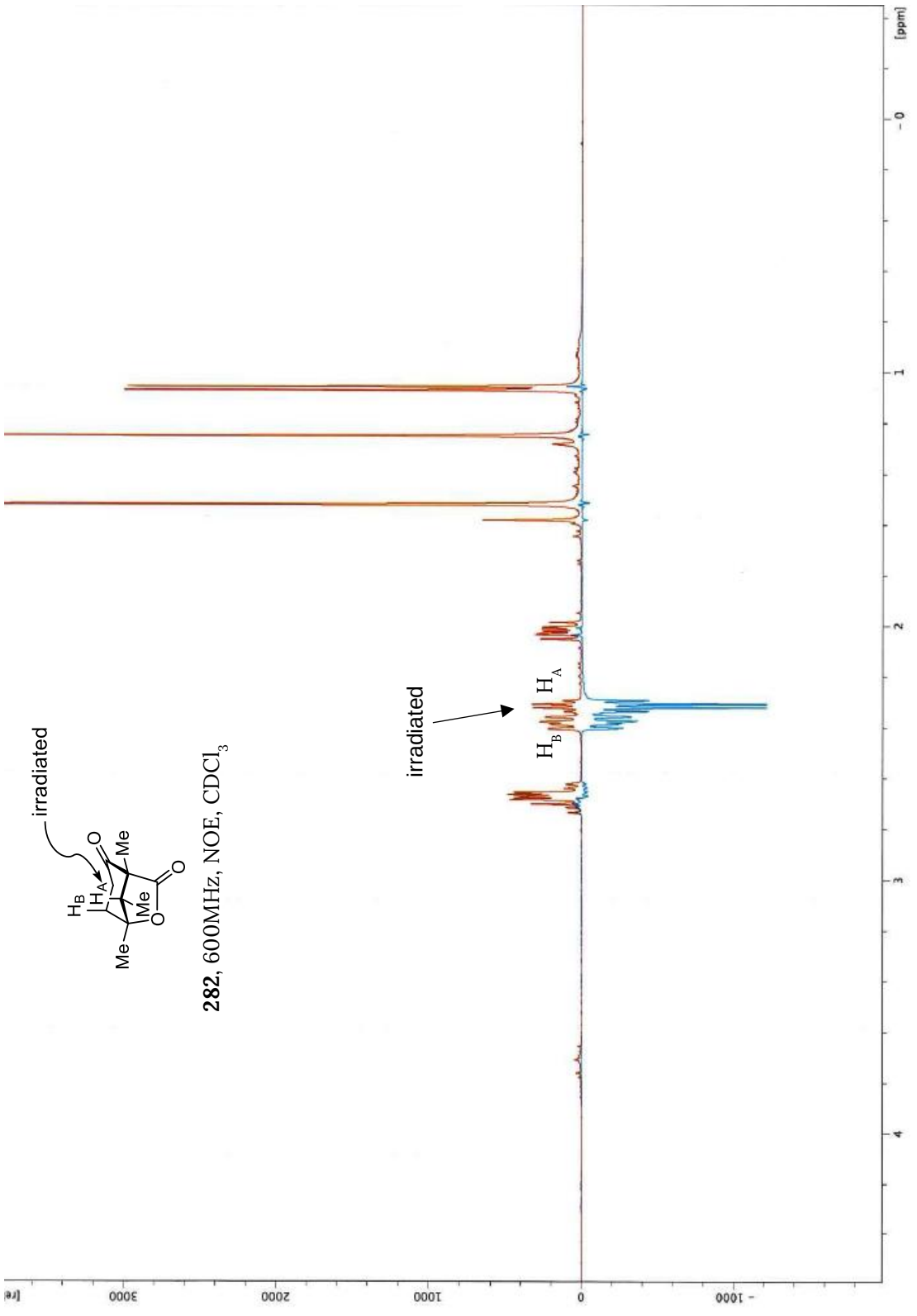
irradiated
H_B
H_A
Me
Me
O
O
Me
O
282, 600MHz, NOE, CDCl3
irradiated
H_A
H_B
[ppm]

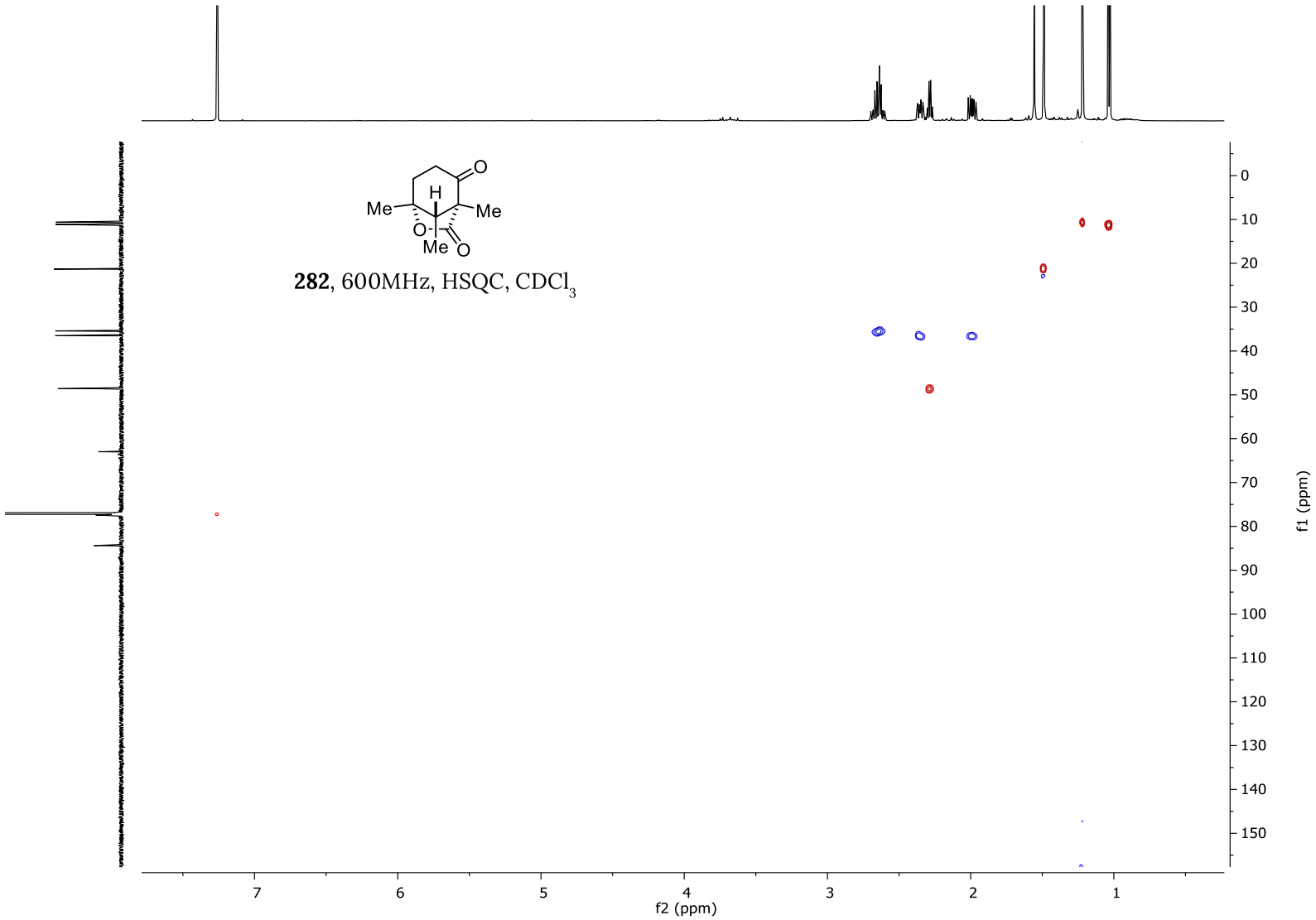

282, 600MHz, HSQC, $CDCl_3$

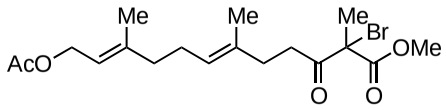

287, 600MHz, $CDCl_3$

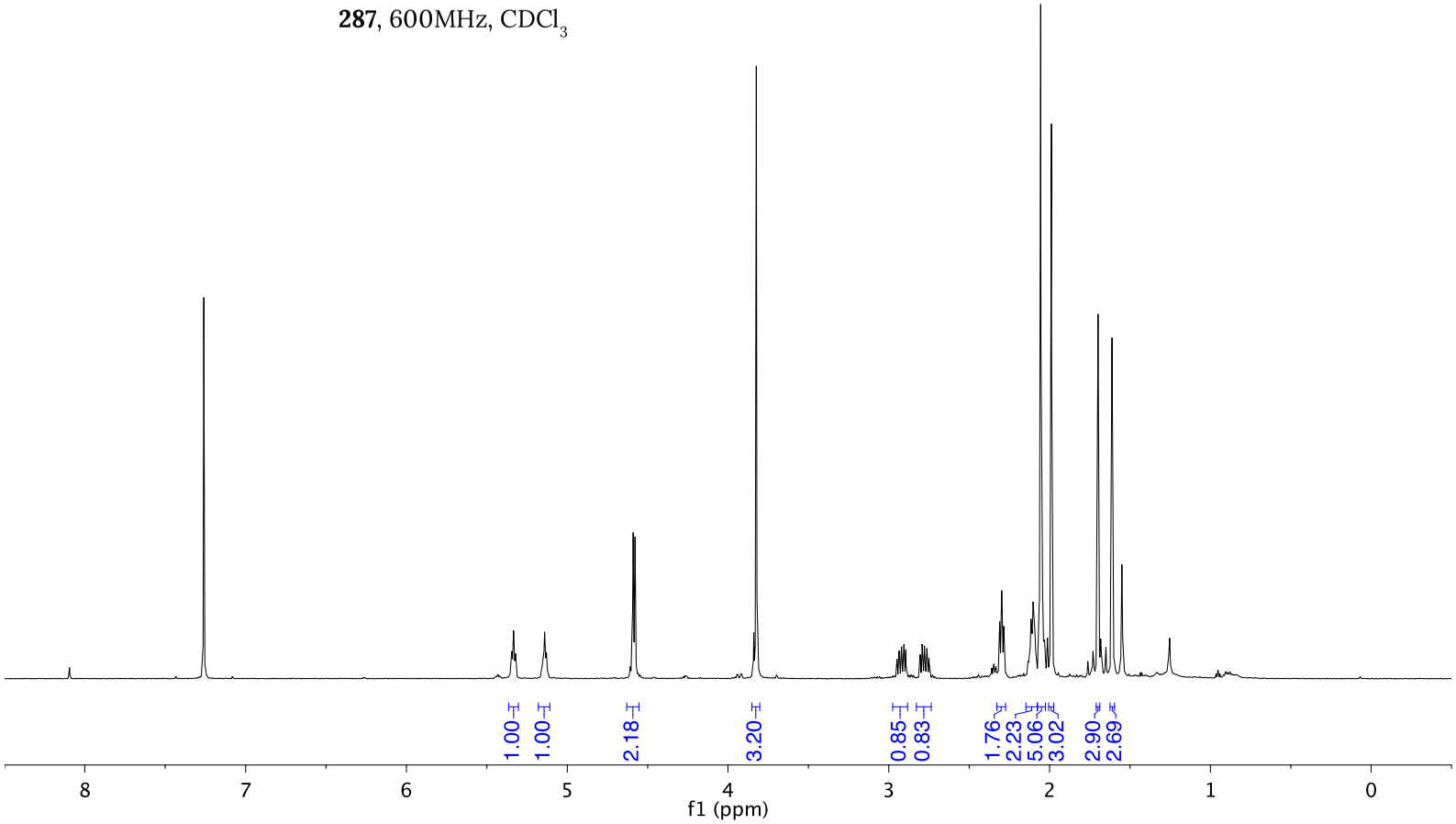

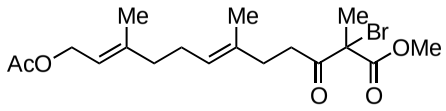

287, 150MHz, $CDCl_3$

287

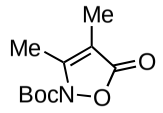

A10, 600MHz, $CDCl_3$

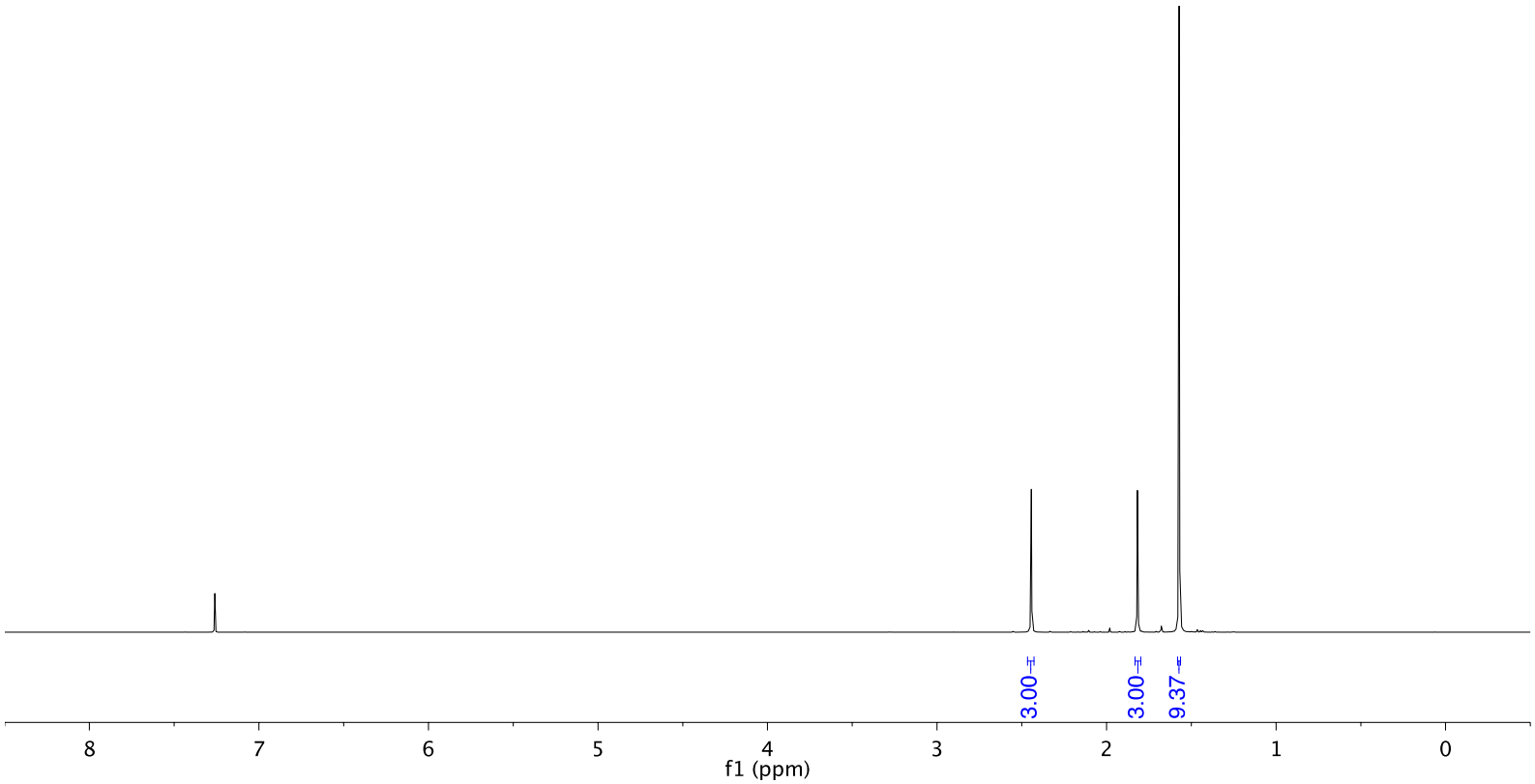

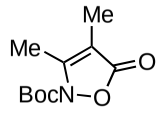

A10, 150MHz, $CDCl_3$

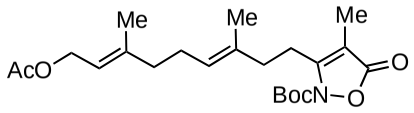

A11, 600MHz, $CDCl_3$

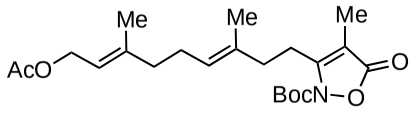

A11, 150MHz, $CDCl_3$

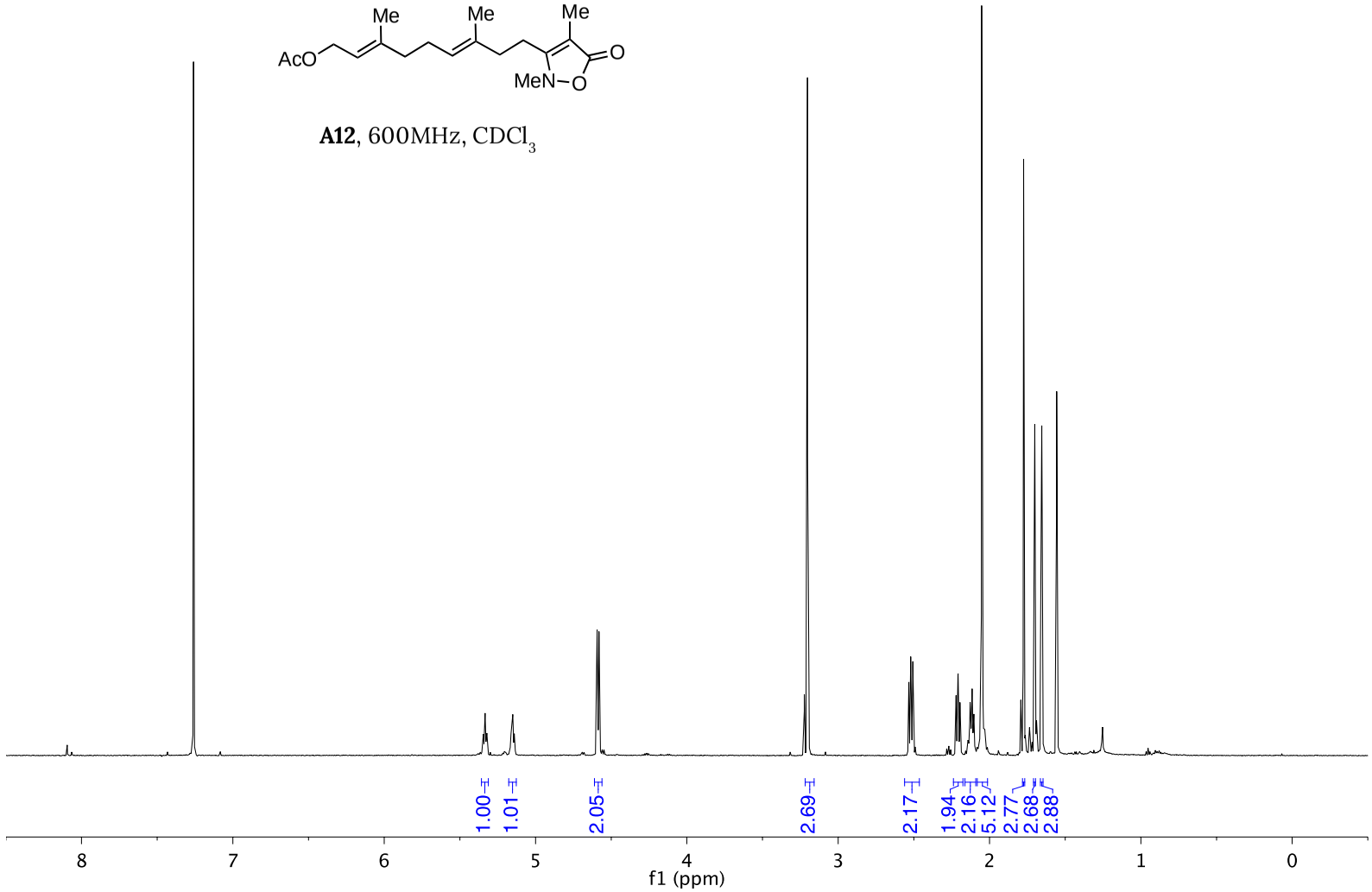

A12, 600MHz, $CDCl_3$

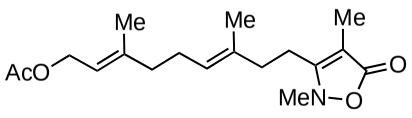

A12, 150MHz, $CDCl_3$

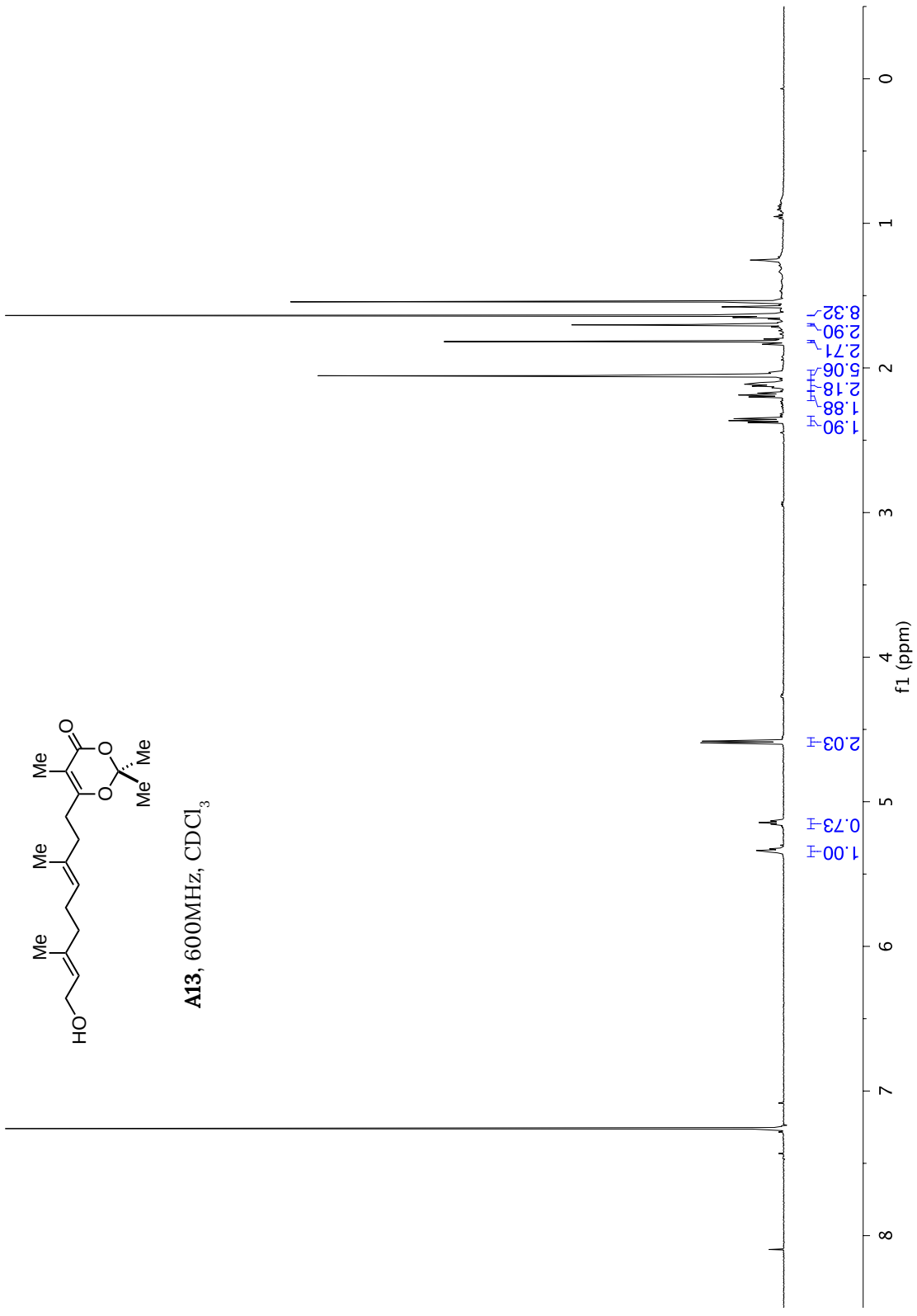
Me
Me
Me
O
O
O
Me
Me
HO
A13, 600MHz, $CDCl_3$
8.32
2.90
2.71
5.06
2.18
1.88
1.90
2.03
0.73
1.00
0
1
2
3
4
5
6
7
8
f1 (ppm)

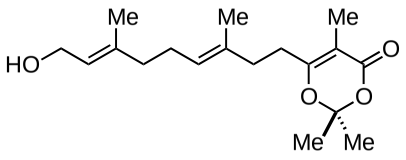

A13, 150MHz, $CDCl_3$